ISBN: 978-3-95450-188-5 doi:10.18429/JACoW-MEDSI2016-MOPE01

STABILIZATION METHODS FOR FORCE ACTUATORS AND FLEXURE HINGES

Carles Colldelram[1*], Josep Nicolas[2], Claude Ruget[1]
[1]CELLS, Cerdanyola del Vallès, Spain
[2]SLAC, Stanford, California, United States

Abstract

In the framework of the design of an adaptive optics x-ray mirror bender a stabilization system for ultra-low spring-constant force springs actuators and flexure hinges with nanometre resolution has been conceived. For this purpose its force resolution is better than 10^{-2}N. Since the actuator must preserve the force at this level and provide both pulling or pushing force the spring force was initially transmitted by a lever arm which was pivoting about a bearing articulation but its friction is up to the level of the required force. We present a novel method to compensate the stiffness of the corrector spring as well as a stabilized flexure, substituting the bearing, allowing to a obtain a system able to introduce a variable force on a which its force insensible to movements of the application point in a range of about 1 mm and a frictionless, torque-free articulation in a range of a 1º. The method is based on a combination of magnets with the flexure, in a way that the elastic force exerted by the flexure is compensated by the force of the magnet. Preliminary results show that it is possible to stabilize the torque exerted by the flexure below 0.005 N·m, in a range of 1 degree.

INTRODUCTION

The Nanobender [1,2], Fig. 1, is an instrument conceived to bend X-Ray mirrors to the required focusing curvature and also correct the optics surface errors by means a force actuator. The role of the actuator is to apply a force to introduce a controlled deformation of the mirror substrate that compensates the surface errors of the mirror.

From the deformation model, it turns that to allow compensating surface errors below one nanometer, the forces have to be tunable in a range of up to 20 N or more, and with a resolution of 10^{-2} N or better. To preserve the induced deformation, and thus the corrected figure, the forces applied by the corrector must be stable also within that range.

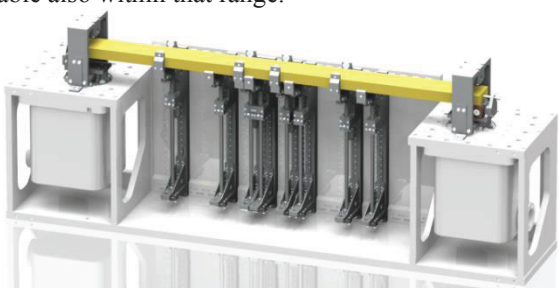

Figure 1: Nanobender.

* ccolldelram@cells.es

For a properly designed actuator, free of friction and parasitic forces, the main source of potential instability comes from mirror transport requirements. Since the mirror has to be moved from the metrology bench to the beamline, or even to a different laboratory, mirror systems must be prepared for transport.

In order to transport safely the mirror, the actuator contact to the mirror must be released. Considering that actuators are applying stress to the mirror, a shock on the transport crate could provoke that some actuator exceeded transitorily the fracture limit of the mirror. Releasing the contact of the actuator from the mirror implies that the repeatability of their relative position is limited to a few tens of microns.

Moreover the original corrector includes and articulation solved by a deep grove ball bearing, that although it has very low friction behaviour could be completely solved by means an also stabilized flexure applying the same compensating principle as for the force mechanism.

The actuator we propose incorporates a mechanism that preserve the force exerted by the actuator for small changes of such position. The working principle of such mechanism is described in this paper.

The paper is divided in two main sections: First the force compensating mechanism for the force actuation and second the stabilized flexure for the articulation.

STABLE-TUNABLE FORCE ACTUATOR

Description

The actuator is sketched in Fig. 2. This corrector have been patented [3]. In this case a pushing actuator is considered. The mechanism can be divided in the four following parts:

1. The frame of the actuator, which is the part of the actuator that supports the other parts of the mechanism, and is mounted on the main frame of the bender.
2. The transmission chain, which includes the lever arm and the contact to the mirror, is the part that transmits the forces exerted by the spring and the magnets, which have different application points, onto a single contact point to the mirror. The transmission also has articulations that absorb all the parasitic components of the forces, which would affect the performance of the system. Although the transmission chain is articulated, it is in practice static, because the reaction force induced

ISBN: 978-3-95450-188-5 doi:10.18429/JACoW-MEDSI2016-MOPE02

STUDIES ON FLOW-INDUCED VIBRATIONS FOR THE NEW HIGH-DYNAMICS DCM FOR SIRIUS

R. M. Caliari*, O.R. Bagnato, L. de Souza Jr, F. R. Francisco, R. R. Geraldes, R. L. Parise, M. Saveri Silva, and D. O. Tavares, Brazilian Synchrotron Light Laboratory, Campinas, Brasil
T. A. M. Ruijl, MI-Partners, Eindhoven, Netherlands

Abstract

The monochromator is known to be one of the most critical optical elements of a synchrotron beamline, since it directly affects the beam quality with respect to energy and position. Naturally, the new 4th generation machines, with emittances in the range of order of 100 pm rad, require even higher stability performances, in spite of the still conflicting factors such as high power loads, power load variation, and vibration sources. A new high-dynamics DCM (Double Crystal Monochromator) is under development at the Brazilian Synchrotron Light Laboratory for the future X-ray undulator and superbend beamlines of Sirius, the new Brazilian 4th generation synchrotron [1, 2]. The disturbances induced by the coolant flows are known to be among the most detrimental influences to a DCM performance, however, quantitative force numbers are not commonly investigated. According to the novel dynamic concept, these forces should be predictably translated into stability performance. Therefore, experimental setups that allow the indirect measurement of such forces in conditions close to those of operation were designed. The results comparing different indirect cooling profiles and manufacturing processes (brazing and additive manufacturing) are shown.

INTRODUCTION

The goal of this work is to present the flow-induced vibrations experiments, an indirect measurement of the force frequency spectrum for the cooling vibrations disturbances at the new high stability monochromator for Sirius [1]. Details about the full system can be found in [3].

DCM CLOSED LOOP CONTROL

The new high-dynamics monochromator introduced in the present conference is a high ending mechatronics system [4], in which the system stability, in particular, is only possible because of a high-bandwidth closed loop control. As it is highlighted in Fig. 1, in order to achieve a nanometric positioning resolution and stability it is essential to understand the disturbances actuating on each element of the closed loop control, so that the effects of each disturbance can be analysed already at project level. Therefore, one must know the frequency domain characteristics and energy content of each component.

A preliminary work has already been dedicated to floor vibration characterization at Sirius [5], whereas amplifier and quantization noise, delays, non-linearities and other disturbances from the chosen equipment are well-known (see [6]). Flow-induced vibrations, on the other hand, are a more difficult subject, to which this work is dedicated.

* ricardo.caliari@lnls.br

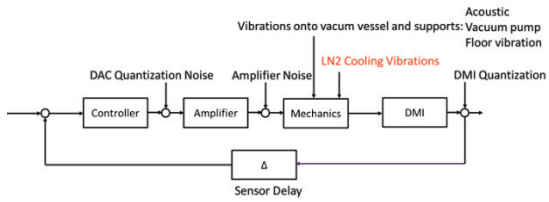

Figure 1: Block diagram of a generic representation of the main disturbances of the closed loop control.

LIQUID NITROGEN COOLING

Due to the high power load that reaches the first crystal in the DCM, liquid nitrogen (LN_2) or water-cooling is generally necessary. An important development front was conducted in this subject to match the LN_2 cooling requirements with the high-dynamics and metrology methods [7].

The problems associated with flow-induced vibrations are known since very long [8], and their negative influence in the performance of monochromators has already been identified and characterized [8, 9]. Indeed, previous works presented vibration results as position vs. frequency plots [10] or acceleration levels (or arbitrary units) in time plots [11, 12]. The state-of-the-art DCMs typically live under given conditions, passively dealing with them by means of mechanical improvements to damp the vibrations and tuning flow and working pressure for each system.

However, in order to guarantee higher bandwidth dynamic control and set the appropriate designing targets for the project, quantitative data of disturbance forces in conditions close to that of real operation should be available. Thus, the force Power Spectral Density (PSD) from the flow-induced vibrations should be characterized.

DYNAMIC MODEL

Discrete Structure Model

The first step was the development of a 1D lumped-mass model, as depicted in Fig. 2(a). The purpose was to design an experimental setup that would be sensitive enough to the expected small force levels. The first approximation was that the flow-induced disturbance forces would be in the range of 1 to 10 mN. These values guided the definition of masses and stiffness for the setups. It was soon realized that the PSD noise floor of the metrology instruments together with parasitic disturbances, such as floor vibrations, would prevent the full frequency range of interest (from about out 5 Hz to 2 kHz), from being evaluated with a single setup.

ISBN: 978-3-95450-188-5 doi:10.18429/JACoW-MEDSI2016-MOPE05

MECHANICAL DESIGN OF SECONDARY SOURCE SLITS FOR HARD X-RAY BEAMLINES AT TAIWAN PHOTON SOURCE

H. Y. Yan†, C. H. Chang, D. J. Wang, C. Y. Chen, J. M. Lin, C. Y. Huang, D. G. Liu, S. H. Chang
National Synchrotron Radiation Research Center, Hsinchu, Taiwan

Abstract

The secondary source slits have been developed for specific hard X-ray beamlines at Taiwan Photon Source. Especially for Coherent X-ray Scattering and X-ray Nanoprobe beamlines, severe specifications of the slits are more necessary to define proper beam sizes in horizontal and vertical directions at sample. The opening size of each pair of slits assembled orthogonally is usually needed to range within several microns, so the UHV-compatible piezo-driven stages with closed-loop system were adopted for the purposes of fine adjustment, precise positional accuracy and repeatability. To reduce X-ray scattering effect, the rectangular single-crystal film was bonded on the edge of the slit blade. The machined rotary weak-link structure and piezo-driven actuators were used to slightly adjust parallelism of each pair of the blades with the method of single-slit diffraction. To enhance structural and thermal stability, the granite plinths with specified shape were designed and the precise temperature controlling system will be set up recently. The overall design, mechanical specifications and procedure of testing for secondary source slits will be introduced in this paper.

INTRODUCTION

As small beam size is more required in hard X-ray beamlines at accelerators of synchrotron radiation around the world, the specifications of slits system become more critical. For example, the beam size between 1 - 10 μm both in horizontal and vertical directions at sample was design for the Coherent X-ray Scattering beamline at Taiwan Photon Source (TPS). The quality of beam spot with small size is influenced by unstable situation very easily, so mechanical stability of slits system needs to be considered comprehensively. For these reasons, the necessity of designing a new type of mono beam secondary source slits was taken into account. Recently we have developed a new type of stable slits system with severe specifications, such as the smallest opening size and parallelism between two blades on each pair of slits. The following sections will introduce design of secondary source slits, testing procedure and result, and precise temperature controlling system respectively.

DESIGN OF SECONDARY SOURCE SLITS

To achieve the expected performance, some commercial components used widely were adopted in the mono beam secondary source slits for their mature developing experience. And the specific design for accurate adjustment and mechanical stability were completed. Fig. 1 and Fig. 2 show the schematic 3-D drawing and on-site view of secondary source slits installed in the Coherent X-ray Scattering beamline and located at 40.52 m from the center of two Insertion Devices respectively. Considering the optical design, the slits system is uncooled type because of locating after the Double Crystal Monochromator (DCM).

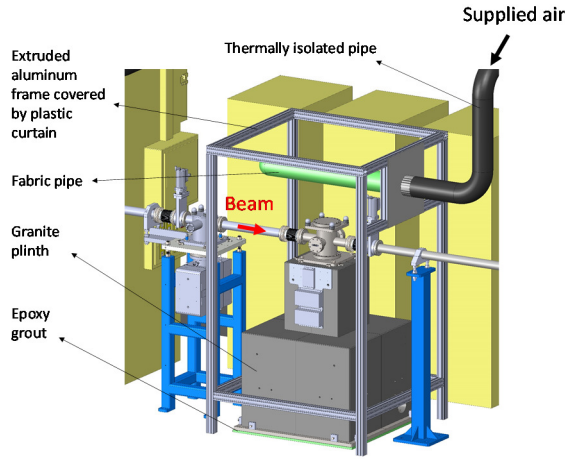

Figure 1: Schematic 3-D drawing of secondary source slits.

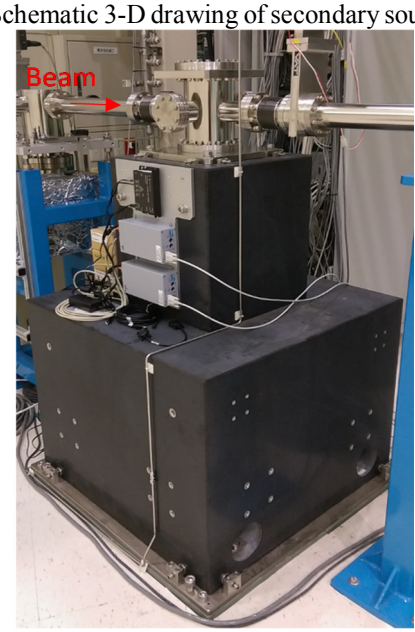

Figure 2: On-site view of secondary source slits installed in the Coherent X-ray Scattering beamline at TPS.

Specifications

Fig. 3 shows a 3-D model of main mechanism for secondary source slits. Gap between blades of each slit is maintained to produce zero beam. Two sets of piezo-driven actuator were adopted for their accurate size for each step and compatibility of ultra-high vacuum (UHV). Piezo stages with closed-looped system function for controlling opening size of each pair of slits, and their positional accuracy and repeatability are both less than 100 nm. Picomotors are used to adjust parallelism between blades of each

ISBN: 978-3-95450-188-5 doi:10.18429/JACoW-MEDSI2016-MOPE07

GROUND MOTIONS MEASUREMENTS FOR SYNCHROTRON

D. Ziemianski†, Cracow University of Technology, Kraków, Poland
M. P. Nowak, Solaris, Kraków, Poland

Abstract

For more than two decades, ground vibration measurements were made by different teams for feasibility studies of linear accelerators. Recent measurements were performed in the SPS tunnel and at different CERN sites on the surface. The devices to measure vibrations of magnitude ranging in nanometres, the analysis techniques and the results are critically discussed and compared with the former measurements. The implication of the measured integrated R.M.S. displacements for the Crab cavities cavern are mentioned.

The equipment used in this study consists of 2 state-of-the-art Guralp broadband triaxial seismometers. Models CMG-T60-0004 (Guralp Systems) performed measurements in three directions V, N/S and E/W.

The first analysis was to evaluate the power spectral density for each direction of sensors and event. The power spectral density is calculated from the auto power spectrum.

The power spectral density shows a typical curve for the geophones with the micro seismic peak between 0.2 and 0.4 [Hz]. It is important to point that ground vibrations should not be ignored in planning accelerator facility. Actually it is one of the limiting factor in the optimization of future accelerators.

SENSORS

Each author should submit the PDF file and all source files (text and figures) to enable the paper to be reconstructed if there are processing difficulties.

Models CMG-T60-0004 (Guralp Systems) performed measurements in three directions V, N_S and E_W. The geophones measure velocity with a sensitivity of about 2000 [V/(m/s)] and a frequency range between 30 [s] and 100 [Hz].

Geophones were adjusted to have the vertical direction parallel to the gravitation force. Longitudinal north-south and east west directions for geophones were pointed in the same directions. The results obtained from these sensors are dependent on good operational conditions and give a good signal to noise ratio only if all conditions are correct. The geophones need to be well protected against fluctuation in temperature and turbulent airflow.

In order to have a constant temperature for the geophones during operation, they were located and switched on 1 hour before any measurement was started. Then they had time to reach thermal equilibrium, this also reduces the DC offset from the measurement.

RESULTS

The first analysis was to evaluate the power spectral density for each direction of sensors and event. The ground motions at several locations measured in are plotted in (Figure 1). These locations are divided into three groups. The first group (red lines) is the synchrotron bunker, the second group (green lines) is the experimental hall and the third group (black lines) is the tunnel linac.

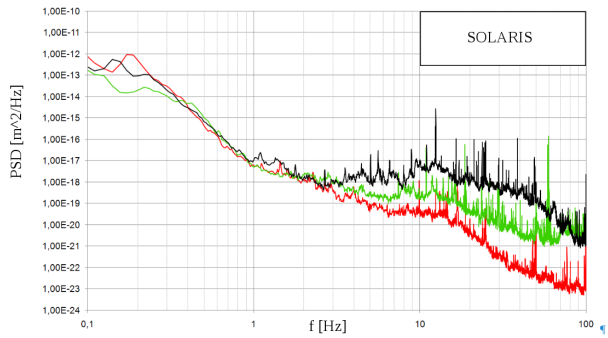

Figure 1: PSD for SOLARIS synchrotron.

RMS Integrated is used to sum up the total vibration of the PSD. It gives the RMS (Root Mean Square) value of the total vibration The integrated RMS ground motion in vertical direction for all these locations are plotted in (Figure 2). The (Table 1) show the value Integrated RMS value at 1 [Hz].

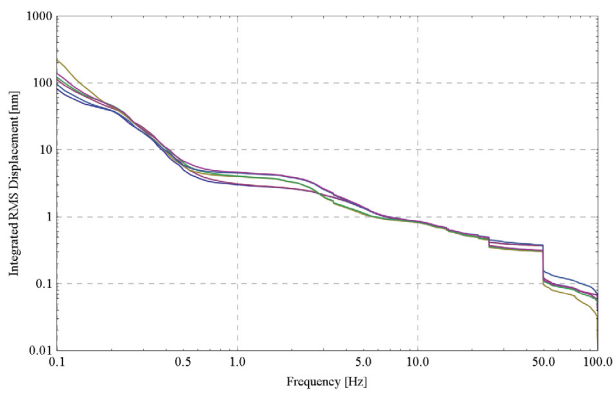

Figure 2: Ground motion all measured locations.

† dziemianski@pk.edu.pl

ISBN: 978-3-95450-188-5 doi:10.18429/JACoW-MEDSI2016-MOPE08

THE LNLS METROLOGY BUILDING*

H. G. P. Oliveira†, L. Sanfelici, C. Esper-Neto, P. T. Fonseca, R. R. Geraldes, B. C. Meyer, M. A. Pereira, G. L. Rodrigues, L. G. Silva, LNLS, Campinas, Brazil
L. Buccianti, M. H. A. Costa, C. Prudente,
Biotec Soluções Ambientais, São José dos Campos, Brazil

Abstract

The increasing demands of instrumentation projects for SIRIUS require more sensitive equipment to be developed and characterized in the micro and nanometer scale. To achieve this level of precision it is necessary to work within a controlled environment, minimizing instabilities and disturbance effects such as temperature variation and vibrations. Based on metrology labs as those at BESSY, ESRF, DLS and others, a new facility is currently under final construction stage at the LNLS, which will be dedicated to high precision optical and mechanical metrologies. This work describes in detail the project of the new LNLS Metrology Building.

INTRODUCTION

Sirius [1] is a 3 GeV synchrotron light source that is currently being built by the Brazilian Synchrotron Light Laboratory (LNLS), with a high brilliance beam which size could be as small as 9.5x3.5 μm and with a natural emittance of 0.25 nm·rad. Most of its beamlines have the requirements for a micrometric beam size up to 50 μm. To achieve these specifications, it is necessary to work with high-end mechanical and optical elements able to guarantee the stability and precision, like the new high-dynamics monochromator under developing at LNLS, aiming a final stability of 10 nrad at the Bragg angle [2]. Moreover, besides the designing and machining steps, it is necessary to validate the mechanisms as a whole, which is achieved with precision metrology. Also, to make reliable measurements, several parameters must be taken into account, like the accuracy and uncertainties of the measurement equipment, the test setup and the environmental disturbances, which could be temperature stability, air convection and turbulence, air cleanness, atmospheric pressure and humidity, and vibration [3]. This paper describes the main design aspects of the new LNLS Metrology Building, with four rooms: Assembly 1 and Assembly 2 for general assemblies, vacuum tests and dimensional analysis, a Mechanical Metrology Lab (MML) and an Optical Metrology Lab (OML); with an advanced environmental control and vibrational stability by means of a high precision HVAC system and inertial blocks with special foundations. The building itself is an 840 m² thermally isolated shed kept within ±1,5°C. Inside there are two 100 m^2 inertial bases and, around them, the mentioned four rooms were erected. The assembly rooms have relaxed environmental requirements (±0,5°C and ±10% RH), whereas both of the metrology laboratories are more restrict (±0,1°C and ±5% RH). The optical lab is also an ISO7 cleanroom.

The authors recommend being with the poster when reading this paper, as they are complementary documents.

INERTIAL BASES

In 2013, a study was held at LNLS in order to define the Sirius tunnel floor foundation, aiming for a high level of stability. First, the site soil geophysics conditions and natural vibration were analysed. Then, two special blocks prototypes were proposed and constructed, based on the MAXIV and DLS ring floor foundation. Several vibrational tests were carried out on the prototypes. Both bases perform very well concerning external vibration attenuation, but the MAX-based performed better (faster) on dissipating vibrations generated internally, which led to the choice of this foundation type to be used at Sirius.

As vibrational issues are an important matter for metrology purposes, it was decided that the LNLS metrology building would be erected around these inertial bases, being the assembly rooms around the DLS-based floor and the metrology laboratories around the MAXIV-based foundation.

CONCEPT

The LNLS Metrology Building was designed following a layer-based architecture, in which the outer layers have a proper environmental control that contributes for the stability of the inner ones. The goal of this architecture is to provide the laboratories (inner layers) a highly stable environment, minimizing the influence of the large thermal and humidity variations that may naturally occur outside the building. There are three layers: the machine room (MR), the building itself and the laboratories, that can be seen in Figure 1. Each layer has one or more rooms controlled by independent air handling units (AHUs). The environmental requisites for each room are presented in Table 1:

Table 1: Environmental Parameters

Room	T [°C]	RH [%]	Clean Room Class
Building	23±1.5	-	-
Assembly 1	22±1.0	50±10	-
Assembly 2	22±0.5	50±10	-
Mech. Metrology	22±0.1	50±5	-
Gowning Room and Buffers	22±0.1	50±5	ISO 8
Opt. Metrology	22±0.1	50±5	ISO 7

* Work supported by the Brazilian Ministry of Science, Technology, Innovation and Communication
† henrique.oliveira@lnls.br

ISBN: 978-3-95450-188-5 doi:10.18429/JACoW-MEDSI2016-MOPE09

PRELIMINARY DESIGN AND TEST OF DAMPING MECHANISM FOR REDUCING VIBRATION OF TPS SR VACUUM CHAMBER

K. H. Hsu†, H.C. Ho, C.K.Kuan, C.M. Cheng, W.Y. Lai, S.Y. Perng, T.C. Tseng, D.G. Huang, M.L. Chen, C.J. Lin, H.S. Wang, National Synchrotron Radiation Research Center, Hsinchu, Taiwan (R.O.C)

Abstract

Since flow-induced vibration of vacuum chamber effects of the stability of the electron beam storage ring in Taiwan Photon Source (TPS), a damping mechanism was designed and installed to reduce vibration. The damping mechanism is composed of a clamper of vacuum chamber, a fixed fixture on the girder and a sandwiched stainless steel support with damping materials inside. Different kinds of materials were applied in the damping mechanism for vacuum chamber. The vibration of vacuum chamber were obtained and compared. The design and vibration measurement results of damping mechanism for vacuum chamber are presented in this paper.

INTRODUCTION

Taiwan Photon Source (TPS), a third-generation accelerator, was constructed with a circumference of 518.4m with 24 girder magnet assembled (GMA). It reached its goal of 500mA in 2015. However, it was found that the vibration of vacuum chamber is major especially in the upstream of the dipole magnets. The source of vacuum chamber vibration are thought to be generated by cooling water passing through the pipe as shown in figure 1.The vibration of vacuum chamber affect the motion of electron beam due to eddy current effect [1]. In order to reduce the vibration of vacuum chamber, the damping mechanism was designed.

Figure 1: cooling pipe of vacuum chamber.

DESIGN OF DAMPING MECHANISM

Due to limited space between the touch sensor module and quadruple magnet on the girder, the damping mechanism is designed as a thin support as shown in figure 2 .The damping mechanism was composed of a clamper of vacuum chamber, a fixed fixture on the girder and a sandwiched stainless steel support with damping material inside. The clamper is designed to clamp the vacuum chamber with two M8 bolts with two sets of screws to adjust the vacuum chamber from the top surface. The fixture is fixed on the girder with two M16 bolts, and linked with the stainless steel sandwiched support with three m8 bolts. The thickness of stainless steel is 2mm. The sandwiched stainless are mounted with six M8 bolts with damping material inside. The six bolts are fastened lightly at the last step of assembling the damping mechanism in order to prevent from deforming the vacuum chamber.

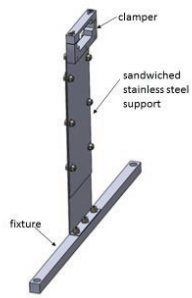

Figure 2: Design of damping mechanism for vacuum chamber.

MATERIALS IN DAMPING MECHANISM

Since it is difficult to obtain commercial passive damping material in Taiwan, only 3 types of material applied in the damping mechanism were chosen to study the performance of vibration reduction. These materials for our test are listed in Table 1 and Figure 3.

Table 1: Testing Materials

Material	Thickness (mm)	Loss factor	Storage module(Mpa)
3M ISD 112	0.127	1.0	0.22
Nitto D-300N	1.5	N/A	N/A
3M 4026	1.6	N/A	N/A

Figure 3: Different materials (from right: 3M ISD112, Nitto D-300N and 3M 4026).

3M ISD112, a kind of viscoelastic damping polymers, is used in many engineering designs to reduce vi-

† khhsu@nsrrc.org.tw

ISBN: 978-3-95450-188-5 doi:10.18429/JACoW-MEDSI2016-MOPE10

DYNAMIC ANALYSIS AND MEASUREMENT OF GROUND MOTION FOR THE SOLARIS - NATIONAL SYNCHROTRON RADIATION CENTRE IN CRACOW

D. Ziemianski†, Cracow University of Technology, Cracow, Poland
M. Nowak[1], National Synchrotron Radiation Centre SOLARIS, Cracow, Poland

Abstract

The paper presents the results of the ground motion measurements and dynamic analysis performed in The Polish synchrotron radiation facility Solaris. The analysis has been carried out within the framework of the installation experimentals lines inside SOLARIS bilding and accelerator tunnel. The equipment used in this study consists of 4 seismic, high sensitivity, ceramic flexural ICP accelerometer. Models 393B31. (PCB) , which performed measurements in one vertical directions. The first analysis was to evaluate the power spectral density for each sensors and event. The power spectral density is calculated from the auto power spectrum. The power spectral density shows a typical curve with the micro seismic peak between 0.2 and 0.4 [Hz]. It is important to point that ground vibrations should not be ignored in planning accelerator facility. All over the measurement, the RMS integrated level in the vertical direction at 1 [Hz] were calculated and presented in paper.

SENSORS

Four mono-axial seismic accelerometers were used to measure the ground motion, with a sensitivity of about 1000 [mV/m/s2].The mass of each transducer is 635 [g] and 771[g] (PCB 393831, ENDEVCO 86). The usable frequency range of a sensor is from about 0.1 Hz up to 1/3 to 1/2 of the natural resonance frequency (700/370 [Hz]). In order to increase the frequency, either the stiffness should be increased or the mass decreased. Since decreasing mass also decreases sensitivity, increasing stiffness is preferable. In most cases, a combination of the two approaches is required.

The accelerometers were glued on the floor with wax. The natural frequency of an umounted sensor is different from that of a mounted sensor, because the mounted sensor has a stiffness determined by the stiffness of the structure in which it is mounted. Attaching the sensor to a structure can lower the natural frequency by a substantial amount.

† dziemianski@pk.edu.pl

EVOLUATION OF ACCELEROMETER

In addition to seismometers, seismic accelerometers can be a suitable motion transducer for the SOLARIS measurement. The signal and noise of two different seismic accelerometers has been evaluated. These are PCB393831 (Figure 1) and Endevco Model 86 (Figure 2).

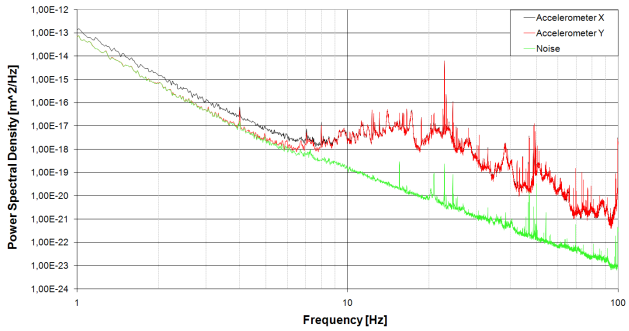

Figure 1: Integrated RMS signal and noise PCB393831.

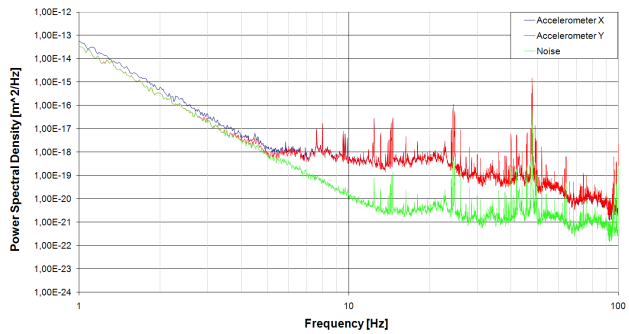

Figure 2: Integrated RMS signal and noise Endevco Model 86.

Two curves show that all accelerometers tested are able to measure above 7 Hz according to the signal to noise ratio. For the SOLARIS measurement this is not sufficient. The motion should be measured down to 1 Hz. However, seismic accelerometers can be used as a supplement to seismometers at high frequencies.

INTEGRATED RMS VALUES

Integrated RMS is used to sum up the total vibration in a spectrum. As the name indicates it give the RMS (Root Mean Square) value of the total vibration.

$$\sigma_{\omega} = \sqrt{\sum_{k_1}^{k_2} \Phi_{\omega}(v)\, dv} \qquad (1)$$

ISBN: 978-3-95450-188-5 doi:10.18429/JACoW-MEDSI2016-MOPE11

PRELIMINARY ACTIVE VIBRATION ELIMINATION STUDY OF THE TPS GIRDER SYSTEM

T.C. Tseng, S.Y. Perng, H.S. Wang, K.H. Hsu,W.Y. Lai, M.L. Chen, H.C. Ho, C.J. Lin, D.G. Huang, C.W. Tsai, C.K. Kuan, National Synchrotron Radiation Research Center, Hsinchu, Taiwan

Abstract

Taiwan Photon Source (TPS) had delivered the first synchrotron light on the last day of 2014 and is to open to the users from September 2016 after one and half years of commissioning and insertion devices installation. However, the instability is still an obvious problem to the beam quality and the deviation amplification factor of the magnets to the electron beam plays an important contribution role. Since the magnets are firmly installed on the girders and the contribution is mainly transferred from the girder vibration. This study tries to eliminate the obvious vibration frequencies amplitude exerted on the girder from outside sources such as the utility system with the PZT actuators installed on the locking wedges between girder and pedestals. By the amplitude and inverse phase searching iteration, some vibration frequency peaks in phase domain can be eliminated and the instability is also reduced.

INTRODUCTION

The Taiwan Photon Source (TPS) storage ring began the installation at Oct. 2013 as shown in the Figure 1 and had delivered the first synchrotron light on the last day of 2014[1]. After one and half years of commissioning and insertion devices installation, TPS is scheduled to open to the users from September 2016.

However, the instability is still an obvious problem to the beam quality and the deviation amplification factor of the magnets to the electron beam plays an important contribution role[2]. Since the magnets are firmly installed on the girders and the contribution is mainly transferred from the girder vibration.

In order to align the girders precisely and quickly with less manpower, an automatic-tuning girder system was proposed and fulfilled[3,4,5]. This girder system showed prominent adjustability and stability[6]. However, due to the heavy load of magnets the natural frequency as showed in Figure 2 is still not high enough although a locking system has applied. From the vibration spectrum inspection on the girder set and ground, there are frequency peaks other than the natural frequencies from outside sources such as the utility system as shown in the Figure 3.

This preliminary study tries to show the ability to eliminate the obvious vibration frequencies amplitude exerted on the girder system from outside sources. And eventually an active system will be set up to improve the stability.

Figure 1: TPS Storage ring bending section.

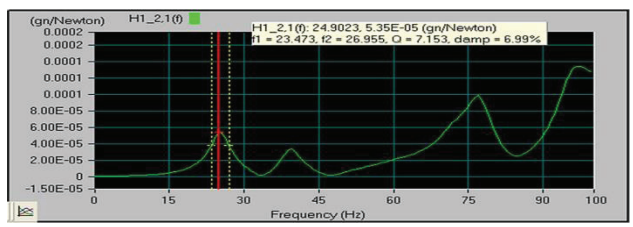

Figure 2: Natural frequency of one girder set with locking system.

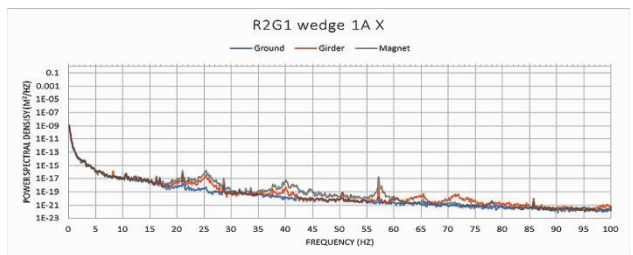

Figure 3: Vibration spectrum measurement around a girder set.

TESTING GIRDER SETUP

An extra testing girder set had been installed at the TPS inner ring lab for the preliminary study instead of the storage girder for convenient. The TPS storage ring girder configuration is shown as in Figure 4. Two modified locking wedges with PZT modular as in Figure 5 are installed at the same side of outside two pedestals as the anti-vibration actuators.

Two 3-axes PCB 356B18 accelerometers are placed on the girder surface top of the outside pedestals. These accelerometers serve as the monitors at the preliminary study stage and will be the feedback sensors for the active system.

A computer with labview program was prepared to control the system. The accelerometer signals are received

ISBN: 978-3-95450-188-5 doi:10.18429/JACoW-MEDSI2016-MOPE13

THE 20M/S CERN FAST VACUUM WIRE SCANNER CONCEPTUAL DESIGN AND IMPLEMENTATION

J. Herranz†, Proactive Research and Development, Barcelona, Spain
W.Andreazza, N.Chritin, B. Dehning, J. Emery, D.Gudkov, P.Magagnin, S.Samuelsson
J.L. Sirvent Blasco, R. Venness, CERN, Geneva, Switzerland
A.Barjau[1], Universitat Politècnica de Catalunya, Barcelona, Spain

Abstract

In the next years the luminosity of the LHC will be significantly increased. Therefore a much higher accuracy of beam profile measurement than actually achievable by the current wire scanner is required. The new performance demands a wire travelling speed up to 20 m/s and a position measurement accuracy of the order of 1 µm. In order to minimize the error source of the wire position measurement, a challenging concept has been developed which consists of the placement of the motor rotor and the angular position sensor in vacuum. The implementation of this new concept requires the use of a magnetic brake, hybrid vacuum bearings, the design and production of very thin (<0.5mm) wall vacuum chamber regions and the production of titanium components by 3D additive technologies. The implementation of this new concept has required different optimization processes as the structural optimization under dynamic load of the most critical rotating elements or the optimization of the control system and the motion pattern. This contribution gives an overview of the new device design and shows the different technical solution applied to develop the new concept in a successful way.

INTRODUCTION

A wire scanner (Fig. 1) is an electro-mechanical device which measures the transverse beam density profile of a particle beam by means of moving a thin wire across the beam in an intermittent manner. As the wire passes through the beam the interaction generates a cascade of secondary particles. These are intercepted by a scintillator, which couples the photons generated by the incident particle to a photomultiplier (PMT), which provides an electrical signal proportional to the incident photon flux.

The wire is stretched by a fork directly mounted on a shaft. The wire, fork and shaft are located in a vacuum chamber while the actuator is outside that chamber. The actuator provides a motion pattern consisting of three distinct phases (acceleration, constant speed and deceleration) fulfilling a set of requirements in order to achieve a suitable wire speed and position at beam crossing. Therefore the wire is crossing the beam in motion and consequently subjected to dynamic effects.

The strong peak acceleration in the motion pattern induces deflections and vibrations on the measurement chain (shaft, fork and wire) [1], which result in discrepancies between the true position of the wire and the position measured by the position sensor (Fig. 2).

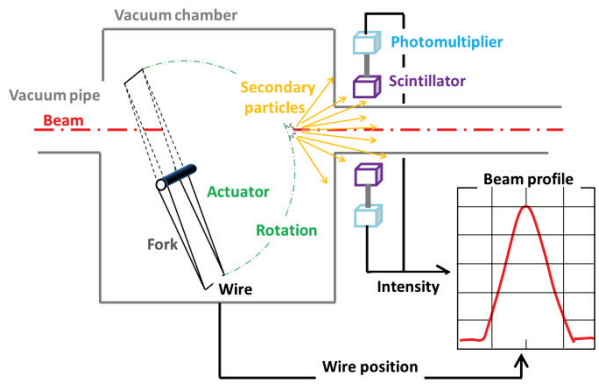

Figure 1: Illustration of the rotating wire scanner instrument.

Errors on the wire position when intersecting the beam have a direct consequence on the profile and position measurement accuracy. Thus, identifying and minimizing the uncertainties and error sources is a priority [2].

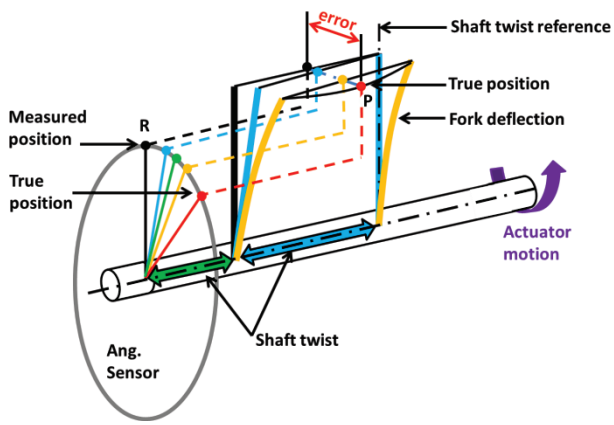

Figure 2: Deflections of the measurement chain for a rotating wire scanner.

The measurement requirement of the transverse beam distribution in the LHC rings [3] established the maximum uncertainty for the beam size determination for the LHC beam to be 1.8%. Minimum LHC beam size is in the range of 160 µm therefore the uncertainty in the beam size determination by the wire scanner has to be lower than 2.8 µm.

Experimental studies have been performed in order to determine wire damage limits due to the beam-wire energy deposition [4]. The conclusions of these studies advocate a wire traveling speed on the range of 20m/s.

†jherranz@proactiverd.com

ISBN: 978-3-95450-188-5 doi:10.18429/JACoW-MEDSI2016-MOPE15

CAM MOVER ALIGNMENT SYSTEM POSITIONING WITH WIRE POSITION SENSOR FEEDBACK FOR CLIC

J. Kemppinen[1, *], Z. Kostka, H. Mainaud Durand, CERN, 1211 Geneva 23, Switzerland
[1]also at Institute of Machine Tools and Manufacturing, ETH Zürich, Zürich, Switzerland

Abstract

Compact Linear Collider (CLIC) is a study of an electron-positron collider with nominal energy of 3 TeV and luminosity of $2 \cdot 10^{34}$ cm^{-2}s^{-1}. The luminosity goal leads to stringent alignment requirements for single quadrupole magnets. Vertical and lateral offset deviations with regards to a given orbit reference in both ends of a quadrupole shall be below 1 µm and quadrupole roll deviation shall be below 100 µrad. Translation in the direction of particle beam is not controlled but mechanically locked.

A parallel kinematic platform based on cam movers was chosen as system for detailed studies. Earlier studies have shown that cam movers can reach the CLIC requirements through an iterative process. The paper presents new modular off-the-shelf control electronics and software including three optional positioning algorithms based on iterations as well as a more advanced algorithm which can reach target position in one movement. The advanced algorithm reads wire position sensors (WPS), calculates quadrupole orientation based on the readings and updates the remaining trajectory during motion. All of the optional positioning methods reach the CLIC positioning requirements within minutes.

INTRODUCTION

CLIC final stage nominal energy is so high that two 21-km-long main linacs are needed, even though a very high acceleration of 100 MV/m is foreseen. Both main linacs are composed of 2.01-m-long modules. The modules are composed of either accelerating structures (AS), main beam quadrupoles (MBQ) or a combination of the two. There are four different types of MBQ which differ from each other only by length. Type 1 is the shortest and type 4 is the longest MBQ. The lengths are 420 mm, 920 mm, 1420 mm and 1915 mm. [1, pp. 393]

Each MBQ is equipped with a beam position monitor (BPM). In order to reach the CLIC luminosity target, all MBQ magnetic centres have to be within 17 µm and all BPMs within 14 µm from straight line fit on any sliding window of 200 m along the linacs, as shown in Fig. 1. The requirements include uncertainties related to linking the MBQ magnetic centre to the alignment sensors, uncertainties of the alignment sensors themselves as well as positioning accuracy of the alignment stage of a single MBQ. The maximum contribution of single MBQ misalignment is defined as ± 1 µm in transversal (x) and vertical (y) offset with regards to a given orbit reference with ± 3 mm travel in each end of the MBQ. In addition, maximum deviation in rotation around the beam (roll) is 100 µrad.

* Juha.Kemppinen@cern.ch

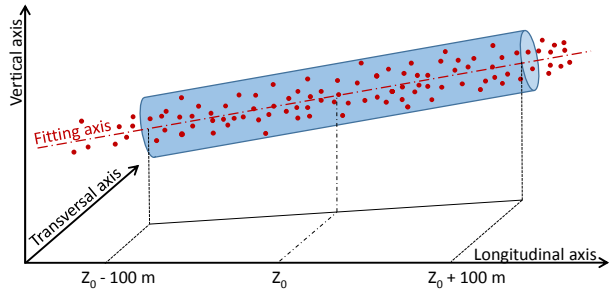

Figure 1: Objectives of CLIC active pre-alignment. [1, pp. 602]

It was demonstrated in an earlier study that the CLIC positioning requirement is reached when a mock-up girder with dummy weights, simulating type 4 MBQ and stabilisation system, is aligned using a parallel kinematics machine (PKM) based on cam movers [2]. In this paper, the same PKM and girder are used but the control electronics have been replaced. The new electronics allowed more advanced motion control. Four different positioning algorithms were developed. They are presented and compared.

The type 4 cam movers and the test setup are presented in the next section. Then, the new control electronics are introduced. Next, the positioning algorithms are described, followed by test results and comparison. Finally, conclusions are drawn.

TEST SETUP

Left side of Fig. 2 shows CLIC type 4 MBQ together with a system that stabilizes its mechanical vibrations. The combination weighs 570 kg. It is mounted on five cam movers which control five degrees of freedom (DOF). Only translation in the direction of beam is not controlled but rather blocked mechanically. The five DOFs are measured redundantly with two stretched wires and two wire position sensors (WPS) around each wire, manufactured by Fogale Nanotech and measuring both x- and y-offsets with 0.1 µm resolution.

Actual type 4 MBQ prototype together with its stabilization system has not been built. Therefore, a mock-up girder was used in the alignment study. Right side of Fig. 2 shows the girder, mounted on CLIC type 4 cam movers (ZCM), manufactured by ZTS VVU Kosice. The same setup was used also previous study [2]. The girder weighs 185 kg. In the previous study, 590 kg of dummy weights were installed on top of the girder, resulting in total load of 775 kg and it was seen to make positioning more difficult. This time, only the girder was installed due to lack of time. Two stretched wires and four WPS sensors are used to measure the girder position.

ISBN: 978-3-95450-188-5 doi:10.18429/JACoW-MEDSI2016-MOPE16

DEVELOPMENT OF THE RIXS MANIPULATOR

H.Joehri†, Leonard Nue, Thorsten Schmitt, Christoph Hess, Luc Patthey,

Sebastian Sonderegger, Paul Scherrer Institut, Villigen, Switzerland

Abstract

The RIXS Manipulator (RIXS = Resonant Inelastic X-ray Scattering) is a further development of the Carving Manipulator.

The carving manipulator has six independent degrees of freedom (three translations and three rotations). All three rotations are exactly in the middle of the sample surface.

The head of the manipulator is in UHV and the sample can be cooled down to 14K.

For the RIXS manipulator there is a new requirement to have a field of view from 0 – 180°. There are mainly two parts in the carving manipulator that set the probe in the shadow of the beam at small angles.

- A bellow
- The bearings

To solve these problems we shifted the bellow behind the pivot point. This gives some strange movements of the bellows and we had to analyse this in a separate test installation.

For the bearings, we developed a goniometer bearing with ceramic bearing shells.

Meanwhile the RIXS manipulator is implemented and in routine operation.

CARVING MANIPULATOR

The RIXS manipulator is a further development of the carving manipulator which is used to position solid samples. It has six degrees of freedom and the kinematics is designed in a way that all tree rotations can be executed without moving the center of the sample (Figure 1).

The head is in a vacuum chamber and the sample can be cooled down to 14°K.

All motors are outside of the vacuum chamber. The rotation of the sample and the movement of the tilt angle are transmitted into the vacuum.

The transmission is realized by shafts and gears (Fig 2).

For the rotation of the sample, one step of the transmission is done by a bellow (Figure 3)

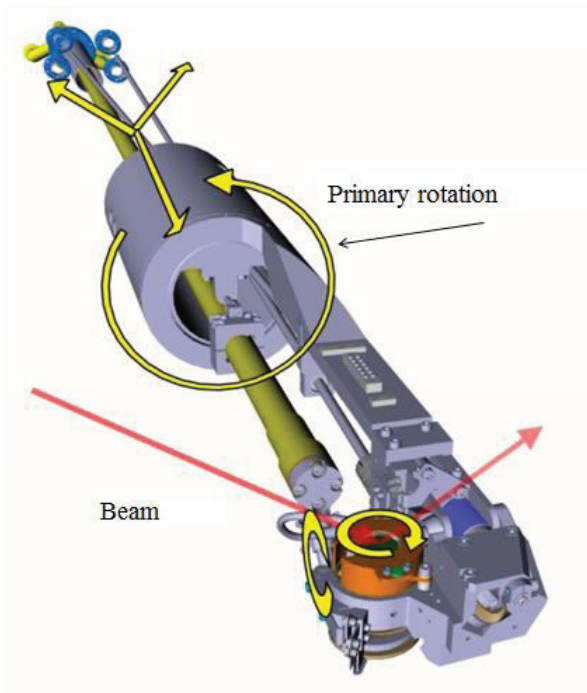

Figure 1: Carving manipulator with 6 degrees of freedom.

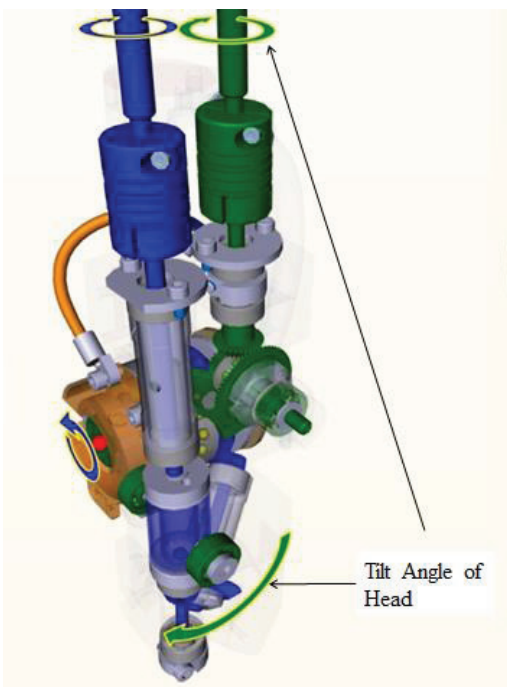

Figure 2: Transmission of sample-rotation (blue) and tilt angle of head (green).

† haimo.joehri@psi.ch

ISBN: 978-3-95450-188-5 doi:10.18429/JACoW-MEDSI2016-MOPE17

OCTOGLIDE – TABLE POSITIONING DEVICE FOR DIFFRACTION APPLICATIONS

G. Olea†, N. Huber, HUBER Diffraction GmbH & Co.KG, Rimsting, Germany

Abstract

A new Table Positioning Device (TPD) for high precision and heavy load manipulations has been developed. Conceived as an alternative to the precision hexapods, it fulfils the gap of sample (and/or, instruments) positioning in smaller (height) available working spaces of synchrotron Diffractometers (Dm). The concept is based on a Redundant Parallel Kinematic Structure (Rd-PKS) with four (4) legs having 2dof active joints (actuators). In the Proof of Functionality (PoF) step, a stacked solution has been adopted for the actuators' design using precision XY translation Positioning units (Pu). The symmetrically 6-4(**PP**)PS mechanism – OCTOGLIDE(OG) having eight (8) gliding actuators (**P**) is implying also a pair of wedges–Elevation (El) and socket/ball–Guiding (G) Pu, as passive joints (P and S) forming one of the Positioning modules (Pm). Spatial positions in the working space can be reached without any singularities and planar motions along X or Y axis performed very intuitively with only some of the actuators (decoupled) motions. The first tests of the prototype are revealing both, high precision geometry of motion (straightness, flatness, etc.) and stiffness capabilities.

INTRODUCTION

Diffraction using standard or advanced X-ray methods is still the most common techniques to investigate the structure of various materials [1]. In the synchrotron case, the dedicated machines – Diffractometers (Dm) have been built in a large variety to fulfil the specific requirements (NEWPORT, HUBER, KOHZU, etc). Sometimes, these requirements implied the use of special environmental conditions' instruments. They could be sophisticated, large in size and heavy; but, must be manipulated with high precision (i.e. I07/DLS [2]), too. In order to comply with the actual existent space of standard available Dm machines, the designers of positioning devices must adapt. Till now, the serial stacked solution has been largely used. Each of the motion axes – X, Y and/or Z (translation and/or rotations) has been materialized through standard independent stages to pose the sample (and, instrument) in the right position. However, in the case of more than 3 dof, the available space cannot be enough for packing all axes, or doing the necessary tasks-especially, variable distance rotations around Dm - Center of Rotation(CoR) point, which in this case is fixed. Precision Hexapods has been foreseen as next solution [3]. By being more compact, they are precise and able to freely choose the pivot point (P). However, when the combination of the specifications is including heavy load, and appreciable rotation distance (dP), the design of the products could be a challenge [4], especially the height (250mm). In order to fulfil the gap, a new product has been developed. The specificity of its kinematics, design and performance are now presented.

† go@xhuber.com

KINEMATICS

Topology

The new Table Positioning Device (TPD) is based on a more general parallel kinematic (PK) [5] topology having four (4) legs. This QUADROPOD (QP) family has a good natural static stability, being perfect adapted to the common shape of a working table. With all the actuators at the base, the 6-4(**2**)13 structure is a redundant one (Rd=2) which can be an advantage (power). By choosing DD (or, in-parallel) actuated joints, the dynamic capabilities will increase [6], too.

Mechanism

However, the Figure 1 shows a TPD kinematic structure with 2dof active joints ($\mathbf{P_iP_{i+4}}$, i=1…4) stacked on two levels (i,i+4). In the Prove of Functionality (PoF) step, the standard (electromechanically) motorized stages were an easy way of implementation and the motor / screw mechanical principle (stability) another one. 6-4(**PP**)PS mechanism (6-dof, PPPS-kinematic chains, P-prismatic/linear and S-spherical joints) can be seen as composed from two pair of orthogonal arranged kinematic chains (K_i,K_{i+2}, i=1,2), each having a pair of active joints with motion axis perpendicular on each other ($\mathbf{P_i \perp P_{i+4}}$) and parallel on the opposed ones($\mathbf{P_i \parallel P_{i+2}}$).

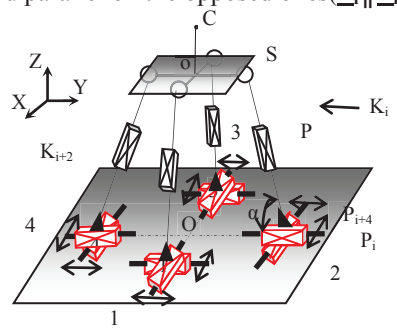

Figure 1: Mechanism kinematics.

By this symmetric arrangement of the eight (8) planar sliding/gliding actuators (OCTOGLIDE), together with the specificity of the passive joints on the next level (P, α

Table 1: Basic Motions

Motion	Actuation	Ki
X	P_i(i=2,4)P_{i+4}(i=1,3)	2
Y	P_i(i=1,3)P_{i+4}(i=2,4)	2
Z	P_{i+4}(i=1,...,4)*	2

* ±X & ±Y sign should apply.

ISBN: 978-3-95450-188-5 doi:10.18429/JACoW-MEDSI2016-MOPE18

REAL-TIME MOTOR CONTROL SYSTEM FOR BEAMLINES

Chia-Feng Chang, NSRRC, 101 Hsin-Ann Road, Hsinchu 300, Taiwan

Abstract

To improve the stability and accuracy of motor control system for Beamline, the beamline with motor adjustment mechanism collocates with the real-time firmware motor control system through the high-definition motor mechanism. Because the real-time motor control system doesn't need to be connected with the computer for a long time, it improves the speed, stability and accuracy of closed loop operation thus promote the controlling ability of motor. As a result, the real-time motor control system will improve the stability and accuracy of the entire motor control system with beamline.

INTRODUCTION

Closed-loop control is a vital part of a control system. The parameters of closed-loop control and the advantage and disadvantage of an analog input/output system will lay influence on the control system results. This text is designed to discuss about the applications for Closed-loop control and analog input/output system, in order to enhance the stability and accuracy of beamline motor control system. Consequently, we adopt analog input/output system, FPGA and closed-loop control for design.

Because the stepper motor equipped with a reducer can analyze mobile platform to 10 nanometers per stepper, with FPGA accompanied to simultaneously trigger the activation of an analog input/output system, the addition of a closed-loop control mode firmware into this hardware structure can enhance the stability of the beamline motor system, and the convenience of real-time adjustment against stability. Thus, the beamline control system will be about stability, accuracy and convenience.

SYSTEM ARCHITECTURE

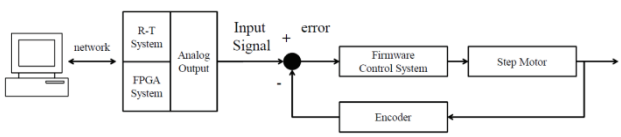

Figure 1: Close-loop Control architecture of Motor control system.

The control system structure in this text is designed by way of R-T closed-loop control (Fig. 1), with the analog input/output module acting as the reading and processing center, and FPGA module and firmware controllers acting as the hardware. The computer end serves to give location orders and besides, the stepper motor serves as the hardware of actual motion and the reading sensor serves to return its actual moving distance for the Encoder.

Control System Description

The hardware related to the control system in the text is composed of three portions: the first is, the computer-controlled center, including the PXI-8108 multi-core processor equipped with R-T module, the analog input/output module, FPGA module; the second is the firmware, the stepper motor control system, responsible for converting the analog output of the analog input/output module into digital forms, and use this data as motion signal; the third is Encoder, which will act according to the moving distance of motion signal after receiving that signal. The information on distance changes can be accessed the value of Encoder Count (Fig. 2).

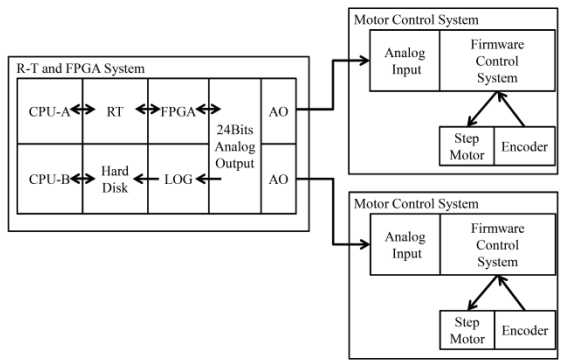

Figure 2: System architecture of R-T control system.

System Process Flow

After the system is activated, R-T System produces voltage signals by way of analog output module, and later synchronizes two sets of voltage signal through FPGA module, to avoid time errors of voltage signal. Then, the analog signals will be converted into digital ones by way of firmware. After signal processing and the user-set distance confirmed, the CPU will take the voltage signals under control, with these signals connected to the voltage input module of the motor-controlled system and the converted voltage signals for the stepper motor, at the same time the apparatus in cooperation will change the length. This way, we repeat the procedure and the closed loop control of the firmware system will continue modification of locations (Fig. 3).

ISBN: 978-3-95450-188-5 doi:10.18429/JACoW-MEDSI2016-MOPE19

MECHATRONICS CONCEPTS FOR THE NEW HIGH DYNAMICS DCM FOR SIRIUS

R. R. Geraldes†, R. M. Caliari, G. B. Z. L. Moreno, LNLS, Campinas, Brazil
M. J. C. Ronde, T. A. M. Ruijl, R. M. Schneider, MI-Partners, Eindhoven, Netherlands

Abstract

The monochromator is known to be one of the most critical optical elements of a synchrotron beamline, since it directly affects the beam quality with respect to energy and position. Naturally, the new 4th generation machines, with emittances in the range of order of 100 pm rad, require even higher stability performances, in spite of the still conflicting factors such as high power loads, power load variation, and vibration sources. A new high-dynamics DCM (Double Crystal Monochromator) is under development at the Brazilian Synchrotron Light Laboratory for the future X-ray undulator and superbend beamlines of Sirius, the new Brazilian 4th generation synchrotron [1, 2]. Aiming at an inter-crystal stability of a few tens of nrad (even during the Bragg angle motion for flyscans) and considering the limitations of the current DCM implementations, several aspects of the DCM engineering are being revisited. The system concept is chosen such that a control bandwidth in the order of 200 to 300 Hz can be achieved. This requires well-designed system dynamics, which can be realized by applying a fundamentally different architecture than that used in common DCM designs, based on the principles used in ultra-precision systems for semiconductor manufacturing. As a result, a lot of the known disturbances can be attenuated or suppressed, and internally excited modes can be effectively handled. The mechatronics concepts and analyses, including the metrological details, are shown.

INTRODUCTION

In the recent years it has become clear to the synchrotron community that the stability performance of DCMs would turn out to be one of the main bottlenecks in the overall performance of many X-ray beamlines, particularly for the new 4th generation machines, the so called Diffraction Limited Storage Rings (DLSR). Indeed, their performance is typically affected by well-known vibration sources, as the cooling system, the experimental floor and vacuum pumps in the surroundings. In addition, the self-induced disturbances, caused by servo and piezo actuators, for instance, have recently been more carefully investigated [3, 4].

Even though some incremental progress has been achieved in mitigating such disturbances, examples from applications in other industries show that the required stability could not be achieved by these incremental changes, based on the common architecture. A fundamentally different overall system approach is necessary to successfully design and realize such ultra-precision system. This work shows the mechatronics concepts used at the new high-stability DCM for Sirius [5]. More details about the full system and its specifications can be found in [6].

†renan.geraldes@lnls.br

CONCEPTUAL DESIGN

The concepts applied in the present design aim at a high-bandwidth closed-loop control, in which the main target is a control bandwidth of the inter-crystal parallelism in the order of 200 to 300 Hz. Thus, the disturbance rejection capacity of the control loop can suppress errors to the required nm levels, both in stand-still and during flyscan. By a proper design of the mechanics, the internal errors (noise sources) are minimized.

To achieve such a high closed-loop control bandwidth, a very well designed mechanical system, based on a fundamentally different dynamic architecture, is applied, and the use of voice-coil (VC) actuators is crucial. Whereas common DCM systems typically use piezo actuators or other inherently stiff actuators systems (like spindle drives), the use of inherently compliant actuators, as VCs, allows for another dynamic architecture. By this principle, the dynamics of the system can be designed to reach a significant higher closed-loop bandwidth, as only the essential mechanical components will act in the control loop. Namely, by means of a mechanical filter, established by a so-called reaction mass, or balance mass, the non-essential so-called reaction path dynamics can be filtered and, as such, be eliminated from the close-loop dynamics in the sense of control stability and disturbance amplification.

Essential for a successful design of such high-end system is predictive modelling, not only with respect to dynamics, but also thermal and other physical and mechanical aspects. Starting with the right overall architecture and taking all the essential requirements into account, predictive modelling, error-budgeting and proper design principles based on experience are crucial to design such complex high-end system. With respect to dynamics, dynamic system models, lumped-mass as well as FE-models are made. From these models, transfer functions are derived and evaluated to guide the conceptual choices and mechanical design to finally reach the required performance. Based on PSD analysis quantitative error budgeting is applied to finally predict the expected performance.

Dynamic Model and Control Tools

Figure 1 shows a schematic drawing of the DCM, which was used as the basis for a 1D-lumped-mass dynamic model of the system. The chosen degree of freedom to be used in this model was Rx, since pitch requirements are the most critical in terms of stability. Starting with such relative simple lumped-mass model, several

ISBN: 978-3-95450-188-5 doi:10.18429/JACoW-MEDSI2016-MOPE20

ULTRA STIFFNESS AND ULTRA LOW WAVING LM GUIDE

Martí Miret, THK GmbH Sucursal en España Sales Manager, Badalona, Spain

Abstract

Since the launch by THK of the first Linear Motion Guide in 1972, these products have evolved in order to overcome different challenges. A current challenge consists on improving the precision of THK's products up to a nanometric scale. Optimizing the internal design of the block of a linear guide according to concrete specifications can reduce the waving phenomenon caused by the changing load condition of the rolling body in the block. However, this optimization is not enough for improving the precision of the LM Guides in a microscopic level. Increasing the number of effective balls by reducing their diameter, expanding the length of the block and increasing the number of rows in the Guide is a solution that allows a high increase of the rigidity and the reduction of the waving to the desired level.

GEOMETRIC ACCURACY OF MOTION

Straightness and waving are two phenomenons that appear due to the movement of the table of a LM Guide.

Straightness indicates the range of how much the table movement deviates from its ideal line, since this movement should be the straight line.

Waving shows the microscopic wave where it characteristically appears in the rolling motion guidance of the infinite circulation.

As shown in Figure 1, and in order to anticipate the geometric accuracy of the LM Guide, it is important to know how much the table would deform its postural change by the load and the moment influenced to it.

Therefore, it is necessary to know the load distribution of the block interior establishing the theory of the load distribution.

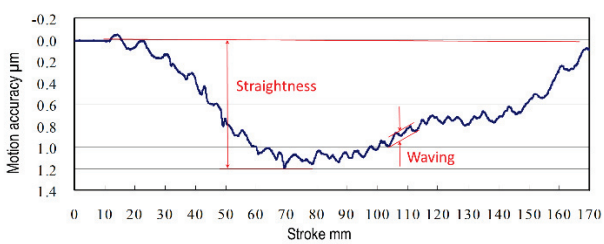

Figure 1: Geometric accuracy of motion.

THEORY OF THE LOAD DISTRIBUTION

This is the theory that consider those respective blocks illustrated in Figure 2 as a single unified system, and varies the external force affecting to the table to a postal change finally by converting the load, elastic deformation, and the contact angle variation where generated at the contact of the rolling body.

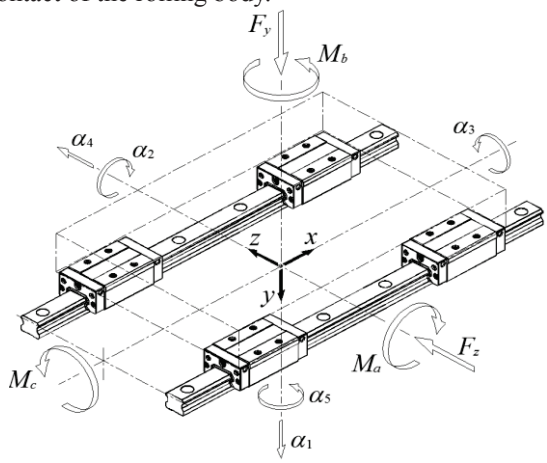

Figure 2: Theory of load distribution.

GENERATING FACTOR OF WAVING

The waving phenomenon occurs due to the movement of the LM block. By this movement, the number of effective balls (balls which are carrying the load) changes increasing and decreasing constantly (Figure 3). This causes a change of the load distribution that creates a changing balance of the load. For this reason appears the factor of waving. The difficulty of correcting this phenomenon is a problem to overcome in order to provide LM Guides of a greater accuracy for ensuring their optimal use in high performance machines.

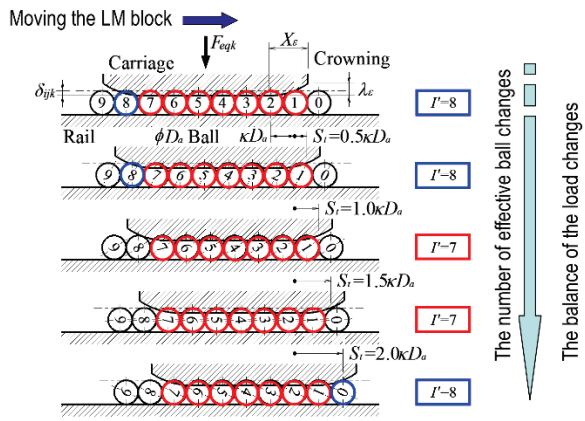

Figure 3: The factor of waving.

OPTIMIZED DESIGN

The initial solution for minimizing the waving consists on determining the optimized design of the block interior for meeting the clients specifications.

ISBN: 978-3-95450-188-5 doi:10.18429/JACoW-MEDSI2016-MOPE22

MECHANICAL DESIGN OF THE MID SPLIT-AND-DELAY LINE AT THE EUROPEAN XFEL

B. Friedrich[1,2], T. Noll[1], W. Lu[3], T. Roth[3], A. Madsen[3], S. Eisebitt[1,2]
[1] Max-Born-Institut, Berlin, Germany, [2] Technische Universität Berlin, Berlin, Germany,
[3] European XFEL, Schenefeld, Germany

Abstract

A new split-and-delay line (SDL) is under development for the Materials Imaging and Dynamics (MID) end station at the European XFEL.[1] The device utilises Bragg reflection to provide pairs of X-ray pulses with an energy of (5 … 10) keV and a continuously tunable time delay of (-10 … 800) ps – thus allowing zero-crossing of the time delay. The mechanical concept features separate positioning stages for each optical element. Those are based on a serial combination of coarse motion axes and a fine alignment 6 DoF Cartesian parallel kinematics[2]. That allows to meet the contradictory demands of a fast long-range travel of up to 1000 mm and in the same time a precise alignment with a resolution in the nanometre range. Multiple laser interferometers monitor the position of the optical elements and allow an active control of their alignment. All optical elements and mechanics will be installed inside an UHV chamber, including the interferometer and about 100 stepper motors.

With this paper we present the mechanical design for the SDL. It will additionally show the design of a prototype of a positioning stage which allows extensive testing of the implemented concepts and techniques.

INTRODUCTION

The intention behind the presented project is the provision of pairs of X-ray pulses with picosecond delay times at the MID end station at the European XFEL. This is to be achieved by a SDL system, which splits the XFEL beam into two branches and merges both after delaying one branch with respect to the other branch. Osaka et al. proofed such a split and delay concept to work with an in-air system for hard X-rays and a delay times up to 220 ps [3]. Earlier, Rosecker er al. developped a SDL working at fixed energy and in air [4].

The SDL under development allows for a window-less integration into the MID beamline and thus places all mechanics into an UHV environment. The SDL is designed to work with an energy in the range of (5 … 10) keV and to achieve a continuously tunable delay time of (-10 … 800) ps. This range also covers the zero crossing of the delay time. The mechanics for the positioning of the optical elements feature a precision in the range of single nanometer and tens of nanoradians, while in the same time allows long-range travel of up to 1000 mm. Full adjustability and an efficient operation will be possible due to the motorisation of most of the controllable dimensions of freedom (DoF) and multiple monitoring and measurement systems.

GENERAL CONCEPT

Bragg reflections of silicon crystals in 220-orientation is utilized to generate the intended beam paths. This, in contrary to grazing incidence mirror optics, is working at high reflection angles, which allow a much shorter and space saving design.

The general concept of the SDL is shown in Fig. 1. It features an upper and a lower branch, in which the incoming beam is divided to by a beam splitter. Both parts of the beam are brought back together at the end of the system by a merger crystal. The two crystals in the upper branch are adjustable in position and angle in order to realise different path length and therefore different delays, and different working energies. The lower branch features two channel cuts, creating a fixed delay to allow also small negative overall delay times.

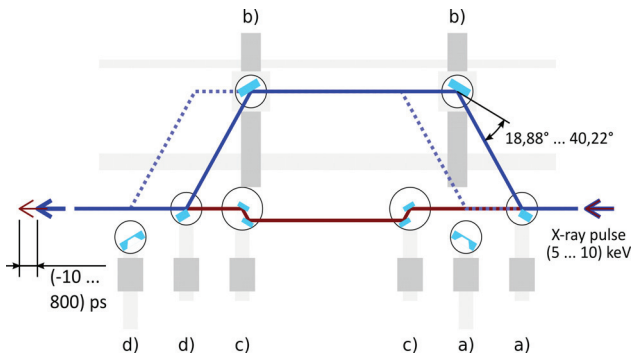

Figure 1: Conceptual view of the SDL indicating the mechanical concept. a) beam splitters; b) upper branch crystals; c) channel cuts; d) beam merger.

Two different splitter and merger stages are foreseen, either using extremely thin crystals and an intensity splitting of the X-ray beam, or the edge of a thick crystal, to split the beam geometrically. The unused version can be translated out of the X-ray beam. Moving all optical elements out of the beam allows the beam to pass through the system without any reflection, i.e. when the SDL is not required for an experiment.

In order to have a most versatile control and evaluation of the system, various measuring and monitoring systems will be integrated. This includes:

- a visible feedback laser, guided parallel to the FEL beam on dedicated mirrors, monitored by nano cameras
- Two 3-axis laser interferometers with sub-nanometre resolution, monitoring the upper branch crystals

ISBN: 978-3-95450-188-5 doi:10.18429/JACoW-MEDSI2016-MOPE23

AN ASSEMBLING CALIBRATION METHOD OF XBPM DIAMOND BLADES IN TPS

H.C. Ho, C.K.Kuan, W.Y. Lai, S.Y. Perng, T.C. Tseng, D.G. Huang,
M.L. Chen, C.J. Lin, H.S. Wang, K.H. Hsu

NSRRC,Hsinchu 30076, Tiwan, R.O.C

Abstract

Diamond blade type X-ray Beam Position Monitors (XBPM) were adopted to monitor photon position at the beamline front-end in Taiwan Photon Source (TPS) [1]. Due to the thin thickness (125um) and fragile characteristic, the assembling precision of the diamond blades is difficult to measure and influences the accuracy of monitor. A non-contact method was thus developed by using a LED laser with telecentric objective lens and a CCD-array to calibrate the diamond blades assembling configuration within micrometer accuracy. According to the measurement results, XBPM can be correlated to four fiducial points for survey network. This paper describes this method and calibrating results in detail.

INTRODUCTION

XBPM are adopted in synchrotron machine to monitor the photon beam position in beamline frontend [2]. It can eliminate controversy for beam position and stability for machine user. The blade position accuracy will influence the accuracy of the monitor. Due to the thin thickness (125um), vacuum parts and fragile characteristic, the assembling precision of the diamond blades is hard to measure. At the begging, we use non-contact method like telescope and microscope, which may have vision and projection lens error, we need to move and rotate the XBPM, XBPM 3D accuracy error will be over 0.2 mm. Now we developed a new non-contact method by using LED laser with telecentric objective lens and a CCD-array assembling configuration instead of a microscope and accuracy of 5 um. Measurement space can be minimized perfectly and measurement time can be saved. Finally, XBPM can be correlated to four fiducial points for easy survey alignment network installation.

MECHANICAL DESIGN

We hope the measurement accuracy will reach within 5 um with this CCD method and easy blades alignment. During measuring process, moving or rotating the XBPM is forbidden (XBPM weight over 15kg, 240x240 mm). Finally, XBPM measurement data can be correlated to four fiducial holes at about 1/4" for survey alignment network installation. Here is a telecentric objective lens which provides an image of the same size in the so-called telecentric range, which produces a constant accuracy [3]. The line scan camera in the receiver which measures the projected outer contour of the fiducial as shown in Figure 1.

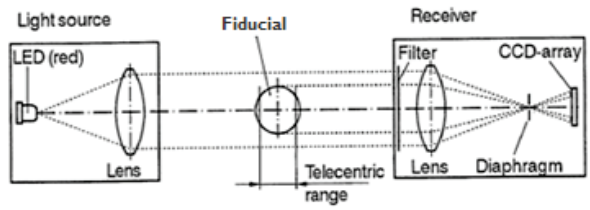

Figure 1: CCD array measurement range of 40 mm, resolution of 0.1 um, and LED wavelength of 670nm.

We make four fiducial holes on the XBPM base template, move the light source and receiver to the fiducial at about 150 mm by using sliders sliding on the rail, and mount and scan fiducial round bar contour. We can make a centre line relative to the rail movement direction by a receiver. Due to the limitation of CCD array area of 40x2 mm, fiducials round bar has a full length which was set up to 75 mm. And the round diameter Ø8 mm concentricity required 2 µm in 55 mm length relative to the hole, the 55mm full length accuracy was controlled within 2 µm. If the measurement range exceeds CCD array range, we can thus move the X-Z stage (450x400 mm travel range) in 1µm resolution. Using a rotatable arm pivot, we can rotate the light source and receiver in 90°. In vertical direction, we measure the blade by using the top surface of the fiducial as a standard point for measurement. In the horizontal direction, the blade is measured by using the side of the fiducial and a side of the blade as a standard point. Scanning step by step, we can measure the gap in the diamond blades and the fiducial centre length. Figure 2 and 3 show the vertical and horizontal sensor scanning.

ISBN: 978-3-95450-188-5 doi:10.18429/JACoW-MEDSI2016-MOPE24

THE PRECISION ADJUSTMENT HOLDER FOR MONTEL MIRRORS

Bo-Yi Chen†, Gung-Chian Yin, Shi-Hung Chang, Huang-Yeh Chen, Chien-Yu Lee, Bi-Hsuan Lin, Shao-Chin Tseng, Jian-Xing Wu, and Mau-Tsu Tang, National Synchrotron Radiation Research Center, Hsinchu 30076, Taiwan
J. Raynien Kwo, National Tsing-Hua University, Physics Department, Hsinchu 30076, Taiwan
Minghwei Hong, National Taiwan University, Physics Department, Taipei 10617, Tawian

Abstract

The focusing of X-ray nanoprobeat Taiwan Photon Source (TPS) relay upon the special designed Montel mirrors and its adjustment holder, which significantly shorten the length of beamline to 75 meters. Moreover, the focal spot size and working distance are expected to be 40 nm and 55 mm, respectively. To achieve this, the precision adjustment holder was designed and made to align Montel mirrors. The holder includes two major parts: (1) fundamental-position alignment part and (2) relative-position adjustment part.

The fundamental-position alignment part has the ability to adjust the two mirrors together in six degree of freedoms, such as X, Y, Z, pitch, roll, and yaw. These translation stages have several-tens mm travel range and nm resolution, while the rotational stages have around 40 mrad azimuthal angular range and 0.1~0.01 μrad resolution.

The relative-position adjustment part can further adjust the two mirrors to minimize the focal spot. During the pre-alignment process, one of the mirrors can be manual adjusted by micrometer heads (Mitutoyo®) in three translation directions with several mm travel range and micrometers resolution. These micrometer heads also provide this mirror three rotational degree of freedoms with sub-mrad resolution. For the further alignment in vacuum chamber, the additional four piezo-motor (PiezoMotors®) actuators can precisely adjust the other Montel mirror in the Y and Z direction with several nm resolution, and its pitch and roll with 1 urad and 0.05 urad resolution, respectively.

The precision adjustment holder will be installed in TPS-23A endstation and start commission before the end of this year.

MONTEL MIRRORS FOR HARD X-RAY FOCUSING

The Montel mirrors were adopted to focus the hard x-ray down to hundreds even tens of nano-meters in synchrotron beamlines[1-4]. There many nano-focusing optics, such as K-B mirror, Zone Plate, refractive lens, and Montel KB mirror. Different optics have different focusing ability.

According to the study done by Gene E Ice et. al [1], The numerical aperture is limited by the critical angles of the mirrors. Besides, the numerical aperture can be enlarged if more reflections are accompanied for focusing. Therefore, it is very clear that the numerical aperture is enlarged by factor of root 2 theoretically, because the Montel mirrors consists two reflections from identical two plane-ellipse mirrors close to each other. The focus principle is to hit one side of the mirror than the other side.

The Montel KB mirror has better chromatic dependence, higher flux and longer working distance. For the application in TPS-23A, we adapt the Montel mirror as the nano-focusing optics, which gives a larger numerical aperture as well as higher flux than conventional K-Bs.

TPS-23A BEAMLINE

There are two horizontal focusing mirrors and one horizontal DCM in the beamline. In order to preserve the coherent in vertical direction, there no other focusing optics before montel KB mirrors, and it is windowless. Finally, we use montel KB mirror to focus the beam down to 40 nm, and the photon flux can be larger than ten to the power of 10. The length of this beam line is less than 70 m. In order to fully use the symmetrical manner of the Montel mirrors, the horizontal optics is more complicated. The HFM1 focuses the horizontal beam at slits3 and he HFM2 defocuses and pull back the source back to the center of the undulator. With this plan, the source becomes a symmetrical source. The sketch of TPS-23A is shown in Fig. 1.

According to the ray tracing simulation results, if the beam energy is 10 keV and average reflection coefficient is 0.83, the source is 65m up stream to the mirrors, the source size is 12.5 μm x 12.5μm, and the source divergence is 6μrad x 6μrad, we can found that the final spot size is around 40 nm and the divergence is 6.29 mrad. The flux is estimated to be 2x1010 Photon/second.

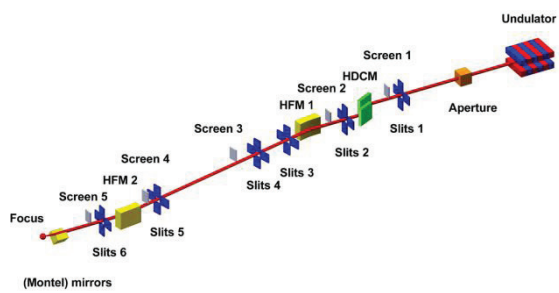

Figure 1: The beamline sketch of TPS-23A.

MONTEL MIRRORS OF TPS-23A

The specification of Montel mirrors adopted in TPS-23A is described as following. The length of the mirror is 110 mm, and the working distance is 55 mm. The very high demand on the slope error is 0.05 μrad, which is the best quality that can be made which is limited by the

ISBN: 978-3-95450-188-5 doi:10.18429/JACoW-MEDSI2016-MOPE26

FRONT END PHOTON SHUTTER WATER LEAK TO VACUUM AT THE CANADIAN LIGHT SOURCE

G. Henneberg*, G. Barkway, M. J. P. Adam, Canadian Light Source Inc., Saskatoon, Canada

Abstract

A leak in the Hard X-Ray MicroAnalysis (HXMA) front end (FE) Photon Shutter (PSH1) absorber was found and temporarily repaired with no delay in returning the CLS to normal operations. The leak was caused by a large amount of erosion to the interior surface of the cooling channel, due to excessive flow rates (>7.0 m/s). Similar photon shutters currently operating under similar conditions are at risk to fail (19 photon shutters in total). Due to damage they may have sustained operating under similar operating conditions, photon shutters of this design currently in service should be either examined or replaced.

INTRODUCTION

Leak Discovery & Repairs

July 2nd, 2016 Accelerator Operations and Development (AOD) discovered a vacuum event at the Canadian Light Source (CLS) for Storage Ring (SR1) cell 6. Initially, the event was believed to be a air leak located in either the SR1, Soft X-ray for Microcharacterization of Materials Beamline (SXRMB) FE, or the HXMA FE.

A collaborative decision was made to wait to find the exact location of the leak. The mechanical technicians first activated a scroll pump in an attempt to pump down the affected section. Water was discharged from the exhaust of the scroll pump, which indicated the water leak. After determining that the leak had originated in the HXMA FE, the technicians identified which components may have failed. By the afternoon, they had discovered a small pinhole leak on the absorber head of the first HXMA photon shutter (Fig. 1).

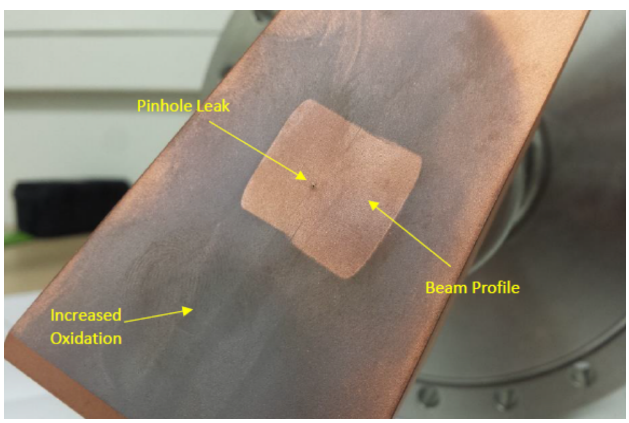

Figure 1: Illustration of the pinhole leak discovered on HXMA PSH1. Leak location is aligned precisely with water jet location of the tube in tube cooled absorber.

* grant.henneberg@lightsource.ca

HXMA Front End Photon Shutter

Estimated heat load for the absorber was found to be 200 W–300 W (for 250 mA ring current). Fortunately, a spare photon shutter previously ordered for the Industry Development, Education, Applications, and Students (IDEAS) beamline was available that satisfied the heat load requirements. The replacement was a Phase II type photon shutter. Technicians oversaw the initial bakeout of affected components (lasting four days). The electron beam was activated to further improve the vacuum quality, using four injections per day to maintain current in the SR1. Equipment testing continued until July 12th, at which point the CLS resumed regular operation. The leak delayed standard start up procedures performed by AOD at the end of the shutdown by seven days, but beam was available to users as scheduled. The PSH1 had been operational since HXMA was commissioned in 2006 (Fig. 2). This type of absorber is similar to a Advanced Photon Source (APS) design and is used to stop bend magnet radiation from the SR1 dipoles when the HXMA Insertion Device (ID) and beamline are turned off. Cooling for the component is provided by running water

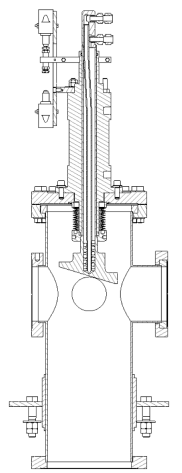

Figure 2: PSH1 absorber style from the front end location of HXMA beamline. The beam path as the absorber is shown is from left to right, with absorption of photon energy along the grazing surface of a tube in tube OFHC absorber.

through the head of the absorber. The leak developed at (or very near) the centre of the absorber's face (Fig. 1). There are six other photon shutters that employ this exact same design currently in use at CLS. There are also 12 photon shutters that are derivatives of this design. Their cooling system and operational parameters are almost identical. Therefore, it is necessary to identify why failure occurred, how it can be prevented, and/or if other components are at risk to fail.

ISBN: 978-3-95450-188-5 doi:10.18429/JACoW-MEDSI2016-MOPE27

THE INFLUENCES OF MATERIAL PROPERTIES TO MICRO DAMAGES ON VACUUM CHAMBER CF FLANGES

S. Vilcins, M. Holz, M. Lemke, D. Nölle, Chr. Wiebers, DESY, Hamburg, Germany

Abstract

The European-XFEL, a 3.3 km long X-Ray laser facility, powered by a 17.5 GeV superconducting linear accelerator, is located at DESY in Hamburg [1]. For the diagnostics ultra-high vacuum components with high mechanical precision and strict requirements on particle cleanliness had to be developed, designed and produced. For the screen system of the facility, enabling to observe the size and shape of the electron beam, massive vessels, precisely milled out of stainless steel blocks 1.4435 (316L) have been produced. For these chambers all flange-connections are milled into these blocks. This paper will report on micro damages in these integrated knife edges and will present simulations of the damage mechanisms. It will also describe the influences of material properties of two different stainless steel brands, effects on the "knife edge" due to the penetration into the gaskets as well as the non-elastic deformation of the sealing area. The dependence of tightening forces under special conditions, like the very clean conditions in particle free applications due to the non-lubricated conditions will be reported. A "cooking recipe" to avoid such micro damages will be given.

INTRODUCTION

Particle accelerators are used as standard as well as and special diagnostics, also for the European XFEL (E-XFEL) at DESY, Hamburg. A scintillation screen monitor system [2] has been designed for diagnostic purposes in particle beams. For this system two different types of special vacuum chambers have been fabricated. More than 50 vacuum chamber with weights over 50 kg have been fabricated out of massive blocks. These two versions of chambers are varied, one with five and the other with eight Conflat (CF) [3] knife edge flanges allowed attaching other diagnostic devises. In this paper the two types call type A/C and B. For type B see Fig. 1.

The biggest amounts of the chambers have to be assembled and installed in particle reduced environment in different sections of XFEL. The vacuum leak for the UHV system rate has to be below $1*10^{-10}$ mbar l/s and tightened with copper flat gaskets.

The geometry of these chambers had to be chosen so that they match the requirements of independency and stability; therefore a massive stainless steel (SST) block was used.

SST is one of the most commonly used constructional materials for vacuum chambers and other vacuum components in general. Applications like vacuum vessels in linear accelerator or storage ring facilities require ultra-high vacuum (UHV). Finding an appropriate source for the raw material in 316 LN was the first step. The dimensions of these vessels are bigger than all designs at DESY have been in the past. Since it was very difficult to find any supplier for material in 316 LN, a compromise was found to use 316 L.

The raw material was ordered according to DESY material specification for 316 L. Essential a 3.1 certification was sent before the order was placed. In this specification of DESY the boundaries of hardness are between 160 and 200 Brinell Hardness (HB). In the material certification the value for the hardness was a little bit under the minimum bounder of DESY's specifications with 158 HB. The raw material was accepted by DESY. All vacuum chambers were manufactured by outside vendors at two companies. Rest gas analysis was not specified. The final assembling has been done at DESY.

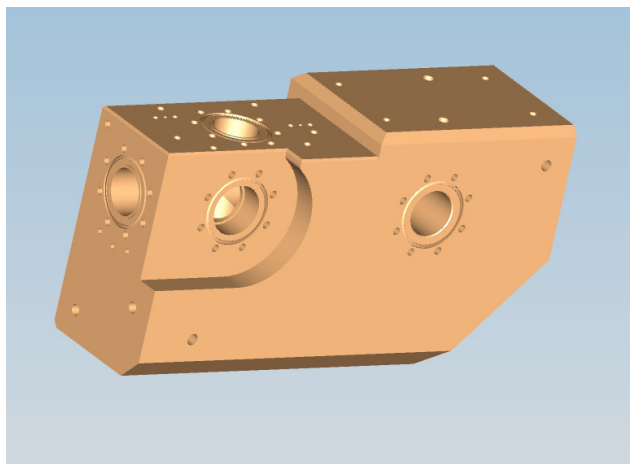

Figure 1: Show a vacuum chamber Type B with adaption ports for other diagnostic devices.

The two prototypes, one for each version, have been successfully tested under UHV conditions at DESY group Machine Diagnostic and Instrumentation (MDI).

After a European wide open call for tender the two versions were placed at two different manufactures in Germany. The cleaned and packaged chambers arrived at DESY and they had to be stored for about 1 year before final assembling. During the final assembling, in a class 5 cleanroom, cleanness problems were detected on one of the attached vacuum window. Due to these problems all chambers had to be dismounted and inspected. During this inspection by chance micro damages on the sealing areas of the CF knife edge were detected. DESY calls this appearance "orange skin" (see Fig. 2). After a few chambers have been cleaned and reassembled the final leak check had shown vacuum tightness problems.

ISBN: 978-3-95450-188-5 doi:10.18429/JACoW-MEDSI2016-MOPE28

VACUUM SYSTEM OF SESAME STORAGE RING

M. Al-Najdawi, E. Huttel, F. Makahleh, M. Shehab, H. Al-Mohammad

SESAME Light Source, P.O. Box 7, Allan 19252, Jordan

Abstract

SESAME (Synchrotron-light for Experimental Science and Applications in the Middle East) is a third-generation synchrotron light source under construction near Amman (Jordan).The storage ring has 16 Dipole arc chambers, 8 short and 8 long straight chambers. The general layout and detailed design of the vacuum chambers, crotch absorbers, RF bellows, injection and RF sections will be presented in this contribution, also the testing of the chambers prototype, bake out process and final installation.

STORAGE RING VACUUM SYSTEM

The storage ring is divided into 16 cells, each cell contains a dipole arc chamber and a straight chamber (long or short) closed by UHV RF shielded gate valve.

There are two types of the vacuum cells, an arc chamber with long straight with a total length of 9.35m and an arc chamber with short straight with a total length of 7.3 m. The overall length is 133.2 m. Lumped absorbers are used to absorb the unwanted synchrotron radiation (SR), there are four types of the absorbers based on the location they are installed.

Diode sputter ion pumps (SIP) are installed near the absorbers with an overall nominal pumping speed of 20500 l/s, also, a NEG pumps are installed near the absorber with the highest SR absorption (higher outgassing)

Valves are installed upstream and downstream of each long straight, 16 in total.

Bellows are installed upstream and downstream of each short and long straight and upstream and in addition up and downstream of the septum.

Inverted magnetron Gauges are installed one at each dipole and each long straight chamber, whereas in the RF section at each of the four cavities

Figure 1 shows the general storage ring vacuum layout and a list of the installed pumps.

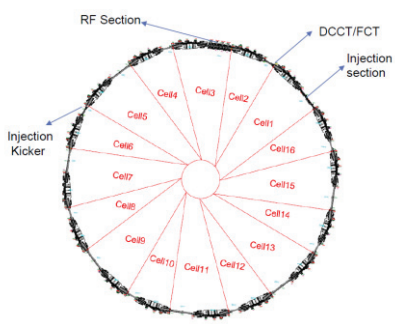

Ion pumps	105 Pumps
Dipole chamber	2 X 300L/S
	2 X 150L/S
Long Straight	3 X 150L/S
Short straight	2 X150L/S
RF Section	4 x 150L/S
NEG pumps	16
IMG	27
Dipole chamber	16
Long straight	7
RF section	4
RF Valves	16
RF Bellows	34

Figure 1: General storage ring vacuum layout.

Crotch Absorber Design

The crotch absorber design follows the same design implemented for the ANKA and SLS [1] light sources, it consist of two parts with 8.8° vertical tooth inclination and 5° horizontal tooth angle and 10mm tooth width. The thermal load has been applied in a conservative way such that the maximum power intensity on each teeth of the absorber has been applied on the whole subjected area the FWHM Area.

FEA analyses for all absorber have been done for a 2.5 GeV 400 mA e-beam; corresponding to 240 kW SR Power. The most critical absorber 2 with the tip located at 641 mm from the source point is exposed to a surface power density of 45.8 W/mm2. At this location the maximum stress is 175 MPa, the maximum strain is 0.15% and the maximum temperature is 300 °C. Figure 2 shows the FEA results for absorber 2 and Table 1 lists the parameter for all absorbers.

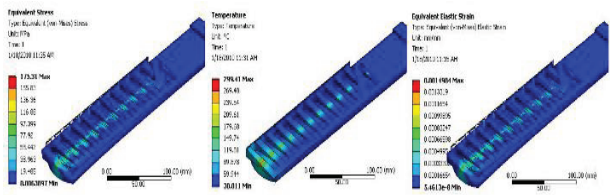

Figure 2: FEA results for absorber 2.

Table 1: Parameter of the SR Absorber

Abs.	Angle [°]	Power [kW]	Lin.Pow. Density [W/mm]	Temp. Max [°C]	Strain [%]
1	6	4.1	41	192	0.14
2	11	7.5	58	300	0.14
3	5	3.2	25	142	0.04
4	0.5	0.4	11	75	0.01

RF Shielded Bellows

The RF bellow design is similar to SLS and ALBA design with some modifications, the bellow has a compact design with a free length of 115 mm and has a sleeve made of 316L stainless steel sheet and 19 fingers made of beryllium copper sheets (0.4 mm thinness). The bellow has a cover made of aluminium; the benefit from the cover is to limit the compression and expansion of the bellow (15mm compression, 3mm expansion and ±2 mm in all transvers directions) also to protect the bellow body from any damage. Figure 3 shows the design concept of the bellow.

ISBN: 978-3-95450-188-5 doi:10.18429/JACoW-MEDSI2016-MOPE29

VACUUM SYSTEM OF HLS-II STORAGE RING*

Y. Wang, X. Pei, W. Wei, L. Fan, Y. Hong B. Zhang†,
National Synchrotron Radiation Laboratory, USTC, Hefei, China

Abstract

Hefei Light Source (HLS) has been operated for more than twenty-five years. From 2010 to 2014, the upgrading project of HLS has been carried out and the new machine is called HLS-II. The main improvement include: the emittance is reduced to 40 nm·rad, 3 new insertion devices (2 IVU and 1 EPU undulators) are added and the injection energy increases to 800 MeV. The typical life time is 300 mins at 300mA, 800 MeV. The average pressure of static and dynamic vacuum are below 2×10^{-8} Pa and 1.2×10^{-7} Pa respectively. The design, installing and commissioning of the vacuum system of the storage ring are detailed stated in in this paper.

INTRODUCTION

The 800MeV electron storage ring of the National Synchrotron Radiation Laboratory (NSRL) is a dedicated VUV and soft X-ray synchrotron radiation light source. The construction of NSRL facility began on November, 1983 and was completed in 1989. HLS comprises of 200 MeV injector, 800 MeV storage ring, 12 beamlines and 15 experimental stations by 2010. In order to supply synchrotron light with higher brightness and stability to the users, the upgrading project of HLS has been carried out during 2010-2014[1]. The main changes of the new HLS (HLS-II) include: The energy of the injector increases to 800 MeV, so the electrons can be injected to the storage ring with full energy. The lattice of the storage ring was changed from TBA to DBA. The beam emittance decreased to 40 nm·rad. A group of multifunctional sextuple magnets are employed and thus the long and short straight section are both lengthened. Five insertion device were installed in the storage ring.

LAYOUT OF THE STORAGE RING

The circumstance of the storage ring is 66.13 m, as shown in Fig. 1. It consists of four DBA cells and each cell has 2 dipoles, 4 quadrupole and 4 sextupole magnets. The synchrotron light is emitted along the direction of 0°and 15° with the beam orbit. There are 8 long straight sections and their length account for 38% of the ring. Insertion devices are located in 6 LSS. Injector and RF cavity are located in the other 2 LSS.

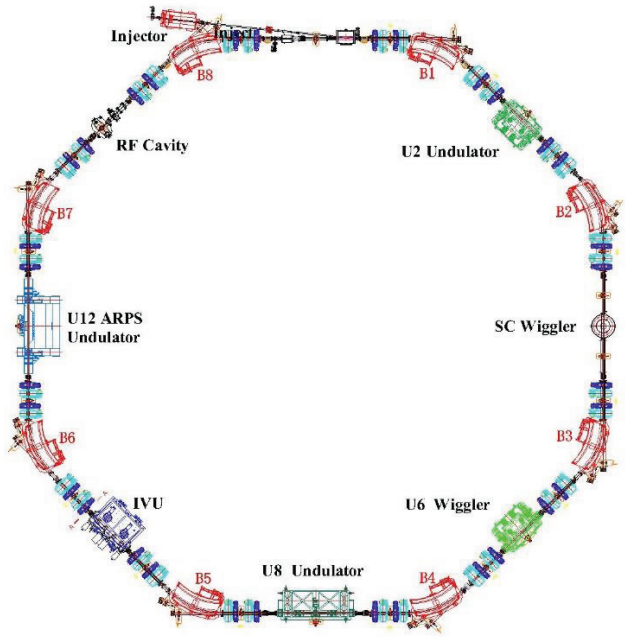

Figure 1: Layout of HLS-II storage ring.

VACUUM SYSTEM DESIGN

The storage ring's circumference is 63.66 meters. The main vacuum pipes are made of 316LN stainless steel by welding. The section is octagonal as shown in Fig.2. To reduce the surface degassing and the magnetic permeability induced by welding, the chambers are baked at 900 °C in the vacuum furnace. After this treatment, vacuum chambers of the total leak rate, outgassing rate and magnetic permeability are below 2×10^{-8} Pa L/s , 2×10^{-11} Pa L/s cm^2 and 1.02 respectively, which meet the design requirements. Considering the convenience of installing, commissioning and maintenance, 3 RF-shielded all-metal gate valves are used to separate the storage ring into three cells. 20 UHV gauges are distributed in the storage ring to monitor the vacuum and for the interlock protection system.

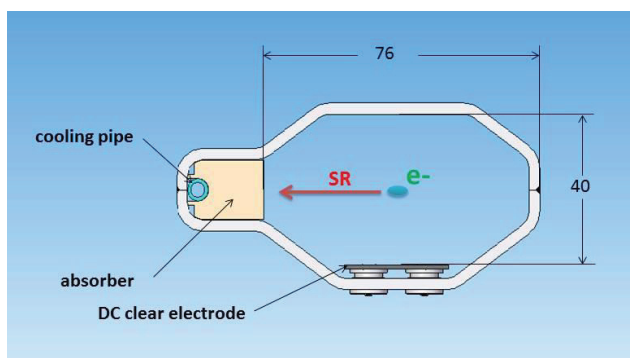

Figure 2: The section of the main vacuum pipe.

* Work supported by Chinese Academy of Sciences
† zhbo@ustc.edu.cn

ISBN: 978-3-95450-188-5 doi:10.18429/JACoW-MEDSI2016-MOPE30

THE DEVELOPMENT OF CUCRZR HIGH HEAT LOAD ABSORBER IN TPS

I. C. Sheng†, C.C. Chang, C. K. Chan, C. Shueh, L. H. Wu, National Synchrotron Radiation Research Center, HsinChu, Taiwan,
Sushil Sharma, Brookhaven National Laboratory, Upton, New York, USA

Abstract

Taiwan Photon Source (TPS) project in National Synchrotron Radiation Research Centre (NSRRC) has reached 500mA design goal. Several upgrades and design enhancements are also under development. CuCrZr copper alloy has been selected to examine its UHV compatibility, machinability and high heat load sustainability as one of the upgrade activities. Most importantly, the absorber is made entirely by CuCrZr (including two end flanges) and installed in the mid-section of double minimum of tandem EPU48 undulators to shadow beam miss-steered synchrotron radiation from upstream EPU. Both the result and fabrication time (without brazing) are promising.

INTRODUCTIONS

As to synchrotron accelerator machine, synchrotron radiation is always associated with high density power, and 99% of them are to be shadowed before it reaches beam line users. Due to its high conductivity and ultra-high vacuum (UHV) compatibility, Oxygen free high conductivity (OFHC) copper and GlidCop® are two of the commonly used materials to shadow the unneeded synchrotron power. OFHC is used to absorber lower power density synchrotron radiation whereas GlidCop® can be much higher due to its excellent mechanical material properties.

However GlidCop® is solely fabricated by the company named North American Höganäs, it is much more expensive and it is not readily available when it comes to specific sizes.

In 2013, we have considered other copper material which can replace OFHC and GlidCop®. The reason being is to marry with stainless steel, both them require brazing process, which either is time consuming or has high failure rate. We searched for couple of candidates and found out CuCrZr alloy is the right material to use due to

- It has high yield and tensile strength.
- It is much cheaper than GlidCop® and is available even in our local supply vendors.
- It can be welded with stainless steel.
- It is UHV compatibility.

As shown in Table 1, CuCrZr alloy has comparable mechanical properties with GlidCop®, with a little bit lower thermal conductivity (16% lower than that of OFHC) but its high yield and tensile strength, this alloy is worthwhile to give a try. Other accelerators have used it for undulator chamber [1].

Table 1: Material Properties

Property	**OFHC**	GlidCop®*	**Cu-CrZr**[2]
Conductivity (W/cm°K)	3.83	3.65	3.23
Thermal expansion (m/°K×10^{-6})	16.6	17	18.6
Poisson ratio	0.31	0.35	0.18
Yield strength (Gpa)	0.049-0.078	0.33	0.27-0.44
Tensile strength (Gpa)	0.215-0.254	0.42	0.37-0.47

**GlidCop-15*

In the following sections, we will present how we carry out vacuum and weld tests of CuCrZr copper alloy.

VACUUM TEST

Templates are provided for recommended software and authors are advised to use them. Please consult the individual conference help pages if questions arise.

An outgassing rate test is performed in our vacuum laboratory. The layout is shown in Figure 1.

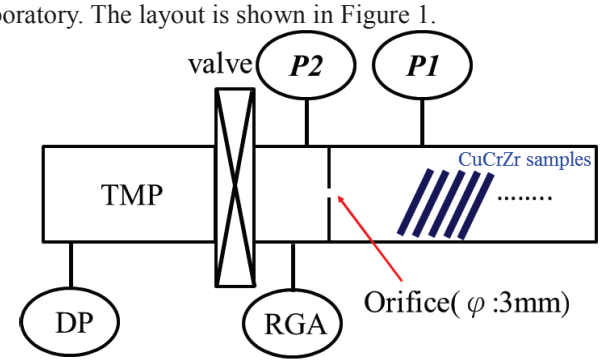

Figure 1: CuCrZr sample outgassing test layout.

The CuCrZr alloy plates has total surface of 4000 cm^2 piled up in the vacuum chamber. They are ultrasonic cleaning in Citranox®, rinsing with de-ionized water for 10 minutes, and dry with 99.9999% nitrogen. Comparing with other materials such as Al and Stainless steel, we list their outgassing rate in Table 2:

The result of outgassing rate comparing with CuCrZr, Aluminum and Stainless steel is illustrated in Figure 2:

† shengic@nsrrc.org.tw

ISBN: 978-3-95450-188-5 doi:10.18429/JACoW-MEDSI2016-MOPE31

DYNAMIC PERFORMANCE OF A SUPPORT SYSTEM FOR BBA COMPONENTS IN SXFEL

F. Gao†, Y.X.Dong, R.B. Deng, Y.M.Wen, S. Sun, Z.Q. Jiang, X. Hu, L.Wang,

Shanghai Institute of Applied Physics, CAS, Shanghai, 201204 China

Abstract

The electron beam orbit stability is very important for the Free Electron Laser (FEL) facility. The high beam position stability requirement results in the high position stability for the FEL key components, such as quadruple magnet (Q) and beam position monitor (BPM). This work focus on the research of the dynamic performance of a mechanical support system composed of mechanical supports（including sheets and adjustments）and a granite block mounted on them. It will be applied for the beam based alignment (BBA) Q magnet and BPM for the Soft X-ray FEL project (SXFEL). The Finite-element（FE）calculations of the model characteristics were carried out to guide the subsequent tests. The test results show that the support system can meet the requirement of the SXFEL project.

INTRDUCTION

Shanghai Soft X-ray FEL (SXFEL) and the Dalian Coherent Light Source project (DCLS) are significant national science and technology infrastructure. The electron beam stability is one of the most important factors that influence the properties of FEL. The increasing demands of beam position stability result in the higher position stability requirement for the FEL key parts such as undulator and quadruple magnet. Since the mechanical support system for the FEL provides supporting, location and position adjustment, the high mechanical stability of the supports is indirectly expected.

Soft X-ray Free Electron Laser (FEL) light in the SCSS project developed a new support-stand composed of cordierite body with low thermal expansion rate attached with two flanges at top and bottom used in undulator line [1]. Sand-filled insulated steel support pedestals were used in undulator line of LCLS (Linac Coherent Light Source) [2]. Swiss FEL also developed a new mechanical support with low thermal expansion for BBA [3].

For the DCLS&SXFEL projects, granite blocks with produced from Shandong Province of China have been used as the main component of the support for BBA. In this work, several kinds of mounting method between granite block with mechanical components and Ground were designed and discussed. The first eigenfrequency is an important index for the stability and performance of supports [4].This paper describes an attempt to understand and increase the first eigenfrequency of different kinds of support for BBA to improve its stability, which based on the fact that the ground vibrations at the SXFEL(SSRF site) are larger than at other light sources [5].

This paper presents two different kinds of support prototype for Beam Based Alignment (BBA). Modal hammering experiments and FE analysis of prototypes are discussed in this work. Finally, vibration measurement result about the final support for BBA mounting in the tunnel is shown in this paper.

PROTOTYPES DESIGN

Design of Prototype 1 (See Figure. 1)

- Prototype1 support contains two components of a granite block with a low thermal expansion coefficient and three dimensional adjustments.
- 3 welding bases are fixed on ground with 12 anchor bolts and non-shrinkage cement having high strength.
- 3 direction adjusting can be done by adjustments located on 3 welding bases and M42 Screws.

Design of Prototype 2 (See Figure. 2)

- Prototype2 support contains two components of a granite block with a low thermal expansion coefficient and three layers of steel.
- The bottom steel is fixed on ground with 4 anchor bolts and non-shrinkage cement having high strength.
- 3 direction adjusting can be done by adjusting blocks located on steel and 4 M16 jack screws.

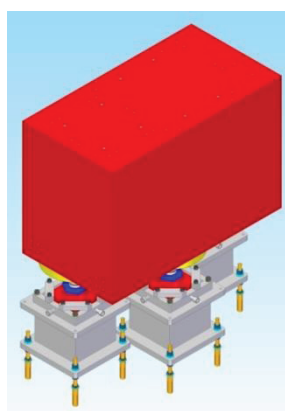

Figure 1: 3-D modal of prototype1.

* Work supported by National Natural Science Fund of China（Grant No.11405255）
† gaofei@sinap.ac.cn

ISBN: 978-3-95450-188-5 doi:10.18429/JACoW-MEDSI2016-MOPE32

PRELIMINARY DESIGN AND ANALYSIS OF THE FODO MODULE SUPPORT SYSTEM FOR THE APS-U STORAGE RING *

J. Nudell†, Z. Liu, C. Preissner, J. Collins, H. Cease, Advanced Photon Source, Argonne National Laboratory, Argonne, IL, USA

Abstract

The most technically challenging module of the planned APS Upgrade (APS-U) project is the Focusing-Defocusing (FODO) module. The girder for the FODO must support a ~6m long string of three transverse gradient dipole magnets and four quadrupole magnets. The challenges which emanate from retrofitting the existing APS tunnel with new hardware along with the stringent requirements for alignment and vibrational stability [1] necessitate a unique engineering solution for the magnet support system. FEA is heavily relied upon in order to create an optimized solution and reduce the number of design iterations required to meet specifications. The prototype FODO magnet support design is presented from the ground up, along with FEA justification and the expected vibrational performance of the module.

INTRODUCTION

The APS is planning an upgrade of the storage ring, which will involve replacing all of the existing hardware in a several month time frame. To meet this difficult schedule constraint, magnets, vacuum chambers, and supports will be assembled to a plinth, and installed as a module. After removal of the existing storage ring hardware, modules will be lifted on air casters and brought to their installation location. Technicians will deflate the air casters and rest the module on three outriggers for initial rough alignment. Next, the plinth will be grouted in place, and the outriggers will be removed. Finally, the magnet support and alignment system will be used to precisely align the girder. A three-point semi-kinematic support system has been chosen in order to reduce the time and effort required for alignment.

Given the large combined mass (~9,145 kg) of the seven magnets which comprise the FODO section, design specifications will be most difficult to meet for this module. To work within the available space around the FODO in the storage ring, all installation and maintenance must be performed on the aisle-side. A prototype FODO module has been procured with a string of dummy magnets which will test fabrication methods, mechanical stability with and without water flow, installation logistics, and vacuum performance (Fig. 1).

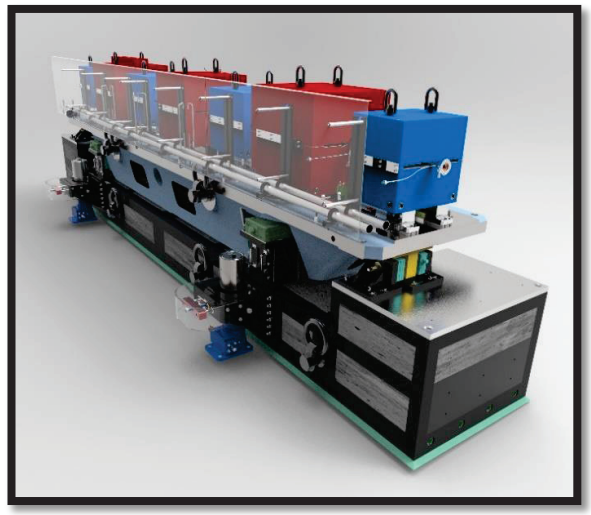

Figure 1: Assembled FODO prototype module.

PLINTH DESIGN

The FODO plinth is a hybrid steel and concrete structure developed through an R&D collaboration with a university, concrete fabricator, steel fabricator, and ANL. Through the use of a proprietary concrete mixture, steel reinforcing bar, and a steel cage which surrounds the concrete, long term shrinkage rates have proven to be acceptably small. The plinth contains all mounting features for the FODO girder support and outriggers, lifting eyes for rigging, and shelves for the two longitudinal gradient dipole magnets, which are positioned directly upstream and downstream of the FODO module. The embedded steel weldments which support the girder have been designed to maximize stiffness while staying within the geometrical boundaries defined by the storage ring walls. The weldments also bring the girder supports as close as possible to beam height in order to reduce the moment of inertia of the girder system and reduce geometric amplification of ground vibrations.

GIRDER DESIGN

The FODO girder has been designed to optimize its stiffness with respect to static deflection and modal response. This was done using a topology optimization software called GTAM [2]. The constraints, an objective function and an initial geometry seed were inputs to the software. An image of the topology optimized geometry is shown in Fig. 2 [3].

* Work supported by: Argonne is managed by UChicago Argonne, LLC, for the U.S. Department of Energy under contract DE-AC02-06CH11357.
† jnudell@aps.anl.gov

ISBN: 978-3-95450-188-5 doi:10.18429/JACoW-MEDSI2016-MOPE34

PRELIMINARY DESIGN OF THE MAGNET SUPPORT AND ALIGNMENT SYSTEMS FOR THE APS-U STORAGE RING*

J. Collins†, Z. Liu, J. Nudell, S. Izzo, C. Preissner, H. Cease
Advance Photon Source, Argonne National Laboratory, Argonne, IL 60439, USA

Abstract

As part of the Advanced Photon Source Upgrade project (APS-U), the storage ring will be upgraded to a multibend achromat (MBA) lattice [1]. This upgrade will provide dramatically enhanced hard x-ray brightness and coherent flux to beamline experiments in comparison to the present machine. The accelerator physics requirements for the upgrade impose very stringent alignment, assembly and installation tolerances and tight vibrational tolerances on the magnet support and alignment system designs. The short installation duration dictates a need for transporting groups of fully assembled magnet modules into the storage ring enclosure while preserving magnet-to-magnet alignment. The current magnet support and alignment systems preliminary design status for the APS-U storage ring will be presented along with an overview of the R&D program required to validate design performance. Magnet module transportation and installation logistics will also be discussed.

INTRODUCTION

The existing APS storage ring will be completely removed and replaced with an MBA lattice as part of the APS-U. The APS-U storage ring will consist of forty repeating arc sectors, each containing nine magnet modules as shown in Figure 1. Each arc sector contains five concrete plinths used to build up groups of magnets that can be installed as a module. The largest magnet module located in the center of the arc sector is the curved Focusing-Defocusing (FODO) module. On either side of the FODO module are straight Multiplet modules followed by Quad Doublet modules. Supported on bridges between the concrete plinths are longitudinal gradient dipole magnets (L-Bend), a total of four per arc sector. The concrete plinths effectively "raise the floor" to help reduce geometric amplification of ground vibrations. The magnet groups on each concrete plinth are mounted to a girder that is supported by a three-point semi-kinematic six degree of freedom (DOF) support and alignment system. The planned installation duration is very short, allowing only one year for removal, installation, testing, commissioning and return to beamline operations. Installing pre-assembled magnet modules will reduce installation time and the three-point semi-kinematic six DOF support and alignment systems will reduce the time and effort required for alignment.

Derived from the APS-U accelerator physics requirements, the survey and alignment assembly and installation tolerances are shown in Table 1. The requirement is that each magnet module girder be aligned to within 100 µm RMS of a neighboring girder at the start of commissioning. The APS-U physics requirements also impose tight vibration tolerances on the magnet support and alignment system designs as shown in Table 2. For instance, a 9 nm RMS vibration tolerance on the vertical magnet-to magnet motion must be satisfied for proper operation. Measurements of the floor vibration spectrum in the APS storage ring indicate that the ground motion will be less than 1 nm above 50 Hz. Therefore, a first mode frequency greater than 50 Hz is chosen as a design goal for the installed magnet modules since it will ensure that vibration tolerances will be met.

Table 1: Survey and Alignment Assembly and Installation Tolerances at Start of Commissioning .

Girder misalignment	100 μm
Elements within girder	30 μm
Initial BPM offset errors	500 μm
Dipole fractional strength error	$1 \cdot 10^{-3}$
Quadrupole fractional strength error	$1 \cdot 10^{-3}$
Dipole tilt	$4 \cdot 10^{-4}$ rad
Quadrupole tilt	$4 \cdot 10^{-4}$ rad
Sextupole tilt	$4 \cdot 10^{-4}$ rad

Table 2: Summary of Vibrational Tolerances

	X (rms) 1-100 Hz	Y (rms) 1-100 Hz	X (rms) 0.1-1000 Hz	Y (rms) 0.1-1000 Hz
u_{girder}	32 nm	40 nm	320 nm	400 nm
u_{quad}	13 nm	9 nm	130 nm	90 nm

In order to validate design performance, a comprehensive R&D program has been established that addresses major risks. Numerous vibration tests are being conducted on prototype modules that will provide substructure stiffness information and allow finite element model validation [2]. Temperature change-driven misalignment tests are planned that will provide insight into how the alignment of a magnet module reacts to local temperature fluctuations. Since fully assembled magnet modules will be transported and installed into the storage ring, transport tests are being conducted to ensure that magnet alignment is retained through this process. Tests are also being conducted that will inform installation planning and logistics.

* Work supported by the U.S. Department of Energy, Office of Science, under Contract No. DE-AC02-06CH11357
† collins@aps.anl.gov

ISBN: 978-3-95450-188-5 doi:10.18429/JACoW-MEDSI2016-MOPE37

DIAMOND MULTI-BEND ACHROMATS FOR LOW EMITTANCE AND NEW INSERTION DEVICES

J. Kay†, N. P. Hammond, Diamond Light Source, Didcot, OX11 0DE, UK

Abstract

Diamond Light Source is pioneering the move to a Multi Bend Achromat storage ring lattice for low emittance combined with the creation of new straight sections available for Insertion Devices (ID). Diamond is at an advanced stage of replacing one Double Bend Achromat (DBA) cell of the existing storage ring with a Double Double Bend Achromat (DDBA). The DDBA cell which is to be installed in Autumn 2016 has 4 dipoles and has been designed with a new straight section in the middle. This allows ID radiation to shine down an existing Bending Magnet port in the shield wall for a new micro-focus protein crystallography beamline called VMX-m. This same principle will be applied to the proposed Diamond II project which will be based on a Double Triple Bend Achromat with 6 dipoles per cell achieving even lower emittance whilst providing many more IDs. This paper describes the engineering challenges of these projects.

INTRODUCTION

The move to replace a DBA cell with a DDBA cell is at an advanced stage with 2 girders measuring 7.5 m long nearing completion for installation in an 8 week shutdown between Oct 7th and Dec 5th 2016. The overall geometry is shown in Fig. 1. and a completed girder in Fig. 2. The engineering design was described more fully in [1, 2].

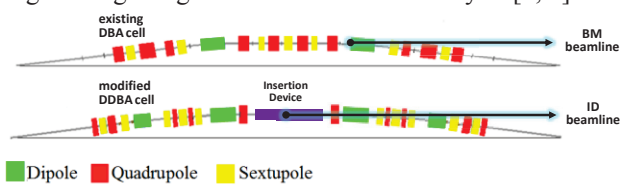

Figure 1: Schematic diagram of the existing DBA and the modified DDBA cell.

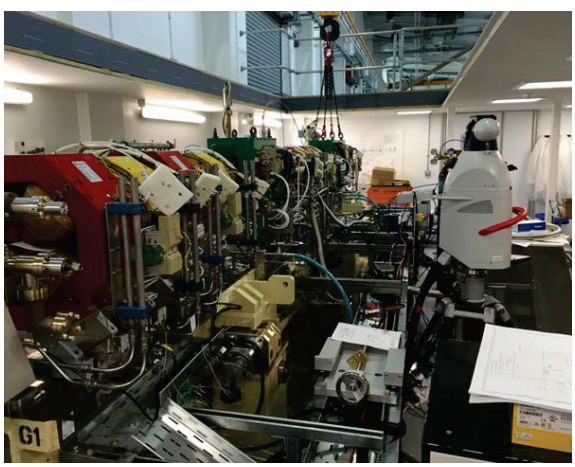

Figure 2: Completed Girder 1 in the assembly room.

† jim.kay@diamond.ac.uk

This paper will give some of the lessons learned from our experience building the DDBA cell as well as point towards a future Diamond II low emittance storage ring.

MAGNETS

A number of issues arose with the magnets to inform future projects. It is essential to keep water connections sufficiently clear of coils and coil terminations to enable pipework and cable connections to be made with good access for hands and tools (see Fig. 3.). Simply identifying 'stay clear' zones in the magnet reference design did not prove sufficient. Another issue on the sextupole magnets which have many terminal connections was the need to space out adjacent terminal blocks to give clear access for different cables to enter the terminal blocks cleanly. Although an overall length for each magnet was specified including coil overhang, the difficulties of achieving the right number of ampere-turns with a real, hollow cross-section conductor meant that this was exceeded which had implications for fitting adjacent components. It is clear that for any significant procurement contract, regular visits are essential to make sure these technical details, overall quality as well as delivery schedule issues are managed. Problems identified during final assembly are just too late and inevitably leave no time for the supplier to put things right and so the client has to compromise.

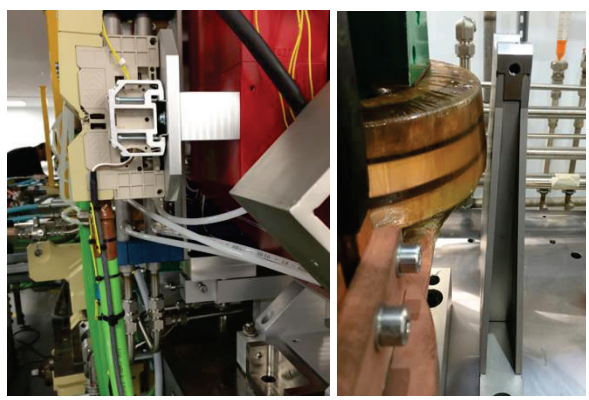

Figure 3: Magnet terminal spacer block added to separate pipes and cables and Dipole coil overhang allowance exceeded.

For more precise alignment of magnets the stretched wire technique was used [3]. This took much longer than was originally estimated by a factor 4 which had a significant impact on programme. The magnets were measured at the manufacturer using the same stretched wire bench and one shim adjustment made per magnet. However this was not checked and in the end all magnets were re-centred and shimmed at Diamond up to 3 times each.

ISBN: 978-3-95450-188-5 doi:10.18429/JACoW-MEDSI2016-MOPE38

MILLIPROBE SCANNER STATION*

J. Divitcos†, M. De Jonge, D. Howard, J. McKinlay
Synchrotron Light Source Australia, Australia

Abstract

The research team at the Commonwealth Scientific and Industrial Research Organisation, Clayton (CSIRO) have developed a the high energy dispersive detector referred to as the Maia. The rapid scanning, high resolution detector offers technological advances, including non-invasive technical study of highly valued artwork.

A vital application of the maia detector is scanning x-ray fluorescence microscopy for obtaining the elemental composition of a large number of materials.
The innovative detector allows connection between scientists and arts communities to increase their understanding of historical artworks, broadening the field of authentication and potentially aiding the fight against art forgery as well as historical information.

We have designed a new dedicated milliprobe station that offers improvements in stability, motion control and mounting. The structure is designed to support and scan various samples in size as well as shape powered by X and Y stages. A slide and hold clamping concept has been implemented, incorporating carbon fiber tubes, which provides easy and rapid assembling of samples. This arrangement provides excellent interchangeability, supporting a variety of planar and non-planar samples for scanning [1].

INTRODUCTION

For several years we have used a prototype 'milliprobe' apparatus to successfully scan large objects. Examples include paintings from the National Gallery of Victoria, historical photos and a Melbourne Cup – Australia's most prestigious thoroughbred horse race trophy.

MAIA DETECTOR

Thanks to the highly sensitive CSIRO and Brookhaven National Laboratory (BNL) developed maia detector. The maia system is a high-throughput x-ray fluorescence detector and real-time analysis system that allows samples to be scanned up to 1000 times faster and in much greater detail than previous methods.

When combined with a focused x-ray source, such as the x-ray fluorescence microprobe beamline, it is able to produce high-definition, quantitative element images with microscopic detail in real-time [2].

* Work supported by:
† jim.divitcos@synchrotron.org.au

TECHNICAL SPECIFICATIONS

Ability to adjust beam addressable sample area: X axis: 600 mm, Y axis: 1200 mm travel.
X Stage: Parker 404XR, Motor Sanyo Denki Stepper 56 mm 103H7128.
Y stage: Parker 406XR, Motor Sanyo Denki Stepper 56 mm 103H7128.
Scanning Speed of X stage & Y stage: 20 mm per second.
Maximum sample size: 1250mm Height x 1750 mm wide x 50 mm thick.
Minimum sample size: 100 mm high x 100 mm wide.
Maia Detector minimum scanning distance: 2 mm from sample plane.
Maximum weight of sample: 15 kg.
Weight of structural stand: 276 kg.
Total Assembly Weight: 420 kg

CONCEPTUAL DESIGN

The design envelope included beam addressable regions to cover 1200 mm by 600 mm for large samples limited only by hutch wall constraints. We proposed several conceptual designs to achieve the specifications generated by our scientists, which were finalized during our design review.

The clamps are secured using knobs where feasible, providing quick release concept, reducing the number of tools required during installation and dismantling of sample. High stability and precision was an essential part of the design criteria. Early structural support of small artwork consisted of aluminium extrusions clamped together to help provide the requirements of this size. As the demand grew for larger format artwork, we introduced a large square tubular frame. This reinforced rigidity of the platform assemblies especially during transit mode.

Vertical carbon fiber tubing can also be disassembled to cater for a combination of smaller size samples reducing any vertical congestion within the surroundings of the hutch. The slots in the vertical side clamps are employed to fine tune any vertical misalignment of the artwork during installation.
Wide linear rails/carriages cater for ease of moment loading, increasing rigidity during motion of the upper and lower platforms. The implementation of counter weights on each side provides reduction of motor load on the vertical stage during transit. The design includes standardisation on same size fasteners to ease the assembly procedure and the number of tools required.

ISBN: 978-3-95450-188-5 doi:10.18429/JACoW-MEDSI2016-MOPE40

DESIGNING THE FLASH II PHOTON DIAGNOSTIC BEAMLINE AND COMPONENTS

D. Meissner*, M. Brachmanski, M. Hesse, U. F. Jastrow, M. Kuhlmann, H. Mahn,
F. Marutzky, E. Plönjes, M. Röhling, H. Schulte-Schrepping, K. Tiedtke, R. Treusch
Deutsches Elektronen-Synchrotron DESY, 22607 Hamburg, Germany

Abstract

From 2013 to 2016 the free electron laser FLASH at DESY in Hamburg, Germany was upgraded with a second undulator line, photon diagnostic line, beam distribution and experimental hall connected to the same linear accelerator. This paper shows the layout of the photon diagnostic section and an overview of the civil engineering challenges. The mechanical design of selected components, e.g. vacuum components, diagnostic equipment and safety related components is presented.

INTRODUCTION

The x-Ray Free Electron Laser FLASH at DESY has been running as a user facility for XUV and soft x-ray photon experiments since 2005. In 2010 the upgrade project FLASH II was started to increase the number of user end stations by adding a second undulator line to the FLASH accelerator and operating both beamlines simultaneously and independently regarding wavelength [1, 2].

Two largely identical photon diagnostic sections had to be developed to provide beam parameters to accelerator operation and user experiments. The first section is located inside the accelerator tunnel starting at 10 m from the source where the beam is very small and intense, the second section is in the experimental hall and is fully accessible to users. Both provide data on beam intensity, position and wavelength. The complete layout is described in [2].

Since most of the components use various gases at different pressures main focus in designing the vacuum system was on differential pumping, especially the gas attenuator located between tunnel and hall where the beam crosses the PETRA III accelerator tunnel. Additional mechanical component development focused on absorbers and mirror chambers for beam steering and radiation protection.

GAS ATTENUATOR AND DIFFERENTIAL PUMPING

The straight section of 12 m between the end of the FLASH II tunnel and the beginning of the experimental hall is used as an intensity attenuator. For the purpose of reducing beam transmission for selected wavelengths this section can be flooded with gas up to a pressure of 0.5 mbar. Gases available are Xe, N_2, Kr and Ar [2].

To separate the beamline vacuum from the attenuator and minimize gas usage five-stage differential pumping stations with small and long apertures are used on both sides of the section. Pumping apertures are 16 mm diameter in the tunnel and 20 mm in the hall. The aperture lengths for stages 2 to 5 are 287 mm in the tunnel and range from 400 mm to 700 mm in the hall. Stage 1 which is closest to the attenuator features a 1 m (1.2 m in the hall) cantilevered tube that protrudes into the attenuator beam pipe and also into the radiation shielding wall of tunnel and hall (see Fig. 1).

Table 1: Pressure at All Pumping Stages from Attenuator to Following Vacuum Chamber [3]

Stage	Diameter mm	Length cm	Pump type mbar l s^{-1}	Pressure[a] mbar
ATT	100	1300	300, TP[b]	5E-01
1.	16	100	300, TP	9E-03
2.	16	29	300, TP	8E-05
3.	16	28	300, TP	7E-07
4.	16	28	300, TP	7E-09
5.	16	29	300, TP	6E-11
6.[c]	25	7	55, Ion GP	3E-11

[a] Simulated prediction of pressure range
[b] with cooling gas option
[c] Aperture of following UHV section

Stages 2 to 5 use turbomolecular pumps with a volume flow rate of 300 mbar l s^{-1} and additionally ion getter pumps for UHV operation. Stage 1 uses a similar turbomolecular pump which can use cooling gas and can bypass the aperture through a DN100 pipe to allow for rapid pumping of the attenuator down to UHV. Table 1 shows the resulting pressures of the setup.

Due to the long and narrow apertures special care must be taken for supports and alignment. All pumping sections are pre-assembled outside of the accelerator tunnel on granite girders with high precision manufactured steel grooves for alignment of the components. The girder itself sits on two sand-filled supports of thick walled steel tubes and a three-point kinematic mount. Since alignment is done only by adjusting the kinematic girder support the manufacturing tolerances of the girder and the pumping stages have to be very small. Precision steel tubing and special welding equipment were used to achieve the desired concentricity of all apertures. The cantilever tube of the first stage is suspended by three wires to compensate for bending due to its span. By adjusting the tension in the wires while measuring the resulting aperture with an alignment laser the aperture can be maximized.

* daniel.meissner@desy.de

ISBN: 978-3-95450-188-5 doi:10.18429/JACoW-MEDSI2016-MOPE41

DESIGN AND CONSTRUCTION OF A PW EXPERIMENTAL SYSTEM OF HV CHAMBER ADAPTABLE, MODULAR AND STABLE

A. Carballedo[1†], J. Hernández-Toro[2], C. Colldelram[1], R. Monge[1], L. Nikitina[1], J.R. García[1], L. Roso[2]

[1]ALBA-CELLS Synchrotron, 08290 Cerdanyola del Vallès, Spain
[2]Centro de Láseres Pulsados, CLPU, Parque Científico, 37185 Villamayor, Salamanca, Spain

Abstract

In the recent years, the number of high power lasers devoted to particle acceleration has increased in Europe. Additionally to this, some synchrotrons and accelerators are integrating these lasers in its lines, increasing the scientific synergies. The HP laser must be transported in HV. The use of HV also permits good cleanliness in the optical setup. As addition, is necessary to create an adaptable and modular design where several chambers could be assembled together. One additional constrain is the stability. A new model of HV chambers is presented. These consist in a frame where the walls are exchangeable panels, which make easier the introduction of a new configuration of ports. The system was designed as construction blocks. For a proper connection of the chambers a new interior fixation and pushers system was designed. Thanks to this, coupling new HV chambers, the volume total can be also easily modified. Finally, a third generation decoupled system is integrated inside, consisting of a stable breadboard, this supported by six columns that implement a preloaded kinematical mount, providing both an outstanding stability and a fine regulation (1st RM: 77Hz).

INTRODUCTION

This project is the result of the collaboration between ALBA-CELLS and CLPU in order to promote the Mechanical engineering related with the high power laser. CLPU (Ultra-short Pulsed Laser Center) is a facility specialized in femtosecond laser pulses with peak powers at Gigawatt, Terawatt and Petawatt levels. Previous collaborations have given the 200TW and 1PW laser compressors. The protagonist of this article is the third one, the 1PW Experimental system consisting in a HV modular vacuum chamber and a stable breadboard for the optical equipment.

MAIN CONCEPT

The functionality of this chamber is as interaction chamber, where the target of the laser and the focus system are mounted. Due to the laser is a high power laser, after the laser is compressed, this cannot be transported in air because the laser properties are deteriorated and a complete HV system ($<5\cdot10^{-6}$ mbar) is required. Furthermore, this also reduces the presence of hydrocarbon contamination on the system.

REQUIREMENTS

A new paradigm of HV chambers is presented. It is necessary to create an open and adaptable design with the following requirements:

- The vacuum chamber should be modular and allow easily modifications in the ports distribution.
- As different experimental setups might need of different optical equipment distribution, a decoupled system is integrated inside the chamber, based in the experience of the two previous laser compressor chambers.

DESIGN

Vacuum Chamber. Modularity

The Experimental vacuum chamber is designed plate-to-plate in a rectangular configuration. Each plate has rectangular ports for lateral covers. Due to the modularity of its design, faces are identical two by two. It implies that the large lateral covers and the short lateral covers are equal respectively. This fact allows not only using a same design of lateral cover for each experimental chamber but also interconnect different vacuum chambers between each other (Figure 1).

Vacuum chamber is made of AISI 304L stainless steel with the exception of AL 6082 aluminium lateral covers, and can be divided on four main parts: bottom cover, walls, top cover and lateral covers. The global dimensions of the chamber are 3000 mm x 1900 mm x 1500mm.

In order of ensure the tightness a system of double joint with different size was designed. This permits either to fix one lateral cover or another vacuum chamber in the same port.

Furthermore, an internal matrix of holes was added to each port in order to allow the connection between chambers.

Due to the big weight of the chamber a complete system of pushers was added. Low friction intermediate plates are placed between chamber and its support to

† acarballedo@cells.es

ISBN: 978-3-95450-188-5 doi:10.18429/JACoW-MEDSI2016-MOPE42

EXPERIMENTAL AND NUMERICAL STUDY OF THE ALBA LINAC COOLING SYSTEM

M. Ferrater†, Universitat Politècnica de Catalunya, Barcelona, Spain
J.J. Casas, C. Colldelram, D. Lanaia, R. Muñoz, F. Perez, M. Quispe*, ALBA – CELLS Synchrotron, Cerdanyola del Vallès, Spain

Abstract

This work investigates experimentally and numerically the performance of the ALBA LINAC cooling system. The main objective is to enhance the hydraulic system in order to significantly improve its thermal and water flow stability. In normal operation some problems have been identified that affect the performance of the LINAC: flowrate below the nominal values and water flow decreasing in time. The cooling subsystems have been experimentally characterized in terms of the pressure drop and flowrate. The measurements were taken using a portable hydraulic unit made at ALBA as well as a set of ultrasonic flowmeters. For the numerical studies the cooling network has been simulated using the software Pipe Flow Expert. The experimental results have shown that a number of components are too restrictive. In some cases the possibility to increase the flowrate is limited. The numerical results show that the velocity magnitude is inadequate in some places, producing air bubble entrapment, high pressure drop at pipes and insufficient flow. Based on this study several modifications are presented in order to raise the nominal flow and to adequate the water flow velocities between 0.5 and 3 m/s.

BACKGROUND

The ALBA facility is composed of a 100 MeV LINAC (see Fig. 1), a Booster that accelerates the beam up to the full energy of 3 GeV, the Storage Ring (SR), and the corresponding transfer lines (LINAC To Booster – LTB, and Booster To Storage – BTS).

Figure 1: The ALBA LINAC.

The LINAC consists of a 90 kV DC thermoionic gun, followed by a bunching system designed to reduce the energy spread and the electron losses. This one comprises a sub-harmonic pre-buncher (500 MHz), a pre-buncher (3 GHz) and 22-cells SW buncher (3 GHz). Two travelling wave constant gradient accelerating sections increase the energy up to 100 MeV. Beam focusing is ensured by shielded solenoids up to the bunching system exit and a triplet of quadrupoles between the two accelerating structures [1, 2].

The LINAC is running reliably since started its operation in 2010. At the early stages of the operation it was experienced that the beam charge is sensitive to variations of more than 0.1 ºC in cooling water temperature of the LINAC bunker and Service Area.

THE LINAC WATER COOLING SYSTEM

Description

The LINAC cooling water system has two different functions. From one side it cools the elements with strong dissipation of power: klystrons, RF cavities, RF loads, RF ceramic windows and magnets. And from the other side the system regulates the water temperature of the RF cavities in order to tune them for working at the nominal RF frequency.

The hydraulic scheme of the cooling water system is illustrated in Fig. 2. The main inlet pipe is connected to the supply ring at the Service Area. The total nominal flowrate is estimated at 100 l/min for a mean increase of temperature of 5.8 ºC. The total power transmitted by the LINAC to the cooling water is 61 kW according with the technical specifications. The inlet pressure of the supply ring is 10.2 bar. However a pressure reducer installed in the supply line set to 8.8 bar protects the downstream piping and components from over–pressurization. The inlet water temperature is 23 +/- 0.1 ºC in nominal conditions.

The main cooling circuit is divided in two subsystems, one for inside and the other for outside the bunker. The resistor load (RL1) and klystron amplifiers (KA1 and KA2) are outside the bunker. Both klystrons dissipate 45 kW.

Inside the bunker the RF cavities are made of copper whose dimensions change with temperature. As the resonant frequency is directly related to the dimensions, any change of temperature will lead to a lower electric field. Calculations of beam dynamics show that a temperature stability of ± 0.2 °C is necessary. The nominal regulation for temperature is around 30 °C.

† marcferrater@gmail.com
* mquispe@cells.es

ISBN: 978-3-95450-188-5 doi:10.18429/JACoW-MEDSI2016-MOPE43

HYDRAULIC FAILURE CAUSED BY AIR IN PIPELINES OF THE EXPERIMENTAL AREA RING OF ALBA SYNCHROTRON LIGHT SOURCE: RESEARCH, SIMULATIONS AND SOLUTIONS

Ll. Macià†, Universitat Politècnica de Catalunya, Barcelona, Spain
J.J. Casas, C. Colldelram, M. Quispe*, ALBA – CELLS Synchrotron, Cerdanyola del Vallès, Spain

Abstract

After five years in operation of the ALBA Synchrotron Light Source a hydraulic failure caused a maximum decreasing of water flow about 40% of its nominal value, hampering the refrigeration of the local components. The problem was mainly caused by the air accumulated in pipes due to very low velocities of water flow. A literature review was conducted about the minimum water flow velocity for removing air in pipelines as design criteria. The aim of this work is to develop hydraulic solutions in order to achieve the minimum flow rate in pipelines of the Experimental Area (EA) ring. In the short term it is proposed to install a controlled bypass in the EA. A numerical simulation using the software Pipe Flow Expert has been implemented in order to determine the requirements of the bypass that works under different conditions to assure a minimum flow rate all along the ring. The velocity map in EA ring is simulated for different scenarios: 180 and 360 degrees distribution for both clockwise and anticlockwise rotation. For the long term a design of pipes with variable cross section is proposed which optimizes the flow velocity magnitude in EA ring in agreement with the design criteria.

BACKGROUND

The ALBA cooling system consists of four main rings which feed the local consumption of the Service Area (SA), Booster (BO), Storage Ring (SR) and Experimental Area (EA) (see Fig. 1). The water is heated through all the rings and it is collected in a common return. The pump P11 takes the heated water from the return and feeds a couple of heat exchangers HE that cool it. The cooled water is brought to a storage tank from which a suction line takes water again to the rings' pumps. In order to regulate the water temperature, a series of controlled mixing valves permit to combine the cooled water with the heated water prior to being pumped to the rings. Finally, a pipe line connecting the tank with the common return line permits to compensate the lack/excess of flow to the cooling loop when the total flow rate changes in the rings' loops.

In 2013 a hydraulic failure in the ALBA cooling system caused a maximum decreasing of water flow about 40% of its nominal value, hampering the refrigeration of the local components. The problem was mainly caused by the air accumulated in the four rings due to very low velocities of water flow [1].

This paper analyses the problem and proposes new solutions. The Experimental Area has been selected for this study. The conclusions will be extrapolated to the other rings.

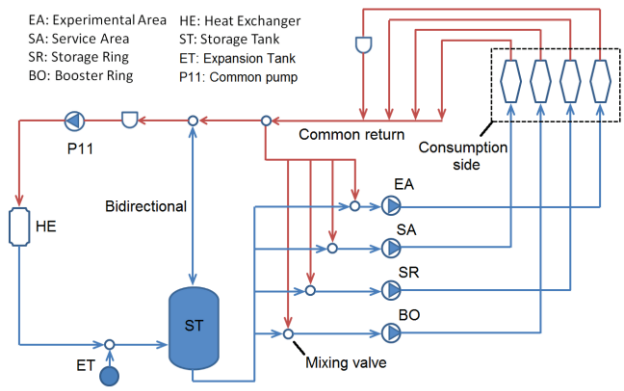

Figure 1: ALBA cooling system scheme.

THE MINIMUM WATER FLOW VELOCITY AS DESIGN CRITERIA

Research studies have shown that a minimum flow velocity is always required to move air pockets in pipelines [2, 3]. Air pockets decrease flow capacity, they induce significant head losses and energy losses, they prompt serious corrosion, and they can trigger and/or enhance pressure surges. Other problems include false flowmeter readings, increased biological activity, vibration and structural damage.

The minimum flow velocity for transporting air pockets depends on the size, shape, and concentration of the bubbles and on the down-slope and diameter of the pipe. The minimum velocity usually increases with increase in bubble size, in down-slope and in pipe diameter. In conditions of low velocity, below the minimum velocity, entrained air bubbles combine to form air pockets at peaks, at the crown of the pipe, at in-line and online fittings and accessories, and at other locations along the pipeline. These entrained air pockets often grow to sizes that even fast-flowing water cannot carry downstream.

Escarameia [3] has studied exhaustibly this issue and analyzes the problem in terms of three variables: diameter of the pipe, angle of inclination and the Froude non-dimensional number. The Froude number, which is proportional to the critical velocity and is inverse proportional to square root diameter, has a range from 0.3 to 0.8 in horizontal pipelines, which is the case of the present paper.

† llorencmaciacid@gmail.com
* mquispe@cells.es

ISBN: 978-3-95450-188-5 doi:10.18429/JACoW-MEDSI2016-TUAA01

PRECISION MECHANICAL DESIGN OF A MINIATURE DYNAMIC MIRROR BENDER FOR THE SSRF BEAMLINE UPGRADE PROJECT

D. Shu[1], A. Li[2], S. P. Kearney[1], C. Mao[2], J. Anton[1,3], and Y. Pan[2]
[1]Advanced Photon Source, Argonne National Laboratory, Argonne, IL 60439, U.S.A.
[2]Shanghai Synchrotron Radiation Facility, Shanghai Institute of Applied Physics, Shanghai 201204, China
[3]University of Illinois at Chicago, Chicago, IL 60607, USA

Abstract

Dynamic mirror benders which enable high precision figuring of planar substrates for x-ray focusing are widely used as conventional optical equipment in various synchrotron radiation beamlines. Especially, in cases for x-ray focusing optics coated with multilayers in a Kirkpatrick-Baez (K-B) configuration [1] as the final focusing elements immediately upstream of the sample, the dynamic mirror benders provide high precision figuring to allow the mirror figure to be tuned to optimize the focusing at different incidence angles to cover a wide energy range [2].

Recently, collaboration between Argonne National Laboratory and Shanghai Institute of Applied Physics has produced designs of a new miniature dynamic mirror bender using Argonne's laminar nanopositioning flexure technique [3-5] for the beamline upgrade project at the Shanghai Synchrotron Radiation Facility (SSRF). The mechanical design and finite element analyses of the miniature dynamic mirror bender are described in this paper.

INTRODUCTION

The SSRF is a 3.5 GeV third generation synchrotron radiation source. Currently, there are sixteen more beamlines under design and construction stage for the SSRF Phase-II beamline construction project. Both SSRF and Advanced Photon Source (APS) have a keen interest in the development of novel K-B mirror mount stages for synchrotron radiation applications. As a part of Argonne Strategic Partnership Project (SPP) (formerly known as work for others or WFO project), collaboration between Argonne National Laboratory and Shanghai Institute of Applied Physics has produced designs of a new miniature dynamic mirror bender using Argonne's laminar nanopositioning flexure technique for the beamline upgrade project at the SSRF. The motivation of the new design is to develop a compact, cost-effective flexure mirror bender with high stability.

TEST MIRROR FOR PROTOTYPE

Figure 1 shows a schematic diagram of a silicon test mirror for the new miniature dynamic bender prototype. The 90 mm long silicon mirror has an effective optical length of 66 mm and thickness of 5.5 mm. The width of the mirror is designed to perform the optical figuring of the mirror under bending [6]. With a dynamic mirror bender, which is capable to provide bent moment tuneable between 0.35 N·m to 0.71 N·m, the elliptical mirror figure radiuses are tuneable between of curvatures of 24 m–88 m to 12 m-44 m.

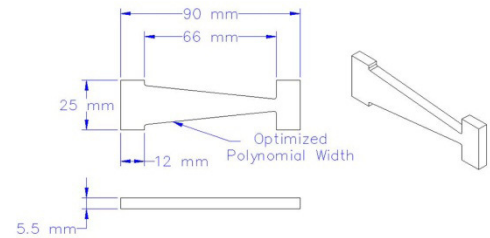

Figure 1: Schematic diagram of a silicon test mirror for the new miniature dynamic bender.

DESIGN OF THE MIRROR BENDER

Based on the type of bending actuators, the miniature dynamic mirror bender is designed with two configurations: the open-loop control configuration with Newportᵀᴹ Picomotorᵀᴹ actuators and the closed-loop control configuration with Newport™ NPM-140 piezo micrometer adapter [7]. Both design configurations use the same flexure bending mechanism module.

Mirror Bender with Newport™ Picomotor™ Actuators

The miniature dynamic mirror bender for open-loop control configuration consists of a base; a pair of laminar flexure mechanism modules; a pair of bending arms; and two Newportᵀᴹ Picomotorᵀᴹ 8301 actuators. The silicon mirror is bonded to a pair of adapters to connect with the bender as shown in Figure 2.

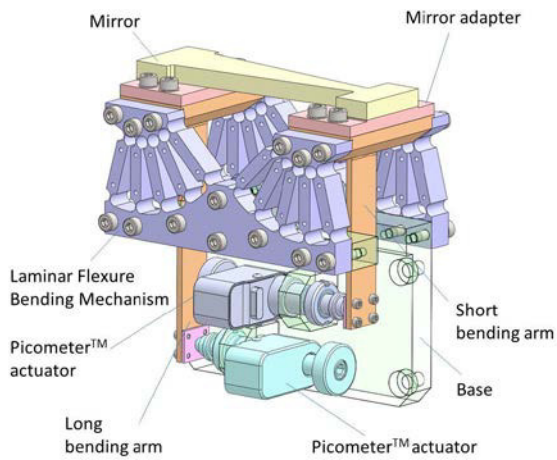

Figure 2: 3-D model of the miniature dynamic mirror bender with Newportᵀᴹ Picomotorᵀᴹ 8301Actuators for open-loop control configuration.

ISBN: 978-3-95450-188-5 doi:10.18429/JACoW-MEDSI2016-TUAA02

EARTH, WIND, AND FIRE: THE NEW FAST SCANNING VELOCIPROBE*

C. Preissner†, S. Sullivan, S. T. Mashrafi[1], C. Roehrig, J. Maser, B Lai, C. Jacobsen, J. Deng, F. S. Marin[2], and S. Vogt, Advanced Photon Source, Argonne National Laboratory, Argonne, IL, USA
[1]University of Illinois, Department of Mechanical Science and Engineering, Urbana, IL, USA
[2]DePaul University, Chicago, IL, USA

Abstract

The Advanced Photon Source Upgrade (APS-U) project will include a suite of new beamlines. In preparation for this, a team at the APS is developing an X-ray microscope with a novel granite (Earth), air bearing (Wind) supported stage to take advantage of the two orders of magnitude increased coherent flux (Fire) that will be available with the APS-U. The instrument will be able to operate as a scanning probe for fluorescence microscopy and as a ptychoprobe for the ultimate in spatial resolution. Both are combined with tomography. The goals for the instrument while operating at the current APS are to demonstrate fast scanning of large samples at high resolution and ptychography at the highest resolution (speed and resolution limited by available flux). This presentation will discuss the unique mechanics, interferometry scheme, the advanced scanning control, and some instrument integration.

INTRODUCTION

The dramatic increase in flux (the Fire) from the APS-U will enable reduced measurement times and increase optical resolution [1]. In fact, to make the best use of available photons and minimize sample damage, the X-ray beam will need to be scanned much more rapidly across the sample than is currently done. The high resolution and fast scanning necessitate a stable instrument platform. A new instrument, the Velociprobe, is being built to explore and push these limits. It will use zone plate optics and be able to operate as a scanning probe for fluorescence microscopy and as a ptychoprobe for the ultimate in spatial resolution. The goal is to scan a 1 µm by 1 µm area in less than 10s with the highest spatial resolution (~10 nm or better in fluoro-microscopy mode).

The goal of a highly stable instrument was considered at each point in the design process. The motion system was designed to minimize the positioning degrees of freedom. The fast scanning control is being developed to maximize bandwidth and disturbance rejection. This will be coupled with state-of-the-art laser interferometry to provide the best possible position information to the fast controller and the image collection systems. This paper covers the overall design of the instrument, including mechanics and controls, and the near-term plans as the Velociprobe is brought online.

INSTRUMENT DESIGN

Mechanics

The Velociprobe consists of a set of granite (the Earth) air-bearing supported (the Wind) coarse positioning X, Y, and Z axes stages. On top of these coarse axes sit the sample stack and the optics stack. The granite coarse stages are used to align the optics to the beam. The optics stack is used for the rapid fine scanning of the beam. The sample stack is used to align the tomographic axis to the optics and to select the region of interest on the sample.

The optics stack consists of a fast (bandwidth of hundreds of Hz) parallel kinematic piezo scanner. The order sorting aperture (OSA) stages are also mounted here. The sample stack consists of a coarse sample X axis, sample tomographic rotation axis, and the X, Y, and Z axes for sample centering. In operation, the optics are aligned to the beam, then the tomographic axis is aligned to the optics. The region of interest is brought to the tomographic axes. The fast scanner is then used to image the sample. The sample region of interest is then indexed to tile out larger sample areas. Basic information about all the axes (except those for the OSA) is shown in Table 1.

Table 1: Velociprobe Axes Listing

Axis	Travel	Design Res.	Model
CRSX	± 12.5 mm	5 µm	Custom
CRSY	± 5 mm	.7 µm	Custom
CRSZ	400 mm	5 µm	Custom
ZPXYZ	30, 20, 30 µm	.1 nm	PI 733.DD
OSAXYZ	± 12.5 mm	1 nm	Smaract SLC-17
SAMCX	± 5 mm	3 µm	Custom
SAMθ	360 deg.	.004 deg.	PI DT-380
SAMXYZ	26 mm	6 nm	PI Q-545

Custom Coarse Stage System

The foundation of the instrument, shown in Figure 1, is the granite coarse positioning stages. The design of these stages was driven by the question: How can the most stable microscope platform for an X-ray microscope be constructed? With this in mind, one of the design considerations was to minimize the number of degrees of freedom. This is because each motion degree of freedom also contributes compliance to the system. This can be particularly true for the degrees of freedom that are used to align the instrument, as they typically carry high loads. In addition, these alignment axes are not used frequently.

* Work supported by: Argonne is managed by UChicago Argonne, LLC, for the U.S. Department of Energy under contract DE-AC02-06CH11357.
† preissner@aps.anl.gov

ISBN: 978-3-95450-188-5 doi:10.18429/JACoW-MEDSI2016-TUBA01

THE DESIGN OF A PRECISION MECHANICAL ASSEMBLY FOR A HARD X-RAY POLARIZER

S. P. Kearney, D. Shu, T. S. Toellner

Advanced Photon Source, Argonne National Laboratory, Argonne, IL 60439, U.S.A.

Abstract

This paper discusses the mechanical design of an x-ray polarizer and the analysis of the design using FEA simulation. In addition, insight was made into the meshing requirements of flexure mechanisms. It was found that the maximum flexure stress will increase in accuracy with a finer mesh, however there is a limit to how well FEA can model stiffness and deflection without incorporating additional advanced FEA analysis techniques such as nonlinear methods. Finally, it was shown that the pitch stages for the polarizer will be capable of a least 80 nrad resolution.

INTRODUCTION

A hard x-ray polarizer is under development for the Advanced Photon Source (APS) at Argonne National Laboratory (ANL). It has been previously shown that polarization of synchrotron radiation can be used to filter a narrow bandwidth of 14.4 keV [1]. This has advantages for Mossbauer spectroscopy (MS) in that it allows for energy spectra to be collected rather than time spectra, which is normal in synchrotron radiation [2].

The paper will first detail and describe the mechanical design of the polarizer device for hard x-rays. Particular attention is paid to the analysis of the flexure mechanism involved in nano-radian level rotations. FEA simulations of a single notch type flexure are conducted followed by simulation of the complete flexure mechanism. Finally, experimental resolution results are shown.

POLARIZER DESIGN

Assembly – Z8-4600

The complete polarizer assembly consists of a total of 7 degrees of freedom (DOF). Three crystals are manipulated using individual actuator stacks, as can be seen in Fig. Figure 1. The left crystal will sit atop two Kohzu™ ST05A-S1T-R tilt stages modified to incorporate Newport™ 8301NF Picomotors™ for controlled positioning in the yaw and roll angles. The middle crystal also has two DOF with the base stage being a custom-designed high precision pitch flexure stage (Z4-4601) and atop that a Kohzu™ ST07A-S1T yaw tilt stage, which also incorporates a slightly larger 8302 Picomotor™ for controlled positioning. Finally, the third crystal has three DOF with the base stage being a more compact version of Z4-4601 designated Z4-4602. Atop this stage is a translation stage Kohzu™ XM05A-C1-R, and another ST05A-S1T-R roll tilt stage with Picomotor™ 8301NF. The detailed design specifications for the assembly can be seen in Table 1.

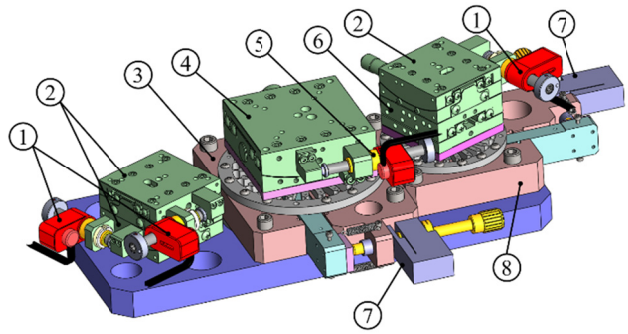

Figure 1: Z8-4600 assembly model view. Numbered items are 1) 3X Picomotor™ 8301NF, 2) 3X Kohzu™ ST05A-S1T-R tilt stage, 3) Z8-4601 pitch stage, 4) Kohzu™ ST07A-S1T tilt stage, 5) Picomotor™ 8302, 6) Kohzu™ XM05A-C1-R translation stage, 7) 2X Newport™ NPM140SG micrometer adapter piezo, and 8) Z8-4602 pitch stage.

Table 1: Design specifications for Z8-4600. The resolutions listed are derived from the published resolutions of the commercial actuators and represent the lower limit.

Specification	Value
Volume (L x W x H) mm^3	(365x214x89)
Mass	4.1 kg
Degrees of Freedom	7
Kohzu™ Tilt Stages Resolution	
ST05A-S1T-R (Open Loop)	0.5 µrad
ST07A-S1T(Open Loop)	0.4 µrad
Kohzu™ Stages Range	
ST05A-S1T-R & ST07A-S1T	±3°
XM05A-C1-R	±3.25 mm
Pitch Flexure Stages Resolution	
Z4-4601 & Z4-4602 (Closed Loop)	15 nrad
Pitch Flexure Stages Range	
Z4-4601 & Z4-4602	±0.7°

Pitch Rotation Stage – Z8-4602

Two laminar weak-link stages have been designed, for fine pitch rotation. For this paper, we will focus on the smaller diameter (73.34 mm vs. 97.78 mm) flexure stage shown in Fig. Figure 2. Pitch rotation is achieved by a Newport™ NPM140SG actuator pushing on an 80 mm sine bar attached to a pair of weak-link flexures. The laminar weak-link structure is comprised of 30 bonded

ISBN: 978-3-95450-188-5 doi:10.18429/JACoW-MEDSI2016-TUBA03

THE GENERIC MIRROR CHAMBER FOR THE EUROPEAN XFEL

T. Noll[1,2], H. Sinn[3], A. Trapp[3]

[1]Max-Born-Institut Berlin, Germany, [2]Helmholtz-Zentrum-Berlin, Germany
[3]European XFEL, Schenefeld, Germany

Abstract

For the high demanding requirements of the beamlines of the European XFEL [1] new mirror chambers were developed, designed and tested. A prototype contains the main features of all needed ten units which are tested extensively. The concept of the mirror chamber is a further development of our Cartesian parallel kinematics for X-ray optics in the UHV. The stiffness and vibration behaviour were further improved and the position resolution was increased compared to earlier implementations at HZB – Bessy II and Desy - Flash. For that the drives were redesigned and now feature a stroke of 100 mm with nanometre resolution.

INTRODUCTION

The new mirror chamber contains a mirror of 800 mm in length with adaptive shape compensation and an eutectic cooling. This mirror assembly has a dimension of 1000 mm x 150 mm x 250 mm (L x W x H). That large assembly requires a chamber of 600 mm in diameter and a length of 1800 mm (entry flange to exit flange). Both ends have doors for easy access to all inner components (s. Figure 1).

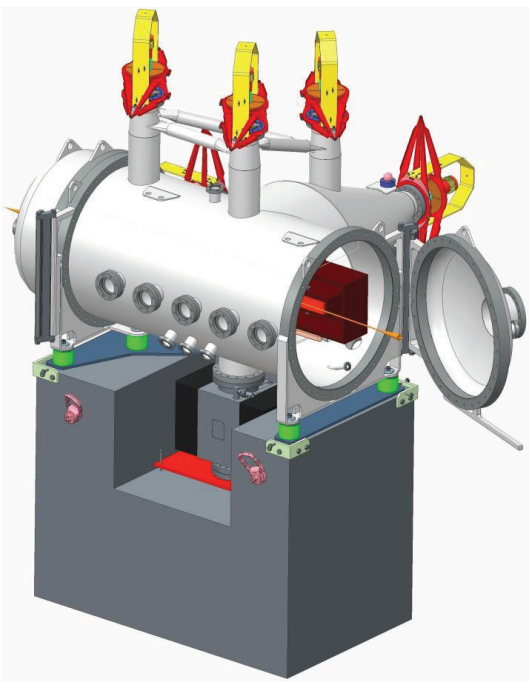

Figure 1: The mirror chamber with one open service flange.

KINEMATIC CONCEPT

The support and alignment mechanics is in principle a six strut parallel kinematics with Cartesian orientation of the movements. This allows the highest possible precision and stability [2], [3], [4] (s. Figure 2).

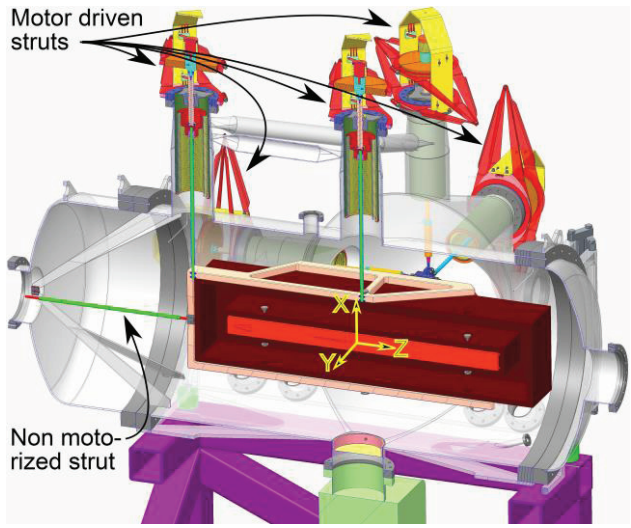

Figure 2: The cross section of the chamber gives a view at the topology of the struts.

The used six struts are the mechanical links between the mirror assembly and the flanges of the UHV-chamber. One of the struts has no motor and is not adjustable because it defines the position of the mirror along the light path which is not of interest for this application. Five of the six struts are motorized with stepper motors and lead screws.

DRIVE DEVELOPMENTS

For the X and Y translations stepper motor driven lead screws are used. For the rotations around X and Z the struts have additional piezo stacks embedded. That allows an even higher resolution and a higher motion dynamic than the stepper motor can deliver. (s. Figure 3).

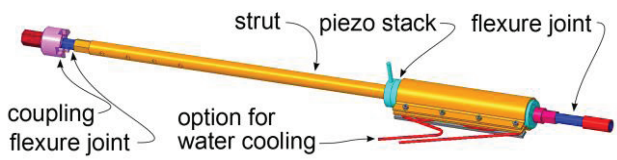

Figure 3: Strut with joints and piezo.

ISBN: 978-3-95450-188-5 doi:10.18429/JACoW-MEDSI2016-TUBA04

MECHANICAL DESIGN AND DEVELOPMENT OF COMPACT LINEAR NANOPOSITIONING FLEXURE STAGES WITH CENTIMETER-LEVEL TRAVEL RANGE AND NANOMETER-LEVEL RESOLUTION

D. Shu, W. Liu, S. Kearney, J. Anton[1], B. Lai, J. Maser, C. Roehrig, and J. Z. Tischler
Advanced Photon Source, Argonne National Laboratory, Argonne, IL 60439, USA
[1] also at University of Illinois at Chicago, Chicago, IL 60607, USA

Abstract

Nanopositioning techniques present an important capability to support the state-of-the-art synchrotron radiation instrumentation research for the Advanced Photon Source (APS) operations and upgrade project. To overcome the performance limitations of precision ball-bearing-based or roller-bearing-based linear stage systems, two compact linear nanopositiioning flexure stages have been designed and developed at the APS with centimeter-level travel range and nanometer-level resolution for x-ray experimental applications. The APS T8-54 linear flexure stage is designed to perform a precision wire scan as a differential aperture for the 3-D diffraction microscope at the APS sector 34, and the APS T8-56 linear flexure stage is designed for a horizontal sample scanning stage for a hard x-ray microscope at the APS sector 2. Both linear flexure stages are using a similar improved deformation compensated linear guiding mechanism which was developed initially at the APS for the T8-52 flexural linear stage [1,2]. The mechanical design and finite element analyses of the APS T8-54 and T8-56 flexural stages, as well as its initial mechanical test results with laser interferometer are described in this paper.

INTRODUCTION

X-ray Laue Diffraction 3D Microscopy developed at 34-ID beamline in the APS has been a unique and powerful tool for spatially-resolved structural studies at submicron level for materials science [3]. A precision linear stage is needed to perform a wire scan as a differential aperture for the 3-D diffraction microscope [4]. The wire scan motion is usually localized in a very short specific travel range after an initial large travel range alignment. Localized wear of the linear bearing stage, which causes an unrepeatable defect in the linear motion straightness of trajectory is always an issue for the results of the 3-D x-ray diffraction microscope.

To improve the linear motion performance and durability of the wire scan stage, a compact flexural-pivot-based precision linear stage APS T8-54 has been designed and constructed at the APS to replace the existing bearing-based linear stage for wire scan using deformation-compensated flexural pivot mechanisms as shown in Figures 1-3 [5]. Based on the experiences gained from the initial operation of the T8-54 flexure stage at the APS sector 34, a few design enhancements have been made to further improve the performance of the T8-54 stage. These design enhancements have also been implemented in the new compact flexure stage design for scanning sample stages at the APS sector 2. In this paper, we present the design enhancements for the T8-54 linear flexure stage, as well as the design of the new compact linear flexure scanning stage T8-56 for APS sector 2. Preliminary tests for the enhanced flexure linear guiding mechanism with laser confocal displacement meter and laser interferometer are also presented.

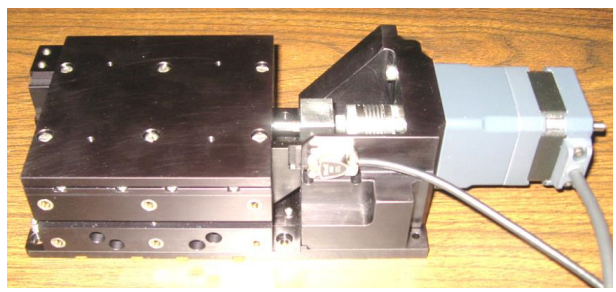

Figure 1: Photograph of the original APS T8-54 linear flexure stage for wire scan as a differential aperture for the 3-D diffraction microscope at the APS sector 34.

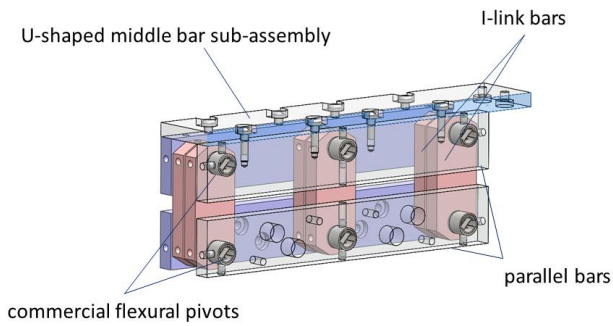

Figure 2: A 3-D model of the basic deformation compensated linear guiding mechanism for T8-54 linear flexural stage.

Figure 3: Photograph of the basic deformation compensated linear guiding mechanism for T8-54 linear flexural stage. A total of 12 C-Flex™ D-20 flexural pivots are applied in the linear guiding mechanism.

ISBN: 978-3-95450-188-5 doi:10.18429/JACoW-MEDSI2016-TUCA02

STRUCTURAL DYNAMIC MODELLING AND MEASUREMENT OF SWISSFEL BUNCH COMPRESSOR

Xinyu Wang†, Thomas Stapf, Haimo Joehri, Florian Loehl, Marco Pedrozzi

Paul Scherrer Institut, 5232 Villigen PSI, Switzerland

Abstract

Magnetic chicanes are used in accelerator facilities to longitudinally compress the accelerated particle bunches. The second compression chicane of SwissFEL consists of four dipole magnets bending the beam on the horizontal plane along a C-shaped orbit and has a total length of 17 m. The position of the two central dipoles can be continuously adjusted to achieve the required transverse offset in order to realize a wide range of compression schemes. To ensure the requires mechanical stability of the accelerator components sitting on the long and movable steel girder (7.7 m), it is essential to design a stiff support structure with high eigenfrequencies. In the design stage, displacement frequency responses are calculated in a modal based linear dynamic analysis using finite element method to ensure vibration amplitude below 1 micrometer. Special considerations are given to the modelling of linear guide systems, as they introduce nonlinear support conditions and need to be adequately simplified in the calculation. After completing the second bunch compressor (BC2) assembly, vibration measurements were performed. Finally, the validation of the numerical model by measurement results will be presented.

INTRODUCTION

BC2 consists of two welded steel girder structures (Figure 1), which are supported on granite tables. Each granite table is fixed to floor by three or four rigid jacks with built-in commercial levelling wedge elements.

From the middle table girders can be moved together with dipole 2 and 3 transversally 505 mm. With a girder length of 7.7 m (dipole separation), the bending angle is 3.8 degree. Girder is supported on pivot bearing for rotation. A linear stage is used for transversal movement. A second linear stage for longitudinal movement is rotatable against the first stage (Figure 2).

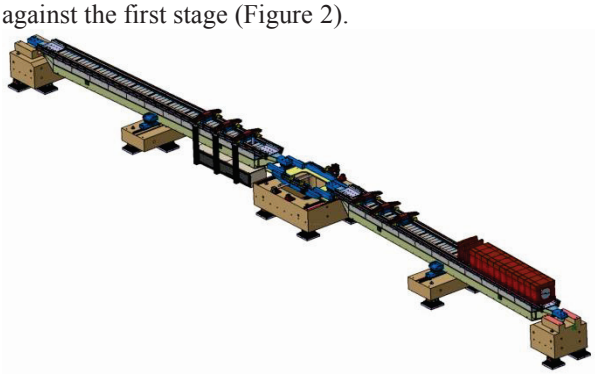

Figure 1: SwissFEL BC2.

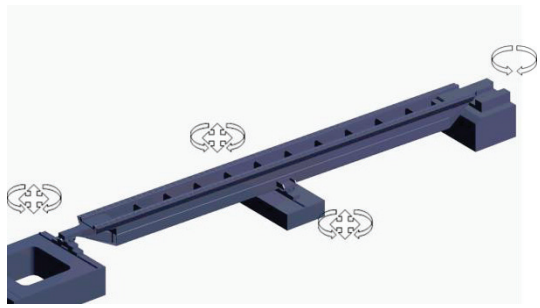

Figure 2: Girder kinematics.

The first steel girder in the beam direction has a total weight of 3'200 kg, including 1'900 kg lead and polyethylene (PE) material for radiation shielding. To ensure the proper operation of accelerator components (BPM and magnets) on the girder, a mechanical vibrational stability below 1 μm is required.

In order to fulfil the stringent design goal of a long and movable steel girder which is in the meantime vibrational stable, finite element (FE) analysis has been performed in the design phase. The modelling is finally verified by vibration measurement.

FINITE ELEMENT MODELLING

The girder structure is welded from rectangular hollow steel sections and steel plates with thickness from 5 mm to 10 mm. Shell elements with 6 degrees of freedom (DOF), three rotational and three translational, have been employed for efficient presentation of in-plane and bending stiffness. Point mass elements have been used to represent shielding masses in 3D space. The voluminous support consoles have been modelled with 3D solid elements (Figure 3). The linear contact connecting shell and solid elements is defined by Multi-Point-Constraint (MPC) formulation with the coupling of rotational DOF to translational DOF.

The FE model has following parameters:

Number of nodes:	329'000
Number of elements:	216'000
Incl. shell elements:	122'000
Degrees of freedom:	1'326'000

Linear static and dynamic calculations have been performed with finite element program ANSYS. FE Modell was prepared from CAD geometry with SpaceClaim Direct modeler.

† xinyu.wang@psi.ch

ISBN: 978-3-95450-188-5 doi:10.18429/JACoW-MEDSI2016-TUCA03

ESTIMATION OF TEMPERATURE FLUCTUATIONS HARSHNESS REGARDING STABILITY OF STRUCTURES IN THE NANOMETER RANGE

N. Jobert†, F. Alves, S. Kubsky, Synchrotron SOLEIL, Saint Aubin, France

Abstract

Along with mechanical vibrations, thermal-mechanical deformations are the primary contributor to positional and pointing errors. This paper deals with specific analysis and interpretation difficulties encountered when designing and validating ultimate stability systems (i.e. in the range of a few nm). When attempting to design such systems, it is not sufficient to simply reduce overall temperature fluctuations, but it becomes necessary to target efforts at the specific components that are detrimental to the dimensional stability of the system. This calls for an integrated approach where temperature measurements, data analysis and reduction are performed in conjunction with a priori knowledge of the thermal-mechanical system behaviour.

1 INTRODUCTION

When dealing with high-accuracy devices, thermally induced distortions are a key contributor to the overall positional and pointing performance of the system. While it is both correct and obvious that the smaller the temperature fluctuations, the more stable the system will be, there is some hidden complexity in the subject.

Firstly, not all temperature fluctuations will actually distort the structure: very short period (i.e. 'fast') variations will not propagate far into the structure, and will induce very little change in overall dimensions. Nevertheless, they can induce local distortions, hence small positional errors but possibly larger pointing errors. Conversely, very long period (i.e. slow') temperatures fluctuations will result in quasi uniform temperature fields and therefore will efficiently change overall dimensions but possibly induce lower pointing errors.

Secondly, there is always some randomness in temperature fluctuations, which somehow obscures the actual severity of a given environment. This randomness occurs timewise, but also space-wise. For a highly stable environment, the random part of the temperature field has magnitude comparable or even higher to that of the general trend, and simply discarding this part becomes questionable.

Surprisingly, no harshness indicator has been developed that could help quantifying the actual severity of a given realistic thermal environment. It is the objective of this paper to provide some insight on the various phenomena at play. Additionally, we propose a simple yet efficient numerical method allowing the evaluation of actual structural responses to any realistic thermal environment. It is the wish of the authors that such approach should help in making more rational decisions, either at design or commissioning phases.

†nicolas.jobert@synchrotron-soleil.fr

2 ENGINEERING DIFFICULTIES

Thermal Mechanical Susceptibility: Intuition vs Quantitative Analysis

To illustrate the relative efficiency of various thermal fluctuations, it is instructive to start with a simple support structure: the following test-case is nearly academic, and merely aims at providing some feeling for the subject at hand. We assume an L-shaped bracket support structure which is a most desirable shape regarding vibrational stability because of its high stiffness/weight ratio along every axis (Figure 1). The engineering question is: "What about the actual thermal mechanical susceptibility of such a system?"

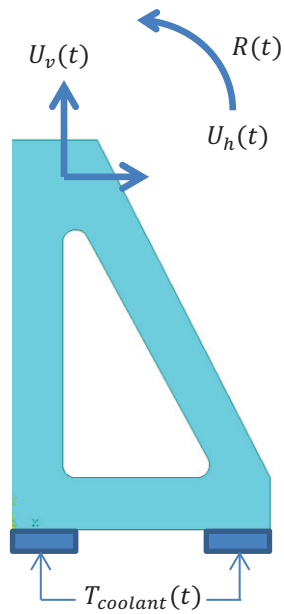

Figure 1: Academic test case.

Clearly, the answer depends on the heat path considered. Generally speaking, this can be either convection through surrounding medium (if any), radiation to the surrounding cavity, or convection to the heat sink. To further simplify the discussion, we will only consider the latter*. Also, we assume a very efficient heat transfer at bottom (which is what we aim for in real life), so that the boundary takes on nearly the same temperature as the coolant fluid.

* Note that, by principle, this is the only heat path that cannot be weakened and therefore ultimate stability will be governed by this disturbance source.

ISBN: 978-3-95450-188-5 doi:10.18429/JACoW-MEDSI2016-TUCA05

THE NEW HIGH DYNAMICS DCM FOR SIRIUS

R. R. Geraldes†, R. M. Caliari, G. B. Z. L. Moreno, L. Sanfelici, M. Saveri Silva,
N. M. Souza Neto, H. C. N. Tolentino, H. Westfahl Jr., LNLS, CNPEM, Campinas, Brazil
T. A. M. Ruijl, R. M. Schneider, MI Partners, Eindhoven, Netherlands

Abstract

The monochromator is known to be one of the most critical optical elements of a synchrotron beamline, since it directly affects the beam quality with respect to energy and position. Naturally, the new 4th generation machines, with emittances in the range of order of 100 pm rad, require even higher stability performances, in spite of the still conflicting factors such as high power loads, power load variation, and vibration sources. A new high-dynamics DCM (Double Crystal Monochromator) is under development at the Brazilian Synchrotron Light Laboratory for the future X-ray undulator and superbend beamlines of Sirius, the new Brazilian 4th generation synchrotron [1]. Aiming at an inter-crystal stability of a few tens of nrad (even during the Bragg angle motion for flyscans) and considering the limitations of the current DCM implementations, several aspects of the DCM engineering are being revisited. In order to achieve a highly repeatable dynamic system, with a servocontrol bandwidth in the range of 200 Hz to 300 Hz, solutions are proposed for a few topics, including: actuators and guides, metrology and feedback, LN2 indirect cooling, crystal clamping, thermal management and shielding. The concept of this high-dynamics DCM will be presented.

INTRODUCTION

In the recent years it has become clear to the synchrotron community that the stability performance of DCMs would turn out to be one of the main bottlenecks in the overall performance of many X-rays beamlines, particularly for the new generation of machines, the so called Diffraction Limit Storage Rings (DLSR). This is because the instabilities in the DCM affect the position and/or the effective size of the virtual source, and, consequently, the spot size and/or the position of the beam at the sample. It is thus imperative that the virtual source instability is kept within a small fraction of the source size. The angular instability between the two crystals is the most critical one because its effects on the virtual source scales with the lever-arm between the monochromator and the source (L_0 in Fig. 1). In the DLSR, the sources are expected to have only a few microns, whereas the typical distances between the source and the monochromator is of tens of meters. Due to that, the stability between crystals is required to be within a few nrad. This scenario has motivated numerous special forums in conferences and even dedicated workshops, as the *ESRF DCM Workshop* in 2014. Since then, an effort has been made by suppliers and the synchrotron engineering community, trying to upgrade the existing systems and come up with new solutions. This work, which is the outcome of such effort at the Brazilian Synchrotron for Sirius beamlines, presents the advanced conceptual design of a DCM with high servo bandwidth closed-loop control. Sirius is in construction phase and the beginning of machine commissioning is planned for mid-2018 [2]. Therefore, a functioning prototype of the DCM has been planned for mid-2017.

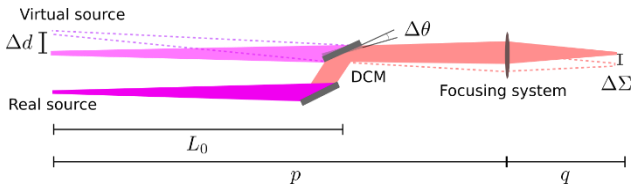

Figure 1: Effects of DCM instabilities in the virtual source.

STATE OF THE ART

Many of the existing DCMs around the world have been recently characterized with respect to stability. Representative cases were shown at the ESRF DCM Workshop, as the one by Ilya Sergeev, in which none of Petra III and ESRF DCMs performed below 100 $nrad_{RMS}$ [3]. Table 1 shows some of the most recent results of one of the state-of-the-art commercial DCMs [4]. The absolute pitch tells the angular instability of the second crystal, whereas the relative pitch shows the instability between the two crystals. The latter not only may affect the monochromatic beam with respect to flux, depending on the energy selection characteristics of the crystals, but, as mentioned, certainly affects the virtual source size and/or position, depending on the acquisition rate and sampling time of the experiments.

Table 1: Pitch Vibrations of State-of-the-Art DCM in the Range between 0 to 2.5 kHz (as reported in [4])

Experimental Condition	RMS (nrad)
Absolute pitch with servoing Bragg	278
Absolute pitch w/ braked Bragg	92
Relative pitch with servoing Bragg	100
Relative pitch w/ braked Bragg	48

From Table 1, it can be seen that this instrument performs around 50 nrad for the braked rotary stage. However, even this lowest value is still too high for the recent and future specs. In addition, given the fast development of detectors and electronics, there has been a lot interest in flyscan experiments, which requires high stability levels to be kept not only with the servoing Bragg, but in actual motion.

SPECIFICATIONS

The project of the DCM at LNLS has started with the case of a beamline with a planar x-ray undulator as the radiation source. Having the DCM at the distance of about 30 m from the source, Fig. 2 shows the variation of the position of the virtual source as a function of the variation of

†renan.geraldes@lnls.br

ISBN: 978-3-95450-188-5 doi:10.18429/JACoW-MEDSI2016-TUCA06

THE GIRDER SYSTEM FOR THE NEW ESRF STORAGE RING

Filippo Cianciosi, Thierry Brochard, Philippe Marion, Loys Goirand, Yves Dabin, Marc Lesourd, Lin Zhang
ESRF-European Synchrotron Radiation Facility, 71 Avenue des Martyrs, 38000 Grenoble, France

Abstract

The ESRF is proceeding with the design and procurement of its new low emittance storage ring (Extremely Brilliant Source project).

This completely new storage ring requires a high performance support system, providing high stability (first resonance frequency about 50Hz) and a precise alignment capability (50µm, manual in transverse direction and motorized in the vertical one).

In order to meet these requirements we decided to support the magnets of each of the 32 cells of the synchrotron with four identical girders that was considered the best compromise between cost, complexity and performances. Each of the resulting 128 girders is 5.1m long, carries about seven tons of magnets, and its weight including fixed basement and adjusting system is six tons.

The adjustment system relies on modified commercial wedges; their stiffness was evaluated through laboratory tests. The FEA calculations carried out to optimize the design will be presented, together with the results obtained on a complete prototype girder system which was built and extensively tested and confirmed the modal calculations..

THE NEW LAYOUT

The present machine presents the lattice called Double Bend Achromat, with two bending magnets and 3 groups of optical magnets in each of its 32 cells. Only the groups of optical magnets are supported by adjustable girders. The dipole, less demanding in term of positiong precision, are placed on fixed supports. The lattice of the new machine is a Hybrid Seven Bends Achromat, constituted by 4 dipoles, 3 dipoles-quadrupoles and 24 optical magnets (Figure 1).

This complexity make unpractical the choice of different support for the different magnets, especially considering that the dipoles are relatively small and light. The solution of supporting all the machine on adjustable girders has been taken. The disposition of the magnets in the lattice led us to divide each of the 32 cells in 4 groups of magnets with almost the same weight (6 Tons) and length (5.1m), and support each of them with an adjustable girder.

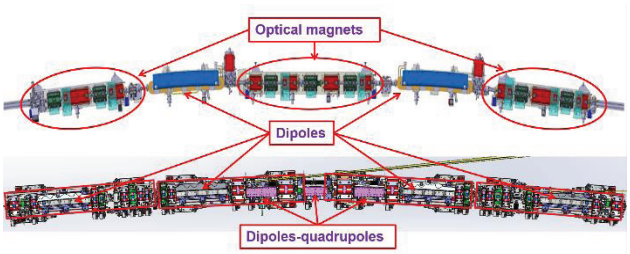

Figure 1: Lattice.

SPECIFICATIONS

The requirement of the girder are summarized in Table *1*.

The positioning precision is due to the physics of the machine and it will not be discussed here.

The re-alignment frequency is linked to the long-term movements and deformations of the ESRF site. During the last years movements of several mm were registered especially in the vertical direction, therefore a fast and convenient alignment method of the machine is required.

The choice of the target value of the first resonance frequency was based upon practical considerations about the behaviour of existing structures and the amplitude of the vibrations present on the site. In theory the important value is the amplification factor of the ground movement as a function of the frequency, but this is nearly impossible to calculate. However this amplification is usually very low for frequency below the 1st resonance. As the amplitude of the ground vibrations is significant mainly for frequency below 30Hz a value of 35Hz was specified for the 1st one.

Table 1: Specifications

Aspect	Value
Length	5.1m
Payload	6-7 Ton
Positioning precision	50µm (Vertical-transv.)
Positioning precision	1mm (Longitudinal)
Alignment freq.	2 times/year
Alignment method	Motorized (Vertical)
Alignment method	Manual (Transv.-long.)
First resonance frequency	35 Hz (minimum)
Planarity of top surface	+/-50 µm

GIRDER DESIGN

Several configurations were considered, with 3 and 4 supports. Three supports permit to not over define statically the girder, but as this solution does not permit to obtain the requested first resonance frequency, we decided to adopt a 4 supports system for this reason. The four supports version hallow holding the load in the vertical direction but not blocking the movements in the horizontal one. Two jacks are used to adjust the transversal position of the girder, while simple pushing screws set the longitudinal one. Figure 2 shows the design of the machine.

ISBN: 978-3-95450-188-5 doi:10.18429/JACoW-MEDSI2016-TUPE01

DMM THERMAL MECHANICAL DESIGN

J. H. Kelly, Diamond Light Source, UK

Abstract

A Double Multilayer Monochromator (DMM) was designed in-house for the VMXi beamline. Thermal mechanical finite element analysis was performed to design a novel optic geometry, employing In/Ga eutectic cooling. The integration of a DMM into the existing beamline required additional power management components, such as a low energy power filter, a power detector and compact CuCrZr masks. This paper describes the thermal management challenges and their solutions. The DMM has been fully commissioned and is operational within the original I02 beamline.

INTRODUCTION

The in-situ Versatile Macromolecular Crystallography (VMXi) Beamline is effectively a new beamline which has been built through the original Diamond Phase one beamline I02. The new fully automated endstation has been built downstream of the original within a novel mini-hutch. A new experimental cabin was built to allow I02 operation during the majority of the VMXi build. The insertion device (ID) is planned to be upgraded from a U23 to a Cryo-cooled permanent magnet undulator (CPMU) giving a factor of 3 useful flux increase. The DMM was designed and installed to give an additional 60 fold increase in flux as compared to a Si(111) DCM [1]. The dramatic increase in flux necessitated a detailed evaluation of the power management within the beamline. This paper details the new power management components designed and procured for the VMXi upgrade.

MULTILAYER EUTECTIC COOLING

The DMM was designed to operate over the energy range of 10 – 25 keV using two multilayer stripes 2.0 nm and a 2.4 nm (See Figure 1). The worst case was assumed to be at 12 keV as the ID is optimised for flux at this energy. This is also a larger angle of incidence and hence small foot print. The absorbed power with the future CPMU K2.04, 500mA would be ~ 480W over a 97.5 x 3.4 mm foot print. This flux density would not be challenging for a cryocooled silicon optic; however concerns over the stability of the deposited layer under thermal contraction lead to a water cooled solution. To minimise turbulence induced vibration, a eutectic bath method was chosen. Numerous geometries were investigated using ANSYS but only the chosen one is presented here.

Two eutectic troughs were machined through the top surface of the bounce down first optic. The original aim of separating the cooling channels by slotting the silicon, was to mimic the ESRF mirror cooling model, of side cooling near the optical surface [2]. The troughs also act as temperature stabilised stiffening ribs to the optical surface. When the heatload is not central, which is always the case for the two stripe design a variation of tangential radius across the foot print is introduced but the effect is small enough to be neglected.

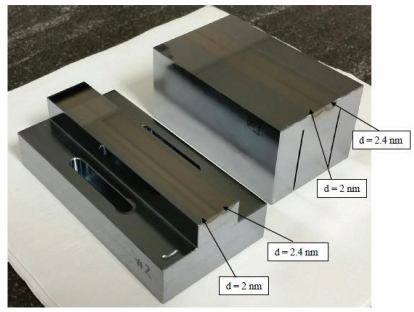

Figure 1: VMXi DMM Multilayer Optics procured from Rigaku, 1st multilayer on the right shown upside-down.

The use of an average young's modulus and poison ratio has been shown to give a good approximation to anisotropic material properties for modelling silicon Zhang [3]; however the non-standard nature of this design may make this finding invalid. The final optimisation was done using the anisotropic material properties. An FEA check was performed see the effect of aligning the X direction with the ML normal and the Y direction normal to the front, side and at ~30º. As expected from the cubic symmetry and Zhang [3], the results are identical for the Y axis aligned with the sides but differ at other angles. The Si(100) surface plane, Si(010) side plane, was found to give the best results and so was used throughout this study.

The eutectic trough was originally designed to come down to within 5 mm of the optical surface; however after manufacturing issues this was increased to 10 mm. This compromised the tangential slope error (fitted parabola radius 50 km to 22 km, 152W absorbed power) but made the optic significantly more robust.

A eutectic wetted area heat transfer coefficient (HTC) of 10,000 W/m^{2}K was chosen after performing a literature review [4-8]. Prandtl, Nusselt and Reynolds numbers extracted from these sources were used to calculate a range of HTCs. This appears to be a reasonable value for natural convection, which has also been used during the design of other instruments for DLS. The optic tangential slope error was relatively insensitive to HTC i.e. double HTC reduced the deformation by 15%. The eutectic troughs were filled to a depth of ~ 10mm. This was deep enough to ensure that the cooling fins remained immersed over the angular range; while shallow enough to minimise the possibility of splashing upon pump-down. After filling the troughs and inserting the Ni plated Cu fins the water chiller was run with a set-point of 50ºC for a few hours. It has been found that this reduces the eutectic viscosity and improves wetting.

ISBN: 978-3-95450-188-5 doi:10.18429/JACoW-MEDSI2016-TUPE02

EXPERIMENTAL VALIDATED CFD ANALYSIS ON HELIUM DISCHARGE

J.C. Chang, Y.C. Chang, F.Z. Hsiao, S.P. Kao, H.C. Li, W.R. Liao, C.Y. Liu
National Synchrotron Radiation Research Center, Hsinchu, Taiwan

Abstract

National Synchrotron Radiation Research Center in Taiwan (NSRRC) had set up three cryogenic systems to provide liquid helium to superconducting radio-frequency (SRF) cavities, insertion devices, and highly brilliant hard X-ray. The first one could produce liquid helium 134 LPH, with maximum cooling capacity of 469 W at 4.5 K. The second one could produce liquid helium 138 LPH, with maximum cooling capacity of 475 W at 4.5 K. The third one could produce liquid helium 239 LPH, with maximum cooling capacity of 890 W at 4.5 K. However, large liquid helium discharge in a closed space will cause personnel danger of lack of oxygen. We performed Computational Fluid Dynamic (CFD) simulation to analyse helium discharge through a SRF cavity in the Taiwan Light Source (TPS) tunnel. We simulated cases of helium discharge flow rates from 0.1 kg/s to 4.2 kg/s with and without fresh air supplied from the air conditioning system. We also set up both physical and numerical models within a space of 2.4m in length, 1.2m in width and 0.8m in height with nitrogen discharge inside to validate the CFD simulation.

INTRODUCTION

Liquid helium for transferring cooling power from the cryogenic plant to the magnets and SRF cavities had been widely applied on the advanced large superconducting particle accelerators. Those superconducting particle accelerators are typically designed in elongated structures and require wide distributed cryogenic system. For requirements of high stable and reliable operation, many efforts have been put into the improvement and modification of the cryogenic system.

One cryogen distribution system has been installed and commissioned to transfer liquid nitrogen and LHe from storage dewars to superconducting radio-frequency (SRF) cavities at TPS. [1] The cryogenic system has maximum cooling capacity 890 W with associated compressors, an oil-removal system, four helium buffer tanks, one 7000-L Dewar, gaseous helium piping at room temperature, transfer lines to distribute helium, and a transfer system for liquid nitrogen. Currently, there are two SRF cavities are located one upstream and one downstream of the distribution valve box.

Personnel safety is another critical issue of the cryogenic system. Once large liquid helium (LHe) was released on the atmospheric tunnel, the volume of helium will expand several hundred times in short time due to sudden change of its density. Therefore, cold helium discharge test in the LHC tunnel at CERN had been experimentally conducted. [2] Numerical simulation of cold helium safety discharges had also been performed at European Spallation Source (ESS). [3] In this study, we applied numerical simulation to analyse helium discharge through a SRF cavity in the TPS tunnel. We also set up a small experiment to validate the numerical simulation.

NUMERICAL SIMULATION

CFD began from the early 30s of the 20th century to solve the linearized potential equations with 2D methods (1972). As rapid development of numerical analysis and computer science, CFD has more advantage of well adaptation than traditional theoretical analysis and experimental measurements. Nowadays, CFD has been widely applied in many fields. Detailed 3D numerical simulation was performed using a commercial general purpose CFD code ANASYS Fluent.

Governing Equation

We set our simulated model as a 3D turbulent flow in this study. The basic governing equations include the continuity equation, the momentum equation and the energy equation.

We apply the k-ε turbulence model and SIMPLEC to solve the velocity and pressure problem.

Mass conservation equation (continuity equation)

$$\frac{\partial \rho}{\partial t} + \nabla \cdot (\rho \mathbf{u}) = 0 \quad (1)$$

where ρ is density of fluid, t is time and $\mathbf{u}$ refers to fluid velocity vector.

Momentum conservation equation

$$\frac{\partial (\rho \mathbf{u})}{\partial t} + \nabla \cdot (\rho \mathbf{u}\mathbf{u}) = -\nabla p + \rho \mathbf{g} + \nabla \cdot (\mu \nabla \mathbf{u}) - \nabla \cdot \tau_t \quad (2)$$

where p is pressure, $\mathbf{g}$ is vector of gravitational acceleration, μ is dynamic viscosity of fluid, and τ_t is divergence of the turbulent stresses which accounts for auxiliary stress due to velocity fluctuations.

Energy conservation equation

$$\frac{\partial (\rho e)}{\partial t} + \nabla \cdot ((\rho e + p)\mathbf{u}) = \nabla \cdot \left(k \nabla T - \sum_j h_j \mathbf{j}_j \right) \quad (3)$$

where e is the specific internal energy, T is fluid temperature, k is heat conductivity, h is the specific enthalpy of fluid, $\mathbf{j}_j$ is the mass flux. In this study, RNG (Re-Normalisation Group) κ - ε turbulent model was used.

Geometry and Grid Generation

A detailed 3D model of 2 of 24 sections of the TPS tunnel, where a SRF cavity is located, was built for the numerical simulation. The space of the simulation zone is about 860.5 m^3. The geometry was built according to the dimensions of the tunnel, as shown in Fig.1. We also take

ISBN: 978-3-95450-188-5 doi:10.18429/JACoW-MEDSI2016-TUPE04

COHERENT SOFT X-RAY EPU VACUUM CHAMBER THERMAL ANALYSIS FOR SYNCHROTRON RADIATION PROTECTION*

Huston Fernandes, Charles Kitegi, David Harder, Dean Hidas, Jim Rank, Marco Musardo, Peter Cappadoro and Toshi Tanabe. Brookhaven National Laboratory, Upton, NY 11973 U.S.A.

Abstract

The purpose of this study was to determine the effect of beam mis-steering, on the temperature of the vacuum chamber. The chamber used for this study was for the Coherent Soft X-Ray (CSX) Elliptically Polarizing Undulator (EPU). Finite Element Analysis was conducted on the vacuum chamber to determine the temperature distribution on the chamber for set values of beam mis-steer, for NSLS-II. These results were then compared with on-site temperature measurements taken using RTD's, as well as thermal sensitive cameras. The accuracy of these results was analyzed and further FEA studies were proposed for steeper beam mis-steers and beam offsets.

INTRODUCTION

The Coherent Soft X-Ray (CSX) Elliptical Polar Undulator (EPU) beam line has two EPU's at a canted angle of 0.16 mrad. The effect of synchrotron radiation of the upstream device was studied on the vacuum chamber downstream. A single vacuum chamber made of Aluminum, as indicated in Fig. 1, covers the entire length of both the EPU's. The maximum aperture of the vacuum chamber is 8 mm as indicated in Figure 2.

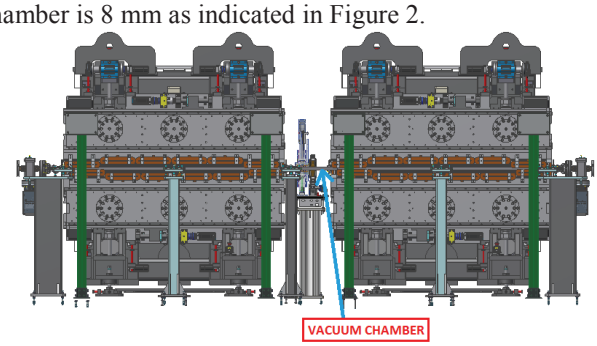

Figure 1: CSX EPU Vacuum Chamber.

The total on axis power of both the devices is around 10.1 KW [2].

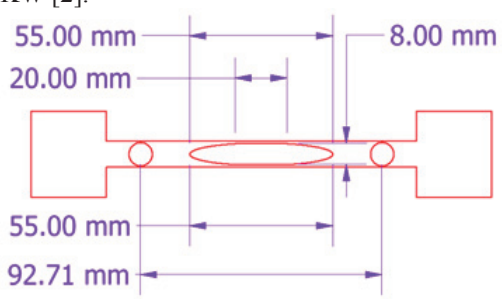

Figure 2: CSX EPU Vacuum Chamber Cross Section.

Since the effect of beam mis-steer of the upstream device is studied on the vacuum chamber, heat fluxes for 0.05 mm beam offset and 0.2 mrad angle beam mis-steer were studied. These offset and mis-steer limits were obtained from the maximum allowable active interlock limits set. After determining the close correlation of the FEA results to the actual measurements, FEA analysis of larger beam mis-steer angles were determined. The maximum beam mis-steer studied was 0.7 mrad.

HEAT LOAD CALCULATIONS

SRW code was used to compute the heat load on the wall of the vacuum chamber. Figure 3 shows the magnetic structure of the CSX EPU.

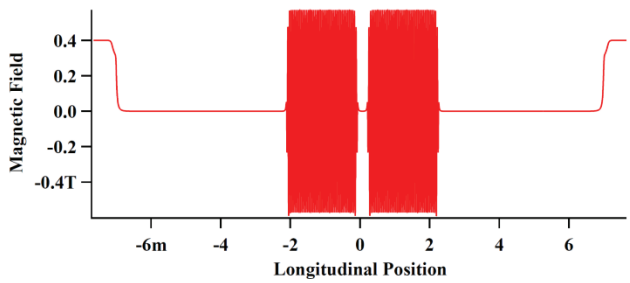

Figure 3: Magnetic Structure of CSX EPU.

The straight section has two EPU's of magnetic length 2 meters placed next to each other with a canting magnet in-between.

Table 1: CSX EPU Parameters Used for Heat Load Calculations

CSX EPU Properties	
Length	2x2 meters
Canted Angle	0.16 mrad
K_{eff}	4.34
Power Total	10.1 KW
Straight	Low Beta
Fan angle (V)	0.79 mrad
Fan angle (H)	0.76 mrad

Table 1 indicates the characteristics of CSX EPU [1]. Figure 4 indicates the power density (heat flux) in SRW code (using Igor-Pro) for synchrotron radiation, on the wall of the vacuum chamber, using a 0.2 mrad mis-steer.

ISBN: 978-3-95450-188-5 doi:10.18429/JACoW-MEDSI2016-TUPE05

NUMERICAL SIMULATION OF THE ALBA SYNCHROTRON LIGHT SOURCE COOLING SYSTEM RESPONSE FOR FAILURE PREVENTION

X. Escaler*, Universitat Politècnica de Catalunya, Barcelona, Spain
J.J. Casas†, C. Colldelram‡, M. Quispe§, M. Prieto#, ALBA Synchrotron Light Source, Cerdanyola del Vallés, Spain

Abstract

The ALBA Synchrotron Light Source cooling system is designed with a common return pipe that interconnects the four consumption rings. Such configuration is believed to compromise its optimal operation. To understand its thermo-fluid dynamic behaviour, a detailed 1D model has been built comprising all the components such as the pipes, fittings, bends, valves, pumping stations, heat exchangers and so on, and the various regulation mechanisms. Preliminarily, the model results in steady state operating conditions have been compared with experimental measurements and the maximum deviations have been found below 13%. Then, a series of transient numerical simulations have been carried out to determine the system response. Specifically, effects of the blockage and leakage of a consumption line as well as the increase and decrease of heat duty for the tunnel rings have been investigated. As a result, the stability of the system has been evaluated and the operational limits have been estimated in front of hydraulic and thermal load variations. Moreover, particular behaviours have been identified which can be used to design monitoring and control strategies to prevent unexpected failures.

INTRODUCTION

The ALBA Synchrotron Light Source cooling system presents a common return pipe that interconnects the four consumption rings as outlined in Fig. 1. This design configuration introduces complexity to the system behaviour because strong interdependency among them exists.

As clearly exposed by Swetin [1], it is imperative that water flow and temperature are both maintained with a high degree of reliability because most accelerator components are interlocked. In particular, it is necessary to understand the system behaviour when facing typical piping problems like blockages or leakages to prevent failures. Moreover, the capacity of the system to respond against temporary changes in the required thermal loads must be checked out.

The motivation of such knowledge is to develop and apply correct monitoring and maintenance strategies to optimise system operation and reliability. It is also necessary in order to allow upgrades that improve reliability and integrate new operating parameters.

* escaler@mf.upc.edu
† jcasas@cells.es
‡ ccolldelram@cells.es
§ mquispe@cell.es
# mprieto@cells.es

Consequently, a numerical simulation appears as an economic and reliable procedure if a preliminary adjustment is carried out to guarantee the accuracy. For that purpose, the Flowmaster® software has been chosen because it has been successfully used to simulate complex fluid networks and advanced control systems as demonstrated in the work of Sprengel [2].

NUMERICAL MODEL

A complete model of the generation side of the cooling system has been built up with typical elements such as pipes, junctions, bends, transitions and valves. More particular elements are the pumps, the heat exchangers, the storage tank and the expansion tank. The consumption side, comprising the four rings, has been simplified due to its complexity to a heat exchanger component with the corresponding total heat duty. The properties of each component have been defined from information provided by the manufacturer as well as from data obtained by visual inspections and measurements in-situ. Details and images of the current model can be found in [3].

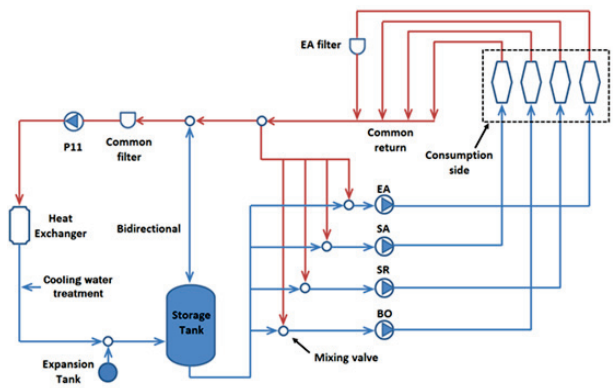

Figure 1: Outline of the ALBA cooling system.

The main regulation systems which correspond to the three-way valves (V3V's) for mixed water temperature at 23 °C, the heat exchangers (EX07) for cooling at 21 °C and the pump engine frequency converters for limiting the delivery pressures have been modelled with PID elements. The four pumping stations have been named P07, P08, P09 and P10 for the Experimental Area (EA), the Storage (SR), the Booster (BO) and the Service Area (SA) consumption rings, respectively.

In order to certify the accuracy of the model, the simulated results under steady state conditions were compared with on-site measured data indicated in Table 1. The hydraulic variables showed maximum deviations around 6 % and the thermal variables around 13%.

ISBN: 978-3-95450-188-5 doi:10.18429/JACoW-MEDSI2016-TUPE06

THERMO-FLUID NUMERICAL SIMULATION OF THE CROTCH ABSORBERS' COOLING PINHOLES FOR ALBA STORAGE RING

X. Escaler*, V. Arbó†, Universitat Politècnica de Catalunya, Barcelona, Spain
J.J. Casas‡, C. Colldelram§, M. Quispe#, M. Prieto$, ALBA Synchrotron Light Source, Cerdanyola del Vallés, Spain

Abstract

The ALBA Synchrotron Light Facility crotch absorbers, that remove the unused storage ring radiation, incorporate an internal cooling system composed by a number of parallel pinholes and by the corresponding stainless steel inner tubes inserted into each of them. Water flows in the resulting annular sections to evacuate the total heat power. Around each inner tube, a spiral wire is fixed along the whole length with a given pitch height in order to enhance the convection heat transfer. The influence of several design parameters on the absorber thermo-fluid behaviour has been evaluated by means of the CFD software ANSYS CFX®. In particular, the wall heat transfer coefficients and the pressure losses through a single pinhole have been evaluated for a range of different flow rates and pitch heights. Moreover, some modifications of the end wall geometry have been simulated as well as the effect of reversing the flow direction inside the channels. Finally, the critical crotch absorber type 3 has also been simulated and the limiting pitch height-flow rate combinations have been found based on the available driving pressure of the cooling system.

INTRODUCTION

Most of the synchrotron radiation generated by the bending magnets in the Storage Ring (around 95%) is absorbed in the crotch absorbers. An important challenge in the engineering of the crotch absorbers is the ability to withstand the temperature and thermal stress induced by the high heat load in the component materials within the accepted safety limits. For the critical crotch absorbers the peak linear and surface power densities at normal incidence are about 64.4 W/mm and 246.2 W/mm^2 respectively, and the maximum total power is about 6.78 kW as presented in [1].

Due to this thermal load, the crotch absorber must be carefully designed to guarantee longevity and good performance. A flow of water at 23 °C circulates inside the absorber through a series of pinholes to cool it. Hence extensive Computational Fluid Dynamics (CFD) work has been conducted on various aspects of a single pinhole design such as the spiral wire pitch height, the flow rate, the direction of the flow and the end wall geometry. This work is of interest since few information is available for design, only the empirical correlations from [2] provide the wall heat transfer coefficients for a couple of pitch heights in a similar pinhole design but with different dimensions. Based on the previous results, several pinholes connected in series have also been simulated.

The current design of ALBA crotch absorbers is shown in Fig. 1. A detail of the spiral wire at the end wall and the two possible flow directions, forward and reverse, are indicated in Fig. 2.

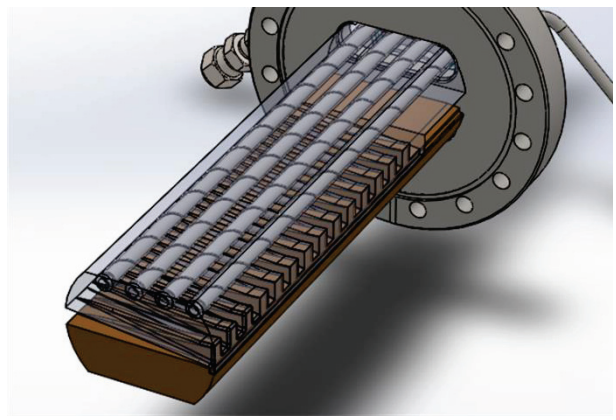

Figure 1: Transparent view of a crotch absorber to visualize the internal cooling pinholes with the spiral wire.

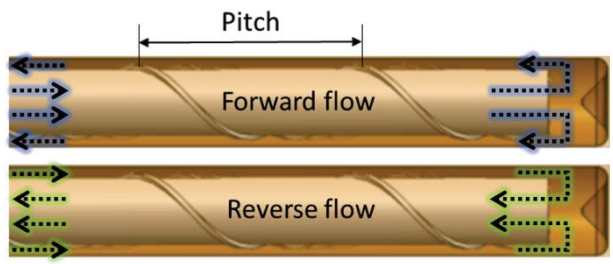

Figure 2: Pitch height of the spiral wire. Forward and reverse flow rate directions inside the pinholes.

CFD MODEL

A mesh sensitivity analysis has been carried out to identify the optimal mesh for the model. As a result, a final mesh of about 1.5 M elements with good quality has been used for a single pinhole. The total thermal load has been uniformly distributed along the contact wall surface with the fluid. At the inlet, the mass flow rate has been imposed ranging from 0.03 to 0.09 kg/s. At the outlet, the boundary condition has been set constant to a relative

* escaler@mf.upc.edu
† victorarbo@gmail.com
‡ jcasas@cells.es
§ ccolldelram@cells.es
# mquispe@cell.es
$ mprieto@cells.es

ISBN: 978-3-95450-188-5 doi:10.18429/JACoW-MEDSI2016-TUPE08

FINITE ELEMENT ANALYSIS OF A PHOTON ABSORBER BASED ON VOLUMETRIC ABSORPTION OF THE PHOTON BEAM

K. J. Suthar* and P. Den Hartog, Advanced Photon Source Engineering Support Division, Argonne National Laboratory, Lemont, USA

Abstract

A photon absorber is a device used to protect vacuum chambers and other hardware from synchrotron radiation by intercepting unwanted radiation, converting its energy to heat, and then removing that heat. Design of a photon absorber requires careful consideration of the high temperatures and steep thermal gradients that are possible with highly localized absorption of these photons. For next-generation machines, like the multi-bend achromat envisioned for the APS Upgrade (APS-U), a designer is likely to be simultaneously faced with more intense synchrotron radiation beams, more limited available space, and closer proximity to the particle beam than have been designed for in the past. Volumetric absorption of synchrotron radiation, which makes use of materials that are semi-transparent to x-rays, is an attractive option which gives the designer greater freedom by spreading the heat load due to the absorbed photons. Volumetric absorption may also help to reduce residual gas pressures in a vacuum system by reducing the photon-stimulated desorption that results from photons reflected by the incident absorber surface. This paper describes simulations which were performed to evaluate the benefit of utilizing volumetric absorption for a conceptual "crotch" photon absorber for the APS Upgrade (APS-U), so-called because of its location in the vacuum system where the chamber is forked to permit x-ray extraction. Results of these simulations show clear benefits of volumetric photon absorption and suggest that such an approach may help to substantially relax constraints on the size, shape, and materials used for such absorbers.

VOLUMETRIC ABSORPTION

Two crotch absorbers are planned for each APS-U storage ring sector. These are expected to intercept roughly 1-3 kW each with power densities, as would be intercepted on a normally-intercepting surface, that approach 100 watts/mm^2. Conventionally, photon absorbers are made using high opacity and high thermal conductivity materials such as copper and GlidCop™ which cause the heat load to be concentrated on the absorber surfaces. A designer typically struggles with reducing the incident angle of those surfaces and increasing the efficiency of cooling to those surfaces as much as possible to manage the thermal stresses that result. In addition, the high reflectivity of these materials to x-rays, coupled with the grazing angles, causes scattering of a considerable fraction of incident photons which can then be a significant driver of photon-stimulated gas desorption. Finally, the high water flow rates required to maintain surface temperatures at safe levels can introduce vibration that may upset critical, precisely-aligned hardware in the accelerator.

A potential solution is the use of an absorber which is semi-transparent to incident x-rays. Such an arrangement allows the heat load into the absorber to be gradually deposited in the body of the component, reducing the associated thermal stresses. In doing so, a designer can find a solution which is more compact than would otherwise be possible. Another approach is to combine an opaque absorbing body with a more transparent, but thermally conductive, material. Doing so similarly limits the resulting temperature rise of absorber materials by allowing the heat generated on the opaque body to be more effectively conducted away.

Such approaches have three distinct advantages over a conventional, surface-absorbing design:

1. The material temperatures and the thermal gradients may be reduced, reducing potentially-damaging thermal stresses, fatigue, and structural softening.
2. Reflection of photons may be reduced, thus reducing the outgassing associated with photon-stimulated desorption.
3. Heat transfer may be more efficient due to overall greater proximity of cooling to the heat load, relaxing water flow requirements.

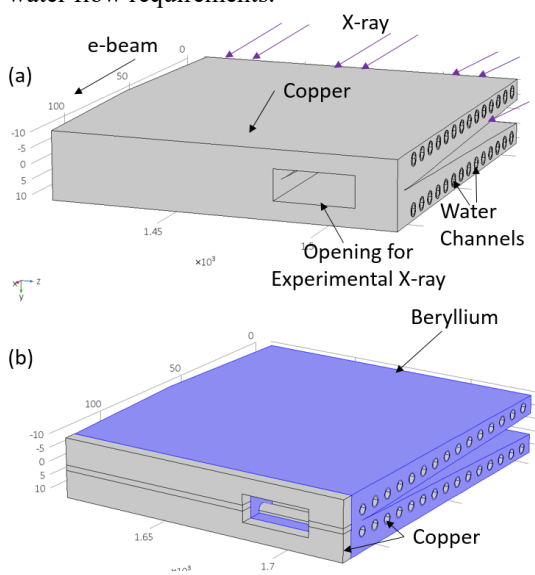

Figure 1: Conceptual APS-U crotch absorber options (a) copper body design (b) beryllium and copper design.

* Corresponding author's email: suthar@anl.gov

ISBN: 978-3-95450-188-5 doi:10.18429/JACoW-MEDSI2016-TUPE09

THERMO-FLUID STUDY OF THE UPC RACE-TRACK MICROTRON COOLING SYSTEM*

X. Escaler†, Departament de Mecànica de Fluids, UPC, Barcelona, Spain
Yu.A. Kubyshin, V. Blasco, J.A. Romero, A. Sánchez, Institut de Tècniques Energètiques, UPC, Barcelona, Spain,
M. Prieto, ALBA Synchrotron Light Source, Cerdanyola del Vallès, Barcelona, Spain
V.I. Shvedunov, Skobeltsyn, Institute of Nuclear Physics, Moscow State University, Moscow, Russia

Abstract

The cooling system of the race-track microtron (RTM), which is under construction at the Universitat Politècnica de Catalunya (UPC), has been simulated by means of a computational fluid dynamics (CFD) software. The hydraulic and thermal performance of the system for various operation conditions has been studied. Firstly, the hydraulic model has been validated by comparison with experimental measurements at different flow rates. Then, the cooling fluid temperatures and the pressure losses of the system have been determined and the capacity of the current design to remove the generated heat at nominal power has been confirmed. Finally, the maximum and average wall temperatures and heat transfer coefficients inside the accelerating structure have been calculated. These results have allowed us to localize sections of the cooling system with a low convection due to detached flows where, therefore, a risk of zones of high temperatures exists. An optimization of the cooling circuit with the aim to reduce such high temperature zones has been proposed.

12 MEV RACE-TRACK MICROTRON AND ITS COOLING SYSTEM

The UPC in collaboration with the Skobeltsyn Institute of Nuclear Physics of the Moscow State University and CIEMAT (Madrid) is building a compact electron accelerator of race-track microtron (RTM) type with the maximal beam energy 12 MeV. Its main envisaged application is Intraoperative Radiation Therapy. Modification of this low power consumption machine can be used also for cargo inspection and industrial radiography. The design of the accelerator is described in [1], the course of its systems development was reported in a number of papers, see for example [2-4]. Currently the RTM is at the final phase of its construction.

The UPC 12 MeV RTM is a pulsed accelerator with the output beam energies 6, 8, 10 and 12 MeV, energy gain per turn equal to 2 MeV approximately and low average current, of the order of 10-100 nA. The electron beam is produced in a module called accelerator head, its 3D view is given in Fig. 1 where main elements, like 180º bending magnets, usually called end magnets, and the accelerating structure (linac) are shown. All magnets are permanent magnets and therefore do not consume power. These elements are fixed on a rigid platform placed inside a vacuum chamber.

The cooling of the RTM is provided by a chiller that comprises a positive displacement pump with a discharge pressure limited to around $6.8 \cdot 10^5$ Pa (6.8 bar) that can be regulated to reach a maximum flow rate of $2.83 \cdot 10^{-4}$ m^3/s if necessary. The main function of the RTM cooling system is to provide a safe and stable operation of all accelerator systems, in particular guarantee a temperature stability of ±1°C in the end magnets and linac. In addition, at the stationary regime of RTM operation the temperature differences between different parts of the end magnets and linac must not exceed the same limit of ±1°C.

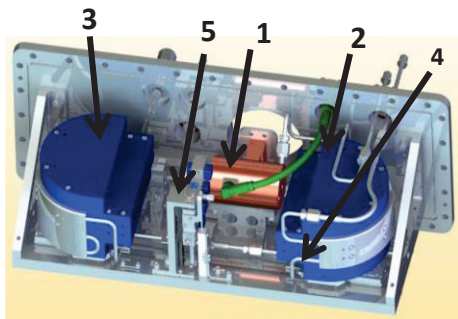

Figure 1: 3D view of the accelerator head of the 12 MeV RTM. The numbered elements are: 1- accelerating structure (linac), 2 and 3 – end magnets M1 and M2, respectively, 4 – cooling tube, 5 – extraction dipoles.

In the present paper we study the performance of the cooling system of the RTM accelerator head. Chilled distilled water is sent through the inlet collector and inlet feedthrough to the vacuum box. Firstly, the cooling circuit, which is a tube of 4 mm internal diameter, passes along the rear walls of the two end magnets, M1 and M2, as one can see in Fig. 1. The tube is partially covered with jackets in order to achieve a good thermal contact with the magnet bodies. After the M2 magnet the cooling tube is connected to the inlet of the linac which has four 4 mm diameter longitudinal cooling channels connected in series. Finally, the outlet of the linac is connected to the output feedthrough and then to the output collector. The connecting tubes are made of stainless steel and also have the 4 mm internal diameter. The total length of the cooling channels and connecting tubes inside the vacuum chamber is about 2 m.

* Work supported by the 2014 SGR846 of AGAUR (Generalitat de Catalunya)
† escaler@mf.upc.edu

ISBN: 978-3-95450-188-5 doi:10.18429/JACoW-MEDSI2016-TUPE10

A THERMAL EXPLORATION OF DIFFERENT MONOCHROMATOR CRYSTAL DESIGNS

J. S. Stimson†, M. Ward, Birmingham City University, Birmingham, United Kingdom
S. Diaz-Moreno, P. Docker, J. Kay, J. Sutter, Diamond Light Source, Didcot, United Kingdom

Abstract

Eight potential monochromator crystal designs were subjected to a combination of three different beam powers on two different footprints. The temperature and thermal deformation were determined for each. It was found that thermal deformation of the lattice is negligible compared to the surface curvature, and that while the thinnest crystal wafer showed the smallest temperature increase, crystals cooled from the bottom alone demonstrated a far more uniform thermal deformation and a larger radius of curvature.

INTRODUCTION

In this work we have explored various monochromator crystal designs. Monochromator crystals are used to select a single wavelength of x-rays from the broad spectrum produced in a synchrotron device [1-2]. The high energies these crystals are subjected to causes them to heat up significantly, leading to thermal deformations that distort the uniform surface of the crystal, leading to multiple wavelengths being selected [3-4]. This is problematic as it is not always obvious whether the change in wavelength at the detector is due to thermal distortion of the monochromator or interaction with the sample being tested.

In order to attempt to reduce or even eliminate this thermal deformation it must be understood how different variables affect the system. To this end we have modelled several different designs of monochromator crystal to see what effect changing the geometry has on the thermal deformation.

As we are concerned primarily with thermal behaviours, we have made a number of approximations. The cooled surfaces remain at 80 K throughout to approximate the flow of liquid nitrogen with an ideal thermal contact [5]. This is a very non-physical boundary condition, which means the results are not directly comparable to real world systems. However, for the purpose of this work it has been used to create a directly comparable baseline between the different models.

It is also assumed that each crystal has thermalized prior to exposure to the beam, and therefore is initially at a uniform temperature of 80 K.

Three beam powers were considered; 110 Watts, 550 Watts and 1100 Watts. This was to simulate exposure to low power, high power and future high power beams as used at the Diamond Light Source. Each of these powers had to be applied using the Beer-Lambert law of beam transmission [6], as shown in Eq. (1) below.

$$I = I_0\, e^{-\mu x} \tag{1}$$

In Eq. (1) I is the intensity of the beam, I_0 is the intensity of the beam at the surface, μ is the absorption coefficient and x is the distance into the material.

As the beam produced by the I20 beamline is broad spectrum, this calculation was done for each energy and then integrated across all energies as shown in Eq. (2).

$$I = \int I_0(E) e^{-\mu(E)x}\, dE \tag{2}$$

In Eq. (2) I_0 (E) is the intensity of the beam at the surface for x-rays of a given energy and μ(E) is the absorption coefficient for x-rays of the given energy in silicon.

This was done for the measured intensities of each wavelength at the I20 beamline for the given power values. The intensity penetrates the surface, decreasing as it propagates.

Two major factors were considered; the deformation of the diffracting surface could change both the spacing of the lattice layers and change the angle of incidence, both of which can damage the Bragg diffraction desired by modifying lattice layer structure [1].

These are only an issue if they are non-uniform across the diffracting surface, as a uniform change can be allowed for when angling the monochromator crystal. As such the radius of curvature of the diffracting surface has been calculated at the centre of the surface for each design.

The curvature, k, can be calculated by mapping some function y to the deformation of the surface, then applying Eq. 3 [7].

$$k = \frac{\left(\frac{d^2y}{dx^2}\right)^{\frac{3}{2}}}{1+\left(\frac{dy}{dx}\right)^2} \tag{3}$$

The radius of curvature is simply the reciprocal of the modulus of curvature [7], as shown in Eq. 4.

$$R = \frac{1}{|k|} \tag{4}$$

A larger radius of curvature relates to a flatter crystal surface, i.e. the larger the radius of curvature the better.

The lattice spacing as a function of temperature was also calculated, to see if a non-uniform temperature gave rise to a non-uniform lattice that would have affected the Bragg diffraction. However, calculations showed that between 150 K and 80 K the lattice spacing varied only by 5.5e-15 m, a statistically negligible change given the lattice spacing is only of the order of Angstroms. This shows that the variance of the lattice spacing directly due to temperature is unlikely to impact the Bragg diffraction.

Despite varying designs between the different crystals, the mechanical boundary conditions used stay the same; each crystal is anchored by a single fixed point in the centre of its base, with a line extending from this point to

ISBN: 978-3-95450-188-5 doi:10.18429/JACoW-MEDSI2016-TUPE11

STUDY ON THERMAL MECHANICAL DESIGN AND OPTIMIZATION ANALYSIS FOR THE ALBA INFRARED MICROSPECTROSCOPY BEAMLINE (MIRAS) EXTRACTION MIRROR BASED ON FINITE ELEMENT ANALYSIS

M. Quispe†, A. Carballedo, J.J. Casas, C. Colldelram, A. Crisol, G. Peña, Ll. Ribó, I. Sics, I. Yousef, ALBA – CELLS Synchrotron, Cerdanyola del Vallès, Spain

Abstract

This paper reports design, modelling, simulation and optimization results for the ALBA MIRAS infrared radiation extraction mirror. Finite element analysis (FEA) was used to simulate the thermal mechanical behaviour of the device. With the aim to ensure a good thermal performance, conservative assumptions were applied: all of the incident Bending Magnet (BM) radiation is absorbed at the mirror surface, constant bending magnetic field and low thermal contact between the mirror Al 6061 and the OFHC copper arm. A novel solution has been implemented in order to provide an effective cooling by a natural convection on the in-air part of extraction mirror assembly. This has voided the necessity for a water cooling that often causes problems due to the associated vibrations. The power conditions were calculated by using SynRad+. The main ALBA Storage Ring design parameters are: 3 GeV, 400 mA and 1.42 T. According to these conditions, the mirror absorbs 15 W with a peak power density of 0.51 W/mm^2. The peak temperature calculated was 63.2 ºC. The real measurements reported during the commissioning stage showed a good thermal performance, in agreement with the results predicted by FEA.

BACKGROUND

MIRAS is one of phase II beamlines, currently under commissioning stage at the ALBA synchrotron light source. It will go into operation with official users in October 2016 and will be dedicated to Fourier Transform Infrared spectroscopy and microscopy [1].

The MIRAS engineering (conceptual design and production drawings), assembly and qualification metrology tests have been performed at ALBA. One of the key elements is the infrared extraction mirror that will collect the infrared radiation and reflect it back to the storage ring tunnel in order to be transported to the experimental hall.

The ALBA infrared extraction mirror is based on the slotted, non-cooled, type. The concept of the slotted mirror not only avoids interaction with the central high energy core of the dipole emissions, but also allows to realize a simple design that functions reliably without additional water cooling that often causes problems due to the associated vibrations [2, 3]. A novel solution has been implemented in order to provide an effective air cooling system by natural convection on the in-air part of extraction mirror assembly.

THE ALBA INFRARED EXTRACTION MIRROR

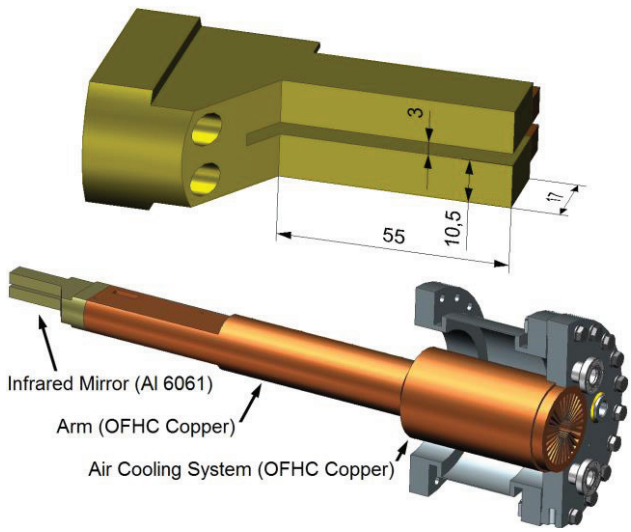

Figure 1: The ALBA infrared extraction mirror. Top: mirror Al 6061, dimensions in mm. Bottom: overall view of the device.

The main parts of the infrared extraction mirror are shown in Fig. 1: the mirror Al 6061, a copper arm and the cylindrical air cooling system made of copper.

The mirror is a rectangular bar 17x24x55 mm with the reflective face at an angle of 63.7º to the electron beam trajectory in the upstream vacuum chamber (see Fig. 2). A 3 mm slot in the mirror allows the high-energy radiation to pass through it. The much wider vertical divergence of the infrared radiation is collected on both sides above and below the slot and redirected towards the emission port. The mirror is attached to the copper arm using screws; indium foil is placed at the interface to improve the heat transfer to the copper arm.

The air cooling system consists of a cylinder made of copper, 65 mm internal diameter, 10 mm thickness and 131 mm long which is provided with 32 longitudinal, straight fins of 1 mm thick and 22.5 mm height. The copper cooling system is brazed into the stainless steel flange providing a perfect contact for the heat transfer.

† mquispe@cells.es

ISBN: 978-3-95450-188-5 doi:10.18429/JACoW-MEDSI2016-TUPE12

DEVELOPING WHITE BEAM COMPONENTS OF TPS BEAMLINE 24A

Ming-Han Lee†, Chien-Hung Chang, Shih-Hung Chang, Din-Goa Liu, Yi-Jr Su, Liang-Jen Huang, Cheng-Chi Chen, Chao-Chih Chiu, Longlife Lee, Hong-Yi Yan, Chao-Yu Chang, Lee-Jene Lai
National Synchrotron Radiation Research Center,
101 Hsin-Ann Road, Hsinchu Science Park, Hsinchu 30076, Taiwan

Abstract

The TPS 24A, Soft X-ray Tomography (SXT) beamline, is one of the beamlines in the second construction phase at the Taiwan Photon Source (TPS). This bending magnet (BM) beamline has high flux in the range between 260 eV and 2600 eV. It is designed for transmission full-field imaging of frozen-hydrated biological samples. At the exit slit, the beam flux optimized in 520 eV is 2.82×10^{11} photons/second with resolving power 2000, the beam size is 50×60 μm^2 (V×H, FWHM) and the beam divergence is 1.73×1.57 mrad^2 (V×H, FWHM). By contributions of the generic beamline components project in recent years, modular mechanisms would be used in this beamline such as mask, X-ray beam position monitor (XBPM), photon absorber (PAB), and screens. However, these beamline components were designed for ID beamlines, so they should be redesigned for BM beamlines. This paper generally introduce these beamline components decided and redesigned for the TPS 24A. They will play important roles at the BM beamlines in the future.

BEAMLINE LAYOUT

Figure 1 shows the layout of the SXT beamline.

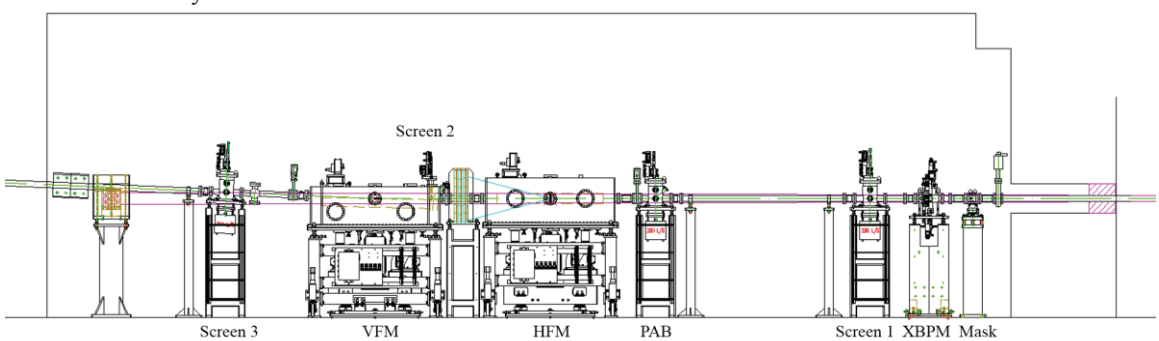

Figure 1: White beam components layout of the SXT beamline.

MASK

The mask as shown in Figure 2 is used to confine the beam size of 21 mm (H) × 20 mm (V) with small range adjustment. Due to the much larger beam size and lower heat load of BM beamlines, we cancelled the tungsten blades used in ID beamlines and simplified the route of cooling water in the chamber of the mask. The entrance and exit ports were also changed from 2.75 inch to 4.5 inch CF flanges. Furthermore, a local shielding which contains of lead and Polyethylene (PE) was added to the mask to prevent the bremsstrahlung radiation.

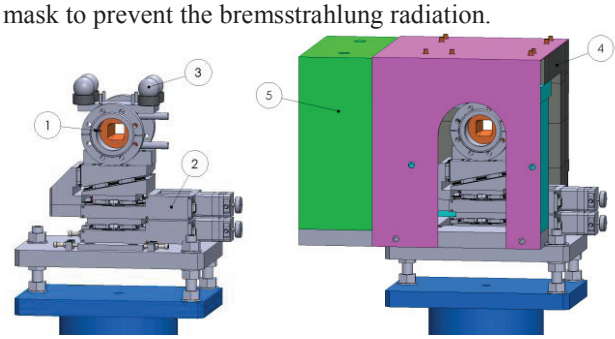

Figure 2: The schematic drawing of the mask and local shielding.
1. UHV water-cooling chamber, 2. Motorized XZ stage, 3. Laser tracker target, 4. Lead, 5. PE.

XBPM

The XBPM with high precision and current detecting function is used to confine the beam size and observe the beam fluctuation. Four tungsten blades moved by linear stages are used to confine the beam size. The stroke of the linear stages and bellows was changed from 10 mm to 30 mm to make sure that the blades travel longer than the beam size. The beam could fully pass through when the blades are opened, and would be cut off when the blades are closed. Optionally, eight M16 × 2.0 screw holes made on the granite stand could be used if a bremsstrahlung stopper is needed. Figure 3 shows the schematic drawing of the XBPM.

† lee.mh@nsrrc.org.tw

ISBN: 978-3-95450-188-5 doi:10.18429/JACoW-MEDSI2016-TUPE13

NUMERICAL SIMULATION OF THE ALBA SYNCHROTRON LIGHT SOURCE COOLING SYSTEM RESPONSE TO PUMP START-UP AND SHUT-DOWN

X. Escaler*, D. Juan†, Universitat Politècnica de Catalunya, Barcelona, Spain
J.J. Casas‡, C. Colldelram§, M. Quispe#, M. Prieto$, ALBA Synchrotron Light Source, Cerdanyola del Vallès, Spain

Abstract

The ALBA Synchrotron Light Source cooling system is submitted to regular pump start-ups and shut-downs. Moreover, pumps can trip due to motor power failures. As a result, the piping system can be subjected to surges and pressure oscillations. The 1D thermo-fluid simulation software Flowmaster® has been used to predict these transient conditions taking into account the fluid compressibility, the pipe elasticity, the characteristic time response of the check valves and the pump/motors moments of inertia. During pump start-ups, significant pressure rises are detected that can be reduced by readjusting the PID controller parameters. Unexpected pump shut-downs do not appear to provoke significant water hammer conditions. However, pressure fluctuations are generated mainly in the same pumping line but also in the rest of the system due to the particular common return configuration. In all the cases the pressure regulation mechanisms acting on the pump rotating speeds serve to attenuate the consequences of these transients. Finally, the feasibility of the model to simulate the effect on the system response of trapped air inside the pipes has also been evaluated.

INTRODUCTION

The Consortium for the Exploitation of the Synchrotron Light Laboratory (CELLS) is in implementation state of a transversal project whose objective is to develop and improve the ALBA's synchrotron cooling system. It is aimed at improving the system reliability and stability faced to flow changes induced during normal operation and occasional failures.

One particular activity consists of understanding the cooling system response to start-up and shut-down of any pump device in the cooling system and detecting if pressure variations created in transient events may lead to failures and/or piping components' deterioration.

It is well known that transient flow conditions in piping systems with large flow rates can cause unwanted water hammer problems. Water hammer creates high amplitude pressure waves that travel back and forth inside the pipe network until they are dissipated by friction [1-2]. Excessive high pressures can lead to damage or rupture of pumps and valves. Excessive low pressures can lead to air entrance, cavitation and release of large amounts of dissolved air.

Faced with the difficulty and risk of carrying out experimental tests on the actual pipe network, it has been decided to use the existing Flowmaster® model [3] to simulate numerically the system response. For that, the model has been modified to take into account the inertial and compressibility effects in pumps and pipes by replacing and adding the adequate components. In addition, it has also been necessary to program new scripts and to make changes in the PID controllers in order to simulate the real pumping system start-up/shut-down procedures.

NUMERICAL MODEL

A key parameter to calculate water hammer phenomenon in pipes is the pressure wave propagation speed, a, that can be estimated with Eq. (1) where B is the bulk modulus of elasticity of the liquid, ρ is the fluid density, D is pipe diameter, e is the pipe wall thickness and E is the modulus of elasticity of the pipe wall material.

$$a = \sqrt{\frac{B/\rho}{1+\frac{DB}{eE}}} \quad (1)$$

For example, the wave speed a is around 1200 m/s for water at 23 °C flowing inside a stainless steel pipe of size DN 150 Sch 10. Accordingly, the adequate wave speed for all the different pipe sizes of the network have been calculated and used in the model.

Most common causes of transient problems in pipe systems are the pump start-up and pump shut-down due to a power failure (pump trip). To correctly simulate these effects the pump and the motor moments of inertia must be included in the model. For that, the Thorley empirical equations have been used [4]. The motor inertia, I_m, and the pump inertia, I_p, have been calculated with Eq. 2 and Eq. 3, respectively, where P is the brake horsepower in kW and N is the rotational speed in rpm.

$$I_m = 118\left(\frac{P}{N}\right)^{1,48} \quad (2)$$

$$I_p = 1{,}5 \cdot 10^7\left(\frac{P}{N}\right)^{0,9556} \quad (3)$$

The generation side of the cooling system is comprised of four pumping stations named P07, P08, P09 and P10 for the Experimental Area (EA), the Storage (SR), the Booster (BO) and the Service Area (SA) consumption rings, respectively. In P08 and P10 two pumps operate simultaneously in parallel, meanwhile in P07 and P09 only one pump is working. Another pump, P11, is in

* escaler@mf.upc.edu
† david_78jg@hotmail.com
‡ jcasas@cells.es
§ ccolldelram@cells.es
# mquispe@cell.es
$ mprieto@cells.es

ISBN: 978-3-95450-188-5 doi:10.18429/JACoW-MEDSI2016-TUPE14

STUDY, DESIGN AND OPTIMIZATION ANALYSIS OF THE ALBA LOREA DIPOLE VACUUM CHAMBER AND CROTCH ABSORBERS BASED ON FINITE ELEMENT ANALYSIS

M. Quispe†, J. Campmany, J.J. Casas, C. Colldelram, A. Crisol, J. Marcos, G. Peña, M. Tallarida,
ALBA – CELLS Synchrotron, Cerdanyola del Vallès, Spain

Abstract

This work deals with the FEA study, design and optimization of the LOREA dipole vacuum chamber and Glidcop Al-15 crotch absorbers. At present LOREA is the ninth beamline being designed at ALBA with an Insertion Device (ID) consisting of an Apple II-type helical undulator. For the standard dipole chamber the vertical polarized light hits the walls because of the very narrow vertical aperture between the cooling channels. In vertical mode the ID vertical divergence equals +/- 2.2 mrad and the peak power density and total power are 5.6 kW/mrad² and 5.5 kW, respectively. Due to the high power a temperature as high as more than 600 ºC is calculated. In consequence the dipole chamber has to be modified and the absorbers have to withstand the Bending Magnet (BM) and ID radiation. The new absorbers have to be thicker and its cooling channels are farer from BM power deposition than the standard absorbers. The thermal mechanical simulations show good results, the new absorbers are in a safe range, the maximum temperature, stress and strain are 309.2 ºC, 164.2 MPa and 0.14%, respectively. The main ALBA Storage Ring design parameters used in the simulations are: 3 GeV, 400 mA and 1.42 T (BM).

BACKGROUND

LOREA is the ninth beamline being designed at ALBA synchrotron light source. It will deliver photons with high resolution and high photon flux for Spin and Angle Resolved Photoemission Spectroscopy. Its Insertion Device (ID) consists of an Apple II-type helical undulator (EU125) [1]. This type of EPU can produce horizontal, circular and vertical modes of polarization of the magnetic field.

The radiation emitted by the ID at low photon energies has a very large angular divergence. Although the large divergence is not a problem in case of horizontal and circular polarization, it is instead a problem, considering the "V profile" of the dipole vacuum chamber. Here, the "V profile" necessary to allow the cooling channels produces a very narrow aperture, and the vertical polarized light hits the chamber. This problem is described in Fig. 1: the green fan depicts the ID radiation in a vertical plane at the middle of the cone radiation. The schematic fan is calculated for vertical mode polarization which vertical opening is +/- 2.2 mrad. Because of this large angular divergence there is an interference with the cooling channel and a big amount of heat is deposited on the dipole vacuum chamber.

† mquispe@cells.es

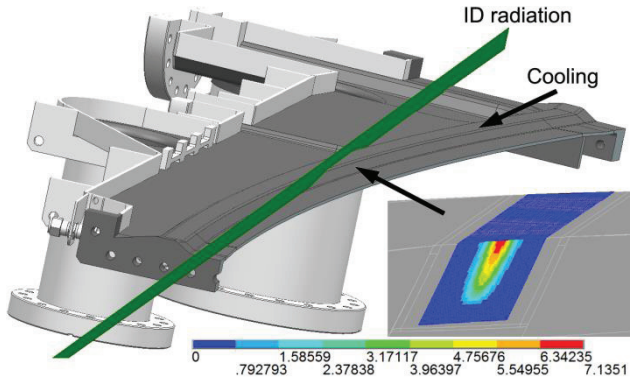

Figure 1: Schematic cross-sectional view of standard dipole vacuum chamber, displaying the lower longitudinal cooling channel and ID radiation interference for vertical mode polarization. The footprint is in W/mm².

THERMAL STUDIES OF THE STANDARD DIPOLE CHAMBER SUBJECT TO ID RADIATION

Thermal Boundary Condition

Thermal simulations (FEA) were used to study the effect of the ID radiation (vertical mode) on the standard stainless steel dipole chamber.

The power deposited on the chamber is calculated with the parameters of Table 1. It is imposed a nominal trajectory of the beam. The power calculated for each cooling channel is 693 W and the peak power density is 7.1 W/mm². Figure 1 shows the footprint for the lower cooling channel.

Table 1: Main Parameters of Insertion Device for LOREA (vertical mode). The Emitted Power and Power Density are Computed for an Electron Beam Current of 400 mA.

Parameter	Magnitude
Maximum magnetic field	1.06 T
K	12.37
Power density	5.6 kW/mrad²
Total power	5.5 kW

Fluid Boundary Conditions

The cooling channels have originally been designed to dissipate the reflected heat radiation from the crotch absorbers. Under this condition the amount of power is very low, the heat is spread uniformly on the chamber and a laminar regime of water flow is sufficient for heat dissipation.

ISBN: 978-3-95450-188-5 doi:10.18429/JACoW-MEDSI2016-TUPE15

THERMAL MANAGEMENT AND CRYSTAL CLAMPING CONCEPTS FOR THE NEW HIGH-DYNAMICS DCM FOR SIRIUS

M. Saveri Silva*, R. R. Geraldes, A. Gilmour, LNLS, Campinas, Brazil
T. A. M. Ruijl, R. M. Schneider, MI Partners, Eindhoven, Netherlands

Abstract

The monochromator is known to be one of the most critical optical elements of a synchrotron beamline, since it directly affects the beam quality with respect to energy and position. Naturally, the new 4th generation machines, with emittances in the range of order of 100 pm rad, require even higher stability performances, in spite of the still conflicting factors such as high power loads, power load variation, and vibration sources. A new high-dynamics DCM (Double Crystal Monochromator) is under development at the Brazilian Synchrotron Light Laboratory for the future X-ray undulator and superbend beamlines of Sirius, the new Brazilian 4th generation synchrotron [1, 2]. In order to achieve high-bandwidth control and stability of a few nrad, as well as to prevent unpredicted mounting and clamping distortions, new solutions are proposed for crystal fixation and thermal management. The design is based on flexural elements, aiming for a highly predictable performance, like support stiffness, crystal distortion and thermal insulation. It was optimised by using mechanical and thermal FEA, including CFD. Efforts were made to predict thermal boundaries associated with the synchrotron beam, including incident, diffracted and scattered power, for which the undulator spectrum was employed in the Monte Carlo simulation package – FLUKA.

INTRODUCTION

The goal of this work is to present the thermal management and the mechanical clamping concepts for the new high stability DCM for Sirius. Details about the full system and its specifications can be found in [3].

THERMAL MANAGEMENT

The first step towards modelling the thermal behaviour of the system was collecting power loads and boundary conditions.

Incident Power

Taking 19 mm period undulator as the source (with 105 periods and at 350 mA current), its spectrum was simulated using SPECTRA [4] and post-processed in MATLAB [5] in order to find both the total incident power and the power variation for energy scans as a function of energy. The results are presented in Fig. 1 and it can be seen that the power load does not exceed 150 W. However, the DCM has to deal with a variation of more than 100 W over the full range, and as much as 38 W for 1 keV scans.

From the total incident power, most of it is absorbed by the 1st crystal (CRYS1), whereas a small fraction of it is diffracted and the remaining of it is scattered. These quantities have been estimated for a better comprehension of each contribution to the system.

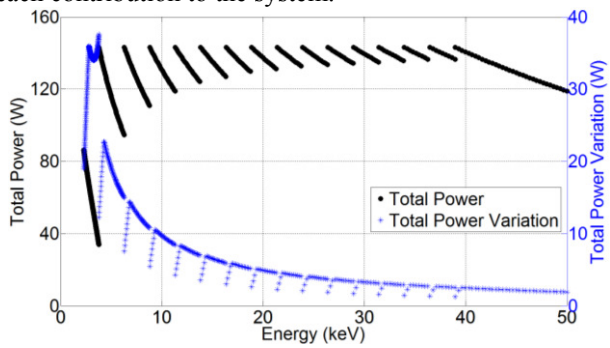

Figure 1: Incident power and power variation in ±0.5 keV scans as a function of energy for Si (111) with an acceptance of 60x60 μrad^2.

Absorption and Scattering

A user routine was implemented into the Monte Carlo package FLUKA [6, 7] in order to guide the design of the shielding structure, to estimate the radiation doses in sensitive elements and to evaluate the deposited energy in the main components after scattering and absorption. Both the Bremsstrahlung flux, generated inside FLUKA from the electron beam, and the synchrotron flux, imported from SRW [8], have been evaluated. The first was found to be several orders of magnitude smaller than latter, so that its contribution could be neglected regarding power levels. Super MC [9, 10] was used to convert CAD drawings in FLUKA geometries. Figure 2 shows the original simplified CAD model and its conversion inside FLUKA, as well as some results of the photon track length density for different shielding designs.

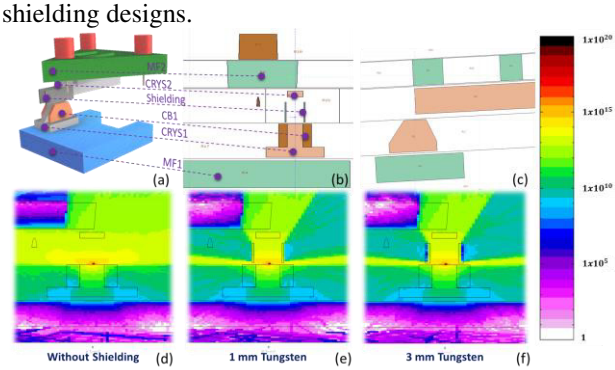

Figure 2: FLUKA simulations: (a) original CAD model; (b) upstream view of the model in FLUKA; (c) side view of the model in FLUKA; (d) to (f) upstream view of photon track length density (Particles/cm²/s) for three shielding designs.

* marlon.saveri@lnls.br

ISBN: 978-3-95450-188-5 doi:10.18429/JACoW-MEDSI2016-TUPE16

DESIGN OF A LEAF SPRING BENDER FOR DOUBLE LAUE CRYSTAL MONOCHROMATOR AT SSRF *

H. Qin†, H. Zhang[1,2], L. Jin[1], W. Zhu[1], K. Yang[1]
[1]Shanghai Institute of Applied Physics, Shanghai 201800, P. R. China
[2] University of Chinese Academy of Sciences, Beijing 100049, P. R. China

Abstract

A leaf spring bender geometry for water-cooled double Laue crystal monochromator (DLM) is presented. The DLM will be employed to acquire high energy monochromatic X-ray (60keV to 120keV) on the ultra-hard applications beamline at SSRF. A compact bending mechanism is designed in order to get horizontally focused high energy monochromatic X-ray as small as 0.5mm. The bender applies a piece of thin asymmetric crystal and a pair of leaf springs which push the crystal to a sagittally bent radius as small as 1 meter by a pair of symmetry moments. An optimized crystal geometry is achieved by taking into account the meridional and sagittal bendings coupled and defined by the anisotropic elasticity of the asymmetric crystal. Furthermore, thermal slope error and structural stress of the bent crystal are analyzed by finite element method (FEA).

INTRODUCTION

Ultra-hard applications beamline will be constructed during phase II project at Shanghai Synchrotron Radiation Facility (SSRF). High energy focused monochromatic X-ray (60 to 120keV) will be chosen for materials science experiments on ultra-hard applications beamline which is derived from a superconductive wiggler light source whose horizontal divergence is as large as 6 mrad. It is critical how to utilize the light source effectively. The sagittally bent double Laue crystal monochromator (DLM) is a desirable optics for hard X-ray beamline and it's very attractive at high energies for its flux, energy resolution and tunability properties [1,2].

In bent Laue-Laue configuration, as illustrated in Figure 1, the first crystal is arranged in inverse-Cauchois geometry, with the source on its Rowland circle at a distance of F_1 from it. Consequently, a virtual-image point is formed on its Rowland circle at a distance of $R_{m1}\cos(\chi-\theta_B)$ from the crystal. The second crystal is bent so that the virtual image point of the first crystal is on its Rowland circle at a distance of $R_{m2}\cos(\chi+\theta_B)$ from it, while its focus point is at a distance of F_2 from it, where R_{m1} and R_{m2} are the meridional bending radius of the first and second crystal, respectively. Both crystals focus the X-rays sagittally and are in the inverse-Cauchois geometry in the meridional plane. The overall focal length of the DLM is:

$$f_s = R_s/(4\sin\theta_B \sin\chi)$$

when both crystals are bent to radius R_s. θ_B and χ are the Bragg angle and asymmetry angle respectively.

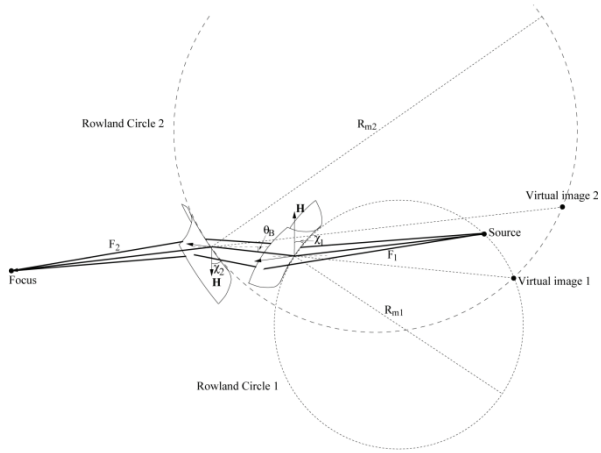

Figure 1: Principle of DLM.

DESIGN AND OPTIMIZATION

Specifications for DLM

The DLM is located at 97 meter from the light source and adopts a pair of thin rectangle crystals with an asymmetric angle of 64.76°. (100) and (311) are the silicon crystal surface and diffraction plane respectively. It will focus the beam horizontally from 30 millimeter to about 500 microns. Main specifications for the DLM is shown in table 1.

Table 1: Specifications for DLM

Parameter	Value
Energy range	60-120 keV
Energy resolution	10^{-3}
Minimum energy step	1eV
Sagittal radius	1-3m
Incident beam size (H×V)	30mm×2.5mm
Beam vertical offset	50mm
Thickness of crystal	1mm
Sagittal residual slope error (RMS)	<6μrad
Meridional residual slope error (RMS)	<10μrad
Vacuum pressure	< 10^{-5} Pa

Optimization for Crystal Dimension

In order to keep the energy resolution at the order of 10^{-3} and obtain a flux of 10^{12} photons/s within the energy range, we set the sample spot at 15 meter (F_2) from the second crystal, due to the limitation for the layout of beamline, whereafter the diffraction plane and asymmetry

† qinhongliang@sinap.ac.cn

ISBN: 978-3-95450-188-5 doi:10.18429/JACoW-MEDSI2016-TUPE18

DESIGN AND FEA OF A 3D PRINTED DETECTOR WINDOW FRAME

W. Tizzano*, Diamond Light Source, Didcot, United Kingdom

Abstract

The purpose of the project was to design and simulate a window assembly to be used in GISAX/GIWAX[1] experiments. The window lies between the sample and the WAXS[2] detector, a modified, in-vacuum detector, with modules removed to allow scattered radiation to pass through to a SAXS[3] detector positioned downstream. The window uses 75 µm thick Kapton® HN film and given the size, pressure and the short distance to the sensors, it was necessary to support it on a frame.

To avoid any information loss from shadowing of the detector, a frame was designed so that shadows will be projected into the gaps between the detector modules. The geometry was such that DMLS[4] was an effective way of producing the item. Given the slenderness of the structure and the forces it supports, the material approaches or exceeds its yield point, so a bilinear, isotropic, hardening material model was chosen; moreover, large deflections were enabled. Also, the contacts were modelled with augmented Lagrange frictional formulation. All these assumptions made the analysis strongly non-linear.

INTRODUCTION

I22 is a non-crystalline diffraction beamline for physical and life sciences that records simultaneously both SAXS and WAXS [1]. A recent upgrade project made GISAX/GIWAX experiments possible.

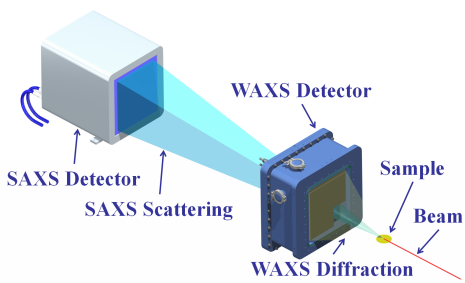

Figure 1: I22 Layout.

I22 is structured as follows (Fig.1): the beam coming from the BCO[5] hits the sample, and the diffracted light goes through a nosecone and is recorded by a 2D in vacuum WAXS detector; the above mentioned detector has some missing modules on the bottom right (Fig.2), allowing part of the radiation to pass through a snout and a camera tube, so the SAXS scattering can be recorded as well, by a detector at a distance that can vary up to 10 m [2] from the sample; three beamstops prevent the direct and reflected beam, and the glare from hitting the detector damaging it.

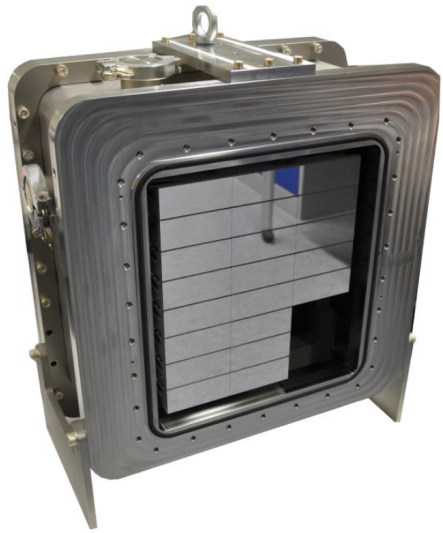

Figure 2: PILATUS3 2M-DLS-L [3].

WINDOW DESIGN

The PILATUS3 2M-DLS-L is an in-vacuum detector, so it was needed to design a window to isolate it from the atmosphere. A 75 µm thick Kapton® HN film was used, because of its transparency to X-ray and low scattering [4]. However, given the area of the window ($\approx 5.8 \times 10^4$ mm^2), the force generated by the differential pressure between the two sides of the film was considerable ($\approx$5.8 kN); for this reason it was necessary to support the Kapton film, or it would have deformed too much, and eventually would have broken.

Nonetheless, any support frame would project a shadow on the detector, and some information would be lost. However, the detector is made up of multiple modules, with gaps between them; the horizontal gaps are 17 pixels tall, and the vertical ones are 7 pixels wide. Since the pixels are square, and have a size of 172 µm^2, the gaps sizes are 2.9 mm and 1.2 mm, respectively. Hence, it was decided to design a support frame consisting in different ribs positioned and angled in such a way that, given a specific relative position between the sample and the detector, the shadow would be projected into the gaps (Fig. 3); in this way no information would be lost.

A rib section was drawn in PTC Creo, and all the necessary constraints were chosen so that in the software the ribs would adapt to the sample position, until this was fixed and the design finalised.

* walter.tizzano@diamond.ac.uk
[1] Grazing Incidence Small/Wide Angle X-ray scattering
[2] Wide Angle X-ray Scattering
[3] Small Angle X-ray Scattering
[4] Digital Metal Laser Sintering
[5] Beam Conditioning Optics

ISBN: 978-3-95450-188-5 doi:10.18429/JACoW-MEDSI2016-TUPE19

APLICATION OF A NEG COATED CHAMBER AT THE CANADIAN LIGHT SOURCE

S.Y. Chen, D. Bertwistle, M. Kei, C. Murray, T. Pedersen Canadian Light Source Inc., Saskatoon, Canada

Abstract

In the Fall of 2015 a 4800 mm long NEG coated chamber was installed in the Canadian Light Source in cell 9 straight section. The chamber will occupy to majority of the straight length. The chambers vacuum has been monitored for +1 year and no obvious issues has been found.

The chamber body is 10 mm thick and the aperture is an ellipse with an 8 mm height and a 65 mm width. A design feature of the chamber is a lack of support in-between the ends of the chamber. This is due to the double elliptically polarizing undulator (54 mm, and 180 mm period). This proceeding details the following: Structure design and Deflection and strength Finite Element Analysis (FEA); Heat loads and cooling calculation; Supports design and deflection correction; Current strips installation and activation.

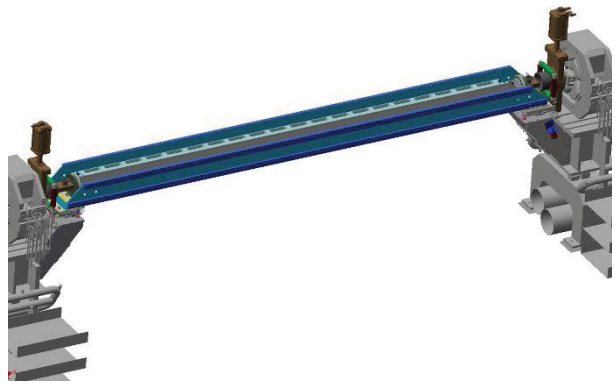

Figure 1: QMSC NEG Coated chamber.

INTRODUCTION

The Canadian Light Source (CLS) is constructing a new phase III Beamline – the Quantum Material Spectroscopy Centre (QMSC). QMSC is designed to cover the energy from EUV radiation to soft X-ray (15 - 1000 eV) with arbitrary polarized light. Two APPLE II type undulators are designed to fulfil this energy range. The 180 mm period Low Energy Elliptically Polarizing Undulator (LE-EPU) covers the photon energy ~15-200 eV while the 55 mm period High Energy EPU (HE-EPU) covers the energy range of ~200-1000 eV. Each of the EPUs are 4 meters in length. The minimum gap for the high energy EPU is 14.5 mm. This double-EPU design required considerable engineering and analysis for the support structure and straight section vacuum chamber.

1. There was no possibility of a middle absorber so the vacuum chamber needed to be capable of absorbing roughly 900 Watts of bend magnet power deposited and an additional 700 Watts heat load from the EPU along the length of the chamber.
2. The chamber could not have a support in-between the two ends, due to the requirement of being able to switch between the HE- and LE-EPU's.
3. The chamber thickness between the magnets was limited to 10 mm, with an aperture of 8 mm. The chamber sag was limited to 0.3 mm. A regular chamber and ion pumps would not be able to be accommodated with the above restrictions.

FMB Berlin supplied a non-evaporable getter (NEG) coated chamber and CLSI designed the two ends supports and put the current strips on the chamber surfaces. Figure 1 shows the chamber assembly.

STRUCTURE, STRENGTH, AND DEFLECTION

Due to the limited space, an H-style structure was required. Both the H-beam width and height were strictly limited by the double-EPU. To ensure the maximum sag was less than 0.3 mm, stiffening bars were attached to the side flanges. The end supports were also designed in such a way that the unti-sag torque could be applied to the chamber. Figure 2 shows the chamber structure. A series of FEA analyses were performed with positive results. Figure 3 and 4 (a), (b) and (c) show the FEA results at different conditions.

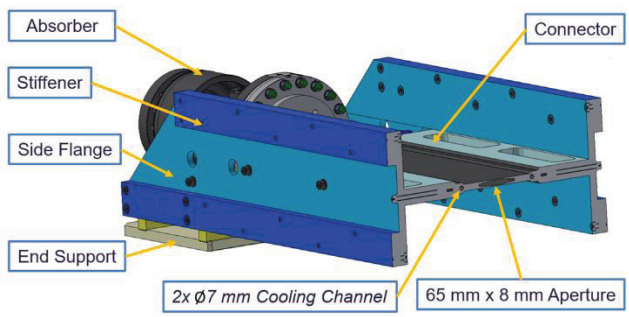

Figure 2: The chamber structure.

ISBN: 978-3-95450-188-5 doi:10.18429/JACoW-MEDSI2016-TUPE21

CLSI BMIT'S SUPER-CONDUCTING WIGGLER CRYOGENIC SAFETY IMPROVEMENTS*

L. Lin †, T.W. Wysokinski, Canadian Light Source (CLS), Saskatoon, Canada

Abstract

4.1 T superconducting (SC) wiggler on CLS Biomedical Imaging and Therapy (BMIT) beamline [1-4] developed a critical problem in the cryogenic safety relief and refill paths. Ice blockage formed and prevented helium gas from relieving during liquid helium (LHe) refill. This resulted in an internal pressure built up, which caused expelling of the LHe and cold gas helium (GHe) from the wiggler cryostat. Several improvements were performed over the years including replacement of the original rupture disk, the pressure relief valves and installation of metal O-ring seals at external ports. Following these improvements, a major upgrade on the wiggler safety relief path was implemented by adding a new vent pipe directly connected to the cryostat for safety exhaust. The LHe refill path was also modified to eliminate possibility of ice blockage. During initial tests after the upgrades, we experienced significant heat load increase which was linked to the thermal acoustic oscillations in the LHe transfer line. The problem was resolved by improving the insulation vacuum in the transfer line and adding a super insulation assembly into the direct vent pipe along with a plug at the refill path.

BACKGROUND

BMIT's 05ID-2 beamline 4.1-Tesla, 25+2 pole wiggler was designed and constructed by Budker Institute of Nuclear Physics (BINP) [3]. The wiggler is equipped with Sumitomo cryo-coolers. During normal operation, the wiggler runs at sub-atmospheric pressure ~50 mbar below zero gauge-pressure with temperature range of 3.1-3.5 K at the second stage of the top cryo-coolers. The minimal no-load pressure recorder during the SR shutdown was –162 mbar. In case of the single quench, the boil-off gas is usually contained within the cryostat with a pressure rise to below 300-400 mbar activation pressure of the two pressure relief valves. There is a rupture disk with activating pressure of 1.7 bar (gauge) in case of further pressure rise for machine safety protection.

During LHe refilling procedure it was observed that the LHe transfer was blocked. Pressure was building up inside the cryostat with no sings and indications from the external pressure gauges. A large amount of cold helium gas was expelled from the cryostat through the refill port when the refill tube was removed.

The ice blockage was experienced several times over the 2-3 years of operation. The wiggler had to be warmed up to about 100 K in order to enable a LHe refill.

INVESTIGATIONS

The following areas were investigated for the refill and pressure built up problems:

1. Air leaks.
2. Vent path
3. LHe refill path

Air Leak Problems

Air leaks were discovered at the followings:

- Air leaked through the pressure relief valves which were not able to seal-back tight after gas release during quench, especially when a large amount of cold helium gas was passing through the seal surface.
- Air also leaked through the mechanical and electrical connection ports that had Buna O-ring seals.
- There was a small leak through the pinhole in the rupture disk.

Vent Path Problem

The air leaking into the cold space eventually froze at the wiggler's vent path – see Figure 1, separating the cold space from the room temperature gas space. The vent path was made of a spiral channel cut in a foam insulation installed in wiggler's central throat. The vent path/channel was about 15 mm wide and 10 mm deep, connecting dewar with the top casing where the vent outlet was located. The pressure relief valves and the rupture disk were both connected to this vent outlet. As a result of the blockage, the helium gas was not able to relief through this vent path during liquid helium refilling procedure, at the same time the pressure gauges were not showing properly the cold space pressure - a safety concern was raised.

Figure 1 Spiral vent path cut in the insulation foam.

*Work supported by Budker Institute of Nuclear Physics under contract No. C60109-029
† Linda.Lin@lightsource.ca

ISBN: 978-3-95450-188-5 doi:10.18429/JACoW-MEDSI2016-TUPE22

LOW-ORDER ABERRATIONS CORRECTION OF EXTREME ULTRAVIOLET IMAGING OBJECTIVE WITH DEFORMABLE MULTILAYER MIRRORS*

Mitsunori Toyoda†, Ryo Sunayama, Mihiro Yanagihara
IMRAM, Tohoku Univ, 2-1-1 Katahira, Sendai, Miyagi, 980-8577 Japan

Abstract

To realize high spatial resolution of an extreme ultraviolet (EUV) microscope, the key technical challenge would be reducing wave aberrations of an imaging objective. Astigmatism arising from figure error of a mirror substrate is the primary aberration which spoils spatial resolution. In this study, we develop a deformable multilayer mirror which is capable of correcting astigmatism on the Schwarzschild objective for EUV microscopy. The deformable mirror is consisting of a concave mirror with a Mo/Si multilayer coating, and a mirror holder with a three-points holding mechanism. This novel device acts as a stigmator, since radii of curvature in mutually orthogonal directions on the concave mirror can be precisely controlled by applying bending forces on the holding points. We report detail of optical and mechanical design of the deformable mirror, which can correct relatively large astigmatism with amplitude of 4 nm rms.

INTRODUCTION

When we apply extreme ultraviolet (EUV) with a wavelength between 3 to 30 nm to optical microscopy, high spatial resolution of a few tens of nanometers can be expected in diffraction-limited imaging. Recently, we have proposed the three-multilayer mirror objective for a full-field EUV microscope [1, 2]. The primary advantage of this novel design would be large numerical aperture (NA). The objective can provide large NA of 0.25, which is at least ten times larger than that for conventional zoneplate optics in EUV and soft X-ray region. The large NA design yields good Rayleigh resolution as well as high image illuminance, which is proportional to the square of NA.

Besides, the objective can bring high magnification, which is essential for fast video observation with an EUV CCD camera with moderate pixel size. To realize a high magnification of 1500, we employ a two-stage imaging configuration by combining the Schwarzschild mirror as primary objective (magnification: x30) and an additional magnifier with a single concave mirror (magnification: x50). To confirm an imaging performance of the objective, we have developed the full-field microscope for at-wavelength observation of an EUV lithography mask [3], and we successfully demonstrated that the microscope can resolve fine line and space patterns with half pitch of 30 nm, at an operating wavelength of 13.5 nm [4].

* Work supported by
JSPS KAKENHI: Grant Numbers. 16H03877, and 16K13693,
Shimadzu Science Foundation.
† toyoda@tagen.tohoku.ac.jp

To provide diffraction-limited resolution on the novel objective, the key engineering challenge would be reduction of wave aberrations, where we should eliminate aberrations below 1/14 of an operating wavelength, so as to satisfy the Maréchal criterion [5]. In case of the EUV microscope, allowable aberrations fall within an extremely small value, i.e., 1 nm rms. Wave aberrations does not only originate from an intrinsic effect of optical design, but also from misalignments and figure errors of multilayer mirrors. Especially, astigmatism resulting from figure error of mirror substrates would be a common issue to spoil resolution of the high magnification objective. We often observe astigmatism on the objective, since a small holding forces or gravity applied to mirrors yield considerable figure error, even if we apply well-polished substrates. This fact motivates us to develop a stigmator which can modify surface figure to reduce astigmatism in real time. In this paper, we report detail of a deformable multilayer mirror which can act as a stigmator for stable operation of the EUV microscope.

MECHANICAL DESIGN OF DEFORMABLE MULTILAYER MIRROR

As shown in Fig. 1, the Schwarzschild objective, which is employed as a primary optics for the EUV microscope, is consisting of the two concave (M1) and convex (M2) mirrors.

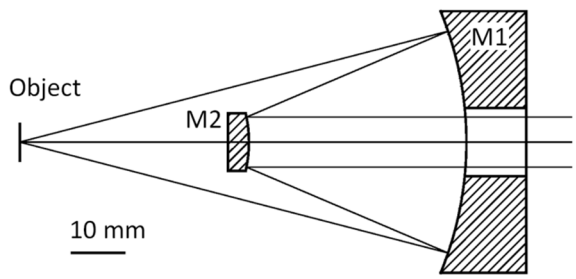

Figure 1: Schematics for the Schwarzschild objective configuration see Table 1.

Table 1: Optical Configuration for the Objective

Magnification	30
Numerical aperture	0.25
Radius of curvature r_1 (mm)	65.935
r_2 (mm)	24.286
Mirror separation d (mm)	41.65
Effective diameter ϕ_1(mm)	42.8
ϕ_2(mm)	9.6

ISBN: 978-3-95450-188-5 doi:10.18429/JACoW-MEDSI2016-TUPE23

GLIDCOP BRAZING IN SIRIUS' HIGH HEAT LOAD FRONT-END COMPONENTS

G. V. Claudiano, O. R. Bagnato, P. T. Fonseca, F. R. Francisco, R. L. Parise, L. M. Volpe
LNLS, Campinas, Brazil

Abstract

Sirius is a 4th generation synchrotron light source in project. Some of Sirius' beamlines will have a very high power density, more than 50 kW/mrad², to be dissipated in components that have a limited space condition. Thus, the refrigeration of these components is complex when one has in mind that the coolant flow cannot be too turbulent in order to not induce much vibration in the components.

Oxygen Free Copper (C10200) has been replaced by the Glidcop on high heat load synchrotron applications due to its good thermal conductivity and preservation of mechanical properties after heating cycles. However, this material is not very workable in terms of union with other materials. It leads to the necessity of development of a brazing process for Glidcop and stainless steel union.

Glidcop samples were submitted to a Cu-electroplating process and a silver base alloy (BVAg-8) was used to join the parts in a high vacuum furnace. Electroplating was used to improve the filler metal wettability. The results were very satisfactory, ensuring water and vacuum tightness. A desirable characteristic not yet proved is the virtual leak property. This paper will discourse about this brazing method.

INTRODUCTION

Currently under construction, Sirius is a 3 GeV, fourth generation synchrotron light source [1]. Sirius is designed to have up to 37 beamlines with ultra-low emittance and high brightness, which will allow high-level research and development on a large range of areas as structural biology, materials science and nanoscience. Development of high-quality technologies is an important point as well (as the Sirius' monochromators and metrology equipment [2]). Figure 1 shows the construction status of the Sirius' project.

Figure 1: Sirius' construction status in August, 2016.

Given its high quality, its components rely on fine requirements on size, safety and cooling capability, having their design on the state of the art. Taking Front-End power absorbers as example: the refrigeration of these components is complex due to their reduced size allied to the high thermal load that is irradiated on them [3]. To solve this problem, engineered materials must be used.

The Glidcop is a good choice due to its good thermal conductivity and preservation of mechanical properties after heating cycles. The difficulty of this project lies on the fact that dissimilar metal components (*i.e.* Glidcop and stainless steel) must be joined and it is needed to isolate both the vacuum and the water chambers. Thus, the joint must be resistant to hold the pressure in the water chamber and must be tight to not allow the transport of small atmosphere molecules to the vacuum chamber. As a trial to manufacture these components, given its specific features, the brazing was chosen as a joining process.

The brazing is a chemical bonding process that consists in heating regions of interest on a set of components in order to reach temperatures at which the filler metal will melt [4]. The liquid filler metal will flow across the gaps by capillary action, covering the mating surfaces and then alloy and create a permanent chemical bond between them. It can join dissimilar metals and porous metal components.

Also, brazing allows the bonding of complex set of components in one operation, saving time and materials that otherwise could be consumed. It is important to emphasize that if the components and the process are properly designed, the brazed joint will be as strong as the base materials and the dimensional stability of the assembly will be maintained. That fact happens because the temperatures reached on a brazing process are much lower in comparison to other processes, as welding.

In addition, if the brazing is done in furnaces the heat is broadly distributed in the whole body volume, reducing the temperature difference between regions. When allied to the smaller heating rates, it results on less stress during the process.

Some other important points are the limitations of the process: stress raisers must be avoided in order to do not result in a fragile brazing joint; and the combination of materials is restricted by the fact that the filler alloy must have its melting temperature below the melting temperature of the base materials.

Brazing is a technique usually applied when there are high demands on strength, fatigue, corrosion and oxidation resistance. Apart from synchrotron technologies, brazing is found on areas such as automotive, aerospace and toll industries.

ISBN: 978-3-95450-188-5 doi:10.18429/JACoW-MEDSI2016-TUPE25

METALLURGICAL EVALUATION OF DISSIMILAR METAL JOINTS FOR ACCELERATOR VACUUM CHAMBER CONSTRUCTION AT THE ADVANCED PHOTON SOURCE UPGRADE PROJECT *

G. Navrotski† and B. Brajuskovic, Advanced Photon Source,
Argonne National Laboratory, Argonne, Illinois, 60439 USA

Abstract

Tubular vacuum chamber assemblies made of aluminum, copper and stainless steel alloys will be used in the new Multi Bend Achromat (MBA) storage ring that is being developed at Advanced Photon Source (APS). Details of the new lattice magnet system design and ring impedance considerations continue to drive these vacuum chambers to smaller dimensions and thinner walls with tighter geometric tolerances under higher thermal loads. It is important to carefully evaluate the methods used to join these dissimilar metal components looking for compromise in primary strength, permeability, electrical and thermal properties while still creating structures that are ultra-high vacuum compatible and leak-tight. This paper visually details the underlying metallurgical changes that occur when joining various combinations of aluminum, OFE copper, GlidCop® and stainless steel using brazing, bonding and welding techniques. Each of the techniques has its advantages and disadvantages with engineering and economic consequences.

VACUUM BRAZING

To support the accelerator systems development program, a series of vacuum test coupons of a style shown in Fig. 1 were prepared and evaluated. The exact sample shown below includes a 316L stainless steel (UNS S31603) CF flange to GlidCop-Al15® (UNS C15715) vacuum braze (left end), a GlidCop® to OFE copper (UNS C10100) TIG weld (left center) and a stainless to OFE copper braze (right).

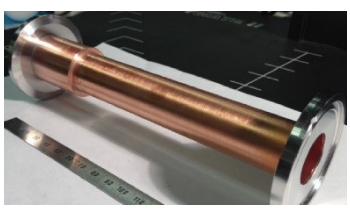

Figure 1: Typical dissimilar metal test coupon.

Joining two different materials using a third intermediate substance that bonds well to both is a highly developed and mature technology. For ultra-high vacuum (UHV) component fabrication using dissimilar metals, vacuum brazing is the 'gold standard' by which other techniques are measured.

A magnified cross-section of a OFE copper to 316L stainless steel vacuum joint is shown in Fig. 2. Both metals are well wet and fused by the gold braze alloy. Excess braze both inside and outside of the joint has a clean well-

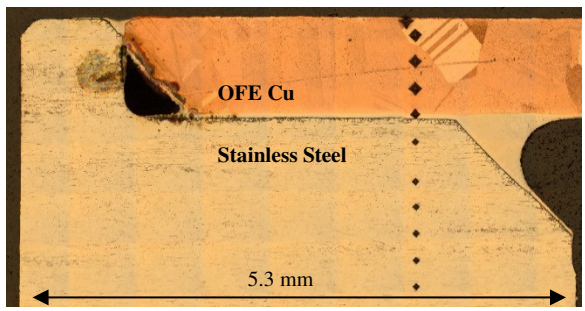

Figure 2: Vacuum braze of stainless to OFE copper.

formed meniscus without voids. The joint design, specifically the chamfer on the OFE copper, creates an unintended trapped volume and potential virtual leak in the component. There has been tremendous grain growth in the copper during processing. Microhardness tests (small diamond indents) show that, as expected, the copper has become fully annealed from its original work-hardened condition.

A similar braze of GlidCop-Al15® to 316L stainless steel is shown in Fig. 3. The reader should carefully consult the literature for the exacting conditions required for GlidCop® brazing [1, 2]. Both metals are nicely wetted and well bonded. There are a few insignificant voids present in the braze metal layer. Microhardness tests confirm that both the stainless and GlidCop® retain their full base metal strength properties, unaltered by the brazing process.

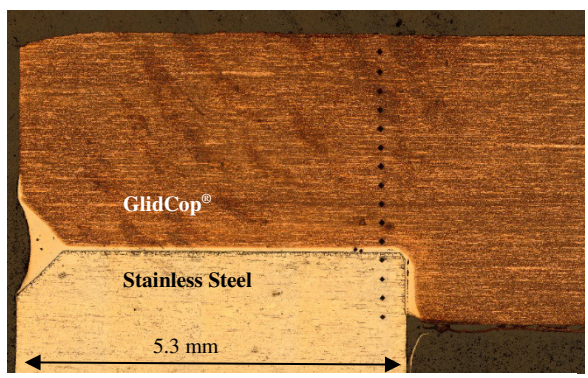

Figure 3: Stainless steel to GlidCop® vacuum braze.

* Funding provided by the Advanced Photon Source, U.S. Department of Energy, Office of Science, Argonne National Laboratory under Contract No. DE-AC02-06CH11357
† email address: Navrotski@anl.gov

ISBN: 978-3-95450-188-5 doi:10.18429/JACoW-MEDSI2016-TUPE26

CARBON-STEEL/POLIETHYLENE RADIATION ENCLOSURES FOR THE SIRIUS BEAMLINES*

L. Sanfelici†, F. H. Cardoso, H. F. Canova, R. Madacki, M. A. Pereira, M. L. R. Santo, J. E. Santos, M. Saveri Silva, L. G. Silva, LNLS, Campinas, Brazil
M. H. A. Costa#, L. Bucianti, E. Palombarini, C. Prudente, Biotec Solução Ambiental, São José dos Campos, Brazil

Abstract

Lead enclosures have been used over the past decades for radiation protection at mid and high-energy synchrotron light-sources, requiring nearly 10% of the investment needed to set up a new beamline. Due to the increasing concern about neutron levels, in part due to the reduction of the photon radiation levels with the increased thickness of the hutch walls, the existing constructive models were revisited and a new constructive approach based on Carbon-Steel (CS) and High-Density Polyethylene (HDPE) is proposed for the SIRIUS beamlines, leading to increased overall radiation protection and potentially lower cost. This work is going to show preliminary simulation results, cost-comparison, as well as a few mechanical design details and prototyping initiatives.

INTRODUCTION

With the progress of the beamlines design for Sirius [1], and driven by the strong bias to foment the national industry motivated by the project sponsors, in 2015 a review of existing constructive options for optical hutches began. In that way the LNLS partnered to Biotec [2], a local company specialized in the design and construction of animal holding houses and clean rooms, not only to develop a solution for optical hutches that meet the radiological requirements but also to explore other companies in the region capable of manufacturing beamline hutches.

As part of an initial survey and assessment of existing solutions, a cost projection was carried out for the main constructive options identified, such as the traditional Pb hutches [3], Barite concrete [4] and CS/HDPE versions. Table 1 presents a simple functional comparison. The price is normalized by reference values obtained from traditional suppliers in the field.

Table 1- Constructive Options for Optical Hutches: Comparing Basic Features and Projected Costs

	Lead	CS/HDPE	Barite Concrete
Wall Thickness	30 mm	50 mm/50 mm	300 mm
Bremsstrahlung	Best	Best	Best
Neutrons	Bad	Best	Best
Synchrotron	Best	Best	Best
Thermal Insul.	Bad	Best	Good
N. Price [0..1]	~1	~0.7	~0.6

The projected costs showed the potential advantage of working with Barite concrete or CS/HDPE combined in comparison to conventional Pb hutches, not to mention the occupational benefits brought by avoiding handling a toxic material such as Lead. The selected option to mechanical-design was the double-walled CS/HDPE due to their dust-free and easy-machining characteristics.

It is not the aim of this work to present deep details regarding radiation protection of the Sirius beamlines or the mechanical design attained but offer a panorama and perspectives of the whole study and development process.

FIRST SIMULATION RESULTS

Table 2: Main Simulation Parameters for Sirius

Simulation Parameters	Value	
Straight section (SS) length	10.34	m
Pressure in the SS	5.10^{-8}	mbar
Distance to hatchet wall	24	m
Electrons energy	3	GeV
Fill current	500	mA
Max. dose rate ($\gamma + n^0$)	0.5	µSv/h

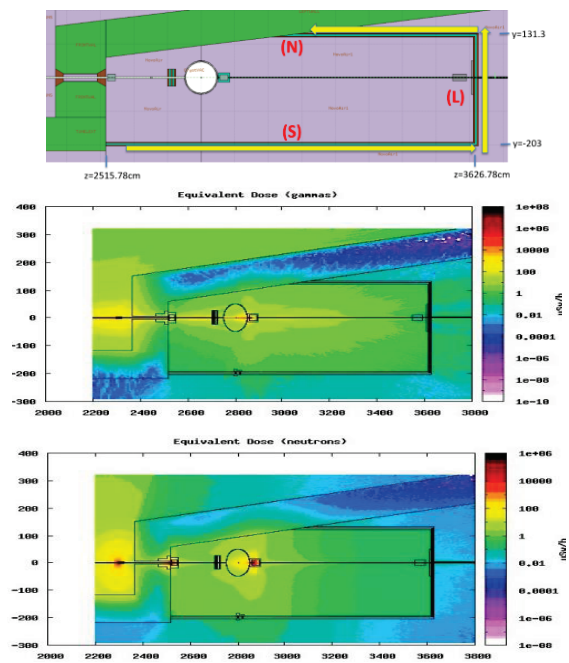

Figure 1: Results for a double-wall hutch composed of 50mm CS followed by 50mm HDPE at Sirius. Top: geometric model. Middle: effective dose distribution for photons. Bottom: effective dose distribution for neutrons.

* Work supported by the Brazilian Ministry of Science, Technology, Innovation and Communication
† lucas.sanfelici@lnls.br
# mhc064@gmail.com

ISBN: 978-3-95450-188-5 doi:10.18429/JACoW-MEDSI2016-TUPE28

CHARACTERIZATION OF THE ACOUSTIC FIELD GENERATED BY THE SINGLE-AXIS ACOUSTIC LEVITATOR

A. H. Chavan[1], B. Hu[2], A. D. Dichiara[2], P. Den Hartog[1], K. J. Suthar[1*]
[1]Engineering Support Division, Advanced Photon Source, Argonne National Laboratory, USA
[2]X-ray Science Division, Advanced Photon Source, Argonne National Laboratory, USA

Abstract

The acoustic levitator utilizes two vertically-aligned, face to face, transducers that emit identical acoustic waves. A standing wave is generated between the two transducers that allows the levitation of liquid droplets at the nodes. These levitated droplets experience an instability. In order to aid in the process of solving this instability, the acoustic field created by one of the transducers was characterized in this experiment and simulated using numerical methods. This characterization and simulation helps to understand the intensity and shape of the acoustic field at different points throughout the region and how the acoustic wave diverges as it travels away from the transducer.

INTRODUCTION

X-ray characterization of the liquid sample usually needs to be held in a container. While x-ray passes through liquid sample, it also passes through the glass capillary. [1, 2] Thus, resulting spectra will have background information with the capillary material. In order to provide container less and contamination free environment, acoustic levitator is utilized for x-ray characterization of material.

When using the acoustic levitator in experiments, levitated particles experience an instability in the acoustic field. This instability can steer the levitating sample away from the X-ray beam. The acoustic field that is generated by the levitator is affected by various components, such as the driving voltage, the frequency and amplitude of the acoustic wave, and the distance between the two transducers that emit the acoustic waves. [3] This paper presents our efforts to understand the instability by characterization and finite element analysis of the acoustic field. We simulated the acoustic field generated by a single transducer using finite element analysis. The simulation results of a sound level profile were compared to the experimental results. The results are discussed in the following sections.

EXPERIMENTAL SET-UP

The characterization of the acoustic field was performed using a high precision microphone (B and K, 4138 - 1/8-inch pressure-field microphone, 6.5 Hz to 140 kHz, 168 dB, 200 V polarization). [4] The position of the microphone was controlled using three stepper motors in Cartesian geometry. The goal was to manipulate the motors to have them move the microphone incrementally throughout a three-dimensional region.

The microphone received the acoustic signal transmitted by the transducer of the acoustic levitator. We placed microphone body away from the measuring point to avoid any interference. The microphone signal was sent to an oscilloscope that digitized the acoustic signal and passed it to a computer for processing. In order to complete accurate and detailed characterization of the acoustic field, a step size of 1 mm was used in the X-Y plane and a step size of 7.5 mm was used on the Z-axis. The wavelength of the acoustic wave is 15 mm; half of this wavelength, 7.5 mm, was chosen as the step size for the Z-axis so as to achieve characterization at key points throughout the acoustic field.

The motion of the motors, control of the microphone, data acquisition, and post processing was performed using LabVIEW. [5] Fig. 1, as seen below, depicts the experimental set-up of the motors along with the microphone and how they are positioned with respect to the transducer.

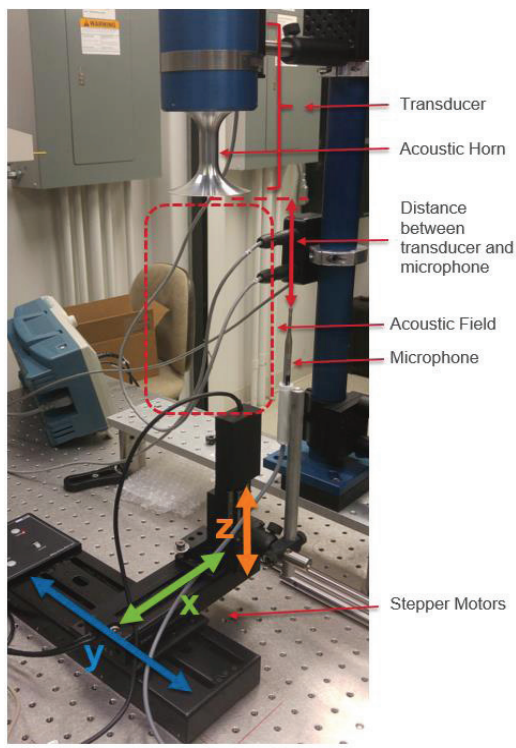

* Corresponding Author : Suthar@anl.gov +1(630)-252-2000

ISBN: 978-3-95450-188-5 doi:10.18429/JACoW-MEDSI2016-TUPE29

INTEGRATION OF A STRIPLINE KICKER PROTOTYPE FOR CLIC PROJECT INTO ALBA STORAGE RING

R. Monge†, J. C. Giraldo, J. Ladrera, M. Llonch, L. Nikitina, M. Pont, M. Quispe
ALBA – CELLS Synchrotron, Cerdanyola del Vallès, Spain

Abstract

The Compact Linear Collider (CLIC) project is an international collaboration working on the development of a high-energy and high-luminosity machine which will accelerate and collide electrons and positrons at energies between 0.5 and 5 TeV. The extraction system for the Damping Rings of CLIC shall follow very tight requirements in order to maintain the ultra-low emittance of the extracted bunches. A first prototype of the extraction kicker based on stripline technologies has been built and characterized at CERN without beam. The stripline will be shortly installed in the ALBA Synchrotron to be tested under beam. In situ measurements of the impedance, transversal field homogeneity and flat-top ripple aims to complete its characterization. This contribution presents the design of the set up for the integration of the stripline in one of the medium straight sections of ALBA storage ring.

INTRODUCTION

The CLIC project is an international collaboration working on the development of a high-energy and high-luminosity machine which will accelerate and collide electrons and positrons at energies between 0.5 and 5 TeV. The Pre-Damping Rings (PDR) and Damping Rings (DR) are required for reducing the emittance of the beams before being injected into the main linac. The injection and extraction from the PDR and DR are performed by kicker systems based on stripline technologies which allow to maintain a low beam coupling impedance and acceptable broadband impedance matching to the electrical circuit [1].

A first prototype of the extraction kicker for the CLIC DR has been designed, built and studied without beam in previous works from C. Belver-Aguilar et al. [1, 2, 3]. In order to complete its characterization, the stripline kicker will be shortly installed in the ALBA Synchrotron to be tested under beam. The results of the in situ tests and measurements of the beam coupling impedance, transversal field homogeneity and flat-top ripple will be compared to the simulations to validate the final design.

This contribution presents the design of the measurement set up for the integration of the stripline kicker into the ALBA storage ring.

LAYOUT INTEGRATION

ALBA Synchrotron was elected for the kicker testing under beam due to the similarity of characteristics in terms of beam energy and low emittance. Figure 1 and Table 1 shows the accelerator layout and main parameters of ALBA machine respectively.

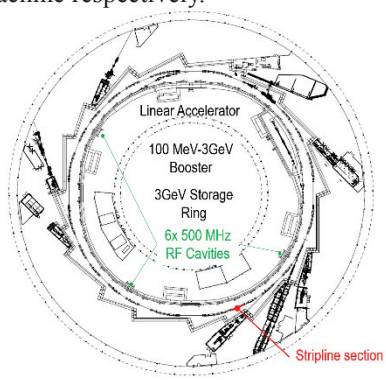

Figure 1: Location of the stripline installation.

Table 1: ALBA Machine Main Parameters

Energy	3 GeV
Design Current	400 mA
Circumference	268.8 m
Horizontal Emittance	4.58 nm·rad

The kicker chamber will be installed in a medium straight section of 3200 mm length, between Sector 07 and Sector 08 of ALBA storage ring. The adjacent vacuum chambers and absorbers have been designed in order to not disturb the beam performance and to protect the stripline from the synchrotron radiation. Figure 2 shows the general layout of the final assembly.

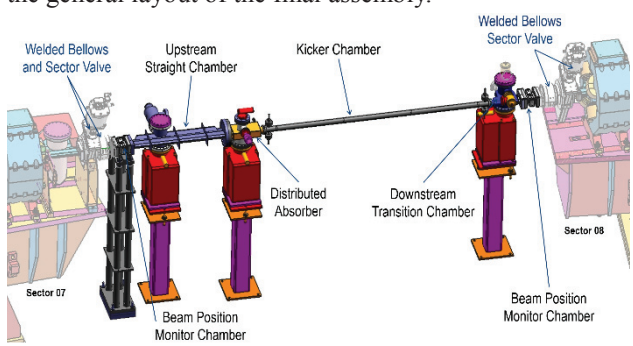

Figure 2: General assembly of stripline section.

Ray Tracing Study

To avoid the incidence of synchrotron radiation over the new elements of the section, ray tracing calculations have been performed. A safety margin of 1 mm has been considered between the inner part of the kicker chamber's ring supports and the x-ray fan. The position and dimensions of the distributed absorber were optimized taking into account the available space of the section, the dis-

† rmonge@cells.es

ISBN: 978-3-95450-188-5 doi:10.18429/JACoW-MEDSI2016-TUPE31

MANUFACTURING OF PHOTON BEAM-INTERCEPTING COMPONENTS FROM CuCrZr

F. DePaola, C. Amundsen, S. Sharma, NSLS-II, Brookhaven National Laboratory, New York, USA

Abstract

Photon beam-intercepting components in synchrotron light sources have usually been made as water-cooled Glidcop® bodies brazed to stainless steel Conflat type flanges. This fabrication method involves many manufacturing steps which result in increased cost, long procurement time and lower manufacturing reliability. A new design approach was recently proposed which simplifies fabrication by eliminating brazing and utilizes a readily available copper alloy, CuCrZr. This paper describes the manufacturing experience gained at NSLS-II from fabricating many components of this new design. Results of an investigation of various techniques for joining CuCrZr to itself, to SS304, and to AL-6061 are also presented.

INTRODUCTION

For over 20 years synchrotron facilities have used Glidcop® material to make photon beam-intercepting components. Glidcop® was chosen because of its good thermal conductivity and because it retains its strength at high temperature. These Glidcop® components require advanced procurement planning because of their high cost, long lead time to produce, and the high risk associated with manufacturing them. Brazing Glidcop® can be challenging due to the tendency of the braze alloy to diffuse into the Glidcop®. Braze repairs are often required to produce vacuum leak-tight joints. This paper is based on the new design approach that was proposed at MEDSI 2014 [1] which eliminates brazing and substitutes Glidcop® with a less expensive and readily available copper alloy, CuCrZr.

NSLS-II CuCrZr COMPONENTS

NSLS-II has installed (1) bending magnet (BM) and (2) 3-pole wiggler (3-PW) frontends to date with total of (24) components made from CuCrZr (Installed components include: Absorbers, Masks, Slits, and Photon Shutters). There are (24) new components currently being manufactured from CuCrZr for future installation of three additional 3-PW frontends. A typical BM/3-PW slit body and fixed mask are illustrated in Fig. 1 and 2, respectively.

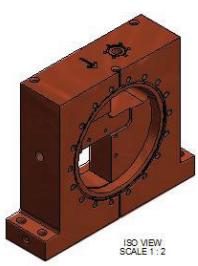

Figure 1: Typical BM/3-PW frontend slit body.

Prototype development of absorbers, masks, slits, and photon shutters based on the new design is ongoing for the insertion device (ID) frontends. The current Glidcop® design for an ID frontend fixed mask is illustrated in Fig. 3 and the proposed CuCrZr design is shown in Fig. 4.

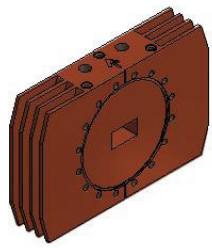

Figure 2: Typical BM/3-PW frontend fixed mask.

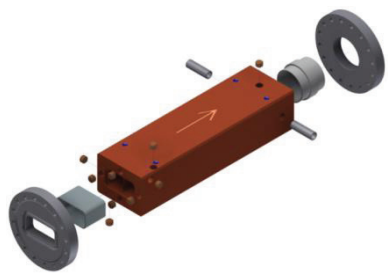

Figure 3: Current design of ID frontend components.

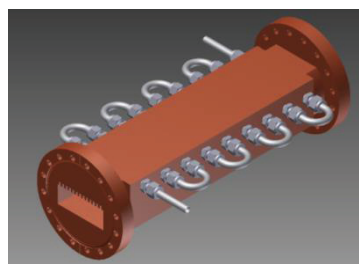

Figure 4: Proposed design of ID frontend components.

EXPERIENCE GAINED AT NSLS-II

General Machining and EDM of CuCrZr

The machinability of CuCrZr was found to be about the same as that for GlidCop® but significantly better than that of oxygen-free copper. Wire EDM of CuCrZr was also straight forward although cutting an aperture into a component 16" long is a slow process as would be expected of a high conductivity copper alloy.

Conflat Flange Knife Edge

The original design incorporated the standard 70° knife edge which is typically machined in stainless steel Conflat flanges. During incoming inspection a number of

ISBN: 978-3-95450-188-5 doi:10.18429/JACoW-MEDSI2016-TUPE32

A GIRDER-FREE MAGNET SUPPORT SYSTEM DESIGN

S. Sharma, NSLS-II, Brookhaven National Laboratory, NY, USA

Abstract

Magnet support systems for the new light sources are required to satisfy several rigorous performance specifications. The support system must be rigid so that its static deflection under its own weight and the combined weight of the magnets is small and repeatable. For vibration stability the lowest natural frequency of the magnet-support assembly should be greater than 50 Hz. To meet thermal stability requirements it is desirable to minimize bending deformations of the support system when subjected to temperature changes. In addition, the magnet support system should be easy to transport, easy to align, and cost effective. Altogether these requirements are difficult to satisfy, especially if the main structural component of the support system is a girder of length greater than 3 meters.

In this paper we propose a magnet support system design consisting of column-type supports joined by removable C-channel beams. The column-type supports provide a superior stability performance without compromising the alignment capability. Analysis results are presented to characterize the performance of this support system.

INTRODUCTION

The storage ring (SR) magnets of new high-brightness light sources have stringent mechanical alignment and stability requirements. The magnets are usually grouped together for assembly on girders in such a way that the stricter specifications apply to magnets on the same girder whereas the specifications for the girders are substantially relaxed. Table 1 shows the alignment and stability specifications for the NSLS-II storage ring magnets [1].

Table 1: NSLS-II Alignment and Stability Specifications in X (horizontal) and Y (vertical) Directions.

Specifications	Alignment (μm)		Stability (nm)	
	Δ X	ΔY	Δ X	ΔY
Magnets	30	30	150	25
Girders	100	100	600	70

Magnets are usually assembled on long girders (in 3–7 m range) outside the SR tunnel. This allows advanced preparation of magnet-girder assemblies as well as use of better techniques for magnet alignment such as the vibrating wire method. Long girders support the weight of the magnets primarily by bending (flexural) deformations which are not conducive to magnet alignment. Bending vibration modes and thermal bending deformations also work against meeting the magnet stability specifications. This is illustrated below for a simple box-beam girder.

A BOX-BEAM GIRDER

A steel box-beam girder of 0.5 m height, 0.5 m width and 0.04 m wall thickness (inset of Figure 1) is analysed for deflection under its self-weight and the weight of the magnets. The weight of the magnets is approximated by doubling the weight density of steel. The deflection for simply-supported boundary conditions is calculated both by a flexural beam equation and by 3-D Ansys analysis that includes shear and compression deformations. As shown in Fig. 1, the gravity loads are resisted primarily by shear and compression deformations for span-to-height ratio R of < 3. For R > 7, the loads are resisted mainly by bending deformations which increase as R^4. As a comparison, the measured gravity deflection of a 5 m long (R = ~ 10) NSLS-II girder was 117 μm, and had a scatter of ~ 15 μm (half of the alignment tolerance) because of friction at the support points.

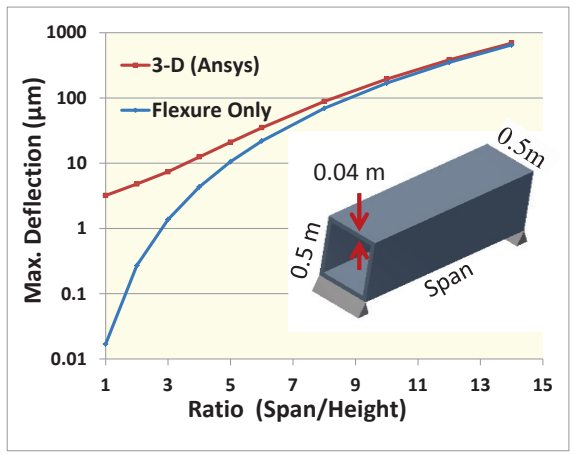

Figure 1: Gravity deflection of a box-beam girder under its self-weight and weight of the magnets versus R (Span/Height).

The box-beam girder can also be used for an insight into its mechanical stability. A natural frequency of > 50 Hz in bending (or torsion) mode is commonly used for the magnet-girder assembly to ensure that the vibration stability specifications are met for the ambient ground motion. Thermal bending deformations are induced in the girder when the girder's expansion or contraction due to change in the tunnel-air temperature is constrained. Because of thermal inertia, a girder typically experiences only a fraction (~ 10%) of the change in the tunnel air temperature. Thermal bending also occurs due to diurnal expansion/contraction of the floor.

The first natural frequency in bending mode and thermal bending (for 1° C change in girder temperature) of the box-beam girder are plotted in Fig. 2. The weight of the magnets is again included approximately by doubling the weight density of steel. As can be seen the natural frequency decreases as $1/R^2$ whereas the thermal bending deformation increases as R^2. A natural frequency of > 50 Hz is obtained for R < 9. Assuming that the stability

ISBN: 978-3-95450-188-5 doi:10.18429/JACoW-MEDSI2016-TUPE33

NSLS-II BEAM APERTURE SLIT VIBRATION STUDIES

C. Spataro, C. Amundsen, H. Bassan, S. Sharma
Brookhaven National Laboratory, Upton, NY 11973 USA

Abstract

Beam aperture slits mounted on stepper-motor driven X-Y stages are used in NSLS-II frontends to define the beam size and to limit thermal loads on downstream optical components. The X-Y stages have positional and resolution requirements of 1 µm and 0.1 µm, respectively. This is achieved by micro-stepping the stepper motor by a Delta-Tau GeoBrick-LV-NSLS-II controller. During the initial operation of the X-Y stages unacceptable levels of vibration when the stages were in motion, and an intermittent sharp squealing when they were at rest, were discovered. In this paper we present the studies that were undertaken to investigate these issues and the solutions that were implemented.

INTRODUCTION

The NSLS-II frontend slit assembly consists of an invar stand, a baseplate, X-Y stages, and water cooled Glidcop slit (Fig. 1).

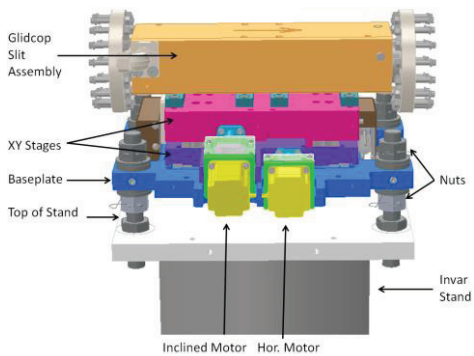

Figure 1: NSLS-II Frontend Slit Assembly.

A pair of slit assemblies is used for the adjustment of the beam size exiting the front end. The L-shape aperture of the upstream slit trims the lower and left edge of the beam while a similar aperture of the downstream slit trims the upper and right edge of the beam. X-Y stages provide the required motion in the horizontal and vertical directions taking into account the coupling of the two motions by the inclined stage. In canted beamlines one pair of slits is used (total of 4 slits) to trim each beam independently. The slit assembly is mounted on a thermally stable invar stand to meet the long term positional stability requirements of 1 um.

XY STAGE MOTOR CONTROLLER

The X-Y stages have position and resolution requirements of 1 µm and 0.1 µm, respectively.

A stepper motor system incorporating a Delta Tau GeoBrick-LV-NSLS-II controller with relative encoders are used for precise positioning of the slits. The horizontal and inclined axis motors are identical. The horizontal position is controlled by the horizontal axis motor. The vertical position is controlled by the horizontal axis motor and the inclined axis motor which is at a 14 degree angle to the horizontal plane. This design was implemented to minimize the vertical size of the slit assembly, thus improving its mechanical and thermal stability. The motors have a micro-step resolution of 160 nm. Both stages are equipped with Renshaw optical encoders with a resolution of 40 nm.

PRE-INSTALLATION TESTING

The motors were installed and configured on the X-Y stage assembly before installation. Extensive tests were performed on the X-Y stages to verify their performance, vibration characteristics, and number of cycles to failure. A slit was mounted on the stages during these tests but the water lines and bellows were not connected. The tests were deemed successful as all performance specifications were met.

RUNAWAY VIBRATION

After the slit assemblies were installed in the SR tunnel, initial testing and calibration revealed that there was a vibration problem which did not occur during the laboratory tests. A homing test routine was used for calibration in which the stages were exercised in both horizontal and vertical directions. During execution of the homing routine, the stages often experienced runaway vibrations, causing the controller to quit the routine. With two slit assemblies side by side, the excessive vibrations from one stage in motion caused the other to move as well. The large vibrations between the stages were being transmitted through the vacuum and water connections.

One of the potential sources of this vibration was identified as the electrical noise picked by long instrumentation wiring. At NSLS-II, the controllers are located on top of the storage ring tunnel about 20 meters away from the motors. However, electrical noise was ruled out as a source when the same vibration problem occurred even when the motors were run locally by an identical controller brought in a close proximity to the motors.

A closer mechanical inspection of the slit assembly revealed some twist in the baseplate. This occurred because the final set-screw adjustments for alignment were performed after the nuts were already torqued, causing distortions in the baseplate. The alignment procedure was modified so that most of the torque was applied after final adjustments. The vibration levels were reduced but not sufficiently to eliminate the runaway incidences.

An experiment was then performed in which a viscoelastic pad was added to the top of the slit to help dampen

ISBN: 978-3-95450-188-5 doi:10.18429/JACoW-MEDSI2016-TUPE36

GROUND VIBRATION MONITORING FOR SXFEL CONSTRUCTION AT SSRF*

R. B. Deng†, F. Gao, L. X. Yin
Shanghai Institute of Applied Physics (SINAP), Shanghai 201204, P. R. China

Abstract

Shanghai X-ray Free Electron Laser test facility (SXFEL) began construction on Dec.30 2014. It is quite important to monitor the ground vibration influenced by the construction at Shanghai Synchrotron Radiation Facility (SSRF), because the SXFEL is just in the north of SSRF and the nearest distance is only 20m. In this paper, the results of ground vibration measurement during the construction period at SSRF experimental hall, tunnel and experimental room near the SXFEL site are shown. Vibrations at different hours, frequency bands and directions are discussed to provide more detailed information on the influence of SXFEL construction to SSRF.

INTRODUCTION

Shanghai X-ray Free Electron Laser test facility (SXFEL) with total length about 300 meters is being built at Zhangjiang campus of Shanghai Institute of Applied Physics (SINAP), where Shanghai Synchrotron Radiation Facility (SSRF) is situated [1]. SXFEL began construction on Dec.30, 2014. It is quite important to monitor the ground vibration influenced by the construction at Shanghai Synchrotron Radiation Facility (SSRF), because the SXFEL is just in the north of SSRF and the nearest distance is only 20m.

METHODOLOGY AND EQUIPMENT

Large-scale pile foundation construction of SXFEL started on Mar. 9, 2015, so a series of vibration measurements were carried out at the SSRF Experimental Hall, Tunnel and Experimental Room since Mar. 2015. The measurement points of A, B, C at SSRF are shown in Fig. 1. Point A locates on the floor of Experimental Hall,

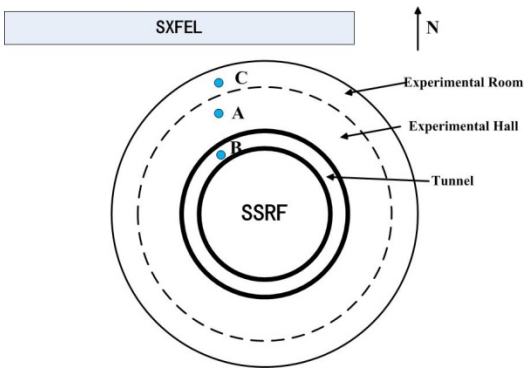

Figure 1: Measurement points at SSRF.

* Work supported by the National Natural Science Foundation of China (Grant No. 11405255)
† dengrongbing@sinap.ac.cn

with B on the floor of Room 1049 and C in the tunnel. We used a DHDAS5927 data acquisition system and DH610 seismometers from Donghua Testing Technology Co., LTD, China. The test site of A is shown in Fig. 2.

Figure 2: Test site on the floor of Experimental Hall.

The displacement power spectrum density (PSD) and integrated root-mean-square (RMS) displacement are derived based on the data analysis techniques [2].The range of the RMS displacement is between 1 Hz to 100 Hz, which is within the effective frequency band of the DH610 seismometer.

MEASUREMENT RESULTS

Contrast of Vibration with and without Pile Foundation Construction

The contrast of continuous RMS displacements of the measurement point A at SSRF Experimental Hall in vertical direction, west-east (W-E) direction and north-south (N-S) direction every Friday in Mar. 2015 before and after large scale pile foundation construction are shown individually in Figs. 3–5. It can be seen that large scale pile foundation construction affects greatly on ground vibration in the vertical direction while affects less on vibration both in the W-E and N-S directions.

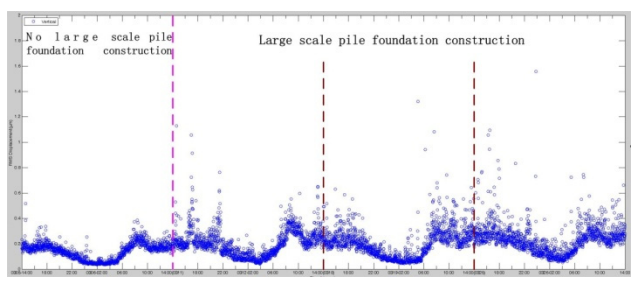

Figure 3: RMS displacement of the point A at SSRF Experimental Hall in vertical direction every Friday in March, 2015.

ISBN: 978-3-95450-188-5 doi:10.18429/JACoW-MEDSI2016-TUPE38

PROGRESS AND MECHANICAL ENGINEERING OF FEL PROJECTS AT SINAP

L. Yin†, L. Wang, S. Sun, W. Zhang, X. Hu, L. Yu, W. Fang
Shanghai Institute of Applied Physics, Shanghai, P. R. China

Abstract

Free electron laser (FEL) technology is the next focus at Shanghai Institute of Applied Physics (SINAP). Shanghai Deep Ultraviolet Free-Electron Laser (SDUV-FEL), a test facility for new FEL principles, was operated for 5 years and got a series of important results. Dalian Coherent Light Source (DCLS), a 50~150nm wavelength FEL user facility based on a 300MeV linac located at Dalian Institute of Chemical Physics, started beam commissioning in August. Shanghai X-ray Free-Electron Laser (SXFEL), a soft X-ray FEL test facility based on an 840MeV linac, will be installed in this month and the commissioning is scheduled at the beginning of 2017. The Progress of the FEL projects and the mechanical engineering in the design and construction are presented.

INTRODUCTION

Shanghai Synchrotron Radiation Facility (SSRF) is a 3.5 GeV light source opened to users from 2009. There are 15 beamlines in operation and the SSRF Phase-II Project, including 16 new beamlines, will be started at the end of 2016. In the meantime, the free-electron laser (FEL) projects are also performed at Shanghai Institute of Applied Physics (SINAP). The Shanghai Deep Ultraviolet Free-Electron Laser (SDUV-FEL) source is a test facility for new FEL principles and techniques. A series of experiments have been successfully carried out in it. It will be closed when SXFEL starts operation in 2017. Dalian Coherent Light Source (DCLS) is developed jointly by Dalian Institute of Chemical Physics (DICP) and SINAP. It is a EUV coherent light source based on ultrafast lasers and electron accelerator techniques. The installation was just completed at DCIP campus and the first light is hoped to be obtained in this autumn. It will be the first user FEL user facility in China. Shanghai X-rays Free-Electron Laser (SXFEL) project, approved by the central government at the beginning of 2015, is under construction. It is located at the north of Zhangjiang campus, just adjacent to the SSRF facility. Fig. 1 shows the view of the SXFEL building. Installation of the facility was started in August and will be completed by the end of 2016. The FEL commissioning is scheduled in early 2017.

Figure 1: The SXFEL building adjacent to SSRF.

SDUV-FEL

SDUV-FEL is an integrated multi-purpose test platform for FEL principles and techniques. The linac is mainly composed of a low emittance photocathode injector, five 3 m long S-band accelerating structures and one bunch compressor. The undulator line includes six 1.5 m long planar undulators with period length of 25 mm and fixed gap of 10 mm. Fig. 2 shows the undulators of SDUV-FEL. The FEL experiments were began in 2009. Some major milestones are achieved. In the end of 2009, SASE experiments were carried out and the SASE light at the end of the 9 m long undulator were obtained. Seeded FEL experiments were began in May 2010. The HGHG saturation was achieved at the end of 2010. The FEL with an EEHG scheme was obtained at the 10th harmonic of the seed in 2013 (shown in Fig. 3). Besides these, a widely-tuneable HGHG, cascaded HGHG and the polarization control via crossed-planar undulators are demonstrated in the following years [1- 3].

Figure 2: Undulators of the SDUV-FEL.

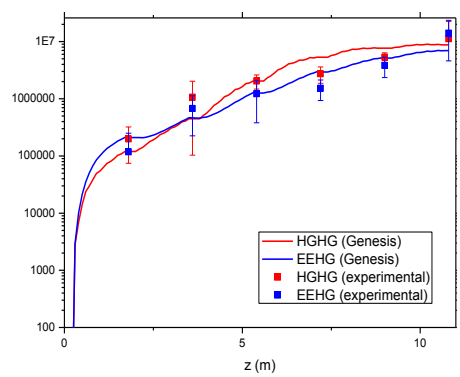

Figure 3: Gain curves of HGHG and EEHG.

† yinlixin@sinap.ac.cn

ISBN: 978-3-95450-188-5 doi:10.18429/JACoW-MEDSI2016-TUPE40

CRYO-READY UNDULATOR U15: PASSING SOLEIL'S 2 METER THRESHOLD IN USEFUL MAGNETIC LENGTH

M. Tilmont, F. Briquez, N. Bechu, L. Chapuis, K. Tavakoli, C. De Oliviera, J. P. Duval, M. Sebdaoui, M.E. Couprie, J.L. Marlats, J.M. Dubuisson, C. Herbeaux, A. Lestrade
Synchrotron SOLEIL, Saint-Aubin, France

Abstract

The U15 is an in-vacuumundulator designed to operate at room temperature and at 70K. It is the first in-vacuum undulator designed, assembled and which will be used in SOLEIL's storage ring that have support beams for magnets longer than 2 meters.A clear gap is felt in the technologies used for manufacturing and assembling compared to our standard 2m length in-vacuum undulators. This is due, in part, to the tolerances imposed by the maximum phase error admissible in SOLEIL's storage ring. The poster will shine lights on those difficulties from a design and manufacturing point of view.

INTRODUCTION

The SOLEIL Synchrotron is in operation since May 2006. 18 of its beamlines use undulators as sources. The first undulators were electromagnet-built (such as HU 640[1]) and Apple-IIs followed since a few years by in-vaccum (cryogenic or not) undulators.

The U15 undulator will be first used in the frame of the LUNEX5 (free electron Laser Using a New accelerator for the Exploitation of X-ray radiation of 5th generation) project of advanced and compact Free Electron Laser (FEL). It will be used for a test experiment of FEL with a laser wakefield accelerator under preparation in the frame of the COXINEL ERC Advanced Grant project[2]. It has been designed as the longest possible magnetic field that can be used for this experiment: 3 meters.

In the design and building phases of the U15, there was a clear threshold that complicated nearly every step of the project compared to the U18s even if the basis of both instruments are very close to one another.

CONTEXT

The in-vaccum in used at the moment are U20s, functioning at room temperature and one cryogenic U18 (a second one is being built). Both are two meters long (with a magnetic period of 20 and 18 mm respectively). The Apple-IIs are typically 2m long when electromagnet-based undulator can reach 6 meters. In the past, HU640 was so long and heavy, that it has been partially reassembled directly in SOLEIL storage ring. This process is not compatible with in-vaccumundulators considering the level of cleanliness required for a storage ring.

The phase error disturbs the electron dynamics in the storage ring, and causes a reduction in the intensity of synchrotronradiation in an undulator as well as impacting the lifetime of the electron beam. In a facility of SOLEIL's size, the beam is very sensitive to the phase error compared to larger storage rings. The definition of the magnetic fields in each undulator (as well as any potentially magnetic instrument affecting the beam) is critical in its impact on the electron beamline.

CHARACTERISTICS OF THE UNDULATOR

- The magnetic useful length of the undulator being 3 meters, its overall length has been designed as 3,4 meters. Its height (2,2m) and depth (1,52m) are closer to U18s and U20s
- It is designed to functions both at room temperature and 70K. The compatibility for both temperatures is a difficulty in itself: the difference in temperature between max and min imply a 12mm shortening of the in-vacuum beams.
- The magnetic forces between the beams are of 10 tonnesfor a 2,6mm gap. The undulator will serve to test the effects of tapering on the electron beam.

PRE-DESIGN AND BUDGETING PHASE

The study of the buildings where the undulator will transit and will be assembled before starting the design is crucial. The most significative element that can be examined beforehand is the assembly of the vessel: adding 1meter to the magnetic length of the undulator adds 2meter at the minimum to the length needed during this stage.

Study of the existing assembly process is then a point to investigate. The beams supporting the magnets are made of aluminium in our IVUs and are light enough to be handled by hand by only two persons. Investigating the efforts needed during manutention and calculating the impacts of adding 50% of length shows that the handling is not possible at all without lifting tools.Are those lifting tools available near the assembly space? Are those lifting tools as long as needed for the new design?

When investigating this second point for example, we saw that our tools and buildings restrained the positions possible for the assembly process to only two options. One of theserequiresto move and recalibrate several instruments in the assembly hall. These questions have several effects on the final budget and the manpower needed for the project and may impact the decision of starting the design or greatly change the time table of the project.

ISBN: 978-3-95450-188-5 doi:10.18429/JACoW-MEDSI2016-TUPE41

DESIGN AND DEVELOPMENT OF A SYSTEM OF HYBRID TYPE TO MEASURE THE MAGNETIC FIELD OF A CRYOGENIC UNDULATOR

Cheng-Hsing Chang†, C. K. Yang, S. D. Chen, J. C. Huang, C. S. Hwang
National Synchrotron Radiation Research Center, Hsinchu Science Park, Hsinchu 30076, Taiwan

Abstract

Cryogenic permanent-magnet undulators (CU) have currently become the most important scheme serving as sources of hard X-rays in medium-energy facilities worldwide. One such set (length 2 m, period length 15 mm) is under development for Taiwan Photon Source (TPS). To obtain a magnetic-field distribution of the cryogenic undulator after it is cooled to an operating target temperature below 80 K, a device of hybrid type combining a Hall probe and stretched-wire method has been designed and developed, to perform the field measurement at low temperature and in an ultra-high vacuum environment. The Hall probe is used to measure the field on axis in the transverse and vertical directions; the stretched wire is utilized to measure the field integral in the vertical and horizontal directions in the horizontal plane. Unlike a conventional field-measurement system in air, this innovative system must be located in an ultra-high vacuum environment with limited clearance. This paper describes mainly the entire system, including kernel components, control systems and preliminary test results in detail.

INTRODUCTION

To obtain great brilliance within the hard X-ray region from an accelerator facility of medium beam energy, approximately 3 GeV, an approach with a cryogenic permanent-magnet undulator (CU) places magnet arrays of short period inside a vacuum chamber [1], which enhances the peak magnetic field strength around 20% compared with an in-vacuum undulator (IU). The deflection parameter (K) is thus kept consistent with an undulator of type out of vacuum. After the entire machine was assembled with the vacuum chamber, the scheme resulted in a difficulty of taking data through a conventional device for field measurement. Many solutions have thus been proposed to solve this problem: BNL designed a customized rectangular vacuum chamber or rectangular port of which one side can be used for access [2, 3]; ESRF adopted a specific dedicated chamber for field measurement [4]; SPring8 has a SAFALI system, and so on [5, 6]. Considering not taking off the main vacuum chamber and using standard vacuum components, NSRRC developed a set of field-measurement system in situ for an undulator in vacuum. It was applied to verify the magnetic field on axis of several undulators in vacuum, but had facilitated only an atmospheric environment [7]. To fulfill a further requirement for the measurement of a cryogenic permanent-magnet undulator in the near future, the device must be able to accommodate to an ultra-high vacuum surrounding without contamination and interference. This paper presents the current efforts of a new design and development of a CU field-measurement system.

SYSTEM REQUIREMENTS

To characterize the magnetic performance of CU15 in operating conditions at low temperature, the field-measurement devices must be placed in a narrow clearance space of the ultra-high vacuum environment around a vacuum chamber, magnet array and a nearby cooling system. Adjacent components in the vicinity of the magnets and the field-measurement device must neither interfere with each other nor perturb the signal source. As stated above, a compact design is a crucial and essential element of the system development. The movement requirements of the measurement system are listed in Table 1. To avoid an accidental collision due to loss of control resulting in component damage or system failure, interlock protection devices must also be taken into account.

Table 1: Movement Requirements of Each Method

Method	Stretch Wire	Hall Probe
Stroke range		
Vertical	±1 mm	±5 mm
Transverse	±22 mm	±1 mm
Longitudinal	-	2.4 m
Scanning Speed	10 mm/s	3 mm/s

System Composition - Hardware

Figure 1 displays the overall construction of the system to measure a magnetic field. The free space between vacuum chambers is used to accommodate the measured undulator. According to the functions of the system, the field-measurement equipment of hybrid type can be divided into two portions, a Hall probe and a stretched wire.

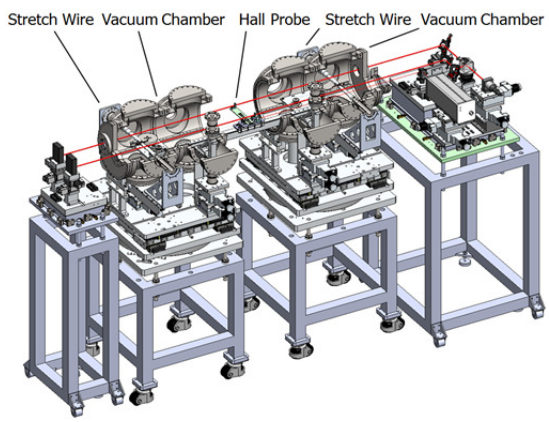

Figure 1: Overview of the measurement system.

† cschang@nsrrc.org.tw

ISBN: 978-3-95450-188-5 doi:10.18429/JACoW-MEDSI2016-TUPE44

OPTIMIZATION FOR THE APS-U MAGNET SUPPORT STRUCTURE *

Zunping Liu †, Jeremy Nudell, Curt Preissner, Jeff Collins, and Herman Cease
Advance Photon Source, Argonne National Laboratory, Argonne, IL 60439, USA

Abstract

The Advanced Photon Source Upgrade (APS-U) is to replace the existing storage ring with a multi-bend achromat (MBA) accelerator lattice [1]. For the APS-U removal and installation, current planning calls for a 12-month shutdown and testing period, prior to resumption of operations. It calls for quick installation of the magnet support system within assembly and installation alignment tolerances. A three-point semi-kinematic vertical mount for the magnet modules is the approach to reduce time for alignment. The longest section is the curved Focusing-Defocusing (FODO) section (four quads with three Q-bends interleaved, and a three-pole wiggler). All magnets of the FODO module sit on a single piece of support structure in order to have good control over the magnet-to-magnet alignment tolerance. It brings challenge to minimize the top surface deflection and maximize the first mode frequency of the magnet support structure that is supported at three points. These constraints require optimizing the magnet support structures. Details of the optimization, including three-point positioning, material selection, and topology optimization, are reported in this study.

INTRODUCTION

Optimization is subjected to constraints. For example, the APS-U removal and installation is planned for a 12-month shutdown and testing period prior to resumption of operations, and the assembly and installation alignment tolerance is specified as 100 microns RMS for girder-to-girder alignment [1]. To meet such specifications within a one-year period, a three-point semi-kinematic vertical mount for the magnet modules is considered as the best approach, in comparison with four-point and/or non-kinematic vertical mount. The conceptual design is based on the three-point semi-kinematic vertical mount, and the goal of optimization is to meet the technique specifications.

The APS-U specifies 9 nm RMS as magnet-to-magnet vibration tolerance and 30 microns RMS as magnet-to-magnet static tolerance within a girder [1], a common term for the magnet support structure. Spacing of the three-point support can be optimized, which helps to minimize the magnet-to-magnet static tolerance due to surface deflection of the support structure. The vibration tolerance is related to the ground vibration spectrum. The floor vibration spectrum in the APS storage ring has 1 nm absolute value at 50 Hz [2,3]. It indicates that the first mode frequency around 50 Hz of an assembled module is guaranteed to meet the magnet-to-magnet vibration tolerance. It leads to a goal, 50 Hz as the lower bound of mode frequency, for optimization. A parametric study of girder height is performed during optimization.

For conceptual design and optimization, topology optimization is an ideal tool. It allows selecting the best elements in a given design space that maximizes the use of material. Research on numerical topology optimization started three decades ago [4] and Genesis® incorporated the discipline nearly two decades ago [5]. It's available for statics, eigenvalue, buckling, frequency response and random response load cases. Among a bunch number of commercially available topology optimization software, the Genesis Topology for Ansys Mechancial (GTAM) [6] is utilized in this study. Two major constraints, minimizing strain energy and maximizing frequency response, are applied during the optimization process.

For a given structure, material of higher elastic modulus produces a higher natural frequency. Fabrication capacity by vendors constrains in material selection because of the structure size and complexity. Fabrication constraints are available in GTAM but not applied for the conceptual design and optimization. A cast iron design was chosen because of its design flexibility, low cost, and favorable vibration damping properties.

The FODO girder, the longest of the APS-U girders at approximating 5.6 meters long, is studied as a representative. All magnets of a FODO module sits on the girder, a single piece of support structure. The girder is then supported on a concrete plinth through a three-point semi-kinematic mount together with horizontal pushers. The plinth sits on a nominal 1-inch thick epoxy grout on floor. The pushers are ignored during optimization. This study focuses on the girder.

SPACING OPTIMIZATION OF VERTICAL SUPPORTS

The FODO girder has a top surface 5.568-meter long and 1.1-meter wide. As an initial step of the conceptual design, a 160mm thick plate is assumed as the girder. Because the length-to-width ratio is as large as 5 times, the three points are arranged with one point at center and the other two symmetrically toward two ends along the long side, as shown in Fig.1. The point at the center along the long side is set at one end along the short side and the other two points at the other end. The support span along the short side is maximized, which is preferred from the point view of stability and the rolling mode of vibration. In such a scheme, the spacing optimization is to find an optimized span between the two symmetrically arranged points along the long side. In the calculation the structure is supported by three bars, each 100mm in diameter and 200mm long. Figure 1 shows the total displacement when the span is set at 4 meters. When the span varies, the maximum value of

* Work supported by the U.S. Department of Energy, Office of Science, under Contract No. DE-AC02-06CH11357
† zpliu@anl.gov

ISBN: 978-3-95450-188-5 doi:10.18429/JACoW-MEDSI2016-WEAA02

X-RAY ABSORBER DESIGN AND CALCULATIONS FOR THE EBS STORAGE RING

F. Thomas[1], J.C. Biasci, D. Coulon, Y. Dabin, T. Ducoing, F. Ewald, E. Gagliardini, P. Marion
European Synchrotron Radiation Facility (ESRF), Grenoble, France
[1] also at Institut Laue-Langevin (ILL), Grenoble, France

Abstract

The Extremely Brilliant Source (EBS) of the ESRF will hold new type of X-Ray absorbers: a new material will be used (CuCr1Zr suggested by [1]) together with a novel design integrating:

- Conflat (CF) flange machined in the absorber body. No weld, no braze.
- Optimized toothed surface profile, reducing the induced thermal stresses.
- Fluorescence Compton and Rayleigh scattering integrated blocking shapes.
- Concentric cooling channels.

A brief overview of the new design and concepts for toothed absorbers will be given.

The presentation will then focus on thermal-mechanical absorber calculations, combining both Computational Fluid Mechanics (CFD) and Finite Elements Analysis (FEA). The calculations were made using the ANSYS packages [2, 3].

The calculations and calculation process will be discussed as well as the design criteria chosen by the team.

The CFD calculations will show that an effective heat transfer coefficient between the water and the copper part can be estimated for concentric cooling channels as well as the pressure drop through the absorber.

Finally, the stress analysis will be emphasized. The type of stresses (tensile, compressive or shear) and their nature (primary or secondary) will be linked to the choice of design criteria.

INTRODUCTION

The ESRF took the strategic decision to make most if not all the X-Ray absorbers of the new EBS storage ring in CuCr1Zr copper alloy instead of classical Cu OFE [4] or Glidcop® AL-15 [5]. In order to reduce the risk of using a new material, we designed absorbers in a way that they work always in the purely elastic regime.

The first paragraph will be a brief overview of the new design and concepts used for toothed absorbers – machined CF flange, toothed scattering blocking shape and concentric cooling channels.

In the second paragraph, we will discuss the CFD model used to determine an effective heat transfer coefficient of 15 kW/m^2/K per cooling channel for a flow rate of 4.24 l/min together with an estimated pressure drop of $\Delta p \sim$ 0.3 bar.

The third paragraph will show thermal and mechanical calculation results of one of the new absorbers: the 2 cooling channels, single jaw, ABS-CH9-1-2 horizontal absorber. The stress analysis will be detailed and linked to stress design criteria.

BRIEF OVERVIEW

In the EBS, the toothed absorbers will have to absorb normal power incident densities up to 110 W/mm^2. In order to spread out the heat load on larger surfaces, one can make triangular toothed surfaces, reducing the power density by $\sin(\beta).\tan(\alpha)$, 2β being the top angle of the triangular tooth and α the tilt angle of the teeth base relative to the beam, i.e. the grazing angle if they were no teeth – see fig. 1. In our case, optimization between large spreading surfaces, implementation in the vacuum chamber, standardization and machinability leads to a 2β angle of 45° and an α angle around 10° (absorber dependent due to geometrical constraints), reducing the power density deposited by ~ 90-95% (theoretically).

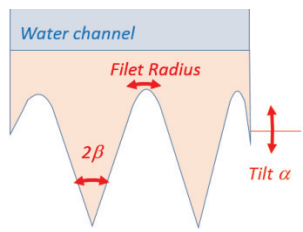

Figure 1: Relevant parameters for an absorber's jaw

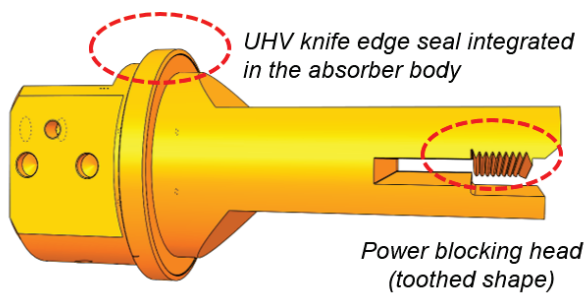

Figure 2: Toothed horizontal absorber overview

Figure 2 emphasizes the innovating design choices made for the EBS absorbers: CF knife edge machined in the absorber body, single jaw absorbers with a longer tooth at the right end of the jaw.

We made the calculations assuming that the angular misalignment was 1.5°, 0.5° from the angular divergence of the X-ray beam and keeping 1° safety margin.

ISBN: 978-3-95450-188-5 doi:10.18429/JACoW-MEDSI2016-WEAA03

THERMAL STABILITY OF THE NEW ESRF EXTREMELY BRILLIANT SOURCE

B.Tampigny, Y. Dabin, F. Thomas[1], J.F. Bouteille, L. Favacque, T. Marchial, F. Favier, P. Roux-Buisson, J.C. Biasci, P. Raimondi, D.Martin, M.Diot, A.Flaven Bois,
European Synchrotron Radiation Facility (ESRF), Grenoble, France
[1]also at Institut Laue-Langevin (ILL), Grenoble, France

Abstract

In the frame of the Extremely Brilliant Source project (EBS), studies dedicated to disturbances have been more intensively investigated. Engineering instabilities have two origins: mechanical and thermal.

Major thermal issues are:

- air conditioning presents a temperature ramp up of 2°C along the sector, in the tunnel
- storage ring requires a warm up period of 4 days for reaching stable orbit

These effects have been observed and corrected for 20 years.

With EBS requirements, we need to identify these thermal effects in order to reduce disturbances, thus improving more systematically source stability. The study is led by the comparison between present and new thermal system.

To do so, it is necessary to evaluate the heat balance in this system, as well as to identify the thermal time constant for each component.

Finite Element Analysis (FEA) models have been performed to explore the sensitivity of these thermal issues. A full scale mock-up cell equipped with a prototype girder was implemented aimed at revealing power cables influence inside. A FEA model was also developed for the present storage ring to analyze the air stream cooling process.

Although investigations have already been developed, some others remain to be achieved by the end of 2016.

OVERVIEW

This is the domain of instability. Light source storage rings errors have been investigated for a long time, however the new EBS project is faced to set new questions within the facility. The present storage ring has been operated for 25 years, and of course, it is highly compensated in many error aspects.

Instabilities We proposed to consider the closed-orbit errors, in the following breakdown:

1. Permanent static errors from the origin
2. Permanent variable errors (quick effects)
3. Errors triggered by the beam operating conditions
4. Long period errors

While the two first have mechanical origins effects (alignments, fiducialisation, vibrations, etc.), the last two have thermal origins effects. The present storage ring has two major thermal issues:

- A longitudinal gradient of 2°C between the air ventilation inlet and outlet along a tunnel quarter
- A transient warm-up period of 4 days before reaching a stable orbit

Resolving these thermal errors requires having a very fine understanding of the storage ring thermal behaviour. We have in fact to deal with a thermal system, which we need to define.

Thermal system Such a thermal system is very complex. It contains many components coupled all together. We proposed to consider the following system:

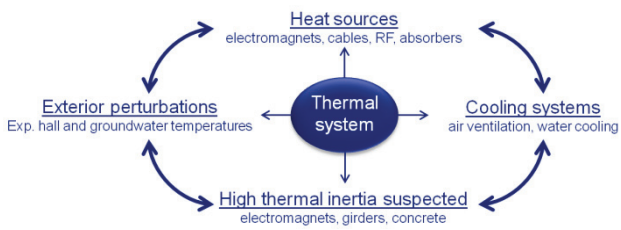

Figure 1: Thermal system of the ESRF storage ring.

As we can see in Figure 1, the thermal system is composed by four main components:

- Components heat sources: electromagnets, cables, Radio Frequency (RF), absorbers
- Two cooling systems of the storage ring: the air ventilation and the water cooling system
- High thermal inertia items: electromagnets, girders, concrete walls and slabs
- External disturbances: experimental hall and groundwater temperatures

Like any usual system vision, most of these components are coupled together.

This paper will not cover all aspects of this system; we will focus mainly on electromagnets as main heat source and thermal capacity. We will discuss also about the air ventilation of the storage ring, girders, external disturbances (experimental hall temperature), power cables and concrete slab.

Our approach is led by some parallel exploration with FEA, as well as full scale mock-ups measurements.

EXPLORATING WORKS

In order to characterize the thermal system of the ESRF storage ring, several components of the lattice were calcu-

ISBN: 978-3-95450-188-5 doi:10.18429/JACoW-MEDSI2016-WEAA04

NOVEL NUMERICAL METHOD FOR CALCULATING THE SHADOW PROJECTION AND COLLISIONS OF A MULTI-AXIS GONIOMETER AT DIAMOND

V. Grama†, A. Wagner, Diamond Light Source, Didcot, UK

Abstract

Beamline I23 is a long-wavelength macromolecular crystallography beamline at Diamond Light Source. The end station is a unique instrument with a bespoke cryogenically cooled multi-axis goniometer and a large curved Pilatus 12M detector in a high vacuum environment. As experiments become limited by radiation damage to the crystals, optimised strategies are needed to orient crystals in the most efficient way to obtain a complete dataset with a minimal X-ray dose.

Two key factors affect the optimisation strategies. Firstly, shadowing on the detector by the goniometer resulting in data loss in this region and secondly, collisions between the goniometer and other components in the end station restricting the available angular range for sample centering and data collection. This paper discusses the numerical methods for calculating the shadowing of a multi-axis goniometer on a semi-cylindrical detector and the calculation of the allowable angles for various conditions to prevent collisions with neighbouring components.

INTRODUCTION

The long-wavelength macromolecular crystallography (MX) beamline I23 at Diamond Light Source is a unique instrument currently being commissioned. Its main use is to solve complicated protein or nucleic acid structures without additional labelling directly from the naturally occurring sulphur or phosphorus atoms in these macromolecules. To eliminate air absorption at longer wavelengths, the complete end station including the goniometer and detector is in vacuum. As diffraction angles increase at long wavelengths, dedicated solutions for the detector and a multi-axis goniometer have been developed. The detector is a large semi-cylindrical Pilatus 12M area detector developed by Dectris. The multi-axis goniometer in inverse-kappa geometry has been built by the UK Astronomy Technology Centre. It has an $\propto_{\kappa}$ angle of 50° which allows the alignment of crystals along any given crystallographic axis [1].

The samples can be exposed to only a certain amount of radiation dose for data collection before they are damaged. Hence, it is vital to predetermine the most efficient way of orienting the crystal to obtain a complete dataset with minimal X-ray dose.

In order to generate strategies for data collection it is important to know two key factors which affect the optimisation in advance. Firstly, the goniometer kappa head assembly has a fairly large footprint. Because of this, at certain kappa and omega angle combinations the kappa assembly interferes with the projected diffraction leading to shadowing on the detector. This results in a data loss in this region. The shape and location of the shadow is dependent on the orientation of the kappa and omega axes. Secondly, it is important to know what angles are accessible for crystal centering and orienting for data collection. There is a restricted angular range which varies due to potential collisions with other moving components, such as the beamstop, backlight and sample viewing system. These share a common space envelope with the goniometer. Also, it is necessary to generate a collision model to ensure safety during operation since all critical systems operate inside a large vacuum vessel with limited visibility.

SHADOW PROJECTION MODEL

There are six main factors which affect the location and shape of the shadow on the detector –

1. The 3D geometry of the goniometer kappa axis assembly
2. The 3D geometry of the detector
3. The omega angle
4. The kappa angle
5. The XYZ offset on the centering stage
6. The sample position

The global coordinate system for the model is in accordance with the Diamond beamline axis orientation standard. The origin of each axis is at the sample position with the axis arrangement following the right had rule.

- The X axis is horizontal and perpendicular to the beam with the positive direction towards the goniometer.
- The Y axis is vertical with the positive direction being upward.
- The Z axis is horizontal and parallel with the beam with the positive direction being in the direction of propagation of the X-ray beam.

The global coordinate system is shown in Fig. 1.

Goniometer Geometry

The multi-axis goniometer is in inverse-kappa geometry. The main rotational axis or omega (ω) axis has an angular range of ±270°, the secondary kappa (κ) axis

Diamond Light Source, UK
† vinay.grama@diamond.ac.uk

ISBN: 978-3-95450-188-5 doi:10.18429/JACoW-MEDSI2016-WEBA01

NOSTRADAMUS AND THE SYNCHROTRON ENGINEER: KEY ASPECTS OF PREDICTING ACCELERATOR STRUCTURAL RESPONSE*

C. Preissner†, H. Cease, J Collins, Z. Liu, J. Nudell,
Advanced Photon Source, Argonne National Laboratory, Argonne, IL, USA
B. N. Jensen, MAX IV Laboratory, Lund University, Lund, Sweden

Abstract

Multibend Achromat (MBA) synchrotron designs are placing stringent mechanical tolerances on the magnet support systems. At the APS-U the magnet-to-magnet vibration tolerances are about 10 nm. [1]. Timelines, installation requirements, and budgets constrain the resources available for prototyping and physical testing. Reliance on FEA to predict dynamic response is paramount in insuring the tolerances are met. However, obtaining accurate results from a magnet support structure FEA is not as simple as analysing the CAD model of the structure.

The 16th century author Nostradamus published a collection of prophecies that since his time, have been held up as predictions of various world events. While it is attractive to think his collection of short poems can be used to foretell the future, in reality it is only the vagueness and absence of any dates that make them easy to apply in a posthoc basis. Arguably, a similar statement can be made about the use of FEA in predicting accelerator support response. In this paper the important contributors to FEA dynamic modelling will be discussed along with techniques that can be used to generate necessary data for models that can accurately predict response.

INTRODUCTION

Background

Numerous multi-bend achromat (MBA) synchrotrons are either under construction or planned [2, 3]. At the Advanced Photon Source (APS) a major upgrade is in the planning stages. The electron beam in this machine will have much smaller transverse dimensions, and consequently more stringent beam stability requirements than the current APS. In addition, the X-ray beams will be focused to ever smaller dimensions, placing more stringent stability requirements on the X-ray source point [4]. Both of these requirements result in magnet-to-magnet vibration tolerances on the order of 10 nm and magnet group-to-magnet group (girder) requirements of a few tens of nanometers.

Along with challenging physics requirements, facility, budget, and logistic constraints cause significant pressure on the design process. For example, the APS-Upgrade (APS-U) project spans multiple years, though the installation and commissioning phase is to take place over a single 12-month dark period. Critical engineering choices need to be made very early in the process. The combination of the physics and project planning constraints push engineering designs in new directions for which limited performance data are available. In the context of magnet support structures, predicting the modal and vibration response before construction are viewed by the APS-U engineering team as essential to completing the magnet support structure designs [5-7] and meeting the machine requirements in and economical and timely manner.

The goal is to have a validated process and set of models, by which the important magnet support system structural response characteristics such as natural frequency, vibration response, static deflection, and thermally-induced distortion can be predicted for each of the magnet support systems. Ideally, the testing of physical prototypes is reduced to an exercise of design verification rather than one of discovery, as shown in the workflow in Figure 1. This level of simulation is commonly referred to as *virtual prototyping* [8]. It is already being done in the automotive sector [9].

While the motivation for virtual prototyping in the automotive or aerospace sectors may be primarily one of reducing the cost of testing and of serial production products, there is certainly significant desire to produce products that have higher levels of out-of-the-box performance than ever before. This is the similarity to the synchrotron world—to engineer and build magnet support structures that have higher levels of mechanical stability than previous generations of synchrotrons.

Analytical and computational simulation have been used extensively in the design of synchrotron components, primarily in the area of absorbers and optics. Thermal finite element analysis (FEA) models for synchrotron radiation absorbers or optics depend on five important aspects: component geometry, boundary condition definition, material properties, thermal load profile and cooling fluid conditions/properties. These have all been characterized sufficiently such that performance can be well predicted from computational models. In fact, recent work has continued to refine the failure criteria through a better understanding of absorber failure mechanisms. The same level of a priori computational confidence is not currently possible in the arena of synchrotron structural dynamics.

* Work supported by: Argonne is managed by UChicago Argonne, LLC, for the U.S. Department of Energy under contract DE-AC02-06CH11357.
† email address: preissner@aps.anl.gov

ISBN: 978-3-95450-188-5 doi:10.18429/JACoW-MEDSI2016-WEBA03

RECENT PROGRESS ON THE DESIGN OF HIGH-HEAT-LOAD COMPONENTS

S. Sharma†, C. Amundsen, F. DePaola, F. Lincoln, J. Tuozzolo, NSLS-II, Brookhaven National Laboratory, NY, USA

Abstract

A new design was recently proposed for the high power masks and slits of the frontends at the 2014 MEDSI Conference. The main features of the new design are integrated knife edges in high conductivity copper alloys, interception of the photon beam only on horizontal surfaces, replacing Glidcop with readily available CuCrZr, and thermal optimization with internal fins. Numerous components based on this design have been built for NSLS-II frontends and some of the design features have been incorporated into other high-heat-load components such as beamline masks and crotch absorbers. In this paper we describe recent progress at NSLS-II in further advancing this design approach by FE analysis, fabrication and testing.

INTRODUCTION

High-heat-load (HHL) components in light sources have usually been made from GlidCop brazed to stainless steel (SS) flanges. GlidCop has high thermal conductivity comparable to that of OFHC copper, but it can also retain a large fraction of its yield strength after brazing. A new design approach was recently presented [1] that allows a wide flexibility in the design of HHL components. The new designs are cost-effective and eliminate long lead-time for procurement [2]. The main features of the new design and their advantages are as follows:

1. **Integral Conflat Flanges**: Conflat flanges are made directly in high strength copper alloys (such as GlidCop and CuCrZr). This eliminates the expensive and time consuming process of brazing the main body of the HHL components to SS Conflat flanges.
2. **Alternate Copper Alloys**: The elimination of brazing allows the use of other hard copper alloys besides GlidCop (specifically, CuCrZr) which are less expensive and are readily available.
3. **Vertical Beam Interception**: Photon beams are intercepted only vertically (on horizontal surfaces). This leads to a common design for all HHL components because the vertical beam size is usually the same. In addition, the design of these components for canted beamlines is considerably simplified since there is no beam interception horizontally.
4. **Internal Fins**: Fins are machined on the inside (beam intercepting) surfaces which significantly improve the thermal efficiency of the components while trapping the scattered beam.

This new design approach is already under implementation not only at NSLS-II but also at other light source facilities [3, 4]. The progress made at NSLS-II is described in the following sections.

† sharma@bnl.gov

BM/3-PW FE COMPONENTS

One bending magnet (BM) and two 3-pole wiggler (3-PW frontends (FEs) at NSLS-II saw the first full scale implementation of the new design. Approximately 25 components consisting of masks, slits and photon shutters were installed in these frontends in May 2016. They have all been performing well as per specifications. Although intercepting comparatively low beam power, they provided the proof of principle of using CuCrZr components with built-in Conflat flanges.

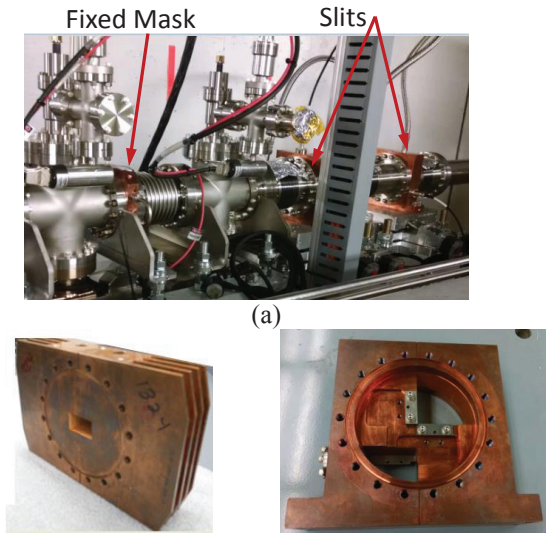

Figure 1: A 3-PW partial FE at NSLS-II, (a) a fixed mask and a pair of slits, (b) air-cooled fixed mask, (c) water-cooled slit.

A partial 3-PW FE is shown in Fig. 1-a consisting of a fixed mask and a pair of slits. Details of the fixed mask and the slit are depicted in Fig. 1-b and Fig. 1-c, respectively. Because of low beam power the fixed mask uses fins for natural convection (air) cooling eliminating the need for flow meters and associated controls. The slits are water cooled for thermal stabilization of the beam aperture. Photon shutters are designed as vertically movable masks. During the pre-installation vacuum processing some of the components were found to have vacuum leaks. This was traced to manufacturing errors resulting in burrs at the knife edges [2].

ID FE AND BEAMLINE COMPONENTS

FE Photon Shutters and Slits

Existing designs of the ID FE photon shutters and slits can be easily replaced with the new designs of very similar overall dimensions. During the prototyping of the new design it was realized that a single piece construction, in which the flanges are machined directly into the main

ISBN: 978-3-95450-188-5 doi:10.18429/JACoW-MEDSI2016-WEBA04

A DISCUSSION ON UTILIZATION OF HEAT PIPE AND VAPOUR CHAMBER TECHNOLOGY AS A PRIMARY DEVICE FOR HEAT EXTRACTION FROM PHOTON ABSORBER SURFACES

K. J. Suthar*, A. Lurie, P. Den Hartog, Argonne National Laboratory, Advanced Photon Source, USA

Abstract

Heat pipes and vapour chambers work on heat exchange phenomena of two-phase flow and are widely used for industrial and commercial applications. These devices offer very high effective thermal conductivities (5,000-200,000 W/m/K) and are adaptable to various sizes, shapes, and orientations. Although they have been found to be an excellent thermal management solution for laptops, satellites, and many things in-between, heat pipes and vapour chambers have yet to be adopted for use at particle accelerator facilities where they offer the possibility of more compact and more efficient means to remove heat from unwanted synchrotron radiation. As with all technologies, there are inherent limitations. Foremost, they are limited by practicality to serve as local heat transfer devices; heat transfer over long distances is likely best provided by other means. Heat pipes also introduce unique failure modes which must be considered.

INTRODUCTION

The heat pipe or, more-generally, a vapour chamber, is a device used to facilitate rapid heat transfer via phase-change. The process requires only a moderate temperature gradient and requires no additional power input. Typically, the heat pipe is used to move energy short distances from heat sources to heat sinks. [1,2] Because of the large transfer of heat associated with a phase change and rapid fluid flow that generally develops in these devices, heat exchange can be well beyond the limits seen in simple conduction or convection-based approaches. The operating principle is simple: A fluid in its liquid state enters the evaporative section of the pipe where it is heated, causing it to evaporate. The vapour then travels to the condensation section where it is liquefied and releases the heat it absorbed in the evaporative section.

Present designs for the APS Upgrade call for photon absorbers which are cooled strictly by convective water flow, as it has conventionally been done. However, consideration of the thermal stresses that will result from intercepting the concentrated beams of synchrotron radiation that are expected with the upgrade suggests that absorber design options, particularly material and geometry choices, will be severely limited. Particularly it is critical as there is a little space afforded by the new, higher-performing MBA lattices that are being evaluated. Another issue of concern is vibration. For required beam performance, exceptionally low levels of vibration are needed to ensure that the particle beam can be precisely steered though lattice magnets. Heat pipes would likely help to reduce vibration as they would reduce the amount of cooling water flow needed to maintain absorber surface temperatures to an acceptable level.

Presently, alternatives like heat pipes are being explored for manufacturing feasibility, economic operation, and ease of fabrication. To help answer these questions, analysis of a conceptual absorber utilizing heat pipes was performed. MATLAB was used to calculate heat pipe performance characteristics based on geometry and other factors and ANSYS was used to perform finite element thermal simulations. The results show that heat pipes can meaningfully improve thermal performance. There are, however, lingering concerns about the reliability of heat pipes for *accelerator applications* which cannot be addressed with such analysis.

Heat Pipe Limiting Factors

A number of design options should be considered when choosing to implement a heat pipe. One such option is the *chamber design*. Thin walls and conductive materials may help to enhance thermal transfer but such choices also may mean that the heat pipe is less mechanically robust. Another option is the *fluid type*. Fluids should be selected which optimize the heat transfer process but which also should not cause corrosion or other degradation of the wick and chamber materials. A number of experiments have established a commonly used list of compatible metal and fluid combinations. [3] There is considerable flexibility in the *wick design* as well. Wicks may consist of a mesh that liquids are squeezed through, they may consist of fibers that guide liquid along, or they may even consist simply of grooves built into the heat pipe wall. Each option offers a different set of advantages and disadvantages which should be weighed relative to the needs of the specific application.

There are a number of physical limitations which impact the transport capabilities in a heat pipe. These include: *capillary pressure difference* - which must exceed the limits introduced by the fluid flow in order to properly move and sustain the motion of the liquid and vapour [1]; s*onic limitations*, or *bottlenecking of fluid* at state change regions, which must be avoided [2]; *entrainment*, or the tendency for droplets of liquid to get caught up in the vapour flow can disrupt flow [2]; *boiling and bubble formation* in the liquid filled wick can also limit the heat capacity [1]. Many of these phenomena will be the result of excess heat capacity. Which limiting factor will limit

* Corresponding author: Suthar@anl.gov, +1(630) 252-4256

ISBN: 978-3-95450-188-5 doi:10.18429/JACoW-MEDSI2016-WECA03

EXPERIENCE WITH THE COMMISSIONING OF THE U15-UNDULATOR FOR SWISSFEL-ARAMIS BEAMLINE AND NEW DEVELOPMENTS FOR THE ATHOS BEAMLINE

P.Boehler†, H. Joehri, A.Keller, M.Locher, M.Bruegger, T.Schmidt, M.Calvi, L.Schulz
Paul Scherrer Institut, Villigen, Switzerland

Abstract

The development of the U15 undulator was presented at the Medsi conference 2012 in Shanghai. Meanwhile the undulatorline is finished. The presentation will explain the experience with the production, the assembling and the commissioning of the undulators. We succeeded to implement a robotic system, that did the final adjustment of all the magnets automatically. Therefore, we were able to reduce the time for the adjustment of the magnets dramatically. A whole loop with measuring, adjustment of the columns and final adjustment with the robotic system for the magnets takes 3 days. The presentation will explain these steps.

For the next beamline, we will profit from the experience of the U15 undulator development, but there are new requirements, because it will be a polarized undulator with a period of 38mm. We are developing a new arrangement of the drives, a further development of the magnet keepers and a vacuum pipe with only 0.20mm of wall thickness.

SWISSFEL PROJECT OVERVIEW

SwissFEL with electron energies of 5.8 GeV will have two undulator lines for hard- and soft X-rays. The first beamline is Aramis that will produce hard X-ray (7 – 1) Å

The second beamline will be Athos for soft X-rays.

ARAMIS UNDULATOR U15

Overview

Figure 3 shows the overview with the following main parts:

- Main frame in mineral cast
- Outer beam
- Wedge drive system
- Cam shaft mover
- Vacuum chamber
- I-beam with block keeper, magnets and poles
- Gap measuring system
- Columns
- Power and controls

† Pirmin.boehler@psi.ch

Main Parameters of U15 Undulator

- Magnetic length 3990mm
- Period 15mm
- Gap workspace 3 to 20mm
- K-values 1.0 to 1.8
- Vertical forces max. 27.4kN
- Magnet material Nd2Fe14Br + Diffused Dy

Changes

After the design, manufacturing and measuring the pre-prototype we had to change and add several things:

- Design and thickness of magnets/poles considering existing block-keeper design (Figure 1)
- Design of columns (Figure 2)
- Monitoring system of wedge drive
- Motor cooling
- Temperature stabilised assembling area
- FEM based column adjustment

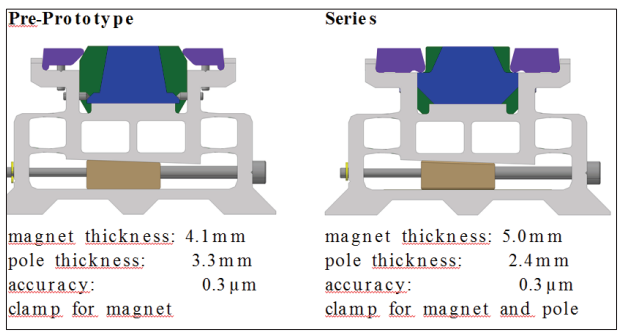

Figure 1: Keeper design changes.

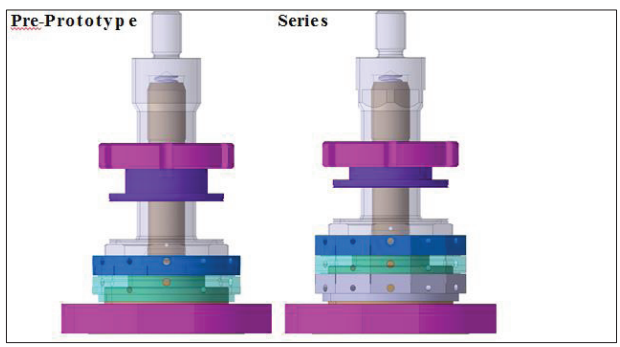

Figure 2: 2nd lock nut to stabilize the fix position. Adjustable range: ± 0.5mm. Accuracy: 1µm

ISBN: 978-3-95450-188-5 doi:10.18429/JACoW-MEDSI2016-WECA04

HORIZONTAL-GAP VERTICALLY-POLARIZING UNDULATOR (HGVPU) DESIGN CHALLENGES AND RESOLUTIONS*

O. Schmidt[1], J. Xu[1], I. Vasserman[1], E. Trakhtenberg[1], K. Suthar[1], N. Strelnikov[1,2], G. Pile[1], D. Jensen[1], E. Gluskin[1]
[1]Argonne National Laboratory, Lemont, IL 60439, USA
[2] Budker Institute of Nuclear Physics, Novosibirsk 630090, Russia

Abstract

The Horizontal-Gap Vertically-Polarizing Undulator (HGVPU) is a compact, innovative, variable-gap insertion device developed by Argonne National Laboratory for the LCLS-II HXR beamline at SLAC. A full sized 3.4-meter-long prototype has been built and fully tested meeting all LCLS-II undulator specifications. An array of conical springs compensates the attractive magnetic forces of the undulator jaws. These springs are designed to exhibit non-linear spring characteristics that can be closely tuned to match the force curve exerted by the magnetic field, thereby minimizing the overall deflection of the strong-backs. The HGVPU also utilizes the existing LCLS-I support and motion system along with other existing equipment and infrastructure, thus lowering overall cost and installation downtime.

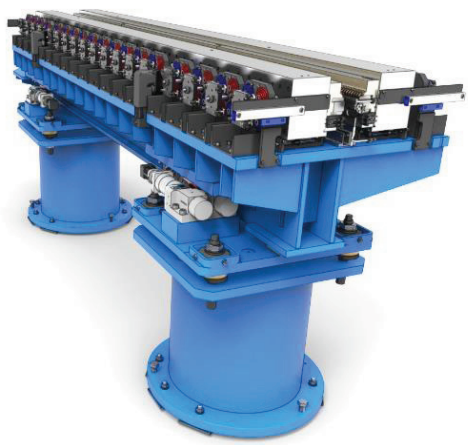

Figure 1: Rendering of final 3.4m HGVPU prototype.

INTRODUCTION

The 3.4-meter-long prototype HGVPU, shown in Figure 1, was successfully developed and built but not without its own unique challenges [1,2]. Very stringent straightness requirements of the strongbacks, temperamental properties of the spring compensation mechanism, mechanical stability over a large temperature range, installation and handling logistics, and unique control system demands all contributed to the development process of this device. Some of the more significant of these challenges will be examined as well as their final resolutions.

* Work supported by the U.S. Department of Energy, Office of Science, Basic Energy Sciences, under contract #DE-AC02-06CH11357.

DESIGN OVERVIEW

The HGVPU is a variable gap undulator that uses an array of springs to compensate for the large attractive magnetic forces between the horizontally opposed undulator jaws. In order to minimize deflection of the strongbacks and to reduce the forces on the actuators, the conical springs are designed with non-linear spring characteristics that approximate the exponential-like force curve induced by the magnetic attractive forces over the variable gap range. Figure 2 shows the cross-sectional view of a single undulator jaw. The magnets and poles are mounted to the magnet/pole mounts which are bolted to the undulator strongback from the back side. Each jaw rests on and is guided by two linear slides that are bolted to the girder surface.

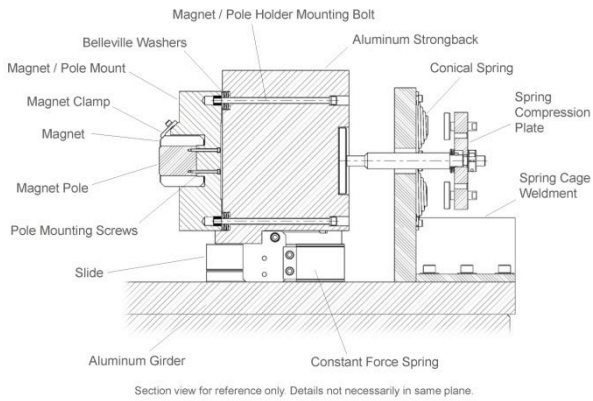

Figure 2: Cross-Section View of Undulator Jaw.

Two actuators, which are not shown in this view, position each undulator jaw at fixed engagement points along the length of the strongback to provide accurate positioning and allow for tapering capability. The springs are affixed to stationary spring cage brackets where they are engaged by the spring compression plates which are directly coupled to the strongbacks. For gaps >21mm, the attractive magnetic forces are negligible and spring compensation is unnecessary. At 21mm, the springs are engaged and increasingly compressed as the gap is decreased to a minimum gap of 7mm.

STRONGBACK STRAIGHTNESS AND ACTUATOR POSITION

Minimizing deflection of the strongbacks was the single greatest design challenge to overcome. The physics requirement for this particular undulator is that the strongbacks deflect less than 19 microns over the full gap range of 200mm to 7mm [3]. The attractive magnetic

ISBN: 978-3-95450-188-5 doi:10.18429/JACoW-MEDSI2016-WECA05

SUPERCONDUCTING RF SYSTEM PLANS AT CLS

C. N. Regier†, Canadian Light Source Inc., Saskatoon, Canada

Abstract

Canadian Light Source (CLS) in Saskatoon, Canada has several cryogenic systems. One of the most critical is a 4.4 K liquid helium system for a superconducting RF cavity. This system consists of a Linde TCF-50 liquid helium plant coupled to a Cornell-designed CESR-B 500 MHz cavity and cryomodule via a 52 metre multi-channel transfer line. Over the years CLS has evaluated failures on the system as well as risks for downtime, and has come up with plans for a major upgrade to the superconducting RF system to improve reliability. An overview of performance and issues to date is presented. Some of the specifics of the risk analysis and upgrade plan will be examined, and details of the process flow discussed.

INTRODUCTION

The Canadian Light Source (CLS) uses a superconducting radio-frequency (SRF) cavity to replace energy lost by the electron beam due to synchrotron radiation. The SRF system operated by CLS consists of a 500 MHz Cornell-designed Cornell Electron Storage Ring B-factory (CESR-B) cryomodule [1] [2] connected via a 52 metre multi-channel transfer line (MCTL) to a Linde TCF-50 liquid helium cryogenic plant. Along with Taiwan Light Source, CLS was one of the first synchrotrons to use SRF for storage ring applications, with the system initially commissioned in 2003. Since then, several other synchrotrons including Diamond Light Source, SSRF, PLS, and NSLS-II have chosen to use the CESR-B design for storage ring radio-frequency (RF) [3] [4] [5]. SIRIUS in Brazil is also planning to use the CESR-B as its storage ring SRF platform.

As with most other synchrotron facilities CLS is a user facility, meaning that operational consistency and reliability are of critical importance. While the SRF system has generally been reliable, over the last 13 years of operation CLS has experienced some problems. Cryogenic transfer line ruptures, cryoplant and compressor issues, and SRF cryomodule vacuum leaks have all occurred at CLS between 2007 and 2013. Based on these experiences, CLS has undertaken several avenues to increase system reliability. Two major projects are planned: The purchase of a third CESR-B cryomodule and a "Cryo Upgrade" project that will see a second cryomodule installed in the storage ring and an additional compressor installed at the plant.

THE CLS SRF SYSTEM

The SRF system at CLS comprises of a single CESR-B cryomodule in Straight 12 of the storage ring, coupled via a cold valve box and a 52 metre multi-channel transfer line (MCTL) to a Linde TCF-50 liquid helium cryoplant. The arrangement of this system is shown in Fig. 1, and a schematic of the system is shown in Fig. 2.

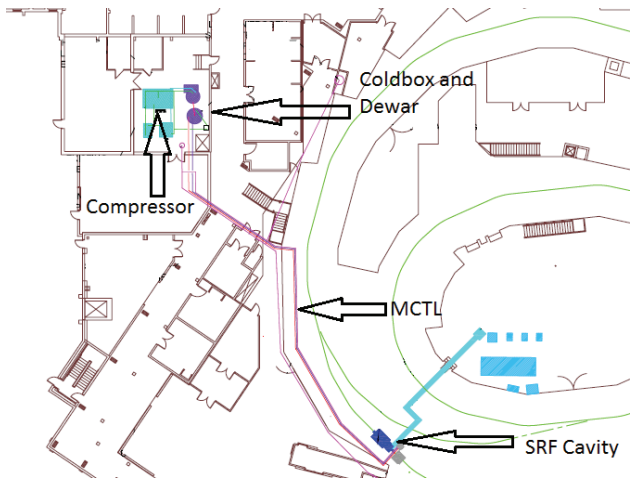

Figure 1: The layout of the CLS SRF system.

The cryoplant is located off of the experimental floor to prevent vibrational interference with ongoing experiments. A 200 kW compressor feeds oil through an oil recovery system (ORS) and gas management panel (GMP) to the coldbox, which deposits liquid into a 2000 L dewar. Pressure head drives liquid down the MCTL to the valve box on top of the storage ring concrete shielding, where a control valve regulates the level in the cryomodule below. Boil-off is returned to the valve box, where a second control valve meters flow back to the plant to regulate the cryomodule helium pressure. Both the liquid supply from the plant and the cold gas return to the plant are piped through the MCTL, along with a liquid nitrogen supply line for the cryostat. The liquid nitrogen is used to cool a thermal shield for the helium along the MCTL and in the cryomodule. A complete spare cryomodule is kept at CLS so that in the event of a cryomodule failure CLS is not required to wait for repair before continuing service. The cryomodules are identified as Cavity 1 and Cavity 2, with Cavity 1 being the first one delivered to CLS.

Figure 3 shows a simple cut-away of the CESR-B cryomodule. Radio-frequency (RF) energy is supplied to the cryomodule via waveguide. The RF passes through a ceramic window located under the cryomodule to transition from the air-filled waveguide into the ultra-high vacuum (UHV) required for the cavity. From there, the RF passes through a pump-out box, which is the point at which turbomolecular pumps can be attached to the UHV, and travels into the waveguide elbow. The elbow curves

† chris.regier@lightsource.ca

ISBN: 978-3-95450-188-5 doi:10.18429/JACoW-MEDSI2016-WECA06

MECHANICAL ENGINEERING SOLUTIONS FOR COXINEL PROJECT*

K. Tavakoli†, T. André, I. Andriyash, C. Basset, C. Benabderrahmane, P. Berteaud, S. Bobault, S. Bonnin, F. Bouvet, F. Briquez, L. Chapuis, M. E. Couprie, Y. Dietrich, D. Dennetière, C. De Oliviera, J. P. Duval, M. El Ajjouri, T. El Ajjouri, C. Herbeaux, N. Hubert, M. Khojoyan, M. Labat, N. Leclercq, A. Lestrade, A. Loulergue, O. Marcouillé, A.Mary, F. Marteau, P. Ngotta, F. Polack, P. Rommmeluère, M. Sebdaoui, F. Thiam, M. Valléau, J. Vétéran, D. Zerbib, Synchrotron SOLEIL, Gif-sur-Yvette, France
J. Gauthier, K. Ta Phuoc, G. Lambert, V. Malka, A. Rousse, C. Thaury, Laboratoire d'Optique Appliquée, Palaiseau, France
E. Roussel, Elettra-Sincrotrone Trieste, Basovizza, Italy

Abstract

COXINEL (COherent Xray source INferred from Electrons accelerated by Laser) is a European Research Council (ERC) advanced grant aiming at the demonstration of Free Electron Laser amplification using electrons generated by laser plasma acceleration. A special electron beam transfer line with adequate diagnostics has been designed for this project. Strong-focusing variable-field permanent magnet quadrupoles, energy de-mixing chicane and a set of conventional quadrupoles condition the electron beam before its entrance in an in-vacuum U20 undulator. This article describes some of the features incorporated into the design of the magnets, girders, vacuum chambers and diagnostic equipment for this experimental machine. Progress on the equipment preparation and installation is presented as well.

INTRODUCTION

When a short multi-TW laser pulse propagates through a gaseous medium, it drives strong plasma waves in its wake. The electric field generated by these plasma waves can exceed by few orders of magnitude those technically achievable with conventional linear accelerators. This accelerating technic is called Laser Wakefield Accelerator (LWFA) [1, 2].

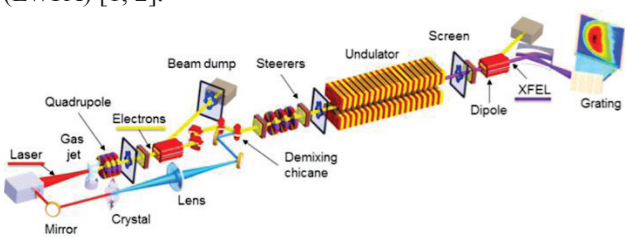

Figure 1: COXINEL's schematic layout.

Using LWFA to operate a Free Electron Laser (FEL) remains very challenging. Among others projects [3, 4] COXINEL aims at using a LWFA to drive an FEL, taking advantage of a specific design of the transfer line to handle divergence and energy spread [5]. The key concept relies on an electron beam longitudinal and transverse manipulation in the transport towards an undulator: a set of strong quadrupoles handles the large divergence of the electron beam and then a "demixing" chicane sorts the electrons in energy and reduces the slice energy spread [6, 7] (see Figure 1).

EXPERIMENT HALL

The experiment hall, called "Salle jaune", is located in "Laboratoire d'Optique Appliquée (LOA)" in Palaiseau, 10 km far from SOLEIL synchrotron site.

The hall is partially covered by a one-tonne crane, which is not sufficient for transportation of the main girders. Some architectural modifications have been performed in the hall in order to free more space for COXINEL installation. Although, there is only 11 meter available between the electron source and the hall's wall. This limited space imposed some trade-off in the choice of installed devices as well as the assembly and alignment sequences. Each different device has been characterized independently and installed on its girder prior to shipping and installation on the LOA site.

GENERAL LAYOUT AND INSTALLATION

Furthermore, all the main components will be presented starting from the electron source down to the final detector following the electron beam direction. A 3D view of COXINEL installation generated by CATIA is presented in Figure 2.

Electrons are produced by one of the two powerful 60 TW laser beam of the LOA "salle jaune laser". The laser beam is focused in a gas jet located in a dedicated chamber called LWFA vacuum chamber. Three permanent magnet variable-gradient (up to 200 T/m) quadrupoles, so called QUAPEVA, placed near to the source inside the LWFA chamber focus strongly the beam. Each QUAPEVA has its independent motorized adjustment table in Z and X directions.

* Work supported by European Research Council
† Keihan.tavakoli@synchrotron-soleil.fr

ISBN: 978-3-95450-188-5 doi:10.18429/JACoW-MEDSI2016-WECA07

ENGINEERING CHALLENGES OF THE VMXi BEAMLINE

J. H. Kelly, Diamond Light Source, UK

Abstract

The in-situ Versatile Macromolecular Crystallography (VMXi) Beamline delivers a high flux density, taking data directly from crystallisation experiments within the plate, using a fully automated endstation. A double multilayer monochromator (DMM) was designed in-house to deliver a 60 fold increase in flux. Two robots and an automated load-lock pass the plates from the crystallisation storage units to the goniometer. A compact endstation was designed to accept the high flux and take data with acquisition times down to a millisecond. This paper gives an overview of the beamline layout and the interesting pieces of engineering design. The beamline is planned to take first user at the end of 2016.

INTRODUCTION

The in-situ Versatile Macromolecular Crystallography (VMXi) Beamline is effectively a new beamline which has been built through the original Diamond Phase one beamline I02. The new fully automated endstation has been designed to obviate the manipulation of individual crystals, preserving crystal integrity and giving diffraction feedback during as well as at the end of growth. A number of new custom components have been designed in-house for this unique beamline. This paper outlines some of the components engineered for the endstation.

The DMM has not been described here as it is the topic of other papers[1][2][3].

VMXI HUTCH

The VMXi hutch is a 4 mm thick fabricated steel construction. The structure is split into four parts. The chicanes are all at floor level. The upper shielding is split in to three rolling sections which may be manually pulled back for access. There are 24 leaded glass windows providing a very good view of the interior. A CAD image of the hutch next to the two plate storage units and external robot is given below (see Figs. 1 and 2).

SAMPLE LOADING AUTOMATION

When either a 20 or 4°C crystallisation plate is deemed ready for either screening or diffraction data capture, it will be ejected from the rear of the Formulatrix crystallisation storage units through a hatch. An industrial six axis robot mounted on a horizontal rail will then take the plate to the Endstation loadlock rotating it to the correct orientation on the way. The loadlock is a pneumatic device with a linear stage mounted upon a 180° rotation. The plate is retracted into the loadlock cylinder, rotated by 180° and driven out, presenting it to the internal gantry robot (See Fig. 3). The loadlock is radiation fail safe so it is not possible to break the radiation containment with a driven axis. It incorporates a bar code reader, a plate in-position switch and stage limit switches to give feedback to the control system.

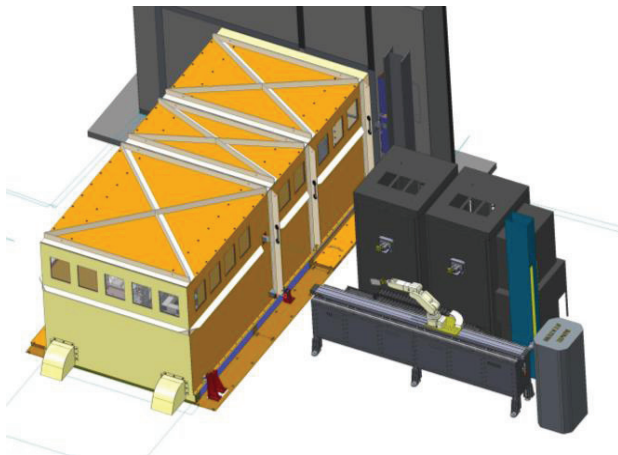

Figure 1: VMXi Hutch with the crystallisation units.

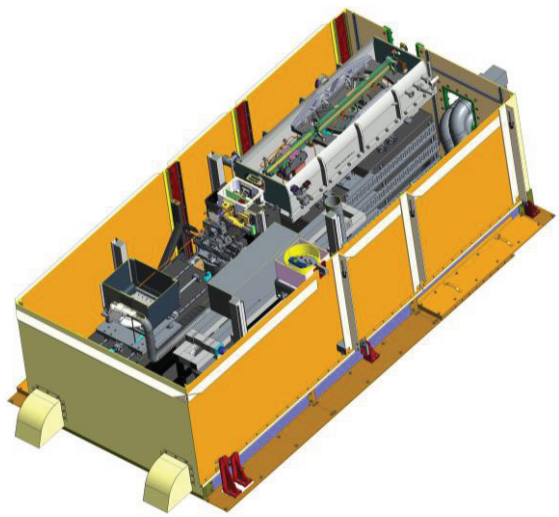

Figure 2: Section view of VMXi Hutch just above the beam path.

The plate will then be transferred into the internal storage buffer, sliding into the goniometer sample mount assembly. The journey from the temperature controlled crystallisation units to the temperature controlled internal storage will take less than 10s. For 4°C plates a thermal stability sleeve will be placed over the plate prior to being transferred onto the goniometer for data collection. The sleeve is designed to slow down the temperature rise of the 4°C plate in the 20°C environment. It was decided that active cooling on the goniometer would be likely to have a detrimental effect on the goniometer motion errors and thermal stability. The passive sleeve has been de-

ISBN: 978-3-95450-188-5 doi:10.18429/JACoW-MEDSI2016-WEPE01

COMBINED FIXED MASK, PHOTON SHUTTER, SAFETY SHUTTER, AND COLLIMATOR DESIGN FOR BXDS IVU AT THE CLS

M. J. P. Adam *, C. Bodnarchuk, Canadian Light Source Inc., Saskatoon, Canada

Abstract

The first shutter assembly outside of the Front End (FE) for Brockhouse X-Ray Diffraction and Scattering Sector (BXDS) beamline required a unique design solution to accommodate all components into the safety shutter position.

Located between the IVW high energy wiggler monochromator and POE1 wall, the total envelope size approximated 1 m x 0.660 m (LxW). Accommodating this smaller space required an alternative shutter design than traditionally used implemented at the CLS.

The alternative design combined the collimator (CLM), safety shutter (SSH), photon shutter (PSH) and Fixed Mask (FM) into one chamber. Finite Element Analysis (FEA) was conducted on the FM and PSH assembly to verify that geometric designs were adequate for reasonable operation in the beamline. FEA was used to determine the steady-state thermal and static-structural response in both operating positions. Missteer was analyzed for both operating positions to a maximum of 2.5 mm (commonly accepted missteer used at the CLS) from center. Finally, two extreme position (partially closed/open) analyses were completed for determination of potential, but unlikely operating conditions.

INTRODUCTION

The first In Vacuum Undulator (IVU) shutter assembly outside of the Front End (FE) for Brockhouse X-Ray Diffraction and Scattering Sector (BXDS) beamline required a unique design solution to accommodate radiation protection of the In Vacuum Wiggler (IVW) IVU secondary optical enclosures.

Located between the IVW high energy wiggler monochromator and the end of POE1, the total envelope size approximated 1 m in length and 0.660 m width. This space required the design and installation of a FM to protect and shield all downstream components, a PSH to absorb incoming beam, a SSH to close and isolate radiation for entrance into the downstream hutches, and a CLM to remove Bremsstrahlung radiation from escaping the IVU beamline. Accommodating a smaller space required an alternative shutter design than traditionally implemented at the CLS (Fig. 1). IVU shutter is located between 27 890 mm and 29 015 mm from the center of straight Cell 04. SPECTRA [1] was used to calculate the heat source data from parameters for the CLS Storage Ring (SR1) (with ring current 500 mA and field energy of 1 T).

The shutter precedes SOE2, POE2, and finally SOE3 along the beamline and has a total power absorption requirement of 1100 W (at 500 mA). The beam spot as seen by the combined shutter is directly apertured by Fixed Mask 3 from the FE.

* madison.adam@lightsource.ca

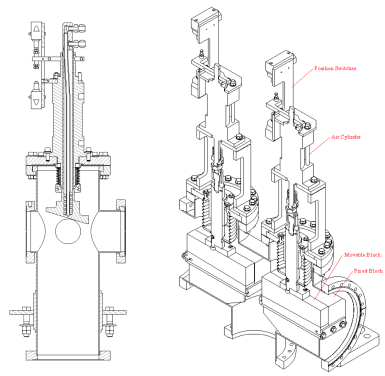

Figure 1: Typical CLS shutter designs. PSH (left) used most commonly in the FE is 300 mm in chamber length. SSH (right) used most commonly within the FE and POE of beamlines ranges between 500 mm–1200 mm in chamber length. And CLM (not shown) 400 mm in chamber length. Total length of a basic arrangement of these components exceeds the allowable space for the BXDS shutter location.

Design Objectives

The key design considerations for the shutter design, in addition the requirements stipulated within CLS Technical Specifications, are:

- The FM and PSH are combined into one component that will act as a photon absorbing surface as well as protection for the CLM/SSH.
- The SSH and CLM have been combined so that as one they block Bremsstrahlung radiation. The SSH must have a movable tungsten block directly in front of the collimator to prevent unintended Bremsstrahlung to pass by when in the closed position.

The FM-PSH must satisfy two operating positions:

- Open – allowing beam to pass through with clearance, while shielding IVW SOE2.
- Closed – stopping all beam energy produced from the IVU and missteered IVW rays. Stopping all associated radiation from the SOE2, POE2, and SOE3 enclosures.

PSH/SSH Requirements at the CLS

The below requirements are particularly important to the safety shutter set (PSH & SSH). The final design needed to ensure that both sets of requirements for the photon and radiation absorbing materials meet facility design expectations.

From "CLS Photon & Safety Shutter Design Specification 8.4.41.1 – Rev. 0" [2]:

ISBN: 978-3-95450-188-5 doi:10.18429/JACoW-MEDSI2016-WEPE02

PERFORMANCE EVALUATION OF FAST CLOSING SHUTTER SYSTEM AT THE SPring-8 FRONT-END

S. Takahashi*, M. Sano, A. Watanabe
JASRI, Hyogo, 679-5198, Japan

Abstract

The fast closing shutter (FCS) system plays an important role in protecting the ultra-high vacuum in the SPring-8 storage ring from an accidental vacuum hazard in the beamlines. In order to predict the transit time of the shock wave and the following pressure increase, a shock tube system with an inner diameter of 35 mm and a total length of 10 m was prepared to measure the shock Mach number. Experiments have been conducted that simulated an inrush of the atmosphere into the high-vacuum (~10^{-3} Pa) pipe by using a trigger system that combines a thin cellophane diaphragm with a plunger. Special ionization gauges with a high-speed amplifier were distributed about every 1 m to detect the transit time of the shock wave and to measure the pressure in the low-pressure chamber (LPC) after the actuation of the FCS system. By inserting larger pipes (inner diameter=390 mm) with various lengths into the shock tube, the attenuation in the shock wave was systematically investigated. The results of the experiment confirmed that the pressure increase in the LPC exhibits a close relationship with the total internal volume of the shock tube.

INTRODUCTION

More than 55 beamlines, which are arranged radially from the SPring-8 storage ring (circumference: ~1.5 km), are now in operation for various experiments. Maintaining the ultra-high vacuum (UHV; 10^{-8}–10^{-9} Pa) in the storage ring is indispensable for avoiding any decrease in beam lifetime and the generation of Bremsstrahlung radiation. Therefore, when a severe vacuum accident occurs in a beamline, it becomes possible for the UHV of the storage ring to break due to an air inrush, which would be followed by the long-term suspension of the user experiments. To prevent such a situation from occurring, a commercially available fast closing shutter (FCS) system (VAT Series 773 linear actuator type) was prepared in each front-end. This system works to detect rapid vacuum deteriorations and is capable of immediately closing the shutter main body, which is installed at the most upstream side of the beamline front end. The shutter does not have an airtight, UHV-compatible vacuum at the seat; that is because typical sealing materials, such as VITON (a type of fluorocarbon rubber), cannot be used because of the severe radiation environment in the 8 GeV ring tunnel. In this way, the FCS system primarily aims to prevent the inrush of a shock wave into the storage ring without delay. Accordingly, a general all-metal gate valve (GV) that is radiation resistant and interlocked with the FCS must also be installed at the upstream side of the FCS in order to prevent further vacuum deterioration.

EXPERIMENTAL SETUP

As shown in Fig. 1, the shock tube system, which has a total length of about 10 m, is mainly composed of vacuum pipes with electro-polishing treatment on the inner surface, a window part with a thin diaphragm made of moisture-proof cellophane and an HV sensor for the trigger, low-pressure and high-pressure chambers at both ends of the pipe, and miniature ionization gauges (MIGs) with a sampling time of 0.1 ms. We defined the low-pressure chamber (LPC) and high-pressure chamber (HPC) as the upstream side and downstream side, respectively. The inner diameter of the vacuum pipe is 35 mm. This corresponds to the standard 2.75-inch ConFlat flange, which has the same nominal aperture size of actual front-end components for the SPring-8 standard undulator beamline. Both the FCS and GV, which are installed just downstream from the LPC, are used with the 2.75-inch ConFlat flange. The window part can simulate momentary fracture of the beryllium window by breaking the cellophane diaphragm using a plunger connected to a pneumatic driving cylinder. The aperture size of the window is 10 mm (diameter), in accordance with the actual component. The MIG measurement spans three orders of magnitude in the range from 10^{-4} to 10 Pa (typically 10^{-3}–1 Pa) by fixing the emission current. Fast pressure measurement with a sampling time of 0.1 ms can be achieved by combining a high-speed amplifier with a generic vacuum controller.

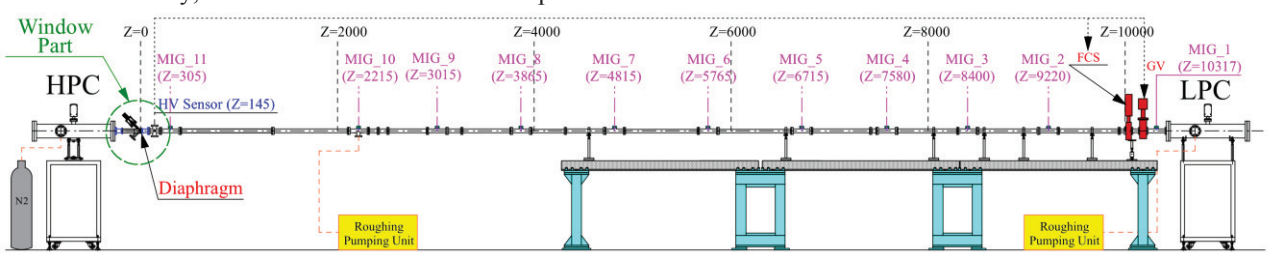

Figure 1: Schematic layout of the shock tube basic system with a total length of 10 m.

* takahasi@spring8.or.jp

ISBN: 978-3-95450-188-5 doi:10.18429/JACoW-MEDSI2016-WEPE03

BEAMLINE FRONT ENDS AT THE 2.5-GeV PHOTON FACTORY STORAGE RING

H. Miyauchi†, S. Asaoka, T. Tahara, Accelerator Laboratory, High Energy Accelerator Research Organization (KEK), Tsukuba, Ibaraki, Japan

INTRODUCTION

Since the first commissioning in 1982, the 2.5-GeV Photon Factory (PF) storage ring has been upgraded third times in 1986, 1997 and 2005, in order to reduce the beam emittance and to produce new short-straight sections for in-vacuum short period undulaters.

In order to adopt the PF storage ring upgrades, the beamline front ends were necessary to be modified. We look back the old and new components of the PF beamline front ends.

MANUAL GATE VALVES

Manual gate valves separate the beamline front ends from the storage ring. We used to use the Viton O-ring seal manual gate valves, but the Viton O-ring seal could not bear the radiation damage. So we replaced the Viton O-ring seal manual gate valves into the all metal manual gate valves (Figs.1 and 2).

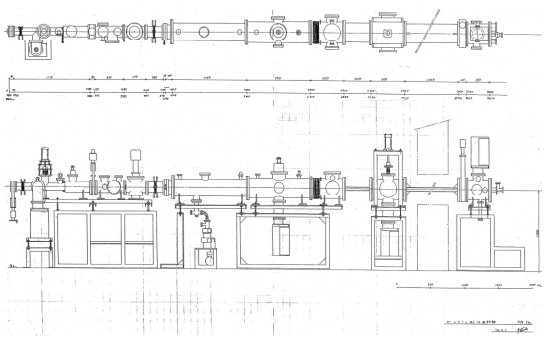

Figure 1: Old BL-15 Front End Layout.

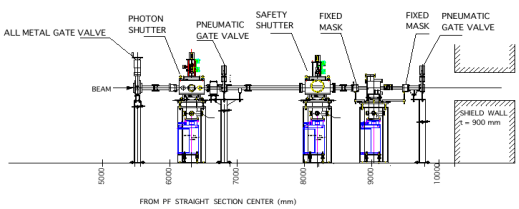

Figure 2: New BL-15 Front End Layout.

PHOTON SHUTTERS

At the first commissioning in 1982, the PF storage ring had only 4 bending beamlines and no insersion devices, the structure of the water cooling Cu absorber inside the photon shutter was very simple (Fig. 3). After installing undulators, we developed the rod type of photon shutter (Fig. 4). And after installing multi-pole wigglers, in order to reduce the loading power density on the surface of shutter, the water cooling Cu absorber inside the photon shutter was made triangle-shaped at the multi-pole wiggler beamline front ends (Fig. 5).

Figure 3: Photon Shutter for Bending BL Front End (Old Type).

† hiroshi.miyauchi@kek.jp

ISBN: 978-3-95450-188-5 doi:10.18429/JACoW-MEDSI2016-WEPE04

DESIGN OF X-RAY BEAM POSITION MONITOR FOR HIGH HEAT LOAD FRONT ENDS OF THE ADVANCED PHOTON SOURCE UPGRADE*

S.H. Lee†, B.X. Yang, J. Mulvey, M. Ramathan
Advance Photon Source, Argonne National Laboratory, Argonne, IL 60439, USA

Abstract

Accurate and stable x-ray beam position monitors (XBPMs) are key elements in obtaining the desired user beam stability in the Advanced Photon Source (APS). Currently, the APS is upgrading its facility to increase productivity and to provide far more highly coherent and brilliant hard x-rays to beamline experiments with a new storage ring magnet lattice based on a multi-bend achromat (MBA) lattice. To improve the beam stability, one of the proposed beam diagnostics is the grazing-incidence insertion device x-ray beam position monitor (GRID-XBPM) for high heat load (HHL) front ends (FEs) at the APS. In this paper, final design of the GRID-XBPM and the high-power beam test results at beamline 27-ID-FE will be addressed.

INTRODUCTION

The APS at Argonne National Laboratory is the largest synchrotron radiation facility in the western hemisphere, providing the highest-brightness high-energy x-rays to users. To provide far more highly coherent and brilliant hard x-rays to beamline experiments, the APS upgrade (APS-U) project team is currently developing a new storage ring magnet lattice based on a multi-bend achromat (MBA) lattice, which offers small electron beam emittance, increases brightness several orders of magnitude, and approaches diffraction limits at higher photon energies. The APS-U project will put the APS on the path to continued world leadership in hard-x-ray science. To fully support the APS-U, the FEs located inside the storage ring tunnel need to be upgraded. Also, because the storage beam size will be down to several microns from one hundred micron in the horizontal plane, a major improvement in beam stability is required in order to realize the benefits of this upgrade [1]. To deliver a high degree of x-ray beam position stability to the users and to achieve the APS-U beam stability goal, the x-ray beam position tolerance and XBPM resolution requirements at 20 m from the source are listed in Table 1. To meet these values, the APS has been conducting research in developing a hard x-ray BPM that uses the 8-keV Cu K-edge x-ray fluorescence (XRF). To implement the XRF-based XBPM in place of the present photoemission-based XBPM, a grazing-incidence insertion device x-ray beam position monitor (GRID-XBPM) has been developed and its first articles were installed for tests at 27-ID and 35-ID FEs in May 2014, as seen in Fig. 1 An experimental test result with two inline undulators showed that the XBPM has approximately 30-fold improvement in rejection of bend magnet radiation background and a gap-independent calibration in one of the two dimensions as shown in Fig. 2.

Table 1: APS–U XBPM Tolerance and XBPM Resolution Requirements (Z=20 m from the Source Point)

XBPM	Plane	RMS AC motion (0.01~1000Hz)	RMS Long-term Drift (7 days)
Position tolerance	Horizon.	5.3 μm	12.0 μm
	Vertical	3.4 μm	10.0 μm
Resolution	Horizon.	3.7 μm	8.5 μm
	Vertical	2.4 μm	7.1 μm

Figure 1: Installed GRID-XBPM at 27-ID FE (Looking upstream) [2].

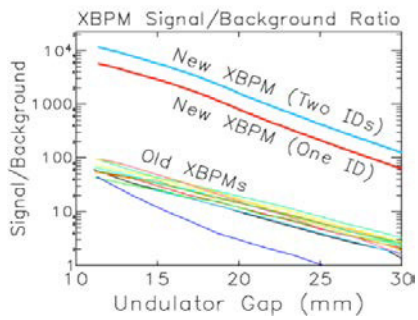

Figure 2: Ratio of undulator signal over BM background for the GRID-XBPM [2].

GRID-XBPM DESIGN

The design has been further value-engineered to make it compact. To reduce the cost, the vertical adjustment capability will be removed because the undulator gap changes are not correlated to the vertical motion of the mask. Fig. 3 shows the final design of the GRID-XBPM which is composed of two masks and two detector assembles mounted on two separate granite block for structural and temperature stability with a translation motion stage. This stage can translate the mask and detector assembly horizontally during machine study. For detecting the XRF signals, both Si-

* Work supported by the U.S. Department of Energy, Office of Science, under Contract No. DE-AC02-06CH11357
† shlee@aps.anl.gov

ISBN: 978-3-95450-188-5 doi:10.18429/JACoW-MEDSI2016-WEPE05

INNOVATIVE DESIGN OF RADIATION SHIELDING FOR SYNCHROTRON LIGHT SOURCES

M. G. Breitfeller, Brookhaven National Laboratory, Upton, N.Y., USA
S. L. Kramer, Operations and Accelerator Design Consulting, Ridge, N.Y., USA

Abstract

Over the course of decades, the shape of the bulk shielding walls for synchrotron light sources has developed into a standard configuration, including a ratchet shape of the outer storage ring wall, to accommodate the clearance needs for front end and first optical enclosure assemblies. New state of the art light sources will have low emittance, high energy beams, which will give potential for higher beam losses. These losses will yield higher radiation dose rates at the downstream wall and stricter safety requirements in the first optical enclosure. Throughout the installation of local shields at NSLS-II, verification dose rate studies of various shielding configurations were performed. Analysis of these studies revealed that a circular outer bulk shield wall could greatly reduce the dose rate to the users who work near the front end optical components. This presentation discusses the benefits of this circular bulk shield wall verses the challenges of component installation near the wall and ways to mitigate them.

INTRODUCTION

The bulk shield wall is the first line of defense from harmful radiation for human health safety, which is the highest of all priorities. A well designed outer storage ring wall attenuates the radiation field to acceptably low level dose rates for people near the wall. A wall with circular geometry presents a large arcing radius, relative to the beam path, that naturally maximizes wall thickness and attenuation. The challenge for engineers is to adapt new methods for interfacing the front ends to the beamline components through the much thicker concrete wall and it's curved outer surfaces.

BENEFITS AND PLANNING FOR THE CIRCULAR WALL

The safety benefits of the circular wall are numerous. The bulk wall shield is the first line of defense for radiation safety, a passive system, and once it is built it requires no additional attention. Other than the penetrations themselves, costly radiation analysis of complex wall geometry is simplified, and fewer local shields are required for hot spots. Next generation light sources will require thicker downstream walls, because higher dose rates will exist in the First Optical Enclosures (F.O.E.) resulting from abnormal losses caused by mis-steering. These higher dose rates can occur even when the safety shutters are actuated to block the X-ray beam path. More details on the advantages of the circular shield wall are given in Ref [1]. Also, cost savings may be significant. The circular wall will require less labor to build forms, less cement to pour, and less lead, needed for strengthening an inferior ratchet shield design.

At NSLS-II, the shape of the existing ratchet wall makes it convenient to connect the front end's gate valve to the first component of the F.O.E. The outer ratchet wall's orthogonal shape allows F.O.E. girders to position close to wall, and their hutches use the bulk wall as the backbone for its boxed shape (see Fig. 1). The downstream wall thickness is 1.5 m, so relatively little layout space is lost by feeding a drift tube through the wall to connect the two systems. To accommodate the new circular wall design, engineering methods must be considered to create penetrations in the thick wall that will gain access to components where needed.

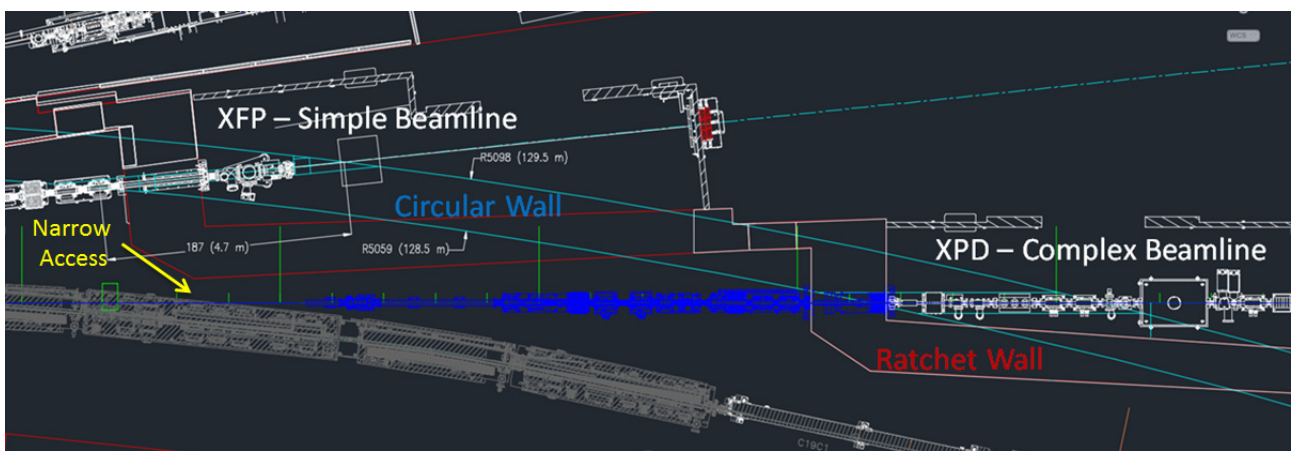

Figure 1: Existing adjacent beamlines at NSLS-II, with ideal circular wall outline overlay.

ISBN: 978-3-95450-188-5 doi:10.18429/JACoW-MEDSI2016-WEPE06

HIGH HEAT LOAD FRONT ENDS FOR SIRIUS*

L. M. Volpe†, P. T. Fonseca, H. F. Canova, P. P. S. Freitas, A. Gilmour, H. G. P. Oliveira, A. S. Rocha, G. L. M. P. Rodrigues, L. Sanfelici, M. Saveri Silva, H. Westfahl Jr., LNLS, Campinas, Brazil

Abstract

Currently under construction on Brazilian Synchrotron Light Laboratory Campus, Campinas/SP, Sirius is a 3GeV, 4th Generation Synchrotron Light Source. In this paper we describe the Front End that has been designed to transmit the intense synchrotron radiation generated by the insertion devices that will generate the most critical thermal stress, with a peak power density of 55.7 kW/mrad² and a total power of 9.3kW at 500mA in the storage ring.

The functions of the main components and their location in the layout are described. Computational fluid dynamics (CFD) and structural simulations, that have been carried out to verify the performance under the high heat loads generated by Sirius, are also detailed along with the limits of temperature and stress that have been employed in the design.

INTRODUCTION

Sirius storage ring uses the multi-bend-achromatic design approach (5BA in this case) to achieve a very low beam emittance of 0.25 nm·rad. The 518 m circumference contains 20 straight sections of alternating 6.5 and 7.5 meters in length, to be used for insertion devices as well as injection and RF systems. The central dipole of the 5BA cells is a permanent magnet with transverse and longitudinal field gradients to reduce the emittance and provide a hard X-ray radiation source. The 3.2 T narrow high field section in its center provides radiation with critical energy of 19 keV. The other low field dipoles (0.58 T), responsible for the main beam deflection, will be electromagnets [1].

A Front End is a group of components connecting the storage ring to the beamline. They are responsible for defining the final aperture, absorbing exceeding beam power, radiation protection, storage ring vacuum protection and photon-beam diagnostics [2]. The first 5 Sirius' beamlines are planned to use in-vacuum and elliptically polarized undulators. An IVU19 front-end was first designed since it is the Insertion Device (ID) that will generate the most critical thermal stress, with a peak power density of 55.7 kW/mrad² and a total power of 9.3kW at 500mA. This paper will present the requirements, design and prototyping details.

FRONT END LAYOUT

The Front End functions are fulfilled by a proposed set of interlocked components, whose locations are shown in Fig. 1. Ion Pumps provide ultra-high vacuum to the Beamline, Front End and Storage Ring, whose level ($\leq 10^{-9}$ mbar) is monitored by vacuum readers placed at strategic locations.

Since for most of the Sirius' Front Ends there is no physical vacuum insulation (such as windows), preserving the pressure levels in the Storage Ring in the case of any event on the Beamline side becomes critical. If a sudden pressure rise is detected, the electron-beam is dumped and the Fast Valve shut to partially seal the vacuum path and stop the pressure wave. It is followed by the Slow Valve, which completely seals the path between Storage Ring and Beamline, preventing a significant pressure rise occurrence in the Storage Ring [3].

Pre-Masks upstream the Front End will be designed restricting the photon beam generated by B1 and protecting the vacuum tubes. Also, a Machine Photon Shutter upstream the Front End will be designed to block the photon beam in maintenance cases.

Table 1 resumes the Front End project, showing the components position, apertures, and the incident/absorbed power. Power values were calculated using Spectra v10.

FRONT END COMPONENTS

Power Absorbers

They are components that absorb the beam power, shape its size and form to the first optical components. The IVU Front End will have a Fixed Mask, a Photon Shutter, and High Power Slits as components responsible for these functions.

There are two materials that are being studied to be used to dissipate the thermal power, Glidcop and Copper Chromium Zirconium (CuCrZr) [4]. The major difference between the two materials is that Glidcop can be brazed and CuCrZr cannot, but CuCrZr can be purchased in the local market and is available in a vast number of suppliers. As CuCrZr is hard enough to be used in flanges, the idea is to make the components without the need of brazing the flanges.

Table 2 presents the design parameters to which the power absorbers are submitted.

Fixed Mask The Fixed Mask (FM) is a static and water-cooled block of high thermal conductivity alloy. It absorbs unwanted or misteered beam, preventing components downstream to suffer from high thermal load effects. It presents an hourglass form orifice, which provides grazing incidence to the beam in order to reduce the power density on its surface, and, at the same time, define the Front End's entrance acceptance. It has four helical water channels for cooling. Figure 2 shows the internal design of the Fixed Mask.

* Work supported by Brazilian Ministry of Science, Technology, Innovation and Communication (MCTIC)
† lucas.volpe@lnsl.br

ISBN: 978-3-95450-188-5 doi:10.18429/JACoW-MEDSI2016-WEPE07

A HIGH HEAT LOAD FRONT-END FOR THE SUPERCONDUCTING WIGGLER BEAMLINE AT SSRF*

Y. Li†, M. Zhang, D. Jia, S. Xue, W. Zhu, Shanghai Institute of Applied Physics, Chinese Academy of Sciences, Shanghai, P. R. China

Abstract

A superconducting wiggler (SCW) will be first employed to generate high energy X-rays for ultra-hard X-ray applications beamline at Shanghai synchrotron radiation facility (SSRF). The front-end will handle a heat load of 44.7 kW with a peak power density of 45 kW/mrad², which is much higher than the commissioned ones at SSRF. Overall design of the high heat load front-end has been completed, including one short absorber with a length of 300 mm and three long absorbers longer than 500 mm. Long absorbers have been designed to be made by medium speed wire-cut electrical discharge machining (WEDM-MS) or electron beam welding (EBW). Thermal analyses of all absorbers have also been done to comply with the failure criteria of SSRF.

INTRODUCTION

Shanghai synchrotron radiation facility (SSRF) is an advanced third generation synchrotron light source with a 3.5 GeV electron storage ring and a designed beam current of 300 mA. A superconducting wiggler (SCW), as source of the ultra-hard X-ray applications beamline BL12SW at SSRF, will be able to generate high-energy X-rays up to 150 keV. Meanwhile, the SCW has an intensive power of over 43.3 kW with a peak power density of 45 W/mrad^2. Overlapping the radiations from upstream and downstream bending magnets, the total power will reach 44.7 kW, which are about 4 to 64 times compared with the commissioned front-ends. This is also the highest heat load for a front-end in SSRF phase-II beamline project.

Overall design of the high heat load front-end, abbreviated as BL12SW front-end, was introduced in this study. Thermal analyses of all absorbers were done to comply with the failure criteria of SSRF. Three long absorbers with lengths bigger than 500 mm were designed to be made by medium speed wire-cut electrical discharge machining (WEDM-MS) or electron beam welding (EBW).

OVERALL DESIGN

Power of SCW

Table 1 is the major parameters of SSRF storage ring and SCW. Power distribution is shown in Figure 1.

Table 1: Parameters of SSRF Storage Ring and SCW

E_e (GeV)	I (A)	B_0 (T)	N	L (m)	K
3.5	0.3	4.2	22	1.08	18.824

Where: E_e is beam energy of the storage ring, I is the maximum circulating current; B_0 is the maximum magnetic field, N is period, L is total length and K is deflecting parameter of SCW.

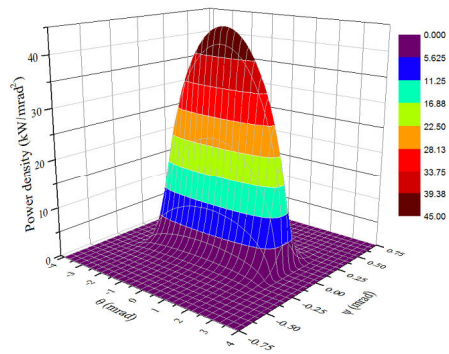

Figure 1: Power distribution of SCW.

Layout of the Front-end

Figure 2 shows the layout of BL12SW front-end with a total length of about 8.9 m. Three fixed masks (FM) confine the photon beam and protect the downstream components from a mis-steered beam. Two photon shutters (PS) intercept the photon beam and protect downstream safety shutter and valves.

Therefore, power from SCW, together with part of the bending magnet, will be absorbed by three FMs and PS2. Technical specifications of these four high heat load photon absorbers are given in Table 2.

THERMAL ANALYSIS

Failure Criteria

Absorbers of FMs and PS2 are all made of Glidcop Al-15. Conservative failure criteria [1] are used as:

- The maximum equivalent stress σ_{max} should be less than 420 MPa.
- The maximum temperature on the Glidcop body T_{max_body} should be less than 300 °C.
- The maximum temperature on the water cooling channel walls T_{max_wall} should be less than water boiling temperature at channel pressure.

Thermal Analysis Results

Direct water cooling and grazing incidence structures are applied to improve heat-absorbing ability for front-end photon absorbers. The temperature and thermal stress distributions of all beam striking components, including pre-mask, FM, PS, fluorescence monitor and XBPM, were simulated carefully and optimized by thermal analysis with ANSYS.

* Work supported by SSRF phase-II beamline project
† email address: liyongjun@sinap.ac.cn

ISBN: 978-3-95450-188-5 doi:10.18429/JACoW-MEDSI2016-WEPE09

DESIGNING THE PHOTON BEAMLINE FRONTENDS IN THE PETRAIII EXTENSION PROJECT

Hilmar Krüger*, W.A. Caliebe, M. Degenhardt, M. Hesse, F. Marutzky,
H.B. Peters, R. Peters, M. Röhling, H. Schulte-Schrepping, B. Steffen
Deutsches Elektronen-Synchrotron DESY, 22607 Hamburg, Germany

Abstract

The new insertion device beamlines in the PETRAIII extension project are arranged in three new sector types. The following will present the designs of the photon beamlines frontends for these sectors. The designs are based on the original design concept developed for the photon beamline frontends at PETRAIII. The aim of this generic approach was to minimize the number of specialized components for all beamlines. The existing girder concept allows a fast and reliable installation phase. The newly designed frontends aimed at using the same proven components and minimizing of the number of girder variations.

There will be 4 new sectors with two undulator IDs in each sector. The canting angle between the undulators was increased from 5 mrad to 20 mrad in difference to the generic beamlines. Additionally, two of the straight sections are modified. One straight section will be transformed in a side station sector with a 1 mrad canting angle. The other straight section with a 40 m long damping wiggler section will be used as a single beamline with a hard X-ray source. The modifications of the original frontend design, the components and the deviations between the sector types are being presented.

INTRODUCTION

For the next step in the development of PETRAIII as a synchrotron radiation source the PETRAIII extension project added up to 10 further insertion device beamlines located in two new additional buildings [1]. The beamlines are arranged in three new sectors types with different layouts to the PETRAIII in the Max von Laue experimental hall. This includes the layout of the frontends of the beamlines in the new tunnel. One of the three sector types contains two beamlines with one new generic frontend for the PETRAIII extension project with an increased canting angle from 5 mrad (PETRAIII) to 20 mrad. Additionally, two of the straight sections are modified. One straight section will be transformed in a side station sector with a 1mrad canting angle (P21) [2]. The other straight section with the 40 m long damping wiggler will be used as a single beamline with a hard X-ray source (P61) [3].

The reasons for the new layout are a different topology of the machine, the space available in the tunnel and the crane system for the transport of the components. This leads to an increased distance between the source of the beamline and the beginning of the girder frontend from at average 4.5 m to more than 35 m. In this section the photon beam is guided only in a UHV tube with vacuum pumps and a mask system. The distance between the beamline source and the optic hutches in the new halls are 50 m for the new generic beamline, 77 m for the side station beamline and 90 m for the the damping wiggler beamline.

GENERIC PHOTON BEAMLINE FRONTEND FOR PETRAIII EXTENSION PROJECT

The aim of the design concept of the old generic frontend as well as the new generic frontend was to minimize the number of specialized components for all beamlines [4, 5]. Additionally a second objective was to use the existing girder concept for PETRAIII with only small adjustments. The already existing girder concept allows a fast and reliable installation phase and is robust and versatile during commissioning and user operation [6].

The major difference of the new generic approach is the change of the canting angle between the two beamlines of one sector. The sector exist 4 times with two undulator IDs in each sector (P22-P23, P24-P25, P62-P63 and P64-P65). The large horizontal gap between the two beamlines in the girder frontend allows the use of a seperate girder system for each beamline per sector (see Fig. 1 at the bottom). The classic generic approach required components for both beamlines per sector on one girder and therefore complex girders. In the new approach the use of only single beamline girder was possible. The only difference in the new generic designs was one additional tube in one beamline to align the girders for a better accessibility during installation and maintenance in the tunnel.

Due to some minor adjustments to some components and the integration of additional components (e.g. water cooled CVD diamond screen) it was necessary to change the arrangement of the components on the girders. Thereby only one girder design of the generic approach for PETRAIII could be re-used. In the the new generic design only four different girders types are used instead of eleven different girder types.

Common to all frontend designs and new in contrast to PETRAIII is the use of the water cooled CVD-diamond flourescent screen with an attached CCD camera system. It is installed on the first girder in front of any other component. This new component allows to image the footprint of the white beam. Also new and common to all beamlines is the modified filter chamber. Now a CCD camera system is attached as well. Right behind the vacuum diagnostic

* hilmar.krueger@desy.de

ISBN: 978-3-95450-188-5 doi:10.18429/JACoW-MEDSI2016-WEPE10

MECHANICAL DESIGN OF PULSE-BY-PULSE X-RAY BEAM POSITION MONITOR USING DIAMOND HEAT SINK*

Hideki Aoyagi†, Sunao Takahashi,
Japan Synchrotron Radiation Research Institute (JASRI), Hyogo, Japan

Abstract

It is indispensable to diagnose dynamics of synchrotron radiation beam for stable supply of the beam in synchrotron radiation facilities. We are developing a pulse-by-pulse X-ray beam position monitor using diamond heat sinks for an undulator beamline. We have designed the monitor aiming at improving heat-resistance property without degradation of high frequency property, and manufactured a prototype to evaluate a feasibility of the design. Thermal finite element analysis was carried out to design an effective structure of a detector head and a holder. Time-domain reflectometry was utilized to evaluate high frequency property of the prototype.

INTRODUCTION

A conventional X-ray beam position monitor (XBPM) is photoemission type, and blade-shaped tungsten is used as detector heads to secure heat resistance. Stabilization of pulse-by-pulse electron beam position has been realized at a high level in the SPring-8 storage ring [1,2]. The conventional XBPM, however, cannot measure pulse-by-pulse beam position, because the time constant of the detector head is long due to the stray capacitance and the impedance is not matched to 50 Ω of cables. To overcome this problem, a pulse-by-pulse XBPM equipped with microstripline structure (stripline-XBPM), which also works as a photocathode, had been developed for the SPring-8 bending magnet (BM) beamlines [3,4]. This monitor has potential to function as (1) a pulse intensity monitor, (2) a pulse-by-pulse XBPM, and (3) a pulse timing monitor [5]. For the undulator beamlines, further improvement of heat-resistance is required. Therefore, we are developing a pulse-by-pulse XBPM for undulator beamlines by introducing heat resistance structure that employed a diamond heat sink.

STRUCTURE OF PROTOTYPE

We started a design work for realization of the pulse-by-pulse XBPM from the following points of view. We decided to suppress an increase in time constant (t = RC) by lowering the stray capacitance as much as possible with securing an effective area of a photocathode, while accepting impedance mismatch around the photocathode [6]. As shown in Fig. 1, the photocathode is mounted on a diamond heat sink as a detector head. We adopted heat-resistant structure to reduce an effective irradiation cross section by aligning four detector heads parallel to a beam axis. A heat sink holder is attached to a cooling base welded to a DN40CF (ICF70) flange. A signal transfer line having microstripline structure is mounted on another ICF70 flange [7]. By separating signal transfer line from cooling mechanism, although high frequency property is degraded compared with the stripline-XBPM mentioned above, the heat-resistant property is expected to be improved. Figure 2 shows a prototype with a 6-way cross chamber. A couple of ICF70 flanges equipped with the detector heads (the signal transfer lines) are mounted on the top/bottom (left/right) ports. Two beam ports are faced using DN63CF (ICF114) flanges with a face-to-face dimension of 120 mm.

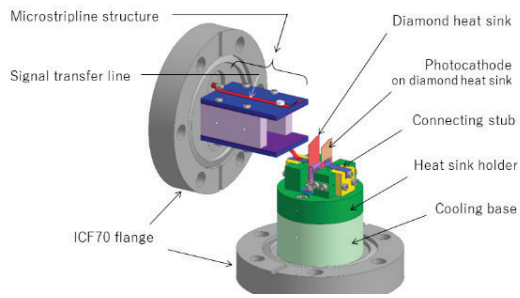

Figure 1: 3D image of the cooling structure (bottom) and the microstripline structure (left).

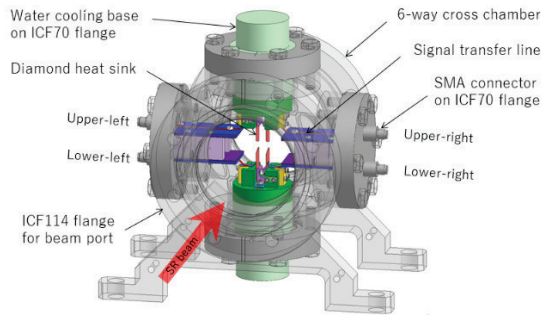

Figure 2: 3D image of the prototype.

THERMAL FINITE ELEMENT ANALYSIS

The thermal finite element analysis (FEA, ANSYS® Release 17.0) was carried out on the diamond heat sink (20 mm × 8 mm × 0.3 mm), the heat sink holder and the cooling base. A quarter model was used for the analysis, and the heat sink holder and the cooling base are treated as an integrated object for simplification. Figure 3 shows an analysis result of the typical case in the normal operation of the SPring-8 standard undulator beamlines. The thermal conductance (TC) of diamond and copper are set to 1,500 and 400 W/(m·K), respectively. Thermal contact conductance (TCC) between the diamond heat sink and the heat sink holder made of copper is assumed to be 10,000W/(m^2·K) in this calculation. The total power of 10W is input with uniform heat flax on the tip (1 mm × 8 mm × 0.3 mm) of the heat sink. This input power is equivalent to the maximum value assumed in the normal operation. The homoiothermal condition (30°C) is put to the bottom of the cooling

* This work was partly supported by Japan Society for the Promotion of Science through a Grant-in-Aid for Scientific Research (c), No. 20416374.
† aoyagi @spring8.or.jp

ISBN: 978-3-95450-188-5 doi:10.18429/JACoW-MEDSI2016-WEPE14

MINIMIZING GRATING SLOPE ERRORS IN THE IEX MONOCHROMATOR AT THE ADVANCED PHOTON SOURCE

M. V. Fisher†, L. Assoufid, J. McChesney, J. Qian, R. Reininger, F. Rodolakis
Advanced Photon Source, Argonne National Laboratory, Argonne, IL, USA

Abstract

The IEX beamline at the APS is currently in the commissioning phase. The energy resolution of the beamline was not meeting original specifications by several orders of magnitude. The monochromator, an in-focus VLS-PGM, is currently configured with a high and a medium-line-density grating. Experimental results indicated that both gratings were contributing to the poor energy resolution and this led to venting the monochromator to investigate. The initial suspicion was that a systematic error had occurred in the ruling process on the VLS gratings, but that proved to not be the case. Instead the problem was isolated to mechanical constraints used to mount the gratings into their respective side-cooled holders. Modifications were made to the holders to eliminate problematic constraints without compromising the rest of the design. Metrology performed on the gratings in the original and modified holders demonstrated a 20-fold improvement in the surface profile error which was consistent with finite element analysis performed in support of the modifications. Two gratings were successfully reinstalled and subsequent measurements with beam show a dramatic improvement in energy resolution.

BEAMLINE

The Intermediate-Energy X-ray (IEX) beamline at the Advanced Photon Source (APS) at Argonne National Laboratory was designed with two separate branches, each with a dedicated endstation: one dedicated to angle-resolved photoemission spectroscopy (ARPES) and the other to resonant soft X-ray scattering (RSXS) [1]. The high energy resolution required by the ARPES endstation is achieved using an in-focus variable line spacing plane grating monochromator (VLS-PGM) [2]. To meet the demands of the two experimental techniques the monochromator is designed to house up to four water side-cooled gratings. It is currently configured with a high-line-density grating (HEG) with a nominal 2400 l/mm and a medium-line-density grating (MEG) with a nominal 1200 l/mm. The HEG is primarily for use with the ARPES branch when conducting higher resolution experiments. The MEG offers higher flux with moderate resolution that can be used by both the ARPES and RSXS branches. Future plans include a low-line-density grating (LEG) with a nominal 400 l/mm that is optimized for photon hungry RSXS experiments.

The diffracted beam downstream of the exit slit was observed to shift in energy depending on the size and position of either the synchrotron beam or the clean-up aperture located just downstream of the monochromator. As a result, the energy resolution was very poor except for the smallest aperture sizes.

GRATINGS

The cause of the poor energy resolution was eventually isolated to the gratings using photoemission measurements at the ARPES endstation. A systematic scanning of a vertical aperture just downstream of the monochromator (before the beam significantly disperses) revealed that the energy of the diffracted beam shifted at the exit slit as one selected different sections of the dispersing beam. This technique essentially allowed one to scan along the length of the grating. Both the HEG and the MEG showed similar energy shifts.

Ruling Line-Density

In order to fully investigate the gratings, the monochromator needed to be vented. The initial suspicion was that a systematic error had occurred in the ruling process on both gratings which had been holographically ruled by the same vendor. No metrology had been performed to verify the variable ruling line density on either grating.

In anticipation of the ruling density being the problem, a new mechanically ruled MEG was acquired. In parallel, plans were made to remove the existing MEG and measure its ruling density. Unfortunately, the long trace profilometer (LTP) at the APS was undergoing an upgrade; as a result, arrangements were made with the optics metrology group at the SOLEIL Synchrotron to measure the ruling density of the original MEG on their LTP. The measurements confirmed that the original MEG was properly ruled. In the meantime, the real problem with the gratings had been isolated to the grating holder itself.

Grating Substrate

The mechanical details of the grating holder were reviewed in preparation for mounting the new MEG. The grating substrate design adopted for the IEX monochromator has three horizontal through-holes to facilitate clamping of side cooling blocks and three vertical holes to facilitate bolting the grating to a support from below as illustrated in Figure 1. The grating substrates were originally specified and fabricated with extremely good surface profiles of better than 1nm RMS. Surface profile measurements were not made after the original MEG and HEG were ruled or after they were installed into their respective

* Work at the Advanced Photon Source is supported by the U. S. Department of Energy, Office of Science, Office of Basic Energy Sciences, under Contract No. DE-AC02-06CH11357.
† mfisher@aps.anl.gov

ISBN: 978-3-95450-188-5 doi:10.18429/JACoW-MEDSI2016-WEPE15

HIGH FREQUENCY UHV MECHANICAL X-RAY BEAM CHOPPER

Nahikari González, Carles Colldelram, Salvador Ferrer, Carlos Escudero
CELLS-ALBA, 08290 Cerdanyola del Vallés, Spain

Abstract

An in vacuum mechanical chopper has been designed and built to perform X-ray Absorption Spectroscopy (XAS) experiments with operating liquid electrochemical cells at the Near Ambient Pressure Photoemission (NAPP) end station of ALBA Synchrotron (BL24, CIRCE Beamline). While operating the liquid electrochemical cell, in order to separate the weak currents induced by the X-ray absorption process at the working electrode in contact with the liquid electrolyte (total electron yield signal or TEY) from the faradaic current stablished between the electrodes when applying a bias, the incoming beam must be chopped at a certain frequency (ω) and then, by means of a lock in amplifier, the signal at this frequency ω can be extracted and measured. The in vacuum chopper developed at ALBA can operate at variable frequencies and when inserted in the X-ray beam path, produces pulses with a certain frequency ω, therefore modulating the TEY signal. This new chopper design, improves previous designs which used piezo-actuated choppers constrained to work at fixed oscillating frequencies [1].

The design consists of a slotted disk that spins around an axis by means of an UHV stepper motor. A LED and photodiode based UHV sensor ensures that frequency drifts do not affect the measurements. The motor is hold by an internally water cooled oxygen-free high thermal conductivity copper (OFHC) support, which allows long duration experiments at high speeds without stopping.

INTRODUCTION

In some soft X-ray absorption experiments, when performing electrochemical characterization of electrode-electrolytes systems under operando conditions, the big currents prevent from effectively collecting the tiny total electron yield currents (TEY) that shape the XAS spectra that contain the information that one wishes to extract from the operating electrode.

In order to separate these weak currents induced by the X-ray absorption process from the dominant faradaic currents (typically 10^6 times bigger), the incoming X-ray is chopped at certain frequency ω and then, by means of a lock in amplifier, the Fourier component of the signal corresponding to the ω frequency is extracted and measured. To modulate the TEY current, ALBA has developed an in vacuum mechanical chopper with variable frequency that, if inserted in the X-ray incoming beam, modulates the TEY signal whose amplitude is measured with a lock in amplifier

This technique has been typically performed using piezo actuated choppers with a fixed oscillating frequency, however, in this paper the viability of using a stepper motor driven chopper and the required surrounding elements is described.

SYSTEM DESCRIPTION

The chopper consists of a slotted spinning disk driven by an UHV stepper motor. The main requirements of the mechanical chopper are the following:

- Sustain a high and stable rotation speed up to 1 kHz continuously for hours.
- Have a controlled and variable frequency.
- Be fully UHV compatible (10^{-9} – 10^{-10} mbar).
- Enable in-out motion in order to remove it from the beam path, if necessary.
- Allow the synchronization with the chopped electron yield current by means of a lock-in amplifier.

The selection of a stepper motor is the key issue of the design since a speed around 2.000 rpm was required. This velocity is beyond the normal working speed for standard stepper motors, which are capable to work at up to 6.000 rpm in air. However, due to the fact that the motor is placed in UHV and therefore, without air cooling at all, the working speed is limited -according to the manufacturer catalogue [2] - to 600 rpm. Because of the negligible cooling capacity in vacuum environments, the motor may overheat, stop and even be damaged in just a few seconds.

The proposed solution to the above mentioned issue is to support the motor with an internally water cooled clamp made of massive oxygen-free high thermal conductivity copper (OFHC). The gap between the motor and the water recirculation path is reduced to its minimum, 2mm. In this way the water arrives as close as possible to the motor's body and hence, the heat exchange between the motor and the water is maximized. A thermocouple connected to the motor's body controls the operating temperature continuously. Fig. 1 shows the basic cooling solution with the motor at the bottom, the holding clamp column with internal concentric water cooling and the brazed CF flange with the corresponding water and electrical connections

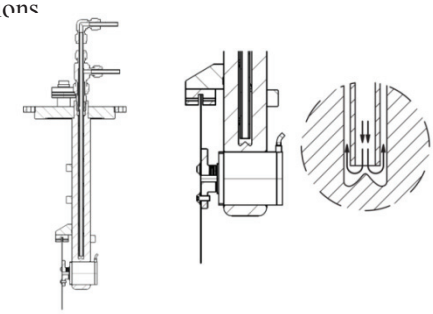

(a) (b)

Figure 1: a) Cross section of the motor cooling elements. (b) Detailed view of the water recirculation.

ISBN: 978-3-95450-188-5 doi:10.18429/JACoW-MEDSI2016-WEPE18

APS 2-ID BEAMLINE, UPGRADE TO CANTED CONFIGURATION *

D. Capatina†, M. Beno, M. Fisher, J. Knopp, B. Lai, E. Moog, C. Roehrig, S. Vogt,
Advanced Photon Source, Argonne National Laboratory, Lemont, USA

Abstract

To provide independent operation of the two 2-ID beamline experimental stations, a new canted beamline design is being developed. The constraint of keeping the existing front end limits the canting angle. The optimal canting angle was determined to be 400 µrad and is achieved by using a permanent magnet. A coil is added to the canting magnet to provide a steering adjustment of maximum 40 to 50 µrad. In order to increase the beam separation as well as to provide power filtering and higher harmonics rejection for the downstream optics, a dual mirror system with focusing capability is used as the first optic at approximately 28 m from the center of the straight section. The inboard mirror (2.6 mrad) reflects the inboard beam outboard while the outboard mirror (4.1 mrad) reflects the outboard beam inboard. The beam presented to the dual mirror system is defined by two 1 mm x 1 mm apertures. The maximum power absorbed by each mirror is 200 W. Two vertically deflecting monochromators with minimum offset of 17 mm are located in the First Optical Enclosure on the outboard branch. The monochromator for the inboard branch is located in the corresponding experimental station.

BEAMLINE LAYOUT

The 2-ID beamline infrastructure consists of three existing shielded enclosures, three mini-hutches and shielded transport. The mini-hutches are existing as well and are relocated as needed. The shielded transport is a new design. The schematic layout of the major optical and shielding components is shown in Fig. 1.

SOURCE

The X-ray source for the beamline consists of two 2.4-m-long undulators with a period length of 3.3 cm (U33), one for each branch, located symmetrically about the center of the straight section. The period may be further optimized in the future.

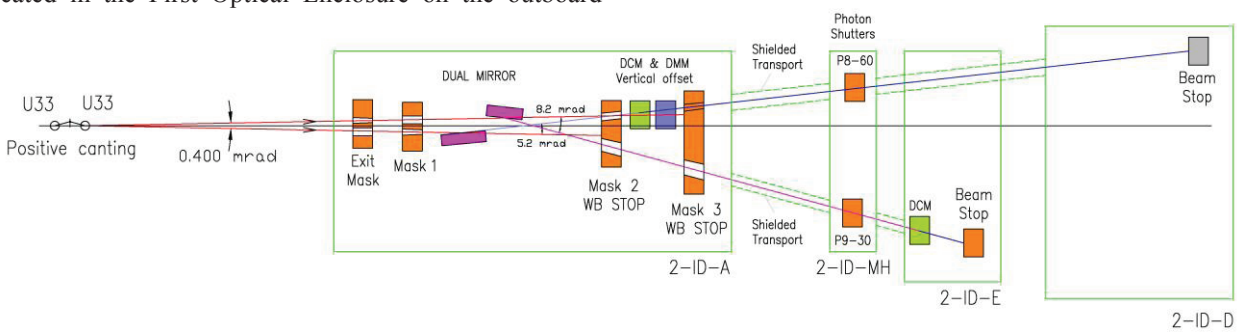

Figure 1: Schematic layout of the major optical and shielding components.

CANTING MAGNET

The design of the canting magnet for 2-ID is based on the permanent-magnet canting magnet planned for Sector 4-ID that introduces a bend of 400 µrad with a magnetic gap of 8.5 mm. Modifications are made to accommodate the larger vacuum chamber and larger magnetic gap in Sector 2. In addition, the ability to adjust the bend by a small amount is desired so the electron beam can be steered independently through the two undulators. A coil is added to the canting magnet to provide a steering adjustment of 40 to 50 µrad, maximum. That limitation on the steering adjustment avoids potential issues with power level increases on downstream masks. The cant centerline is offset 0.61 mm outboard of the traditional centerline (positive canting).

FRONT END

For cost reasons, the existing front end (FE), designed for inline operation, is kept in place, with a new exit mask and collimator. This constraint required that the canting angle be smaller than the typical APS canting angle of 1 mrad. The optimal angle for 2-ID was determined to be 400 µrad. In order for the FE masks and beam stops to remain within the design limits, the undulators cannot be set to their minimum gaps simultaneously. The output power of the undulators is limited to 6553 W. However, in designing the exit mask and the beamline heat absorbers, credit was not taken for the FE power limitation.

DUAL CANTING MIRROR

In order to increase the beam separation as well as to provide power filtering and higher-harmonics rejection for the downstream optics, a dual mirror system with focusing capability is used as the first optic at approximately 28 m from the center of the straight section.

Design Concept

The mirrors are mounted in a vacuum chamber, facing each other, in a staggered configuration, see Fig. 2. The mirror motions are completely independent of each other.

ISBN: 978-3-95450-188-5 doi:10.18429/JACoW-MEDSI2016-WEPE22

F-SWITCH: NOVEL 'RANDOM ACCESS' MANIPULATOR FOR LARGE NUMBERS OF COMPOUND REFRACTIVE LENSES

G.M.A.Duller†, A.Stallwood, D. R. Hall, Diamond Light Source, Didcot, UK

Abstract

The F-Switch is a new concept of device for the manipulation of large arrays of 2D CRLs or similar disc-shaped optical elements (12mm dia, 2mm thick) under high vacuum. Unlike the well-known transfocator devices the optical elements are randomly selectable. This enables a number of potential modes of operation, including the fine adjustment of focal length by adjusting the effective lens centre position when using CRLs or the use of some positions within the array to implement filters or reference foils. Actuation and guidance is achieved within the thickness of the element, so that the overall length of the device is minimised.

The device has been in user operation on the I04 MX beamline at Diamond Light Source (DLS) since 2015. Another device is being assembled for use on the I11 beamline at DLS. It is also hoped to install another device on the I03 beamline.

We present details of the mechanical design of the F-Switch and some examples of its operation.

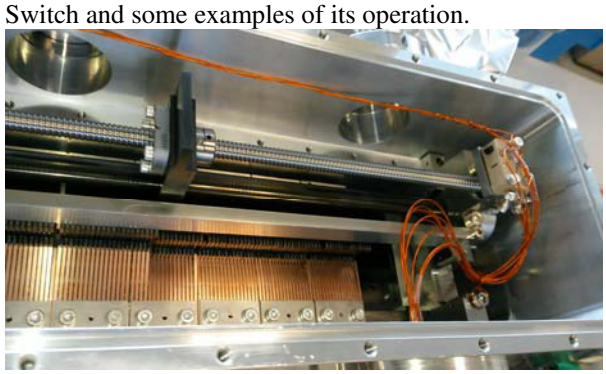

Figure 1: A general view of the F-Switch from above. The leadscrew and claw actuator shaft are visible along with a number of the bistable springs. The lenses are all hidden below this view.

THE RATIONALE

The I04 end-station upgrade [1] created an adaptable and stable platform for the final beam-conditioning elements of the beamline. In order to further enhance its capabilities a specification was developed to add to this platform a transfocator [2, 3] style device. However, it was quickly appreciated that with the short focal length required the limitations of the binary basis of the transfocator would limit the system performance. To illustrate this problem consider a transfocator with a total of 63 lenses. This would consist of six individual moving parts holding 1, 2, 4, 8, 16 and 32 lenses each. To insert 31 lenses the first five holders have to be inserted into the beam. To change to 32 lenses all five of these parts have to be withdrawn and the sixth lens holder has to be inserted. However, the effective centre of the lens has now been translated along the beam direction and so the resulting spot size at a fixed distance from the assembly may be very different from what is predicted if this effect is ignored.

The concept of the f-switch is that each of 120 lenses can be uniquely manipulated in and out of the beam. The benefit of this is obvious when the example above is considered, but it also allows for the number of lenses to be kept constant whilst the effective lens centre may be translated, thus allowing very fine control of the focal spot.

THE BISTABLE SPRING AND ACTUATION BLADE

The lenses used in the F-Switch are now a well-proven technology [4, 5] and are 2-D devices (rotational symmetry) mounted in a disk 2mm thick with a diameter of 12mm. The challenge was to design an actuation system within 2mm measured along the beam direction. The final design implemented a travelling actuator capable of operating on any one of the lenses, which implied that each lens then had to be securely retained in either of two states (in or out of beam) in the absence of an individual actuator. To allow beam to pass a lens which is nominally 'out of beam' the lens holder must be translated by a minimum of 6mm plus half the beam size. The acceptance of the lenses is 900µm, so the total motion required is a minimum of approximately 6.5mm.

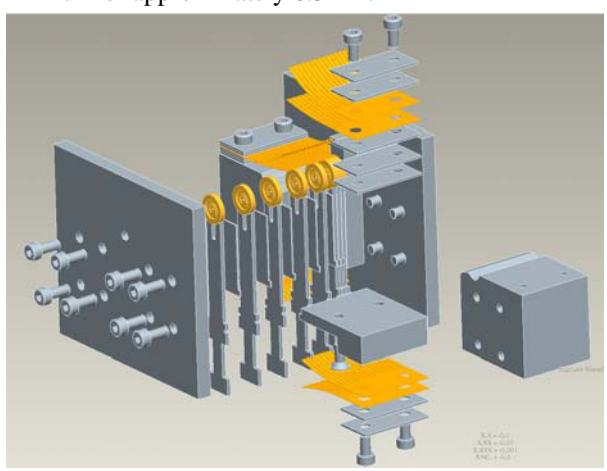

Figure 2: An exploded view of a prototype assembly. In this view the system is inverted wrt the final implementation, with the lenses shown at the top, acted on by a pair of leaf springs. Below this are the fixed spacers and the actuator blades with their bistable springs. The view of each spring is duplicated showing both the in-beam and out-of-beam condition.

†graham.duller@diamond.ac.uk

ISBN: 978-3-95450-188-5 doi:10.18429/JACoW-MEDSI2016-WEPE24

LIVE ANIMAL IMAGING PROGRAM AT BIO-MEDICAL IMAGING AND THERAPY FACILITY AT THE CANADIAN LIGHT SOURCE

M. A. Webb, G. Belev, D. Miller, T. W. Wysokinski, Z. Zhu, Canadian Light Source, Saskatoon, Canada
M. Gibbons, University of Saskatchewan, Saskatoon, Canada

Abstract

The live animal imaging program at the Bio-Medical Imaging and Therapy (BMIT) facility at the Canadian Light Source has been developing for the last 5 years and continues to grow. It is expected to become a large portion of the user activity as numerous groups work towards the goal of live animal studies. Synchrotron-based imaging of live animals is an opportunity for great science that also brings challenges and specific requirements for the experimental end-station. The beamline currently provides basic support and has been improving the facilities available. For example, there have been changes to the lab to allow for longer rodent housing and improved housing during measurements. Remote control of heat lamps and of flow rate for gas anaesthesia allow a veterinarian or animal care worker to make adjustments without interrupting the imaging. Integration of user equipment such as heart/breathing monitoring and ultrasound equipment with the beamline systems can be used for gating control of imaging. Future improvements will be done with consultation with university veterinarians and the user groups.

INTRODUCTION

The Bio-Medical Imaging and Therapy (BMIT) facility at the Canadian Light Source (CLS) provides a world class facility with unique synchrotron specific imaging and therapy capabilities [1 – 3]. BMIT is used to study diverse problems in human medicine, veterinary medicine, micro-beam radiation therapy, dosimetry, agriculture, and other biomedical areas. The facility is comprised of 05ID-2 and 05B1-1 beamlines and supporting laboratories. This paper will first look at the background and requirements involved with working with live animals and then describe some of the engineering solutions which were developed in a collaboration of all those involved.

LIVE ANIMAL PROGRAM AT THE CLS

The live animal imaging program at the BMIT facility at the Canadian Light Source has been developing for several years and continues to grow. It is expected to become a large portion of the user activity as numerous groups work towards the goal of live animal studies. Key goals of the beamline include assuring best practices in animal anaesthesia monitoring and producing the best images and scientific results possible with minimal dose delivered. Figure 1 shows statistics for live animals brought to BMIT. Usage varies considerably depending on the research groups. Note that recent groups have begun to image larger animals such as rabbits and dogs.

There are a number of considerations for the design of the end-station for the imaging of live animals and university veterinarians are consulted closely. The key requirement centres on animal care. In brief, animals arrive at the facility and are under the care of a veterinarian or other animal care personnel. When ready, an animal is placed under anaesthesia and taken into the hutch to be imaged and/or treated. Treatments may include radiation or medical procedures. Imaging may be used to evaluate results. The animal is monitored throughout the process. Once the measurements are finished the animal is removed from the hutch for recovery in the lab. Other requirements are from external bodies. The CLS is regulated by the Public Health Agency and follows the Canadian Biosafety Standards and Guidelines[4, 5]. The CLS is also a member of the Canadian Council on Animal Care (CCAC) [6, 7] and a participant of the University Animal Care Committee [8].

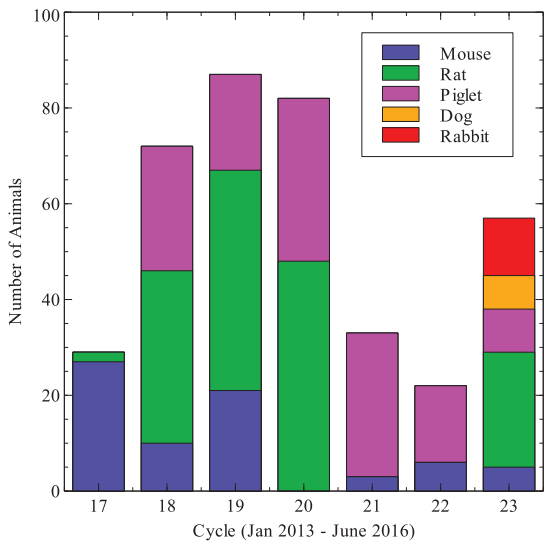

Figure 1: Animal usage statistics. Cycles correspond to 6 month periods.

LABORATORY FACILITIES

The CLS provides basic laboratory facilities and a change-room. There are two labs adjacent to the end-stations, as well as a life science lab nearby. These labs provide equipment for the users and areas for sample preparation. The labs include biosafety level 2 areas.

The BMIT labs also provide a place for the temporary housing of animals, medical procedures and for recovery after experiments. For example rodents may be kept in micro-environment cages up to 72 hours. The lab has red film on the windows and red lights to simulate a day/night

ISBN: 978-3-95450-188-5 doi:10.18429/JACoW-MEDSI2016-WEPE26

UPGRADE THE BEAMLINE PF-AR NW14A FOR THE HIGH-REPETITION-RATE X-RAY PUMP-PROBE EXPERIMENTS

S. Nozawa† , High Energy Accelerator Research Organization, Tsukuba, Japan

Abstract

The time-resolved X-ray measurements at storage ring has achieved successfully in investigating the structural dynamics of excited states, however the most of its experimental repetition rate has been limited to about ~1 kHz . The low repetition rate decided by the frequency of the pump laser system leads to a lack of photon in the time-resolved experiments. In this study, the high-repetition-rate time-resolved X-ray experimental system is reconstructed at PF-AR, NW14A. To use full of the x-ray flux without the x-ray isolation, the precise transient structure could be visualized. This study demonstrated the high-repetition-rate time-resolved X-ray measurements offer an opportunity to understand of the detailed photoreaction process and can be available as a fundamental observation technology for the development of new photo-functional materials.

INTRODUCTION

Time-resolved X-ray measurement is a powerful tool for the investigation of ultrafast science in various research fields ranging from local photochemical or photobiological processes, such as photocatalyzed reaction and photodissociation to photo-induced phase transitions in crystals[1]. Time-resolved X-ray experiments that have been developed with the rapid progress of synchrotron sources have made it possible to study photo-induced ultrafast transformations by synchronizing X-ray pulses with ultrashort laser pulses. This pump–probe synchronization can be combined with established X-ray techniques, such as absorption, diffraction, and scattering experiments [2]. Especially, time-resolved X-ray absorption fine structure (XAFS) is important for studying the molecular dynamics.

The Photon Factory Advanced Ring (PF-AR) is a full-time single-bunch synchrotron radiation source operated for time-resolved X-ray studies with pulsed X-rays. Electrons with a ring current of 60 mA (75.5 nC per bunch) are stored in a single bucket with a lifetime of about 20 h. The radio frequency (RF) for cavities and harmonic number of the PF-AR are 508.58 MHz and 640, respectively. Therefore, the X-ray pulses are delivered at a frequency of ~800 kHz with a pulse duration of about 100 ps.

Previously, the typical laser system, installed in the beam line for time-resolved experiments is a fs Ti:sapphire regenerative amplifier laser system. The Ti:sapphire laser system, which is operated at 800 nm fundamental wavelength, is capable of reaching up to 1 mJ pulse with a repetition rate of ~1 kHz. At that time, the experimental frequency of the laser pump and x-ray probe experiment was limited to ~ 1 kHz to excite samples with an ideal pulse energy. The low-flux condition, attributed to the about one thousandth isolated x-ray, sometimes prevents advanced researches for the dynamic structural analysis [3].

In recent years, the developments of high-repetition laser systems and x-ray focusing technologies has provided the pump-prove experiments without the x-ray isolation. Also at PF-AR, NW14A, the high-repetition-rate time-resolved X-ray experimental system was reconstructed. The improvement of measurement efficiency is described in this paper with an example from time-resolved XAFS.

X-RAY FOCUSIG OPTICS

The X-ray focusing optics are a bent cylindrical focusing mirror and a poly-capillary focusing optics (XOS, USA). In regard to the bent cylindrical mirror, the mirror is coated with rhodium (100 nm thick). The mirror can be bent at a range of bending radii between -2000 m and +2000 m by a mechanical bender. The glancing angle is adjusted by tilting the mirror at the mirror's center. A bending mechanism directly applies the bending momentum to the mirror. By the bent cylindrical mirror, the beam is focused at the sample position with 464 μm (H) ×236 μm (V). In this focusing condition, to add the poly-capillary focusing optics with the 5mm working distance, the beam size at the sample position with 60 μm (H) × 60 μm (V) is achieved.

HIGH REPETITION LASER SYSTEM

For the pump laser with the high repetition rate, a 350 fs Yb fiber laser system (Tangerine, Amplitude Systèmes) was installed. The Yb fiber laser system is operated at 1030 nm fundamental wavelength. The fundamental wavelength can be converted to second (515 nm), third (343 nm), and forth (257 nm) harmonics by a higher harmonics generator for the Tangerine. The fiber laser is capable of reaching up to 30 μJ with a repetition rate of the 794 kHz. The fiber laser is installed at near the sample in the experimental hutch.

TIME RESOLVED XAFS WITH HIGH REPETITION RATE

The time-resolved Ru K-edge X-ray absorption fine structure (XAFS) were measured with the 400 kHz repetition rate by using a scintillation counter, a gated integrator and the fiber laser system. Through the metal filter and the solar slit, the fluorescence signal was detected by the fast scintillation counter, which has a 50 mm diameter of acceptance surface. The experimental condition, where the frequency of laser pulses is a half of the 800 kHz x-ray frequency, removes the low frequency noise components from the laser on/off difference of XAFS spectrum.

† noz@post.kek.jp

ISBN: 978-3-95450-188-5 doi:10.18429/JACoW-MEDSI2016-WEPE28

MINIMIZING EXPERIMENTAL SETUP TIME AND EFFORT AT APS BEAMLINE 1-ID THROUGH INSTRUMENTATION DESIGN

Erika Benda*, Jonathan D. Almer, Peter Kenesei, Ali Mashayekhi, John Okasinski, Jun-Sang Park, Rogelio Ranay, Sarvjit Shastri

Advanced Photon Source, Argonne National Laboratory,
9700 S. Cass Av, Argonne, IL, USA

Abstract

Sector 1-ID at the APS accommodates a number of different experimental techniques in the same spatial envelope of the E-hutch end station. These include high-energy small and wide angle X-ray scattering (SAXS and WAXS), high-energy diffraction microscopy (HEDM, both near and far field modes) and high-energy X-ray tomography. These techniques are frequently combined to allow the users to obtain multimodal data, often attaining 1 μm spatial resolution and <0.05° angular resolution. Furthermore, these techniques are utilized while the sample is thermo-mechanically loaded to mimic real operating conditions. The instrumentation required for each of these techniques and environments has been designed and configured in a modular way with a focus on stability and repeatability between changeovers. This approach allows the end station to be more versatile, capable of collecting multi-modal data in-situ while reducing time and effort typically required for set up and alignment, resulting in more efficient beam time use. Key instrumentation design features and layout of the end station are presented.

BEAMLINE 1-ID

Focus

The 1-ID beamline at the APS delivers high brilliance, monochromatic ($\Delta E/E \approx 10^{-3}$) high-energy X-rays (>40 keV) resulting in exceptional penetrating power and spatial-angular resolution. The Materials Physics and Engineering (MPE) group operates the beamline and takes advantage of this combination to investigate a wide variety of polycrystalline material systems *in situ* / *in operando*, such as structural alloys, chemical compounds used in batteries, and bones to name a few.

Techniques

User experiments are typically performed at the 1-ID-E end station. Three primary techniques are supported at the 1-ID-E end station:

Small and wide angle X-ray scattering (SAXS/WAXS) While these two techniques are typically supported individually, the unique WAXS detector array at the 1-ID-E end station allows the combination of the two techniques. WAXS provides information such as phase volume fraction, preferred crystallographic orientation, and aggregate-average strain. SAXS provides information such as precipitate or void size distribution. The combined technique is capable of interrogating a wide range of length scales and is particularly useful in investigating polycrystalline materials with small grains (1 μm or less) and/or large prior deformations.

High-energy diffraction microscopy (HEDM) This novel technique is capable of non-destructively characterizing an individual constituent grain in a polycrystalline aggregate. Several variants of this technique exist; depending on the location of the detector, the morphologies and intragranular crystallographic orientation information of the grains (near-field) or the average crystallographic orientations, positions, and stress tensors associated with the individual grains (far-field) can be obtained.

Tomography While tomography is a widely available technique, the ability to combine SAXS/WAXS or HEDM with high resolution (1 μm) phase or absorption contrast tomography is quite unique and allows the users to gain a more complete picture of material behavior at these length scales.

Users

The user groups supported by the 1-ID beamline are diverse, ranging from university research groups investigating the micromechanics of materials at a more fundamental level to large corporate users interested in process optimization. Large polycrystalline aggregates with a variety of applications are investigated.

Examples of research performed at beamline 1-ID:

- Understanding the micromechanics associated with microcrack nucleation in nickel based superalloys used for turbine blades. [1]
- Strain development in bovine bone under uniaxial compression. [2]
- Investigating the effects of irradiation on materials used in nuclear engineering. [3]

* benda@aps.anl.gov

ISBN: 978-3-95450-188-5 doi:10.18429/JACoW-MEDSI2016-WEPE29

A NOVEL FILTER AUTO-MOUNTER FOR THE BIOXAS BEAMLINES AT THE CLS

S. Carriere *, D. Beauregard, B. Schneider, G. Steel, D. Taylor,
Canadian Light Source Inc., Saskatoon, Canada

Abstract

The BioXAS beam-lines are a recently completed group of beam-lines at the Canadian Light Source (CLS). The Biological X-ray Absorption Spectroscopy (BioXAS) – Extended X-ray Absorption Fine Structure (EXAFS) beamlines host three 32-element germanium detectors. There was a need to introduce an exchangeable filter between the soller slits and the 32-element germanium detectors. It was further required to have an automated filter exchange system so that users could quickly vary filter thicknesses and types to determine the effect on the signal. An auto-mounting filter system was created to meet these requirements and allows users to quickly exchange filters without breaking experimental hutch lockup. The auto-mounter cartridge can hold up to ten slides that measure 100 mm X 55 mm in cross-section. The device inserts slides in an extremely small envelope between the soller slits and the liquid helium cryostat. The auto-mounter assembly also houses the stages required to actuate the soller slits laterally and vertically. During device commissioning we performed 800 consecutive successful filter exchanges as part of a stress test. The spatial constraints, mechanics, and fabrication of the device will be presented. Software development will also be discussed.

INTRODUCTION

The BioXAS beamlines are a recently completed group of three beamlines at the CLS. The two EXAFS beamlines are sourced from a single "flat top" hybrid wiggler and were designed to be capable of extremely high resolution EXAFS measurements. They are capable of measuring biologically relevant concentrations of metals in dilute samples.

The SIDE EXAFS beamline hosts one 32-element germanium detector mounted at 90° to a liquid helium sample cryostat.

The MAIN EXAFS beamline hosts two 32-element germanium detectors mounted at 90° to a liquid helium sample cryostat (mounted inboard and outboard of the cryostat).

Part of the beamline scope is to allow users to quickly vary filters between the sample and the detector so that they can determine the effect on the signal. Individual users will decide on the type and thickness of filter material. It was decided that the filter exchange would be automated so users could change filters without breaking experimental hutch lock-up.

A Filter Auto-Mounter (FAM) (Fig. 1) was designed to meet these requirements.

Figure 1: Main Beamline Endstation with 2 FAM units.

Constraints/ Requirements

The following were determined to be the FAM design constraints and requirements:

- The design of the FAM has to work for both EXAFS beamlines.
- Users need to be able to pre-load a set of filters according to their needs.
- Two FAM systems are required on the MAIN beamline.
- The system needs to also house the Soller slits and provide them XZ translation.
- Distance from 32-el detector snout and sample is 81mm.
- 1 mm of space between Soller slit and detector snout.
- The sample cryostat is motorized in XYZ, +/- 10 mm in all directions.
- Filters to be placed immediately in front of Soller slits. The available thickness for the filter insert mechanism is 13 mm after accounting for Soller slit thickness, detector position, and cryostat travel.
- The only available route for filters to enter is to be lowered in from above the 32-el detector snout.
- FAM system to be fully automated with the ability to keep track of filter position in order to prevent collisions.
- FAM units to be removable for service without detaching other endstation critical hardware.

DESIGN FEATURES

The overall FAM assembly (Fig. 2).

* shawn.carriere@lightsource.ca

ISBN: 978-3-95450-188-5 doi:10.18429/JACoW-MEDSI2016-WEPE30

INTRODUCTION TO NEUTRON SCATTERING INSTRUMENTS – HOW ARE THEY DIFFERENT?*

R. Connatser, Canadian Light Source, Saskatoon, Canada

Abstract

Neutron scattering is a complementary technique to x-ray scattering scientifically, but while there are similarities, there are some unique challenges in the design, construction, and operations. This poster will provide a brief description of neutron scattering, describe the technical components of spallation neutron scattering instruments, and discuss the engineering challenges found in the design and construction of these instruments.

KEY DIFFERENCES

Neutrons interact with matter via the strong nuclear force (nuclei) and the dipole-dipole interaction between magnetic moments (unpaired electrons). Neutrons penetrate deeply into samples in comparison to x rays, which interact with electrons.

Key differences:

- Weak interaction with matter
- Sources/Generation
- Induced Radioactivity and secondary particle generation
- Time of Flight methodology

SHIELDING

Significant shielding is needed around the energetic production of neutrons and the incidental high energy photons (and associated hadron showers). Where most intense, this shielding will be very thick (meters). This shielding is not just for the protection of humans, but to prevent background radiation from interfering with the experiments (see Fig. 1).

Shielding Composition

To shield against a range of particles and photons involves using multiple materials to account for the varying ways in which they interact with matter. For high energy neutrons and photons, high Z materials are needed, generally steel. For lower energy neutrons, materials containing a high concentration of hydrogen is best, such as concrete (with water) or high density polyethylene.

Complicated Shapes

Similarly to synchrotron beamlines, the technical components of neutron instruments have varying shapes and need utilities supplies to them. Slow neutrons also have a peculiar scattering property in which they almost appear to be a gas. Thus cracks or edges through the shielding must have multiple bends in them. Given the sheer volume of shielding needed on an instrument, the shapes needed meet all the varying needs often more resemble Tetris blocks than Lego.

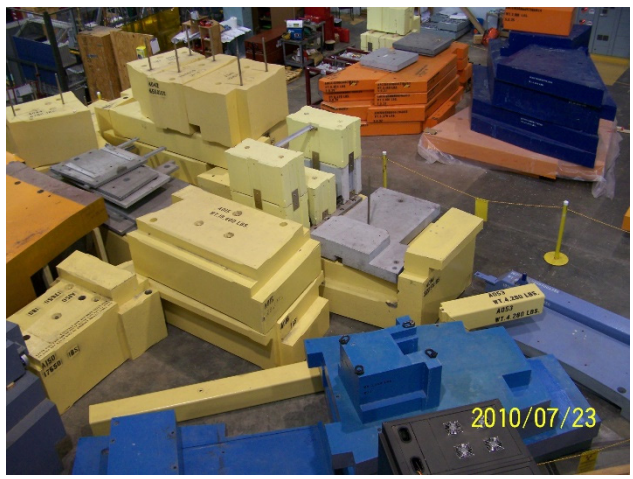

Figure 1: Neutron shielding from the Spallation Neutron Source, Oak Ridge National Laboratory, USA.

Time of Flight Methodology

Unlike photons traveling at the speed of light, neutrons of different energies travel at different speeds – the more energetic, the faster. Neutron instruments must take into account the time of travel from the source to the sample, sample to detector. There must also be methods of removing the prompt pulse and other unwanted neutrons from the beam.

Chopping the Beam

The premise is to physically disrupt the neutron beam with a rotating device. Three examples are:

T0 – to remove the prompt pulse of high energy neutrons with a heavy rotating mass.

Bandwidth – often a cascade of rotating disks that are timed with the pulse to only allow particular energy/wavelengths to pass through to the sample.

Fermi – used to select particular energy/wavelength neutrons.

Sample to Detector

A spectrometer measures an energy change in the neutrons created by the interaction with the sample. The energy change is seen at the detector by measuring the difference in the flight time of the neutrons – e.g. we know when the neutrons of x energy interacted with the sample, we know the precise distance from the sample to the detector and the speed of neutrons of that energy. Neutrons that gain energy will arrive sooner, those that lose energy will arrive later. By having appropriate distances between sample and detector, measurement of these time differentials is possible.

ISBN: 978-3-95450-188-5 doi:10.18429/JACoW-MEDSI2016-WEPE36

DESIGN, CONSTRUCTION AND COMMISSIONING OF TWO HIGHLY INTEGRATED EXPERIMENTAL STATIONS FOR MICRO-FOCUSING MACROMOLECULAR CRYSTALLOGRAPHY BEAMLINES AT NSLS-II

D. K. Bhogadi*, B. Andi, L. E. Berman, M. Carlucci-Dayton, M. R. Fuchs†, J. Jakoncic, T. Langdon, J. Lara, B. Martins, S. Myers, D. K. Schneider, S. McSweeney, R. M. Sweet
National Synchrotron Light Source II, Brookhaven National Laboratory, Upton, NY 11973, USA

Abstract

We present the final engineering design and first commissioning results of two highly integrated experimental stations for macromolecular crystallography (MX) at the National Synchrotron Light Source II (NSLS-II). One of the beamlines will provide micro-focusing (FMX) and the other high automation (AMX). These beamlines will support a broad range of biological and biomedical structure determination methods from serial crystallography on micron-sized crystals, to structure determination of complexes in large unit cells. The experimental stations were designed and fabricated largely in-house to obtain highly flexible and modular units that meet the challenging stability and integration requirements required by the small beam sizes and the limited work envelopes. Key components to meet these criteria are a highly compact beam conditioning unit and exchangeable main and secondary goniometers (sample rotation axes) integrated in a granite support structure.

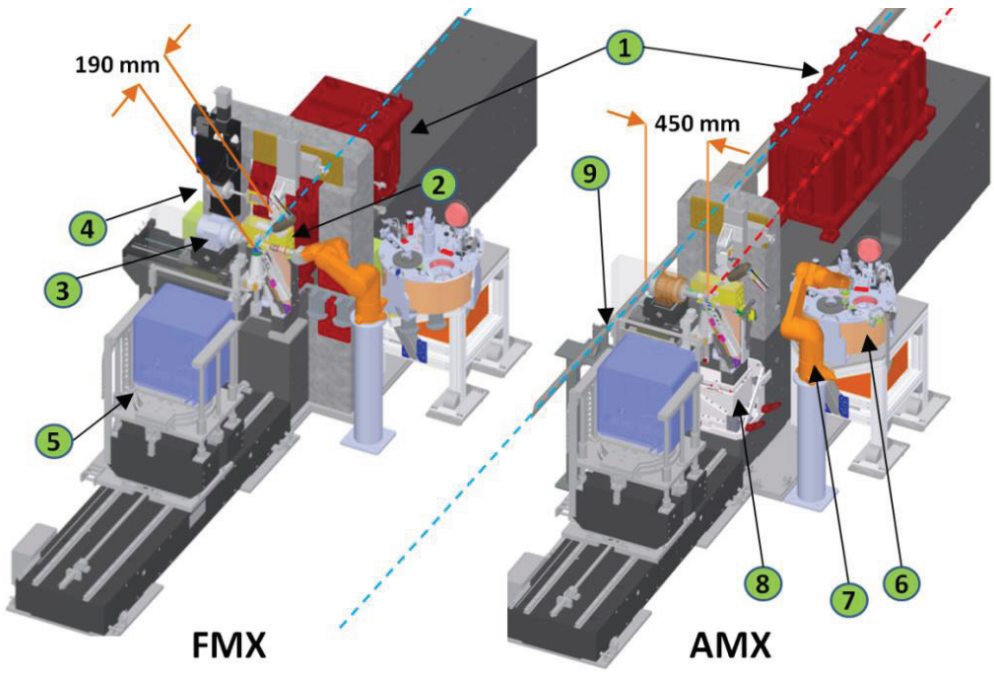

Figure 1: The FMX (left) and AMX (right) experimental stations. The beams come from the top right (FMX cyan dashed line, AMX red dashed line). Devices (identical at both endstation if not indicated otherwise): (1) KB focusing mirror tanks, (2) beam conditioning unit, (3) main goniometer, (4) FMX secondary goniometer, (5) detector support, (6) LN2 sample Dewar (7) Stäubli 6-axis sample mounter (8) AMX XY lift stage (9) FMX beam pipe passing the AMX endstation.

INTRODUCTION

The FMX and AMX beamlines were designed and constructed as part of a suite of Advanced Beamlines for Biological Investigations with X-rays – the ABBIX project [1–3]. The beamlines' layout and scientific mission greatly influence the endstation design: beam sizes of down to 1 and 4 µm respectively require high vibrational stability. The two beamlines share sector 17 of the storage ring in a canted undulator arrangement. Combined with the Kirkpatrick-Baez (KB) focusing mirrors' short focal distances, this layout poses great spatial constraints for the experimental stations and beam conditioning units. To support different measurement

* dbhogadi@bnl.gov
† mfuchs@bnl.gov

ISBN: 978-3-95450-188-5 doi:10.18429/JACoW-MEDSI2016-WEPE37

UPGRADE OF THE SUPER ADVANCED X-RAY SPECTROMETER (SAX-ES) OF THE RIXS ENDSTATION FOR BETTER RESOLUTION AND LARGER DETECTOR SIZE

St. Maag†, P. Hirschi[1], L. Nue, X. Wang, T. Schmitt,
Paul Scherrer Institut (PSI), 5232 Villigen PSI, Switzerland
[1]also at HELVETING Engineering AG, 6331 Hünenberg, Switzerland

Abstract

The RIXS endstation of ADRESS beamline at Swiss Light Source (SLS) is equipped with an ultrahigh resolution X-ray spectrometer as described in [1]. In the scope of a CCD camera upgrade, the modification of the vertical alignment of the guiding structure and ultra-high vacuum tanks became necessary. The new camera with a higher resolution and larger detector size weights around 25 kg. It is required to have a vibration-amplitude well below 2 microns. We will present the critical design parameters of the upgrade, and the effort to increase bending stiffness of vacuum guide structure while keeping major geometry parameters. In addition, kinematic over determinacy was removed. After the upgrade we performed vibration measurements verifying that the dynamic stability of the camera is improved, and the design goal is reached. The site acceptance test confirmed the proper operation of the new mechanism. The redesigned spectrometer is shown in Fig. 1 with the welded bellows only connected on one side.

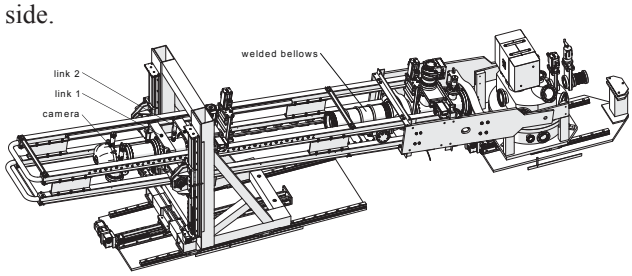

Figure 1: The redesigned spectrometer.

INTRODUCTION

The spectrometer with a length of 5 m is installed on a rotating girder platform and allows varying scattering angles from 30° to 130°. The position of the CCD detector is longitudinally adjustable on the girder and vertically adjustable on a moving frame to allow an angle between 2° to 15° in the vertical plane. For the new and much bigger detector system with 3 inches in width, the whole vacuum section and beam guiding chambers had to be enlarged to get use of a wider beam. The bigger ultra-high vacuum chambers and the new welded bellows were made of stainless steel 316LN.

The retrofit also included a new and larger turbo and ion getter pump as well as an automated vacuum valve on both ends of the bellow. The three separate vacuum compartments allow individual ventilation without ventilating the bellows. The retrofit was performed while aiming at the minimum number of changed parts.

† stephan.maag@psi.ch

The enlargement together with the new vacuum pumps would cause a substantial increase in weight. This could decrease stability of the instrument and it could require changes in the air movers or the girder. To increase the stability and to make sure the instruments weight and centre of gravity could be maintained, the whole supporting structure was built in aluminium with more efficient beam cross-sections. Therefore, the carrier structure is now built with 4 aluminium I-shaped beams with a higher stiffness than the old steel L-shaped beams but with lower weight. The same concept was adapted to the new camera support, which is now made of two big aluminium cross links about 50% lighter than the old design but much stiffer. The revolute joint of the camera support consists of much bigger self-aligning ball bearings, which allows compensation of inaccuracy in all required directions. Thus, the two linear drives at the mainframe are no longer fixed together by an overdetermined structure, they move simultaneous driven by the same motor. The linear bearing, which supports the connection of the carrier structure, also allows this compensation by using cam followers at the floating bearing side. The cam follower is a compact bearing with a high-rigidity shaft and a built-in needle bearing. Contrary to the normal installation case these rollers run on a hardened shaft guideway.

Figure 2: The spectrometer after the upgrade.

For the fixed bearing side normal linear ball bearings were used, running on the same type of shaft guideways. To support the new and bigger vacuum chambers, the carrier structure had to be redesigned and a new bellow guiding system was required. The vacuum chambers are carried by two big aluminium cross links, which allows linear displacement compensation in case of higher temperatures, such as a high bake out temperature of min.

ISBN: 978-3-95450-188-5 doi:10.18429/JACoW-MEDSI2016-WEPE38

THE MECHANICS OF THE VEKMAG EXPERIMENT

T. Noll[1,2], F. Radu[2]

[1]Max-Born-Institut Berlin, Max-Born-Straße 2 A
12489 Berlin, Germany

[2]Helmholtz-Zentrum Berlin, Albert-Einstein-Str 16, 12489 Germany

Abstract

For the experiments at the synchrotron radiation source BESSY II synchrotron of the Helmholtz-Zentrum Berlin a new end station and a new beamline were developed and are now in user operation. The end station contains a 9-2-1 Tesla vectorial magnet and a cryostat with manipulator for the sample cooling and positioning, a deposition chamber, and a UHV detector chamber. We report here mainly on the technical design of the detector chamber which is placed below the magnet chamber and it is also connected to the deposition chamber. Because of various constrains including the limited available space between the bottom flange of the magnet chamber and the floor level, a sophisticated mechanics had to be developed to provide integrated functionality for both the detector holder and the sample transfer units. The detector unit consists of a tubular holder of 5 cm diameter which travels more than 60 cm vertically and exhibits an unlimited rotation degree of freedom of 360 degrees within the magnet bore. The sample transfer unit consists of a telescopic movement mechanism allowing for the sample holder vertical travel within the detector tubular holder. The functionality challenges and their resolve were addressed in an innovative mechanical design at HZB which was financed and build by the VEKMAG consortium.

INTRODUCTION

Soft x-rays are establishing as the most successful probe for a wide range of disciplines seeking answers of fundamental questions at the nanoscale and for different timescales down to femtosecond resolution[1,2]. In particular the magnetism community has benefited greatly from the element specific sensitivity which allows to disentangle the spin and orbital moments through the theoretical prediction and experimental observation of the XMCD effect [3,4,5,6]. Since then, the instrumentation is being continuously developed for advanced methods providing opportunities for magnetic imaging, spectroscopy, and scattering. To this end the VEKMAG consortium [7] has developed, build and comissioned an endstation installed at a newly build beamline located at segment 7.1 in the BESSY II experimental hall of the Helmholtz Zentrum Berlin.

The VEKMAG endstation includes a magnet chamber which includes a superconducting vector magnet and a cryostat, a detector system mounted below the magnet and a deposition chamber connected to the detector chamber which allows for in-situ growth and transfer of the samples. The magnet provides 9T in the beam direction, 2T perpendicular to the beam direction and in the horizontal plane, and 1T in the vertical direction. The available temperature on the sample ranges between 2.5 K and up to 500 K. A more detailed description of the system and the methods (spectroscopy, scattering and X-FMR) will be described elsewhere. Here we describe the technical design of the mechanics for the detector system and for the magnet chamber support frame.

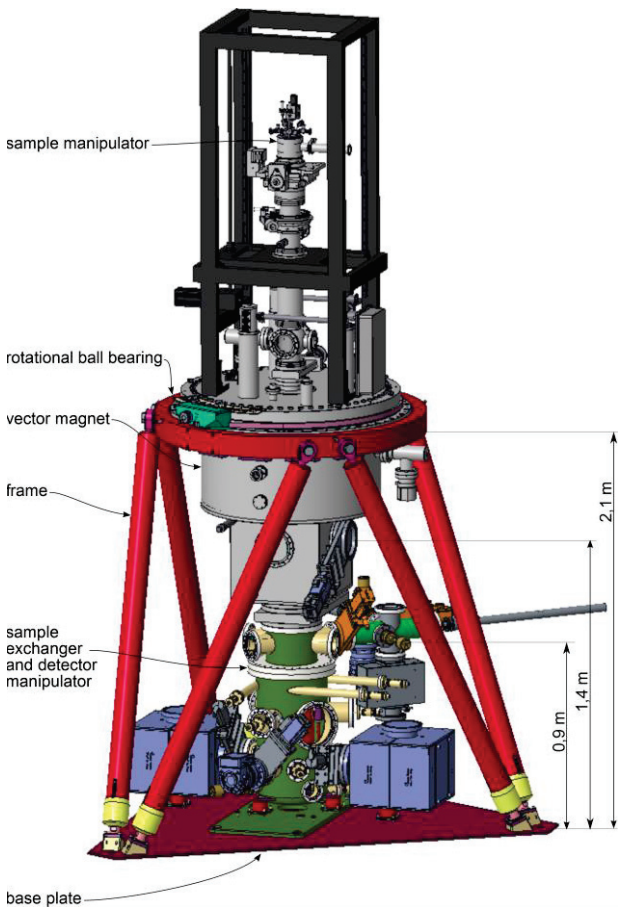

Figure 1: The VEKMAG end-station (the deposition chamber is not shown).

The superconducting vector magnet is accommodated in an individual UHV-chamber which is attached via its upper circular flange of 1 m in diameter to a rotating platform on top of a hexapod frame (s. Figure 1). This

ISBN: 978-3-95450-188-5 doi:10.18429/JACoW-MEDSI2016-WEPE39

FABRICATION, ASSEMBLY, AND METROLOGY METHODS TO OPTIMIZE AN ADJUSTABLE EXIT SLIT FOR A SOFT X-RAY BEAMLINE

J. Takakuwa, C. Hernikl, T. Lipton, T. Stevens, T. Warwick, LBNL, Berkeley, USA

Abstract

Exit slit edge geometry and paired edge parallelism can directly impact performance of a synchrotron beamline. At the same time, maximizing the performance of an existing design is often a financial and logistical necessity. The construction project for beamline 7.0.1 (BL7.0.1, Coherent Scattering and MICroscopy (COSMIC)) at the Advanced Light Source (ALS) facility located at Lawrence Berkeley National Laboratory (LBNL) consists of two branch lines, each of which has vertical and horizontal slit assemblies. These assemblies were fabricated from a pre-existing design, positively impacting project schedule and budget. Apart from orientation, the slit assemblies are identical. The goal for parallelism is +/- 2 microns over the full 25 mm length. Each Slit blade edge can travel +/- 5mm about the beam center with the resolution of a micron; slits can scan over that range with a nominal size of about 10 microns. A variety of fabrication and metrology techniques were implemented to maximize the performance of the current design and feature areas of improvement in fabrication, metrology, and design were identified.

INTRODUCTION

At the ALS, recently constructed beamlines 7.0.2 and 7.0.1 use eight sets of the exit slits described herein. Additionally, beamline 6.0 has five sets of similar design. In constructing new beamlines, existing designs are leveraged for the cost and schedule benefits they provide. Increasingly demanding specifications associated with new beamlines poses a challenge when leveraging these reused designs. After the construction of beamline 7.0.2, efforts were made to improve the performance of the exit slits on beamline 7.0.1 without resorting to a redesign of the assemblies themselves. These efforts resulted in varying degrees of success.

The COSMIC beamline, 7.0.1, has two branchlines and associated end stations. Each branchline uses two exit slit sets where one set confines the beam vertically and one set confines the beam horizontally. The goal was to have an exit slit parallelism of +/- 2 µm over the 25 mm length of the slit. Perpendicularity between the vertical and horizontal sets was not adjustable and resulted from the flange orientations on the welded chamber.

The blades themselves were made from OFHC copper, C10100 alloy, were paddle style blades, electrically isolated (and wired to measure current), and were water cooled for temperature stability. The blades were mounted to the end of actuators for insertion/retraction of the blades into/out of the beam to form a rectangular exit slit with adjustable dimensions and locations. Each blade signal was used in a feedback loop to steer the beam so that the position on the exit slit was consistent. The motion of the exit slit blades was not part of this feedback loop.

BLADE FABRICATION AND EDGE STRAIGHTNESS

The GD&T tolerance for the blade edge was a profile with a 1 µm tolerance zone. The initial fabrication used a fine wire EDM and were considered to be a "best effort". After cleaning, the edge was measured.

First Measurement

Metrology was performed on an Optical Gaging Products, SmartScope Quest 800 machine. Metrology software used was MeasureMind 3D v15.1

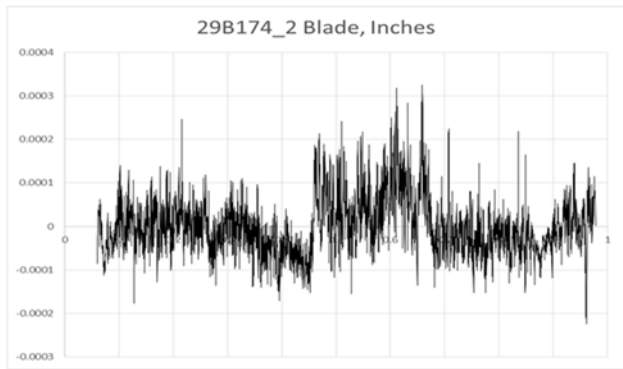

Figure 1: Typical first measurement.

Typical results (see Fig. 1) yielded a variation of the exit slit blade of +/- 2.5 µm to +/- 7.5 µm. As a result a lapping process was chosen for a secondary fabrication operation with the goal of improving the edge geometry of the blades.

Lapping Process

Simple blade fixturing maintained a consistent orientation relative to a surface plate. The blade edges were lapped using a series of graded abrasives (see Table 1). Lapping pressure and motion was done by hand by a journeyman machinist.

Table 1: Graded Abrasives

Abrasive	Grade
Roughing	1200 grit wet/dry silicon carbide
Semi-finish	3 µm (1500 grit), aluminum oxide
Finish	1 µm (2000 grit), aluminum oxide
Final Polishing	.1 µm (2500 grit), diamond

The lapping with grit paper was done by stroking repeatedly in sets of four, in one direction, at ~150 mm per second, along the direction of the blade length. Between sets, the lapped blade surface was visually inspected with a 10 X jeweler's loupe. A new area of abrasive was used after 3-4 sets of strokes. The blades were rinsed with ethanol and dried with compressed air at the time the new area of

ISBN: 978-3-95450-188-5 doi:10.18429/JACoW-MEDSI2016-WEPE40

TWO-ROTATION MECHANISM FOR AN IN VACUUM BEAMSTOP

J.B. González, C. Colldelram, A. Fontserè, G. Jover, J. Ladrera, M. Malfois, J.C. Martínez
ALBA-CELLS Synchrotron, Cerdanyola del Valles, Spain

Abstract

At Small-angle X-ray Scattering beamlines (SAXS), beamstops are needed to block the intense primary beam that has not been scattered by the sample in order to protect the detector from any damage. Beamstops are usually confined inside a vacuum tube minimizing air space between the sample and the detector. For certain experiments, a motorized beamstop is required to achieve a precise positioning in different regions of the detector active area. ALBA has developed a new motorized beamstop consisting of a two-rotation mechanism inside vacuum that composes a movement able to cover all range of the active area of the detector. The presented solution involves a main rotation reached by a gear and a worm drive actuated by a stepper motor and a second rotation relative to the main one produced by a piezo rotation stage. For each position appears two different solutions. This characteristic permits take two equivalent images in the detector with the same beamstop position but different orientation in the beamstop support; thus permitting the compensation of the support shadow on the active area of the detector.

INTRODUCTION

At SAXS beamlines, beamstops are needed to block the intense primary beam that has not been scattered by the sample in order to protect the detector from any damaged. Beamstops are usually confined inside a vacuum tube minimizing air space between the sample and the detector. For certain experiments (for example SAXS/WAXS or GSAXS), a motorized beamstop is required to achieve a precise positioning in different regions of the detector active area.

ALBA has developed a new motorized beamstop consisting of a two-rotation mechanism inside vacuum that composes a movement able to cover all range of the active area of the detector (Fig. 1), permitting for each position appears two different solutions.

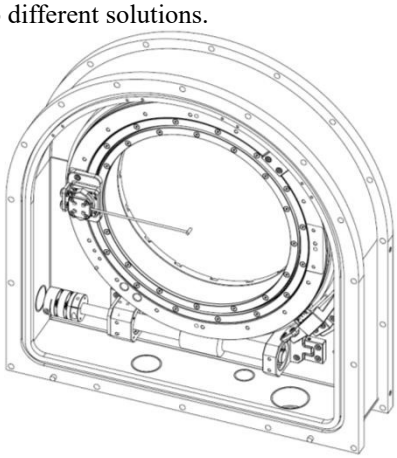

Figure 1: Beamstop main view.

TECHNICAL SPECIFICATIONS

The motorized beamstop must comply with the following specifications:

- Cover all range of the active area of the SAXS detector (210x210mm).
- Obtain two solutions for each position demanded.
- In vacuum motorized movements.
- 5µm resolution.
- 1 rpm speed.
- Compact and integrated in the current Flight Tube of the End Station.
- Mounting interface DN320 ISO-K.
- Vacuum compatible (10^{-2}mbar).

DESIGN

The complete mechanism is confined in a vacuum chamber that belongs to the vacuum flight tube between the sample and the detector. The mechanism involves a main rotation reached by a gear and a worm drive actuated by a stepper motor and a second rotation relative to the main one produced by a piezo rotation stage (Fig. 2). The vacuum chamber contains fixed supports for appropriate bearings which permit the main rotation of the axis. The relative rotation holds the beamstop support that consists of a rod usually made of a material partially transparent to the beam. Finally, the beamstop itself is mounted in the extreme of this support and consists of a cylindrical block of an opaque material to the beam.

This motorized beamstop is more compact and shows a better stability than other conventional alternatives such as linear stages due to a shorter and stiffer beamstop rod and a more packed mechanism.

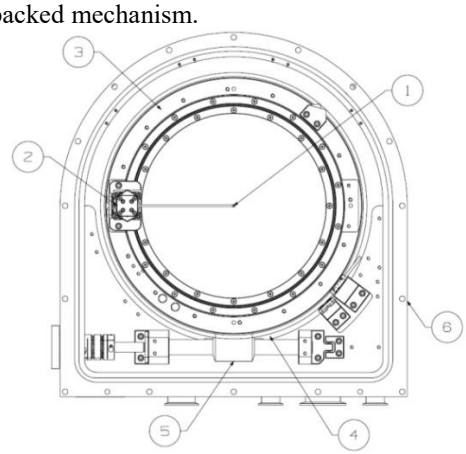

Figure 2: Parts breakdown. (1) Beamstop, (2) second rotation, (3) main rotation, (4) gear, (5) worm drive, (6) vacuum chamber.

ISBN: 978-3-95450-188-5 doi:10.18429/JACoW-MEDSI2016-THAA02

MECHANICAL ENGINEERING OF A CRYO STXM AT CLS*

C. N. Regier†, A. F. G. Leontowich, D. M. Taylor, Canadian Light Source, Saskatoon, Canada

Abstract

A Scanning Transmission X-ray Microscope (STXM) is a useful imaging tool, but its application to certain types of samples is limited by significant rates of x-ray damage to the sample. Cooling samples to liquid nitrogen temperatures can delay radiation damage, but must be done in a vacuum environment to prevent rapid formation of ice on the sample. The Canadian Light Source (CLS) has constructed a Cryo-STXM, which can maintain sample temperatures at 100 K in an ultra-high vacuum environment and rotate the samples in the beam to collect tomographic data sets. This presentation will discuss the mechanical engineering aspects of the development of this Cryo-STXM including the finite element analysis (FEA) for stresses and vibrations, and present the performance parameters being achieved by the instrument.

INTRODUCTION

The Canadian Light Source (CLS) is a third-generation synchrotron located in Saskatoon, Canada. One of the Phase 2 beamlines constructed at CLS was the spectromicroscopy (SM) beamline [1], an insertion device (ID) beamline with an ID in straight 10 of the CLS storage ring. The SM beamline has been operational since 2005, however, the EPU was not installed until May 2006. Before this the beamline used upstream bend magnet radiation to operate. Two end-stations were originally included on the SM beamline: a photon emission electron microscope (PEEM) and a scanning transmission x-ray microscope (STXM) which started operation in 2007.

The SM beamline is currently undergoing an upgrade. The first phase of this upgrade is the construction and installation of a cryo-STXM. The goal is to have a STXM with sub-30 nm resolution that is capable of cryogenically cooling the sample to near liquid nitrogen temperatures, and perform tomography measurements on the sample. There are currently very few cryo-STXMs in the world, and the one at CLS is the first soft x-ray STXM capable of tomography through a 90 degree rotation in both directions. As of August 2016 the cryo-STXM is just completing its final benchmark experiments, and is now operating at the CLS SM beamline.

* Work supported by CFI, the governments of Saskatchewan, Alberta, and Ontario, and the Automotive Fuel Cell Corporation.
† chris.regier@lightsource.ca

The mechanical design phase of the cryo-STXM project presented CLS with some interesting problems. This paper will briefly discuss the SM beamline, and will present an overview of the cryo-STXM. A few specific mechanical engineering issues related to the development of the instrument are examined, and finally the performance of the cryo-STXM to date is reviewed.

THE CLS SM BEAMLINE

Figure 1 shows the layout of the SM beamline at CLS. The SM beamline uses an elliptically-polarizing undulator to supply synchrotron radiation. Downstream of the M1 mirror, a plane-grating monochromator (PGM) filters the desired energy out of the supplied spectrum. The range of energy that the SM beamline is designed to make use of is from a low end of roughly 130 eV to a high end of up to 2500 eV, placing it in the soft x-ray range.

From the PGM the beam proceeds through two further mirrors, M3PEEM and M3STXM, which split the beam and direct it down one of the branch lines. One ray proceeds through another mirror before reaching the PEEM, while the other goes directly into the existing STXM.

Table 1 shows specifications of the CLS SM beamline.

Table 1: CLS SM Beamline Specifications

Spot size (STXM)	30 nm
Spot size (PEEM)	50 nm
Energy Resolution (E/ΔE)	3000-10000
Energy Range	130-2500 eV
Wavelength	95-4.5 Å
Photon Flux (STXM)	~10^8 ph/sec in 30 nm spot
Photon Flux (PEEM)	~10^{12} ph/sec in 50 nm spot

The regular STXM is capable of several techniques, including near-edge x-ray absorption fine structure (NEXAFS) in transmission mode, total electron yield (TEY) mode, and x-ray fluorescence (XRF) mode, soft x-ray tomography, x-ray linear dichroism (XLD), x-ray magnetic circular dichroism (XCMD), and ptychography. The goal of the new cryo-STXM would be to use some of these techniques, specifically TEY and ptychography, on a sample that can be kept at cryogenic temperatures to delay radiation damage and can be rotated +/- 70 degrees in the beam for tomography.

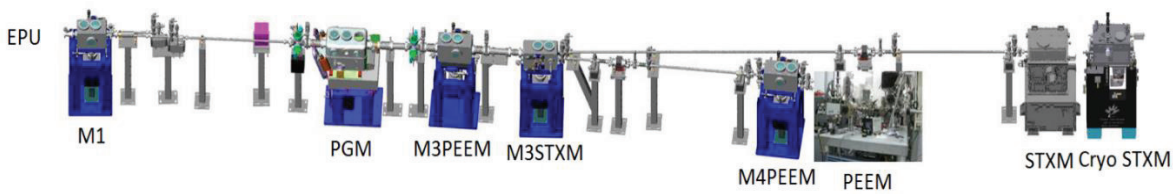

Figure 1: The layout of the SM beamline at CLS.

ISBN: 978-3-95450-188-5 doi:10.18429/JACoW-MEDSI2016-THAA03

MECHANICAL DESIGN OF NEW DUAL PINHOLE MINI-BEAM COLLIMATOR WITH MOTORIZED PITCH AND YAW ADJUSTER PROVIDES LOWER BACKGROUND FOR X-RAY CRYSTALLOGRAPHY AT GMCA@APS *

Shenglan Xu, Nagarajan Venugopalan, Oleg Makarov, Sergey Stepanov and Robert F. Fischetti
GM/CA and XSD, Advanced Photon Source,

Argonne National Laboratory, Argonne, IL60439 USA

Abstract

The GM/CA-developed, quad-mini-beam collimator [1, 2, 3], advanced rastering and vector data-collection software tools [4], have enabled successful data collection on some of the most challenging problems in structural biology. This is especially true for membrane-protein crystals grown in lipidic cubic phase, where crystals are typically small, fragile, and "invisible" when cryo-cooled. There are two main sources of X-ray scattering (besides the sample) that reach the detector, contribute to background and limit data resolution. These are scattering within the collimator that escapes the exit aperture and air-scattering of the direct beam before it terminates in the beam-stop. Scattering from the collimator can be reduced by decreasing the exit aperture size. A quad mini-beam collimator was built consisting of 5-, 10-, 20- and 150 µm beam defining apertures with 50-, 70-, 100- and 300 µm exit apertures, respectively. Previous collimators were positioned in the X-ray beam by two motorized translational motions and two manual angular adjustments via a kinematic mount. The individual beams were selected by recalling stored translational positions. The pitch and yaw angular adjustments were manually pre-adjusted to one optimal position for all four apertures. Due to reduced tolerance in the new design, aligning each of the pin-hole combinations to high-precision required motorizing both translational and angular motions. The novelty of the new mechanical design is the compactness and positional stability of the structure. The new collimator positioning system consists of three frames, four C-flex bearings, two actuators and two high precision stages. The two pairs of commercial flex bearings function as a universal joint.

INTRODUCTION

Since 2007, GM/CA has provided micro-diffraction capabilities at both 23-IDD and 23-IDB beamlines through versatile collimator systems. A robust, monolithic quad-collimator provided user-selectable beam sizes of 5, 10, 20 µm or "full beam" (~25 x ~75 µm FWHM). These quad collimators were positioned in the X-ray beam by two motorized translational motions and two manual angular adjustments via a kinematic mount. The individual beams were selected by recalling stored translational positions. The pitch and yaw angular adjustments were manually pre-adjusted to one optimal position for all four apertures (Figure 1). An active beam stop of 1.0 mm diameter is typically positioned about 35 mm downstream of the sample. A prototype collimator with 5 µm beam defining and 150 µm exit aperture was developed for scanning X-ray micro diffraction studies of tissue architecture. This collimator in combination with a 0.5 mm beam stop resulted in a 30% background reduction, prompting us to develop dual pin-hole collimators for reduced background.

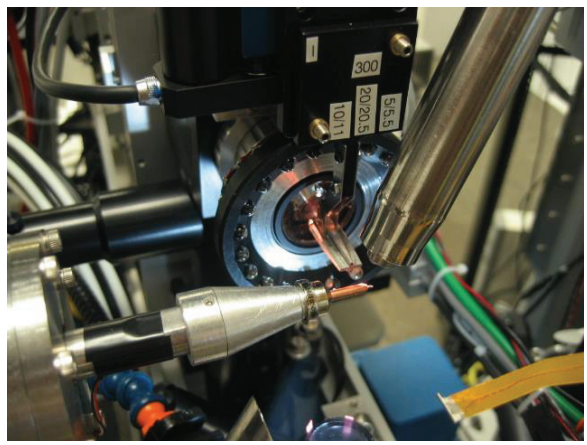

Figure 1: Close up of the Quad collimating system installed at the beamline end station. Two high resolution micro translation stages are combined to form an XY system for the collimators alignment. The travel range is 15 mm for both horizontal and vertical. The design resolution is 0.007 µm and the repeatability is 0.1 µm. The whole system stability is +/- 0.1 µm.

DUAL PIN-HOLE COLLIMATOR

Design of Dual Pinhole Collimator

The dual pinhole collimator design significantly reduces the X-ray scattering that escapes the collimator, Figure 2. The collimator assembly has a steel scatter guard body that hosts an entrance and exit sub-assembly. Both sub-assemblies consist of a steel cap and a Platinum pinhole

ISBN: 978-3-95450-188-5 doi:10.18429/JACoW-MEDSI2016-THAA04

UPGRADING A TRANSMISSION SAX/WAX BEAMLINE TO ALLOW HIGH QUALITY GISAX/GIWAX EXPERIMENTS FOR SOFT MATTER THIN FILM

A. R. Marshall*, Diamond Light Source, Didcot, UK

Abstract

The project required a sample environment to deliver experiments in vacuum or helium, with high humidity, including capacity to use aggressive solvents. The compact, transportable system incorporates a high precision in-vacuum manipulator/ positioning stage (with repeatability better than 1 µm/ 1 mdeg) allowing for multiple sample configurations. Current sample mounts include in-situ film formation (Doctor Blade), thermal annealing/drying heater stage, sample cooling and multiple sample stages; the system has been designed to accommodate many sample substrate formats. The existing end station camera system has been upgraded to include two, in-vacuum, WAXS and SAXS area detectors, which are custom builds based on the Pilatus 6M. The SAX detector module includes three in vacuum, independent ,configurable SAXS beam stop manipulators to block GISAXS transmitted, reflected and specular flare as well as isotropic and anisotropic SAX, a photon sensitive detector shutter plate is included. The 4 mm diameter tungsten beam stops each include a miniature photodiode to measure beam intensity and can be positioned to within 10 µm precision in X and Y over 300 mm x 250 mm motion range.

I22 EXISTING CAPABILITIES

I22 [1] is an insertion device beamline operating at diamond since 2007. The beamline (see Fig.1) is dedicated to Non Crystalline Diffraction including small angle and wide angle x-ray scattering. The beam transmitted through samples in bulk form. Small angle X-ray scattering (SAXS) is a technique that is used to probe the internal structure of condensed matter systems at the micron and nanometre length scales. The Wide Angle X-ray scattering (WAXS) technique measures length scales on the order of Angstroms, and is typically dominated by diffraction processes, suited to study the close chain packing of semi-crystalline polymer chains within polymer blend films. The end station consisted of a 1D WAX camera and a 2D SAX camera of variable length from 800 mm up to 10 m. A single fixed beam stop, with built-in diode, measures beam intensity and blocks the transmitted beam. This paper discusses the changes made and features added to add high quality GISAXS functionality to this beamline.

THE GISAXS UPGRADE

The scope of the project was to replace hardware and reuse existing infrastructure. This limited the work to a GISAXS sample environment and positioning system, and a new SAXS detector module to deliver the greater motion ranges required by GISAXS, with a new motorized beam stop module. The upgrade was combined with replacing the ageing 1D WAX detector with a 2D in vacuum WAX detector.

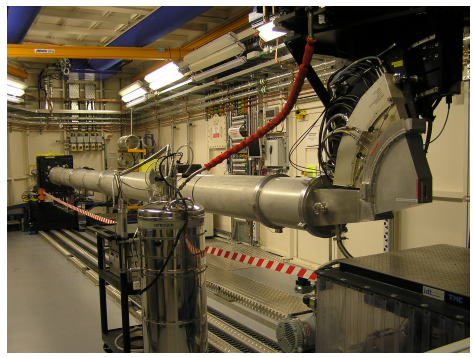

Figure 1: Original camera.

GISAXS Functionality

In transmission Small Angle X-ray Scattering (SAXS) the data is based around the axis of the transmitted beam with the elastic scattering pattern perpendicular to, and centred, on the axis of the primary beam. The technique is used to measure bulk samples where the interaction of the beam with the sample is determined by the size of the beam (≈300 µm × 100 µm) and the sample thickness which range from hundreds of microns to several millimetres. Grazing Incidence

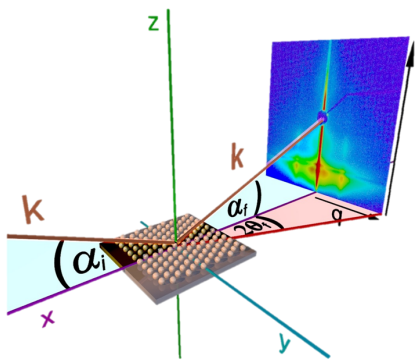

Figure 2: GISAXS theory,GISAXS Image courtesy of Dr Andreas Meyer [7].

Small Angle X-ray Scattering (GISAXS) is based on reflection geometry with the scattering pattern based around the reflected beam axis. It is intended to measure thin films cast on flat substrates. Typical film thicknesses are in the nanometer range and operating at the grazing incidence angles allows

* andrew.marshall@diamond.ac.uk

ISBN: 978-3-95450-188-5 doi:10.18429/JACoW-MEDSI2016-THBA01

AN ENDSTATION WITH CRYOGENIC COILS CONTRIBUTING TO A 0.5 TESLA FIELD AND 30-400K SAMPLE THERMAL CONTROL*

G. A. Scharfstein, D. Arbelaez, J. Jung
Advanced Light Source at Lawrence Berkeley National Laboratory, Berkeley, USA

Abstract

The Engineering Division of Lawrence Berkeley National Laboratory presents a design for an Endstation to enable X-ray Photon Correlation Spectroscopy (XPCS), which is a method to study temperature-induced fluctuation in hard and soft condensed matter systems. XPCS, when applied to a magnetic system, can yield information about how domains fluctuate as the system goes through a phase transition; these phase transitions can occur at low temperatures (less than 100K) and at an applied magnetic field. Therefore, requirements for the Endstation include a 0.5 Tesla (T) field at the sample and temperature control of the sample from 30K to 400K.

INTRODUCTION

Our beamline delivers a 10 micron diameter beam of coherent light and the Endstation can hold and manipulate a maximum sample size of about 7 square mm. Coherent x-ray scattering gives rise to speckles; these speckles can be imaged using a CCD detector. Resonantly tuned coherent x-rays that scatter off a magnetic sample generate magnetic speckles which are representative of the exact lateral magnetic heterogeneity (i.e domains). With the addition of low temperature control, the sample can experience a phase transition. During phase transition the sample morphology will change and causes a subsequent change in the speckle pattern. By monitoring the speckle pattern over time at a particular temperature with magnetic and/or electric fields, it is possible to determine the temporal evolution of the surface features.

The magnetic and thermal systems required to produce the above-mentioned environment present a challenge to the engineering team due to the strength of the field, range and stability of the temperature control for the sample and relatively small volume in which to accomplish this. When the motion control of the sample and pinhole are included, the endstation quickly becomes an extremely complex and tightly integrated system.

*The Advanced Light Source and this work are supported by the Director, Office of Science, Office of Basic Energy Sciences, Division of Materials Sciences and the Division of Chemical Sciences, Geosciences, and Biosciences of the U.S. Department of Energy at Lawrence Berkeley National Laboratory under Contract No. DE-AC03-76SF00098.

MAGNETIC SYSTEM

The magnetic system is based on a three-dimensional Opera Vector Field magnet design with vanadium permendur as the pole material and a 5000 ampere-turn coil as the magnetic source. To obtain the proper field strength and meet the thermal requirements, a cryogenic solution was implemented to keep the energized coils from heating the sample. Liquid nitrogen floods a stainless steel can encasing the coil and the resulting thermal balance exhausts gaseous nitrogen via a vacuum chamber feed through. The geometry of the poles is influenced by the proximity of the pole tip to the sample and its translation normal to beam; 5mm is the vertical range (along gravity vector) and 7mm is the horizontal range of motion, along with about 190 degrees of rotation along the horizontal axis. The tapered shape is required to control the flux as the coils are relatively far from the pole tips and magnetic field target. Overall, the magnet system is optimized for field along the beam axis and it can be rotated along the beam-horizontal-to-gravity plane by controlling the power of opposing coils (see Figure 1).

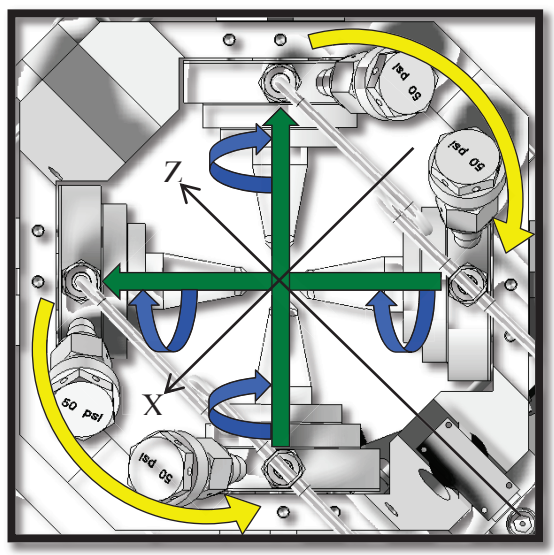

Figure 1: A diagram of the magnet system showing the current direction for each coil (blue arrows), the field vectors (green arrows) and the flux return through the yoke (yellow arrows).

ISBN: 978-3-95450-188-5 doi:10.18429/JACoW-MEDSI2016-FRAA01

ENGINEERING CHALLENGES ON THE I14 NANOPROBE BEAMLINE

A. Peach, Diamond Light Source, Oxford, UK
F. Cacho-Nerin, J. Parker, P. Quinn, Diamond Light Source, Oxford, UK

Abstract

An overview of the double branch 185m I14 Nanoprobe beam-line under construction at DLS will be presented together with the end-station design in further detail. The end station consists of a split vacuum vessel containing a KB mirror configuration (at UHV) and the sample environment (at HV) which is just 50mm from the end of the final KB optic. An in-vacuum detector is mounted between the KB and the sample whilst two externally mounted detectors will operate between 0.25m & 3m from the sample. Four cryogenic samples can be brought into the vessel at a time and transferred remotely to the sample position with cooling provided by a Helium pulse tube cooler. With an initial 50nm size beam, stability is absolutely critical and careful attention has been paid in the design to mitigate any thermal and structural sources of vibration. An array of interferometers reference the KB mirrors and sample position and will be used to actively correct for any drifts. The very tight space constraints involved have greatly increased the complexity and duration of the design but testing of prototypes is now underway. The system is scheduled for build and test through the Autumn 2016.

INTRODUCTION

The long Nanoprobe Beamline currently under construction and commissioning at Diamond Light Source features both a Nanoprobe & Mesoprobe branch. The Nanoprobe branch will be accepting first users in Spring 2017 whilst the Mesoprobe branch will be completed later in a 2nd build phase.

Each branch has a separate experiments hutch within the newly constructed external building, which also features a suite of Electron Microscopes laboratories.

Due to the arrangement of the Mirrors and Double Crystal Monochromator (DCM) it will be possible to deliver pink or mono beam to the end station of either branch.

BEAMLINE CHALLENGES

The goal of the beamline is to provide a sub-50nm X-ray beam through which samples can be scanned in 2D and 3D under various conditions whilst collecting data from several detectors. In particular a nano-KB system was selected to achieve nano-focussing with a cryogenic system able to handle frozen hydrated samples for biological imaging. To achieve this we need:-

- Beam stability of < 50 nrad RMS before the nano-focus endstation and stability at the sample of <3 nm
- A KB mirror and sample stage system designed for flexible sample conditions in air or vacuum whilst maintaining the KB system under UHV at all times.
- Long term thermal stability to minimize thermal drift.
- A detector layout for multi-modal experiments.
- An interferometry system capable of sample rotation.
- Cryogenic cooling for 2D and 3D scanning with associated sample handling and sample staging for frozen hydrated samples.

BEAMLINE LAYOUT

The beamline is 185m long to improve demagnification of the beam at the sample, whilst maintaining a reasonable working distance. This also provides a coherent beam for diffraction limited focussing and coherent imaging applications.

The beamline was designed for a cryogenic in-vacuum undulator, with the main optics installed inside two hutches within the main synchrotron building. The beam propagates through a long vacuum pipe to an external building some 90 m away from the main synchrotron which houses a third Optics Hutch together with the Nanoprobe and Mesoprobe Experiments concrete hutches.

Hutch 1&2 Key Components

Optics Hutch 1 contains the primary optics including the mirrors and DCM.

Nano-focussing and coherence experiments require high stability and the beamline targeted < 50 nrad rms beam movement in both the vertical and horizontal direction from 1-100 Hz.

With the demands for vertical beam stability at the sample ultimately to within a few nanometres, the optical arrangement was carefully considered and an all horizontally deflecting geometry was used.

The Mirrors M1 (with bender) & M2 (flat) use stripes of Si, Rh and Pt to provide harmonic rejection and horizontal beam shaping with respect to the secondary source.

The horizontally deflecting monochromator is a fixed exit system using a pair of Si(111) crystals to provide continuous energies from 4.5 to 26 keV with much attention paid to the mechanism stiffness and arrangement of the cryogenic cooling pipework which has been proven to provide vibration free performance below 100 Hz and less than 50 nrad RMS up to 200 Hz.

A fast feedback system operating at 500Hz will be used to actively control the pitch and roll and suppress low frequency vibrations based on beam position measurements. As nano-probe experiments are flux hungry, a filtered pink beam option was considered by using mirror M3 (to be installed at a later date) with space also available to consider a multilayer monochromator.

ISBN: 978-3-95450-188-5 doi:10.18429/JACoW-MEDSI2016-FRAA03

MECHANICAL DESIGN OF MIRAS, INFRARED MICROSPECTROSCOPY BEAM LINE AT ALBA SYNCHROTRON

Llibert Ribó†, Igors Šics, Artur Gevoryan, Josep Nicolas, Alejandro Crisol, Carles Colldelram, Liudmila Nikitina, Raquel Monge, Marcos Quispe, Ibraheem Yousef
ALBA Synchrotron Light Source, Cerdanyola del Vallés, Catalonia, Spain
Paul Dumas, SOLEIL, Gif-sur-Yvette, France
Gary Ellis, ITP CSIC, Madrid, Spain

Abstract

The infrared (IR) micro spectroscopy beam line MIRAS has been an in-house project fully developed at ALBA as a result of a collaboration of different teams during the period of 2014 when the design started to 2016 It is composed of a horizontally retractile mirror to extract the IR light from the bending magnet radiation and a system of 8 transport mirrors located by positioning systems designed for a high stability performance, to transport the extracted IR light outside the tunnel until the first End Station.

LAYOUT

The layout was defined by the scientific and the optical teams, in close collaboration with Dr. Paul Duma's team (SOLEIL, France) and Dr. Gary Ellis (IPT CSIC, Spain), who contributed a lot during the design phase.

The extraction mirror M1 is located inside a bending magnet vacuum chamber. At the beginning of its bending radius, starts the optical layout: This is named the source point. M1 reflects the infrared fan of the synchrotron radiation of the bending magnet where M1 is located as well as a fraction of emission fan of the upstream bending magnet (in addition to the "edge radiation"). The infrared beam is transported through a layout of 4 transport mirrors with a toroidal mirror used to focus the beam at the focal point F1 just outside the tunnel wall. Subsequently, 3 additional mirrors direct the beam to the focal point F2 located inside the 1st End station. The beam line is prepared to be upgraded up to 3 End stations (See Fig. 1) as the beam splitter mirrors (MBSP1 and MBSP2) are retractile and allow part of the beam to pass through the other possible end stations (F3 and F4). At present, MIRAS is completed up to MBSP1 and F2 with 1st End station being operational.

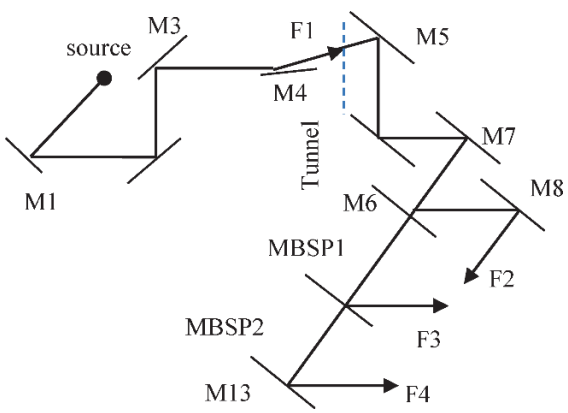

Figure 1: Schematic Layout of MIRAS.

SYSTEMS DESCRIPTION

Extraction Mirror M1

The slotted extraction mirror M1 is inserted inside the Dipole vacuum chamber in a certain angle, facing a portion of the synchrotron radiation coming from the last bending magnet, passing through a 3 mm slot (see Fig. 2a). In order to maximize the optical performance of the mirror the clearances with the inner face of the dipole chamber are very tight, 2 mm nominally with the inner wall and 1.8 mm with the slot end (see Fig. 2b).

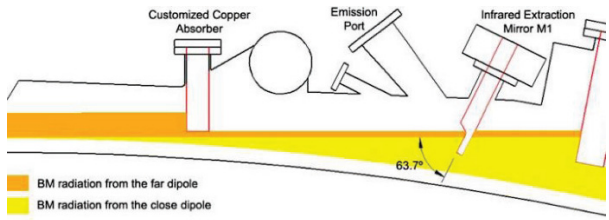

Figure 2a: Schematic of IR emissions collected by M1.

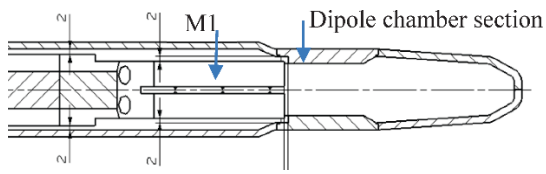

Figure 2b: M1 nominal clearance.

The mirror has been manufactured from polished aluminium 6061, and optical surface is gold plated (unprotected) (Fig. 3). An array of 6 thermocouples is positioned on the back side of the mirror protruding by 0.5 mm into the slot space. With their reading, the vertical position of the extraction mirror in respect to the beam can be fine-tuned. Apart from those, another pair of thermocouples are embedded into the non-reflective surface for temperature measurement of the body of M1.

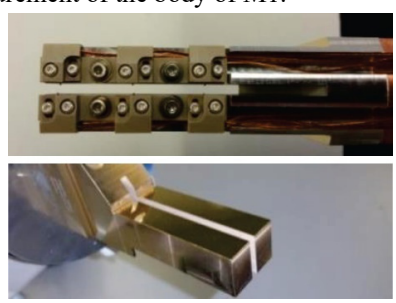

Figure 3: Top: back side of the mirror and portion of the cooper arm. Down: reflective surface.

ISBN: 978-3-95450-188-5 doi:10.18429/JACoW-MEDSI2016-FRBA01

A NEW CRYSTAL BENDER FOR THE ID31 LAUE-LAUE MONOCHROMATOR

M.Magnin-Mattenet[1], P. Got[1], A. Vivo[1], V. Honkimäki[1]
[1]ESRF, 71 avenue des Martyrs, 38043 Grenoble, France.

Abstract

The ID31 beamline is able to provide X-Ray energies ranging from 20 to 150keV. The energy range 50-150keV is covered by a Laue-Laue monochromator located at 105.2 meters from the source. Two asymmetrically cut Si crystals equipped with benders, based on a new concept, provide an energy resolution ranging from few hundreds of eV down to the Darwin width of few eV.

The bender principle, design, manufacture and first commissioning will be described. The virtual source, produced with a white beam transfocator, can be before or after the monochromator. Therefore the bending mechanism must allow both concave and convex configuration with bending radius from 20m to infinite. Each bender is equipped with two home made piezo-jacks controlled in close loop with capacitive sensors. The system is liquid Nitrogen cooled. The thermal behaviour will be described in detail and thermo-mechanical finite element analysis will be presented.

INTRODUCTION

The X-ray source of ID31 is an in-vacuum cryo-cooled undulator with 14.5mm period and the aim of the optical design of the ID31 beamline is to provide the highest possible X-ray beam intensity over the energy range of 20 to 150 keV. The X-ray techniques available at ID31 are tomography, reflectivity, SAXS and WAXS techniques which are used to study fuel cells, solar cells, rechargeable batteries, catalytic materials and various "dirty" interfaces. The beamline is equipped with three focusing devices used in combination with the ID31 Laue-Laue monochromator which is located at 105.2 meters from the source and covers the energy range from 50 to 150keV.

THE LAUE-LAUE MONOCHROMATOR

The Laue-Laue monochromator consists of two bent Si(111) crystals in non-dispersive geometry with an asymmetric cut of −36°. The crystals can be rotated so that other reflections in the (110) and (001) plane can be used, e.g. the Si(113) reflection with an asymmetric cut of −6.5°. The crystals thickness is 5 mm and they are LN2-cooled. Since the virtual source given by the compound refractive lens can be before or after the monochromator the bending mechanism allows both concave and convex bending. The beam offset can vary between 7 and 25mm. To allow the full energy range with 20 mm offset, the second crystal has a translation along the incident beam from 250 to 750mm relative to the first crystal.

THE BENDER

Various benders for mirrors or crystals have been developed in the past at ESRF [1-2], but none of them fully answer the specifications for the ID31 beam line.

Specification

The beam bandwidth is proportional to the inverse of the bending radius of the crystal determined by the virtual source to crystal distance. Therefore a convex and a concave bending with cylindrical shape is needed from ∞ to 20m. A coarse rotation of the crystals (±40°) is used to select reflections from (110) and (001) plane.The liquid nitrogen cooling is mandatory due to the high heat load generated by X-rays. Furthermore, the cooling scheme has to be optimized for both crystals to minimize thermal bump caused by the incident X-ray beam. Moreover, the absorbed power is tuned with the absorbers located in the first optical hutch. The crystals and bending mechanism has to be high vacuum compatible (10^{-8}mbar). The resolution in energy has to be 1ev. All this constraints led to a new principle for the bender.

Principle and Concept

The main difficulty is to fix the cryo-cooled crystal so that it is not sensitive to the vibrations induced by the cooling or other sources. Furthermore, the crystal should be mounted without torsion. Due to these constraints the concepts based on four-bar-bender or cantilever are not suitable. The new concept consists in finding a clever dimensioning of the bender relatively to the crystal so that the fixing points are placed where no significant aberration of the bender and crystal from the cylinder occurs [e.g, Fig.1a]. The new bender described here is very well adapted to provide at the same time a cylindrical shape of the crystal, a very high stiffness with a very good thermal contact for the cooling [e.g, Fig.1b]. The bender has a rigid middle part which is strongly attached to the support. On each side, one flexure is used as a rotating point to allow the motion controlled by the piezojacks. Two piezo-jacks attached on both side provide the push/pull forces. The piezo jacks are controlled in close loop with capacitive sensors located on both sides.

ISBN: 978-3-95450-188-5 doi:10.18429/JACoW-MEDSI2016-FRBA02

THE NANOBENDER: A NEW X-RAY MIRROR BENDER WITH NANOMETER FIGURE CORRECTION

Carles Colldelram[1*], Josep Nicolas[2], Claude Ruget[1], Pablo Pedreira[1], Igors Sics[1], Llibert Ribó[1], Albert Tomas[3], Joan-Manel Casalta[3], Carlos-Martín Nuño[3], David Úbeda[3]
1 CELLS, Cerdanyola del Vallès, Spain
2 SLAC, Stanford, California, United States
3 Sener Ingeniería y sistemas, Cerdanyola del Vallès, Spain

Abstract

Over time X-Ray mirrors are demanded for better focusing, closer to sample refocusing, spot size as well as better beam uniformity at sample position. Based on the experience of ALBA Phase I beam lines a new alternative design of a mirror bender is proposed [1]. The system includes two main functionalities: the mirror bender mechanism and mirror figure error correction. Both mechanisms are based on the introduction of a force constrain on the mirror surface instead of a geometrical one. As being based on a force mechanism they could reach high resolution and especially for the correctors which can achieve nanometre resolution. The correctors are designed to provide high force stability in the mirror side, eliminating the crosstalk between bending and figure correction, and minimizing the sensitivity to drifts. With such controlled deformation of the mirror substrate it is possible to obtain the desired surface figure not only to correct mirror figure errors but also to adapt it to the incident wavefront, thus becoming adaptive system. The mechanical solutions are presented which are able to correct mirror surfaces with a resolution of 1 nm reaching slope errors below 100 nrad.

INTRODUCTION

This new X-Ray mirror bender system has been conceived in the ALBA Beam Lines Phase I framework. The protein crystallography beam line at ALBA, BL13 XALOC [2], has a quite simplified optical lay-out with a channel-cut crystal monochromator and a couple of focusing mirrors placed in a Kirkpatrick-Baez (KB) configuration [3]. The mirror system allows reaching a focus spot of 50×5.5 μm^2 FWHM (H×V). This both mirror system were outsourced. The spot quality at sample position is mainly depending of the optical surface quality of this vertical focusing mirror (VFM), of its slope error, and in order to minimize the striation in the beam it was requested to the manufacturer to include a number of gravity sag compensators to have the possibility to use them not only to correct gravity flexion but also for mirror optics figure corrections.

Already with these correctors [4], thought to compensate gravity sag errors, the system has already an initial rough but enough force resolution allowing the mirror figure correction based on the Elastic Beam Theory [5] and a high-accuracy profile metrology, the ALBA NOM optical metrology system (see Fig. 1).

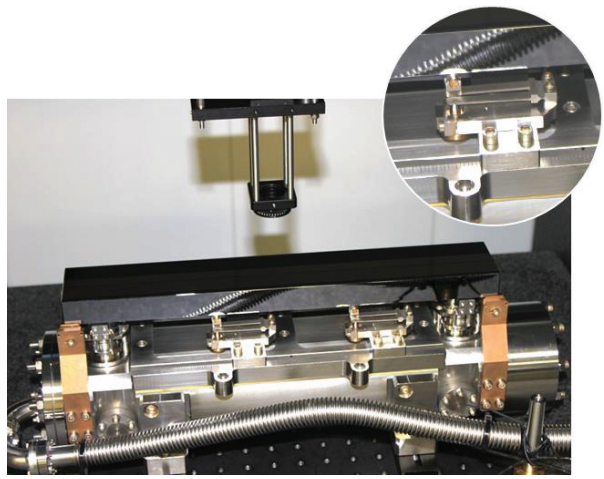

Figure 1: BL13 Xaloc VFM at ALBA NOM.

By means this analytical calculation, the actual surface error and an optimization algorithm we were able to calculate the number of correctors, setting force and position along the mirror to improve the mirror figure. Although these corrector were manual and not made to deal with this function the 300mm mirror was corrected from its initial slope error of 0,242µrad up to 0,055 µrad (see Fig. 2) by mean two of these gravity sag compensators and both pushing from below.

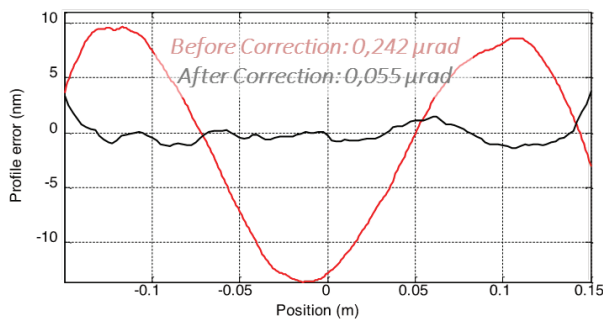

Figure 2: VFM optical surface height.

A ray tracing simulation of the mirror before and after the correction give a picture of the beam quality at sample position and its undesired striations improvement (see Fig. 3).

* ccolldelram@cells.es

ISBN: 978-3-95450-188-5 doi:10.18429/JACoW-MEDSI2016-FRBA03

DESIGN OF THE DIAMOND LIGHT SOURCE DMM FOR THE VMXi BEAMLINE

D. J. Butler†, J. H. Kelly, Diamond Light Source, Didcot, UK

Abstract

A Double Multilayer Monochromator (DMM) was designed in-house for the VMXi beamline. This paper describes the novel engineering solutions employed to build a high stability instrument. PiezoMotor® actuators drive sine-arm Bragg axes for both optics providing the coarse and fine motion in a single actuator. The long translation of the second multilayer is driven externally via a linear shift to eliminate in-vacuum pipe & cable motions. A high stability air bearing translates the whole DMM across the two multilayer stripes. The optics are water cooled via an Indium / Gallium eutectic alloy bath to minimise coupled vibrations. The DMM is operational on the VMXi beamline, experimental and performance data is presented.

INTRODUCTION

The in-situ Versatile Macromolecular crystallography (VMXi) beamline due to enter into service December 2016 is a high performance, high throughput autonomous upgrade to beamline I02. I02 currently operates a Double Crystal Monochromator (DCM) and the new DMM sits upstream of the DCM to allow both DCM and DMM based experiments. The DMM provides a broad energy band pass providing approximately 60x more photons to the sample. The overall design can be seen installed in the optics hutch (Fig. 1) and an isometric 3D CAD view (Fig. 2).

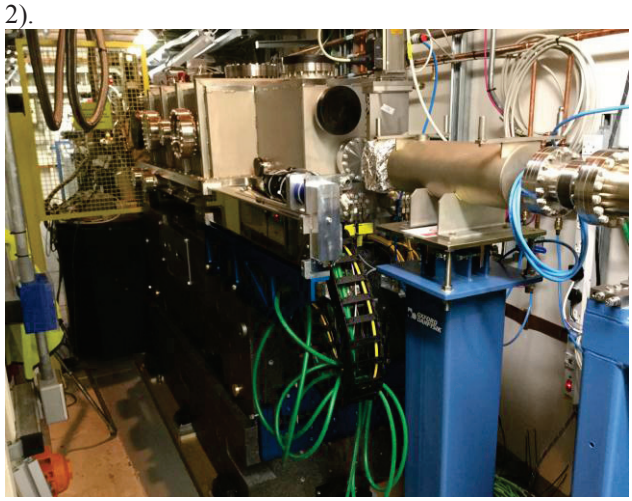

Figure 1: DMM installed in I02 optics cabin.

Stability of the beam was a critical criterion so throughout the design, care was taken to provide rigid mounting and stiff supports. Due to the shallow angles the DMM operates with, a relatively long travel in the beam axis is required. This is defined by the angular range and difference in multilayer heights. To maintain compatibility with the DCM, the DMM has a 25 mm vertical fixed offset so ML2 requires approximately 600 mm travel in the Z-direction (see Fig. 3).

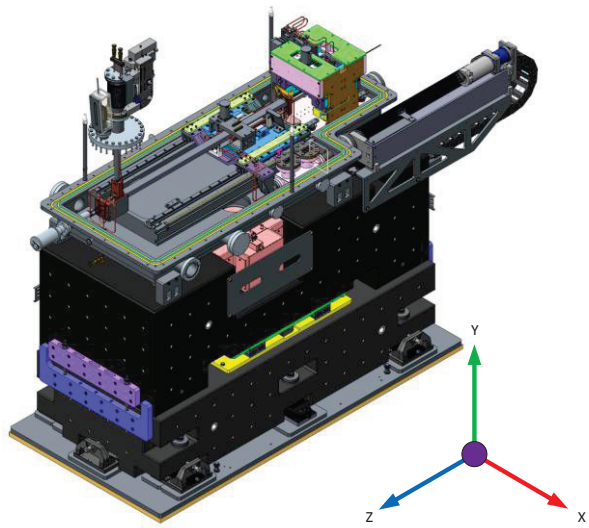

Figure 2: 3D CAD model of the VMXi DMM.

This posed a number of design challenges to maintain pitch stability over this range (the DMM is largely insensitive to roll and yaw). From previous experience with commercial DMMs and DCMs it was decided that an in-house design would be developed. The storage ring at DLS currently operates at 300 mA but future upgrade to a Cryogenic Permanent Magnet Undulator (CPMU) would increase the ring current to 500 mA. The DMM has therefore been designed with this in mind. Table 1 details the specification and achieved performance.

Table 1: DMM Specification

Incident design power (CPMU @500mA)	~590 W
Incident beam size	3.4 x 2.1 mm (max)
Deflection Geometry	25 mm down
Energy Range	10-25 keV
Beam stability (measured)	34 nrad (RMS)

DMM COMPONENTS

At the heart of the design are the multilayers – a silicon substrate on which layers of heavy and light elements are deposited. The multilayer can therefore be produced with a prescribed d-spacing and the VMXi multilayer has 2x stripes at d-spaces of 2 nm and 2.4 nm. This allows an energy range between 10-25 keV with some energy overlap between the two multilayers. To select either multilayers the whole vessel is translated in the X-direction on a granite air bearing.

† d.butler@diamond.ac.uk